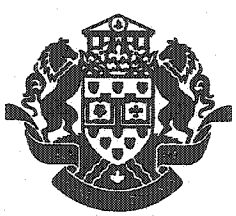

Université d'Ottawa • University of Ottawa

Université d'Ottawa · University of Ottawa

FACULTÉ DE ÉTUDES SUPÉRIEURES ET POSTDOCTORALES

FACULTY OF GRADUATE AND POSTDOCTORAL STUDIES

Samantha DROUIN

AUTEUR DE LA THÈSE - AUTHOR OF THESIS

Ph.D. (Chemistry)

GRADE - DEGREE

Department of Chemistry

FACULTÉ, ÉCOLE, DÉPARTEMENT - FACULTY, SCHOOL, DEPARTMENT

TITRE DE LA THÈSE - TITLE OF THE THESIS

Design and Transformation of Versatile Ruthenium Catalysts

D. Fogg

DIRECTEUR DE LA THÈSE - THESIS SUPERVISOR

CO-DIRECTEUR DE LA THÈSE - THESIS CO-SUPERVISOR

EXAMINATEURS DE LA THÈSE - THESIS EXAMINERS

R. Crutchley

K. Fagnou

J. Louie

D. Richeson

J.-M. De Koninck, Ph.D.

LE DOYEN DE LA FACULTÉ DES ÉTUDES SUPÉRIEURES ET POSTDOCTORALES

SIGNATURE

DEAN OF THE FACULTY OF GRADUATE AND POSTDOCTORAL STUDIES

DESIGN AND TRANSFORMATION OF VERSATILE RUTHENIUM CATALYSTS

By

SAMANTHA D. DROUIN

Thesis submitted to the
Faculty of Graduate and Postdoctoral Studies
University of Ottawa
In partial fulfillment of the requirements for the degree of

Doctor of Philosophy

Ottawa-Carleton Chemistry Institute
University of Ottawa
Ottawa, Ontario
Canada

Your file Votre référence
ISBN: 0-612-89993-4
Our file Notre référence
ISBN: 0-612-89993-4

ABSTRACT

Ruthenium metathesis catalyst $RuCl_2(PCy_3)_2(CHPh)$ (**1a**) was transformed into hydrogenation-active species via hydrogenolysis of the alkylidene ligand. Several different hydride products were identified, including novel dihydrogen complex $RuCl_2(H_2)(PCy_3)_2$ (**3**), and hydridochloro species $RuHCl(H_2)(PCy_3)_2$ (**4**). In related work, an optimized protocol for tandem ring-opening metathesis polymerization (ROMP)-hydrogenation was developed. Thus, hydrogenation of ROMP derived poly(octene) was accomplished under the very mild conditions of 1 atm H_2 and 60 °C. Strategic regeneration of a metathesis catalyst following hydrogenation allowed implementation of a "double tandem" sequence of ROMP-hydrogenation-ROMP, whereby bimodal polymer blends were generated in a one-pot process starting from a single catalyst precursor.

The potential of perfluorophenoxide ligands for design of metathesis catalysts was investigated via synthesis of vinylidene complex $Ru(OC_6F_5)_2(=C=CHBu^t)$(dcypb) (**18**), where dcypb = bis(dicyclohexyl)-1,4-phosphinobutane. Protonolysis of the perfluorophenoxide ligands in **18** by HCl gave the dichloro analogue $[\{Ru(=C=CHBu^t)(dcypb)\}(\mu\text{-}Cl)_3]Cl$ (**19•Cl**). The structure of **19•Cl** illustrates a common motif in Ru chemistry: the tendency to form trichloride-bridged dimers. By contrast, replacement of chloride ligands in **19•Cl** by perfluorophenoxides yields a stable

mononuclear complex (**18**). While both **18** and **19•Cl** catalyze the ROMP of norbornene, preliminary results suggest that the mononuclear **18** is a more efficient initiator than **19•Cl**.

Replacement of each vinylidene in **19•Cl** by a CO ligand gave [{Ru(CO)(dcypb)}(μ-Cl)$_3$]Cl (**21a**), which is a direct structural analogue of **19•Cl**. While **21a** is stable in air, reaction with hydride reagent KBH^{s}Bu$_3$ gave a highly reactive trihydride K[RuH$_3$(CO)(dcypb)] (**28**). Complex **28** was found to be moderately active for Murai catalysis and extremely active for the hydrogenation of benzophenone. A catalytic intermediate in the hydrogenation chemistry was isolated and identified as orthometallated RuH[*o*-C(O)(Ph)C$_6$H$_4$](CO)(dcypb) (**30**). Interestingly, the Murai activity of complex **30** is lower than that of **28**, suggesting that the orthometallated species is not on the reaction path for the coupling reaction.

The potentially stabilizing effect of a chelating iminopyrrolato ligand was investigated via synthesis of novel metathesis catalysts RuCl(NN$'$)(PCy$_3$)(CHPh) (**34**) and RuCl(NN$'$)(py)$_2$(CHPh) (**35**), where NN$'$ is (2, 6-^{i}Pr$_2$-C$_6$H$_3$N=CH)-2-C$_4$H$_3$N$^-$. The activity of **35** for RCM was found to be very low. However, phosphine derivative **34** is an extremely robust metathesis catalyst, capable of effecting RCM in air in non-distilled, non-degassed solvent. Catalysis via **34** probably involves phosphine rather than imine dissociation. Strong chelation of the iminopyrrolato ligand is an attractive feature for the

design of sterically well-defined catalysts; incorporation of chirality in NN′ is a promising strategy for eventual preparation of stereoselective analogues of **34**.

TABLE OF CONTENTS

TABLE OF COMPOUND NUMBERS

Number	Compound
1	$RuCl_2(PCy_3)_2(CHR)$
1a	R = Cy
1b	$R = CHCMe_2$
2	$Ru(H)_2Cl_2(PCy_3)_2$
3	$RuCl_2(H_2)(PCy_3)_2$
4	$RuHCl(H_2)(PCy_3)_2$
5	$RuCl_2(H_2)_2(PCy_3)_2$
6	$RuCl_2(H_2)(PCy_3)_2$(DMA)
7	$RuHCl(H_2)_2(PCy_3)_2$
8	Cyclooctene (COE)
9	5-Bromo-1-Cyclooctene
10	5-Methoxy-1-Cyclooctene
11	5-Acetoxy-1-Cyclooctene
12	5-Methoxymethylbicyclo[2.2.1]hept-2-ene
13	$RuHCl(CO)(PCy_3)_2$
14	$RuCl_2(CO)(PCy_3)_2$
15	$RuHCl(CO)(IMes)(PCy_3)$
16	$Ru_2Cl_4(dcypb)_2(N_2)$
17a	$RuCl(dcypb)(\mu\text{-}Cl)_3Ru(dcypb)(C{=}CHBu^t)$
17b	$RuCl(dcypb)(\mu\text{-}Cl)_3Ru(dcypb)[C{=}C(OH)Ph_2)$
18	$Ru(OC_6F_5)_2[(C{=}CH(Bu^t)](dcypb)$
19•Cl	$[\{Ru(C{=}CHBu^t)\ (dcypb)\}_2(\mu\text{-}Cl)_3]Cl$
19•PF_6	$[\{Ru(C{=}CHBu^t)(dcypb)\}_2(\mu\text{-}Cl)_3]PF_6$

20	$Tl[\{Ru(C{\equiv}CBu^t)(dcypb)\}_2(\mu\text{-}Cl)_3]$
21	$Ru_2Cl_4(CO)_2(dcypb)$
21a	$[\{Ru(CO)(dcypb)\}_2(\mu\text{-}Cl)_3]^+Cl^-$
21b/c	$[RuCl(CO)(dcypb)]_2(\mu\text{-}Cl)_2$
22	$RuCl_2(CO)_2(dcypb)$
22a	*ccc*-$RuCl_2(CO)_2(dcypb)$
22b	*tcc*-$RuCl_2(CO)_2(dcypb)$
23	$[\{Ru(C{=}CHBu^t)(dcypb)\}_2(\mu\text{-}Cl)_2]^{2+}{\bullet}2\{BAr^F{}_4\}^-$
24	$RuCl_2(C{=}CH^tBu)(PCy_3)_2$
25	$RuCl_2(C{=}CH^tBu)(PPh_3)_2$
26	$RuCl_2(CO)(PPh_3)_2(DMF)$
27	Unidentified decomposition products from **22**
28	$K[fac\text{-}RuH_3(CO)(dcypb)]{\bullet}KBH^sBu_3$
29	$RuCl_2[P(C_6H_4\text{-}4\text{-}CH_3)_3]_2(NH_2CH_2CH_2NH_2)$
30	$RuH[o\text{-}C(O)(Ph)(C_6H_4)](CO)(dcypb)$
31	$RuCl[o\text{-}(C_6H_3\text{-}4\text{-}Me)C(O)(C_6H_4\text{-}4\text{-}Me)](CO)(PMe_2Ph)_2$
32	$RuCl(OC(C_6H_4)(Ph))(CO)(dcypb)$
33	$RuCl[2\text{-}\{(2,6\text{-}{}^iPr_2C_6H_3)\text{-}N{=}CH\}C_4H_3O](PCy_3)(CHPh)$
34	$RuCl[2\text{-}\{(2,6\text{-}{}^iPr_2C_6H_3)\text{-}N{=}CH\}C_4H_3N](PCy_3)(CHPh)$
35	$RuCl[2\text{-}\{(2,6\text{-}{}^iPr_2C_6H_3)\text{-}N{=}CH\}C_4H_3N](py)_2(CHPh)$
36	$RuCl_2(H_2IMes)(py)_2(CHPh)$
37	$RuCl_2(H_2IMes)(py\text{-}3\text{-}Br)_2(CHPh)$
38	$RuCl_2(H_2IMes)(py\text{-}4\text{-}Ph)_2(CHPh)$

LIST OF TABLES

LIST OF FIGURES

LIST OF ABBREVIATIONS

Å	angstrom
atm	atmosphere (1 atm = 760 mmHg, 101.3 kPa, 14.696 psi)
bpy	2,2'-bipyridine
br	broad
c-	cis
$^{13}C\{^{1}H\}$	proton-decoupled carbon-13 (NMR)
CI	chemical ionization (mass spectrometry)
CM	cross metathesis
COE	cyclooctene
Cp	cyclopentadienyl
Cp*	pentamethylcyclopentadienyl, η^5-$C_5(CH_3)_5$
CP/MAS	Cross Polarization Magic Angle Spinning
Cy	cyclohexyl
d	doublet
DCE	1,2-dichloroethane
dcypb	1,4-bis(dicyclohexylphosphino)butane
DEPT	Distortionless Enhancement by Polarization Transfer
DMF	N,N-dimethylformamide

dtbpm	bis(di-*tert*-butylphosphino)methane, $^tBu_2PCH_2P^tBu_2$
dtbpe	bis(di-*tert*-butylphosphino)ethane, $^tBu_2PCH_2CH_2P^tBu_2$
DMA	N,N-dimethylacetamide
dmso	dimethylsulfoxide
dppb	1,4-bis(diphenylphosphino)butane
dppe	1,2-bis(diphenylphosphino)ethane
EI-MS	Electron Impact Mass Spectrometry
ESI	ElectroSpray Ionization (mass spectrometry)
eV	electron Volts (1 eV = 27.2 hartree)
EXSY	Exchange Spectroscopy
$^{19}F\{^1H\}$	proton-decoupled fluorine-19 (NMR)
GC-MS	Gas Chromatography-Mass Spectrometry
GPC	Gel Permeation Chromatography
$HBAr^F_4$	$[H(OEt_2)_2]^+ [(3,5\text{-}(CF_3)_2C_6H_3)_4B]^-$
HMBC	Heteronuclear Multiple Bond Coherence
HMQC	Heteronuclear Multiple Quantum Coherence
Hz	Hertz, cycles per second
IMes	bis(1,3-(2,4,6-trimethylphenyl)imidazol-2-ylidene
IR	Infrared
J	coupling constant, in Hz

L	ligand
LAH	lithium aluminum hydride
λ	wavelength
M	central metal atom in a complex
m	multiplet (NMR)
m	meta
Mes	mesityl
$NaBAr^F_4$	$[Na^+][(3,5\text{-}(CF_3)_2C_6H_3)_4B]^-$
NN′	2-[(2,6-diisopropylphenyl)imino)pyrrolide
NHC	N-heterocyclic carbene
NMR	Nuclear Magnetic Resonance
NBE	norbornene
o	ortho
ORTEP	Oak Ridge Thermal Ellipsoid Projection
$^{31}P\{^1H\}$	proton-decoupled phophorus-31 (NMR)
PP	chelating ditertiary phosphine ligand
P.S.	Proton Sponge
py	pyridine
pyr	pyrrole ring
q	quartet (NMR)

RCM	ring-closing metathesis
ROMP	ring-opening metathesis polymerization
RT	room temperature
s	singlet (NMR)
t	triplet (NMR)
tert-, ^{t}	tertiary
t	trans
TFA	trifluoroacetic acid
THF	tetrahydrofuran
Tp	hydrido tris(pyrazolyl)borate
T_1	longitudinal relaxation time (NMR)
TMS-OTf	trimethylsilyl trifluoromethanesulfonate
XRD	X-Ray Diffraction
δ	chemical shift (in ppm)
ν	frequency (in cm^{-1})
η	descriptor for hapticity
μ	descriptor for bridging

ACKNOWLEDGEMENTS

I thank my supervisor, Professor Deryn Fogg for her vision, her guidance, and her wonderful enthusiasm.

I am grateful to former labmate Dino Amoroso for his kindness and tolerance. I thank Jennifer Snelgrove for friendly companionship through the years. I must acknowledge the contribution of my predecessor, Fojan Zamanian (Fogee), who initiated the tandem project, giving it the initial momentum that was critical to its eventual success. I would also like to thank the generations of "Fogg denizens", including Jay Conrad, Nick Gambarotta, Amir Jabri, Yuwen Liu, and Pawel Czechura who have energized the group with new ideas, and I thank Jay in particular for so many excellent conversations. I am grateful to Dr. Glenn Facey of the NMR Laboratory for his genuine interest and for numerous helpful discussions. I thank Dr. Glenn Yap of the X-ray Laboratory for crystallographic analyses.

I am tremendously grateful to my family, and particularly my parents, for their constant encouragement and support. Finally, I thank Ray, for his loyal and unconditional love.

PUBLICATIONS FROM THESIS WORK

- S. D. Drouin, G. P. A. Yap, D. E. Fogg, "On the Compatibility of the Vinylidene Ligand and Perfluorophenoxide" *Organometallics*, **2003**, submitted.
- S. D. Drouin, D. Amoroso, G. P. A. Yap, D. E. Fogg, "Multifunctional Ruthenium Catalysts: A Novel Polyhydride Complex Containing the Basic, Chelating Diphosphine Bis(dicyclohexyl)-1,4-phosphinobutane, and Its Application to Hydrogenation and Murai Catalysis." *Organometallics,* **2002**, *21*, 1042.
- D. E. Fogg, D. Amoroso, S. D. Drouin, J. L. Snelgrove, J. C. Conrad, F. Zamanian, "Ligand Manipulation and Design for Ruthenium Metathesis and Tandem Metathesis-Hydrogenation." *J. Mol. Catal. A,* **2002**, *190*, 177.
- D. Amoroso, J. L. Snelgrove, J. C. Conrad, S. D. Drouin, G. P. A. Yap, D. E. Fogg, "A Ruthenium Alkylidene Complex Containing Labile Phosphane Donors: One-Step Synthesis from a Commercially Available Precursor." *Adv. Synth. Catal*, **2002**, *344*, 757.
- S. D. Drouin, F. Zamanian, D. E. Fogg, "Multiple Tandem Catalysis: Facile Cycling Between Hydrogenation and Metathesis Chemistry." *Organometallics*, **2001**, *20*, 5495.
- S. D. Drouin, G. P. A. Yap, D. E. Fogg, "Hydrogenolysis of a Ruthenium Carbene Complex to Yield Dihydride-Dihydrogen Tautomers: Mechanistic Implications for Tandem ROMP-Hydrogenation Catalysis." *Inorg. Chem.*, **2000**, *39*, 5412.

Patent:

- D. E. Fogg, S. D. Drouin, F. Zamanian, "Method for Producing Saturated Polymers and Saturated or Unsaturated Blends", US Patent 6,486,263, 2002.

CHAPTER 1

Introduction

1.1. Homogeneous Catalysis by Ruthenium Complexes

Ongoing research in catalysis is largely fuelled by environmental and economic requirements for cleaner, more efficient technologies;[1,2] catalytic methods offer the dual promise of atom economy and energetic efficiency. Most catalysts in current use are insoluble solids. The affordability and robustness of these heterogeneous systems make them attractive for industrial applications, though most are poorly understood at the molecular level. Soluble, or homogeneous, catalysts tend to be more expensive and less robust than heterogeneous catalysts. What soluble catalysts do offer is greater control over product purity.[1]

In general, homogeneous transition-metal catalysts possess structurally well-defined active sites. This structural definition allows for selectivity in catalysis. Judicious choice of ligands extends control over the geometry of the active site, which in turn may influence its affinity for a particular substrate. In its simplest form, catalytic control is manifested as chemoselectivity, or discrimination between functional groups. Higher levels of control include regioselectivity, or site selectivity, and stereoselectivity, or discrimination between stereoisomeric products. Stereoselective, or asymmetric, catalysis by soluble transition-metal complexes represents one of the most important chemical developments of the last century; a

range of enantioselective hydrogenation, isomerization, oxidation, and C-C bond forming reactions have been made possible by such catalysts and many of these reactions are currently applied in industry.[1]

Over the past two decades, ruthenium has played an increasingly important role in homogeneous catalysis. Its versatility, robustness, and low cost relative to other group 8 transition metals make it attractive for both benchtop and commercial applications.[3] The catalytic versatility of ruthenium can be attributed to several key properties, which apply to a broad range of Ru(II) complexes despite relatively drastic changes in the ligand sphere. These properties include: (1) a propensity for π-backbonding, which is reflected in the stability of Ru(CO), $Ru(N_2)$, and $Ru(\eta^2\text{-}H_2)$ complexes; (2) a tendency to undergo intra- and intermolecular metallation reactions; and (3) a tendency to form hydride complexes.[4] The catalytic significance of this last point is illustrated schematically in Figure 1.1.

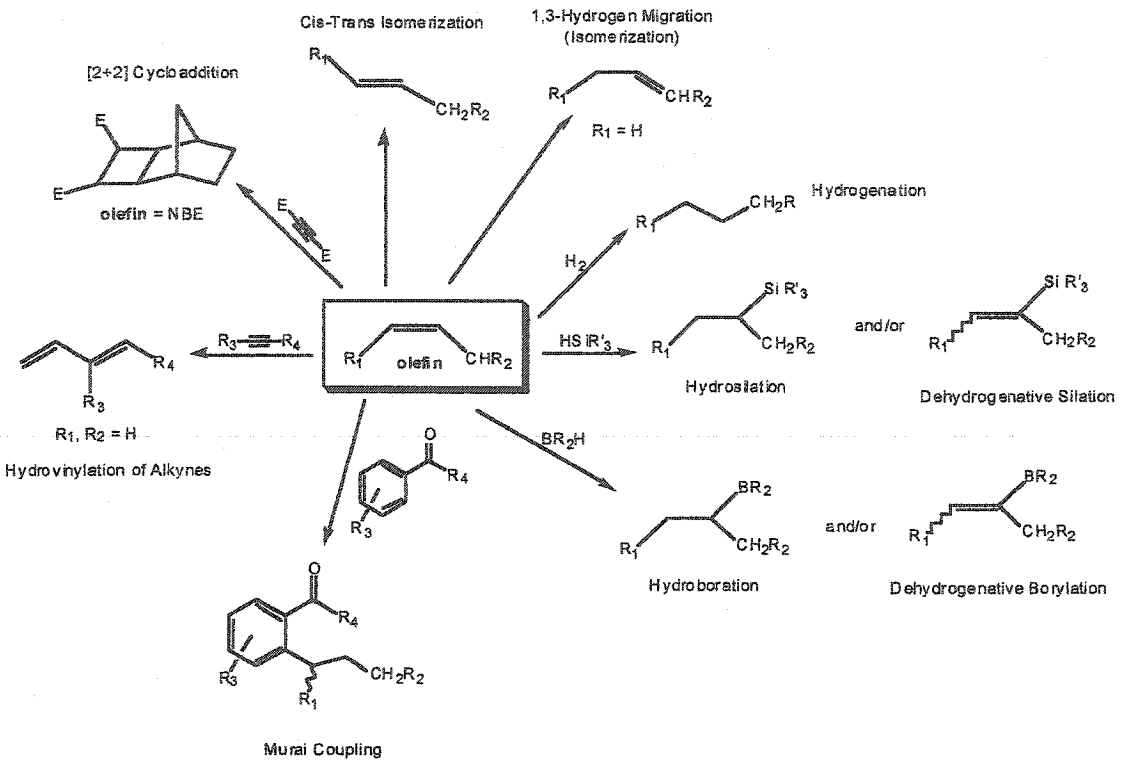

Figure 1.1 Reactions of olefins catalyzed by Ru(II) hydride complexes.

The catalytic chemistry of ruthenium currently embraces a broad range of transformations, including hydrogenation, oxidation (i.e. epoxidation, aziridination and dehalogenation), nucleophilic addition to carbon-carbon and carbon-heteroatom bonds, Kharasch addition, atom-transfer radical polymerization, cyclopropanation and all types of metathesis reactions.[3] This versatility holds great, but largely untapped, potential for *tandem* catalysis, in which a single catalyst precursor effects two or more distinct, sequential catalytic transformations. Key to such reactions is conservation of catalyst structure in the different classes of transformation to be effected. Where a given catalyst can effect several types of reaction, the nature of a given transformation is typically determined by the substrate and

feedstock used. For example, the versatility of Ru-hydride complexes such as $RuHCl(CO)(PCy_3)_2$ is well established;[3] more recently, RuCl(sal)(L)(CHPh) complexes (sal = Schiff base ligand; L = PCy_3 or N-heterocyclic carbene) have been found to catalyze olefin metathesis,[5,6] Kharasch addition,[6] enol ester synthesis,[6] and atom transfer radical polymerization.[7] Startlingly little research effort has been directed at harnessing this versatility in tandem catalysis.[8]

Sequential catalytic transformations may also be effected via catalysts in which *ancillary* ligand structure is conserved, but the active site differs. Such chemistry may be enabled by direct chemical manipulation of the active site. Exploration of the latter class of processes is very recent. Of particular promise are tandem catalyses involving Ru-alkylidenes and Ru-hydrides. Coupling the enormous range of transformations latent within each of these functionalities would greatly expand the efficiency and scope of metathesis chemistry.

1.2. The Olefin Metathesis Reaction

Olefin metathesis, catalyzed by transition metal alkylidenes, effects interchange of vicinal substituents between two alkenes (Figure 1.2). The metathesis reaction is a powerful and versatile tool in organic and polymer synthesis, affording access to both novel molecular and polymeric materials.[9,10]

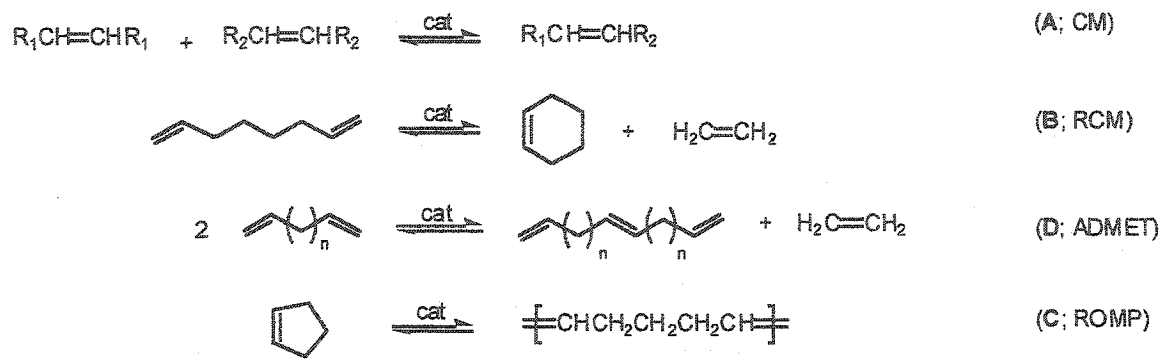

Figure 1.2 Types of olefin metathesis reactions.

Metathesis is grouped into four main classes based on the nature of substrates and products (Figure 1.2). The cross metathesis reaction (CM, reaction **A**) most clearly illustrates the "scrambling" of substituents between the two olefinic substrates. Ring-closing metathesis (RCM; reaction **B**) involves the intramolecular transformation of a *a*, *ω*-diene to give a cycloolefin. RCM is the most widely used metathesis reaction in organic synthesis, and has been applied to construction of both simple and complex ring structures.[9] The reaction is entropically driven by coproduction of ethylene; RCM may, in principle, be reversed in the presence of excess ethylene to give the linear, ring-opened product. Acyclic diene metathesis polymerization (ADMET, Reaction **C**), is an intermolecular variant on RCM, acyclic diene metathesis polymerization (ADMET, Reaction **C**), yielding polymeric products. The utility of ADMET reactions is often limited by formation of complex product mixtures, which include both cyclic and linear oligomers. Ring-opening metathesis polymerization (ROMP, Reaction **D**) offers a cleaner route to polyolefins. In this reaction, ring-opening metathesis is repeated sequentially, resulting in a

growing chain of similarly ring-opened olefins. The equilibrium can be shifted in favour of the products via use of highly strained cyclic monomers; when driven by relief of ring strain, the polymerization is essentially irreversible.

Stereochemical control over metathesis products is manifested in its simplest form by specification of the cis/trans geometry of the new olefinic units. In its most sophisticated embodiment, it allows specification of the relative configurations of chiral centres positioned α-to the new olefinic sites. Tacticity in ROMP polymers is defined in terms of these chiral centres. For example, assignment of tacticity in ROMP-derived polynorbornene is based on the sequence of configurations of the *pairs* of methine carbon atoms on adjacent C_5 rings (Figure 1.3). Analysis of the tacticity of such polymers requires consideration of at least two consecutive repeat units or dyads.[11]

Figure 1.3 Illustration of a dyad of ROMP-derived poly(norbornene). This particular dyad represents the *trans*, syndiotactic configuration (• denotes a chiral centre).[11]

1.3. Olefin Metathesis Catalysts

Early olefin metathesis catalysts were poorly defined systems, in which active catalysts were formed *in situ* from transition metal salts (e.g. $WOCl_4$, WCl_6) and cocatalysts (e.g. $EtAlCl_2$, Bu_4Sn).[10] For the past forty years, these multicomponent systems have occupied an important

position in industry owing to their low cost and simple preparation.[9b,c,g,12] Development of well-defined catalysts began in the late 1970s, growing out of mechanistic insights, and, particularly, from the recognition that the metathesis reaction is initiated and propagated by transition-metal alkylidene complexes. The generally accepted mechanism, first postulated by Herisson and Chauvin in 1971, involves a 2+2 addition of a metal alkylidene to an olefin to form a metallacyclobutane intermediate, which then undergoes retro-addition (Figure 1.4).[13] Productive metathesis yields a new (propagating) alkylidene. Non-productive or degenerate metathesis can also occur, regenerating the parent alkylidene and olefin.

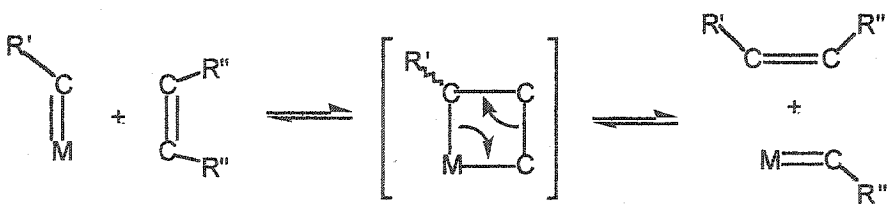

Figure 1.4 Mechanism of olefin metathesis.

The first single-component metathesis catalysts were Group 6 alkylidenes of general formula M(=NAr)(OR')$_2$(=CHR), developed by Schrock.[14] Perhaps the best-known example is the molybdenum complex where Ar = 2,6-Pr$^i_2$-C$_6$H$_3$, R = CMe$_2$Ph, and R' = C(CH$_3$)(CF$_3$)$_2$, which is still used as a benchmark for activity in RCM of tri- and tetrasubstituted olefins.[9f] Chiral variants, bearing chelating biphenolate and binaptholate ligands, were developed during the 1990s: these catalysts are, to date, the most successful examples of *enantioselective* metathesis

catalysts.[15] Catalysts of the type shown in Figure 1.5 have been applied to the asymmetric synthesis of molecular and polymeric products.[15]

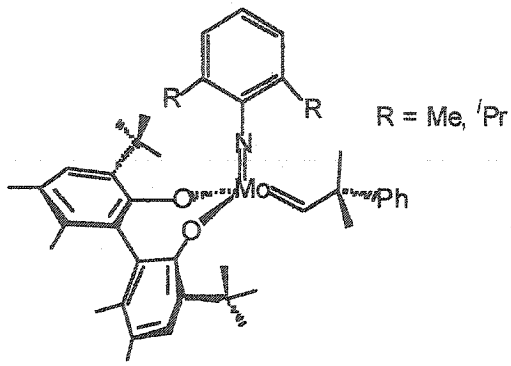

Figure 1.5 Molybdenum catalysts for stereoselective metathesis.[15]

The high oxophilicity of these Group 6 complexes has hampered their uptake by synthetic organic chemists and by industry. More robust catalysts based on ruthenium were discovered by the Grubbs group in the early 1990s.[9c] Of the early Ru systems, the benzylidene complex $RuCl_2(CHPh)(PCy_3)_2$ (**1a**, Figure 1.6) represents a milestone in metathesis chemistry:[16] though less active than the Schrock catalysts, **1a** quickly became more widely used, owing to its versatility and stability.

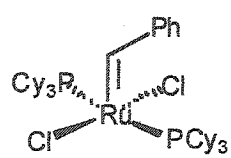

Figure 1.6 The "Grubbs Catalyst", **1a**.

1.4. Bimolecular Deactivation of Chlororuthenium Catalysts

Recent work by the Fogg group has identified a deactivation pathway for chlororuthenium metathesis catalysts involving formation of trichloride-bridged dimers. Thus, solutions of vinylalkylidene $RuCl_2(PPh_3)_2(=CHCH=CMe_2)$ at RT spontaneously form a trichloride-bridged monoalkylidene species, with concomitant extrusion of the alkylidene ligand (Figure 1.7).[17] Related kinetic studies support a bimolecular mechanism.[18] Such deactivation pathways undermine both catalyst lifetime and, indirectly, the potential for tandem catalysis via well-defined transition metal catalysts.

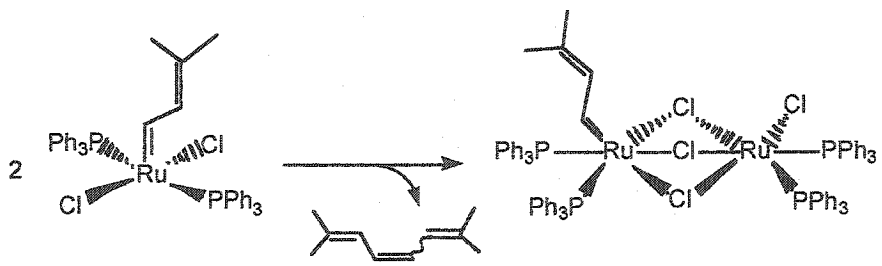

Figure 1.7 Bimolecular deactivation of $RuCl_2(PPh_3)_2(=CHCH=CMe_2)$.[17]

The $Ru_2(\mu\text{-}Cl)_3$ motif is ubiquitous within the chemistry of divalent ruthenium,[19] in which the anionic chloride ligand is omnipresent. Formation of such bioctahedra may represent a common, unrecognized deactivation pathway for dichlororuthenium catalysts. Indeed, the dramatically accelerating effect of alcohol solvents in hydrogenations catalyzed by such species may reflect the ability of the weak donor ROH to reverse dimerization, cleaving the $Ru_2(\mu\text{-}Cl)_3$ bridging unit.[20,21] Alternatively, catalytic lifetime could potentially be enhanced by replacing the

chloride ligands by alternative anionic donors. Circumventing pathways that degrade catalyst homogeneity is key not only to improving catalytic performance in a *given* transformation, but to accessing well-behaved, tandem catalytic processes.

1.5. Scope of This Thesis

This thesis describes the versatility of both known and novel Ru-phosphine catalysts in olefin metathesis, hydrogenation, and Murai catalysis. Choice of electron-rich *alkyl*phosphine ligands, in place of the ubiquitous arylphosphine systems, stems from the observation that these ligands enhance catalytic activity in both hydrogenation[22,23] and metathesis[16,24,25] catalysis, and speculation that electron-rich systems will enhance activity in any reaction for which the transition state involves population of σ^* or π^* antibonding orbitals. In Chapter 3, these synergies were explored in context of tandem metathesis-hydrogenation catalysis, in which the known metathesis catalyst $RuCl_2(CHPh)(PCy_3)_2$ (**1a**, Grubbs catalyst) is transformed into hydrogenation-active Ru-hydride species. The inorganic chemistry underlying this manipulation of catalyst function is delineated, as well as the strategic use of simple chemical switches to reversibly "toggle" between metathesis and hydrogenation chemistry. Ligand and solvent effects on the catalytic chemistry (a recurring theme of this work) are explored, and the largely-overlooked role of alcohol solvents in promoting catalysis is discussed.

In Chaper 3, a monodentate phosphine ligand was employed. With the intention of limiting deactivation chemistry,[18,26] as well as increasing the steric delineation of the active site, chelating ancillary ligands were employed throughout the remainder of this thesis work. Complexes containing the chelating diphosphine 1,4,-bis(dicyclohexylphosphino)butane (dcypb) are utilized in Chapters 4 and 5. Chapter 4 describes the use of perfluorophenoxide anion as a monodentate pseudohalide ligand in Ru-dcypb vinylidene complexes. The capacity of this ligand to circumvent formation of $Ru_2(\mu\text{-}Cl)_3$ dimers is explored. Chapter 5 describes an investigation into the thermodynamic stability of such face-bridged dimers over their edge-bridged isomers, within $[RuCl_2(CO)(dcypb)]_2$ systems. Also discussed is the extraordinarily high hydrogenation activity (and the more modest Murai activity) associated with the mononuclear, hydrido derivatives. This catalytic chemistry reflects the combined effects of an electron-rich diphosphine ligand and a π-acid carbonyl ligand. Chapter 6 describes the synthesis and metathesis chemistry of Ru complexes containing a chelating, monoanionic iminopyrrolato ligand. General conclusions and suggestions for future work are outlined in Chapter 7.

1.6. References and Notes

(1) Parshall, G. W.; Ittel, S. D. *Homogeneous Catalysis*; 2nd ed.; Wiley-Interscience: Toronto, 1992.

(2) Crabtree, R. H. *The Organometallic Chemistry of the Transition Metals*; 3rd ed.; Wiley-Interscience: Toronto, 1994.

(3) Recent reviews: (a) General Ru-catalysis: Naota, T.; Takaya, H.; Murahashi, S.-I. *Chem. Rev.* **1998**, *98*, 2599. (b) C-C bond activation: Mitsudo, T.-A.; Kondo, T. *Synlett.* **2001**, 309. (c) Kharasch and atom transfer radical polymerization: Simal, F.; Demonceau, A.; Noels, A. F. *Recent Res. Dev. Org. Chem.* **1999**, *3 (Pt. 2)*, 455. (d) Biomimetic oxidations: Murahashi, S.-I.; Naruyoshi., K. In *Biomimetic Oxidations Catalyzed by Transition Metal Complexes*; Meunier, B., Ed.; Imperial College Press: London, 2000, p. 563. (e) Lewis Acid and Base Catalysis: Murahashi, S.-I.; Takaya, H. *Acc. Chem. Res.* **2000**, *33*, 225. (f) Olefin metathesis: Trnka, T. M.; Grubbs, R. H. *Acc. Chem. Res.* **2001**, *34*, 18. (g) Oxidation of alcohols: Friedrich, H. B. *Platinum Met. Rev.* **1999**, *43*, 94. (h) Epoxidation and aziridination of alkenes: Che, C.-M.; Yu, W.-Y. *Pure Appl. Chem.* **1999**, *71*, 281. (i) Oxidative dehalogenation of organics: Bressan, M.; d'Alessandro, N.; Liberatore, L.; Morvillo, A. *Coord. Chem. Rev.* **1999**, *185-186*, 385. (j) Murai catalysis: Murai, S.; Kakiuchi, F.; Sekine, S.; Tanaka, Y.; Kamatani, A.; Sonoda, M.; Chatani, N. *Nature* **1993**, *366*, 529. (k) Asymmetric reduction of ketones: Noyori, R.; Ohkuma, T. *Angew. Chem. Int. Ed. Engl.* **2001**, *40*, 40. (l) Copolymerization of aromatic ketones and 1,3-divinyltetramethyldisiloxane: Weber, W. P.; Guo, H.; Kepler, C. L.; Londergan, T. M.; Lu, P.; Paulsaari, J.; Sargent, J. R.; Tapsak, M. A.; Wang, G. *ACS Symp. Ser.* **2000**, *729*, 433. (m) C-C bond formation (non-metathesis): Trost, B. M.; Toste, D.; Pinkerton, A. B. *Chem. Rev.* **2001**, *101*, 2067.

(4) Chaloner, P. A.; Esteruelas, M. A.; Joo, F.; Oro, L. A. *Homogeneous Hydrogenation*; Kluwer: Boston, 1994.

(5) DeClercq, B.; Verpoort, F. *Adv. Synth. Catal.* **2002**, *344*, 639.

(6) DeClercq, B.; Verpoort, F. *Tet. Lett.* **2001**, *42*, 8959.

(7) DeClercq, B.; Verpoort, F. *Macromolecules* **2002**, *35*, 8943.

(8) (a) Sutton, A. E.; Seigal, B. A.; Finnegan, D. F.; Snapper, M. L. *J. Am. Chem. Soc.* **2002**, *124*, 13390. (b) Bielawski, C. W.; Louie, J.; Grubbs, R. H. *J. Am. Chem. Soc.* **2000**, *122*, 12872. (c) Louie, J.; Bielawski, C. W.; Grubbs, R. H. *J. Am. Chem. Soc.* **2001**, *123*, 11312. (d) Watson, M. D.; Wagener, K. B. *Macromolecules* **2000**, *33*, 3196. (e) McLain, S. J.; McCord, E. F.; Arthur, S. D.; Hauptman, E.; Feldman, J.; Nugent, W. A.; Johnson, L. K.; Mecking, S.; Brookhart, M. *Polym. Mater. Sci. Eng.* **1997**, *76*, 246.

(9) For recent reviews on olefin metathesis, see: (a) Barrett, A. G. M.; Hopkins, B. T.; Köbberling, J. *Chem. Rev.* **2002**, *102*, 3301. (b) Frenzel, U.; Nuyken, O. *J. Polym. Sci. Part A: Polym. Chem.* **2002**, *40*, 2895. (c) Trnka, T. M.; Grubbs, R. H. *Acc. Chem. Res.* **2001**, *34*, 18. (d) Dragutan, V.; Dragutan, I. *Platinum Metals Rev.* **2001**, *45*, 155. (e) Buchmeiser, M. R. *Chem. Rev.* **2000**, *100*, 1565.(f) Fürstner, A. *Angew. Chem. Int. Ed.* **2000**, *39*, 3012. (g) Schuster, M.; Blechert, S. *Angew. Chem. Int. Ed. Engl.* **1997**, *36*, 2036. (h) Armstrong, S. K. *J. Chem. Soc., Perkin Trans. 1* **1998**, **371**.

(10) Ivin, K. J.; Mol, J. C. *Olefin Metathesis and Metathesis Polymerization*; Academic Press: San Diego, 1997.

(11) Reference 16 provides an overview of the relevant experimental and theoretical issues surrounding the assignment of tacticity in ROMP polymers.

(12) Lefebvre, F.; Basset, J.-M. *NATO ASI Ser., Ser. C* **1998**, *506*, 341.

(13) Hérisson, J.-L.; Chauvin, Y. *Makromol. Chem.* **1971**, *141*, 161.

(14) For reviews of this area see: (a) Schrock, R. R. *Tetrahedron* **1999**, *55*, 8141. (b) Schrock, R. R. *Acc. Chem. Res.* **1990**, *23*, 158.

(15) (a) O'Dell, R.; McConville, D. H.; Hofmeister, G. E.; Schrock, R. R. *J. Am. Chem. Soc.* **1994**, *116*, 3414. (b) Schrock, R. R.; Lee, J.-K.; O'Dell, R.; Oskam, J. H.; *Macromolecules*, **1995**, *28*, 5933. (c) Alexander, J. B.; La, D. S.; Cefalo, D. R.; Hoveyda, A. H.; Schrock, R. R. *J. Am. Chem. Soc.* **1998**, *120*, 4041. (d) La, D. S.; Alexander, J. B.; Cefalo, D. R.; Graf, D. D.; Hoveyda, A. H.; Schrock, R. R. *J. Am. Chem. Soc.* **1998**, *120*, 9720. (e) Zhu, S. S.; Cefalo, D. R.; La, D. S.; Jamieson, J. Y.; Davis, W. M.; Hoveyda, A. H.; Schrock, R. R. *J. Am. Chem. Soc.* **1999**, *121*, 8251. (f) La, D. S.; Ford, J. G.; Sattely,

E. S.; Bonitatebus, P. J.; Schrock, R. R.; Hoveyda, A. H. *J. Am. Chem. Soc.* **1999**, *121*, 11 603.

(16) Schwab, P.; Grubbs, R. H.; Ziller, J. W. *J. Am. Chem. Soc.* **1996**, *118*, 100.

(17) Amoroso, D. A.; Snelgrove, J. L.; Conrad, J.; Drouin, S. D.; Yap, G. P. A.; Fogg, D. E. *Adv. Synth. Catal.* **2002**, *344*, 1.

(18) Ulman, M.; Grubbs, R. H. *J. Org. Chem.* **1999**, *64*, 7202.

(19) Seddon, E. A.; Seddon, K. R. *The Chemistry of Ruthenium*; Elsevier: Amsterdam, 1984.

(20) Fogg, D. E.; James, B. R.; Kilner, M. *Inorg. Chim. Acta* **1994**, *222*, 85.

(21) Bianchini, C.; Barbaro, P.; Scapacci, G.; Zanobini, F. *Organometallics* **2000**, *19*, 2450.

(22) Burk, M. J.; Martinez, J. P.; Feaster, J. E.; Cosford, N. *Tetrahedron* **1994**, *50*, 4399.

(23) McManus, N. T.; Rempel, G. L. *J. Macromol. Sci., Rev. Macromol. Chem. Phys.* **1995**, *C35*, 239.

(24) Dias, E. L.; Nguyen, S. T.; Grubbs, R. H. *J. Am. Chem. Soc.* **1997**, *119*, 3887.

(25) Amoroso, D.; Fogg, D. E. *Macromolecules* **2000**, *33*, 2815.

(26) Busch, S.; Leitner, W. *Adv. Synth. Catal.* **2001**, *343*, 192.

CHAPTER 2

Experimental Procedures

2.1. Materials

Solvents. Reagent grade toluene, hexanes, diethyl ether and tetrahydrofuran (BDH) were dried and degassed using an Anhydrous Engineering solvent purification system. Anhydrous dimethylformamide (DMF) was purchased from Aldrich and used without further purification. Other solvents were refluxed over and distilled from an appropriate drying agent under an atmosphere of N_2: benzene over sodium benzophenone ketyl; pentane over sodium; dichloromethane, 2-propanol, pyridine, acetonitrile, 1,2-dichloroethane, and dimethylacetamide (DMA) over calcium hydride; methanol over Mg/I_2; acetone over Drierite (anhydrous $CaSO_4$). All solvents (with the exception of methanol and 2-propanol) were stored over Linde 4Å molecular sieves under an atmosphere of N_2. Deuterated solvents ($CDCl_3$, CD_2Cl_2, CD_3OD, C_6D_6, THF-d_8, D_2O and toluene-d_8) were obtained from Cambridge Isotope Laboratories Ltd. $CDCl_3$ was refluxed over and distilled from Drierite under an atmosphere of N_2. C_6D_6 was deoxygenated by consecutive freeze/pump/thaw cycles and stored over Linde 4Å molecular sieves. Ampoules of CD_2Cl_2, THF-d_8, and toluene-d_8 were used as received. All deuterated solvents were stored under N_2.

Gases. Hydrogen (Praxair UHP Grade) was passed through a Deoxo cartridge and a Drierite column in series for procedures at 1 atm, or used without further purification for reactions above atmospheric pressure. Carbon monoxide and argon (Praxair; 99.5% or Research Grade, respectively) were passed through a Drierite column. Deuterium (Aldrich 99.8%) and ethylene (Praxair, Instrument Grade) were used as received.

Phosphines. All phosphines, other than those independently synthesized, were of reagent grade and used as received. Triphenylphosphine (PPh_3) and dicyclohexylphosphine ($HPCy_2$) were obtained from Strem Chemical Co. All phosphines, with the exception of PPh_3, were stored under an N_2 atmosphere.

Monomers. Norbornene (Aldrich) was dried over and distilled from sodium. Cyclooctene (Aldrich) was distilled from CaH_2. Other monomers were independently synthesized (*vide infra*). All monomers were stored under an N_2 atmosphere.

Other Materials. Benzaldehyde, potassium hydride (KH), Proton Sponge™ (P.S.), copper(I) chloride (CuCl), 1,4-dibromobutane, *n*-butyllithium (2.5 M in hexanes), 1,5-cyclooctadiene (COD), 5-norbornene-2-methanol, *m*-chloroperbenzoic acid (57 – 87% purity), lithium aluminum hydride (LAH), HCl (2.0 M in Et_2O), potassium tri(*sec*-butyl)borohydride (1.0 M in

Et_2O), Super-Deuteride (lithium triethylborodeuteride, 1.0 M solution in THF), 3,3-dimethyl-1-butyne, 3-chloro-3-methyl-1-butyne, and pentafluorophenol were purchased from Aldrich and used as received. Triethylamine (Aldrich) was distilled from $CaSO_4$ and stored under N_2. Allylbenzene (Aldrich) was vacuum-distilled and stored over 4 Å molecular sieves in an atmosphere of N_2. Diethyl diallylmalonate (Aldrich, 98%) was deoxygenated by consecutive freeze/pump/thaw cycles and stored under N_2. Hydrated $RuCl_3$ (38-43% Ru), thallium (I) ethoxide (TlOEt) and thallium hexafluorophosphate ($TlPF_6$) were obtained from Strem Chemical Co. and used as received. $[Na(OEt_2)]^+[(3,5\text{-}(CF_3)_2C_6H_3)_4B]^-$ ($NaBAr^F_4$) was generously supplied by Dr. Dino Amoroso (Promerus Inc., Brecksville, Oh, USA). $[RuCl_2(COD)]_x$ was prepared by Jeremy Cheeseman of this group by a literature procedure.[1]

2.2. Instrumentation

Infrared spectra were recorded on a Bomem MB100 IR spectrometer. Nuclear magnetic resonance (NMR) spectra were recorded on a Varian Gemini 200 (200 MHz for ^1H), a Varian XL-300 (121 MHz for ^{31}P, 75 MHz for ^{13}C, and 46 MHz for ^2H) or a Bruker Avance 300 (300 MHz for ^1H, 121 MHz for ^{31}P, 75 MHz for ^{13}C and 282 MHz for ^{19}F) or a Bruker AMX-500 (500 MHz for ^1H, 202 MHz for ^{31}P, and 125 MHz for ^{13}C) FT-NMR spectrometer. For ^1H and ^{13}C NMR spectra the residual proton and carbon signals of the deuterated solvent were used as internal standards. ^{31}P NMR spectra were referenced externally against PPh_3 (δ_P -5.06, C_6D_6;

-5.46, $CDCl_3$; -5.64, CD_2Cl_2); shifts are reported relative to 85% H_3PO_4. ^{19}F NMR spectra were referenced externally against a dilute solution of trifluoroacetic acid (TFA) in $CDCl_3$ (δ_F 0.00 ppm). Downfield shifts are taken as positive for all nuclei. Solid state NMR spectra were recorded on a Bruker ASX-200 MHz spectrometer (81 MHz for ^{31}P). Variable temperature NMR spectra and 2D experiments (HMQC, HMBC and EXSY) were carried out on the Bruker Avance 300 or the Bruker AMX-500 instrument. Elemental analyses were performed by V. Kuznetsov of this department using a Perkin Elmer Series II CHNS/O instrument, or by Guelph Chemical Laboratories (Guelph, ON). Mass spectral analyses were performed by the Ottawa-Carleton Mass Spectrometry Centre. Dr. Glenn P. A. Yap of the departmental crystallographic service carried out single crystal X-ray diffraction studies. Gel Permeation Chromatography (GPC) data were obtained with CH_2Cl_2 as eluent (flow rate 1.0 mL/min; samples 1-2 mg/mL) using a Wyatt DAWN light-scattering instrument equipped with an Optilab DSP refractometer, HPLC system with a Waters model 515 pump, Rheodyne model 7725i injector with a 200 μL injection loop, and Waters Styragel HR3 and HR4 columns in series. High-pressure reactions were conducted in machined steel autoclaves (Parr) equipped with glass liners.

2.3. Laboratory Techniques

Unless otherwise stated, all reactions were carried out at room temperature (RT, ~ 22 °C) under an inert atmosphere using standard Schlenk or drybox techniques.

2.4. Monomers

The following preparations are based on literature methods. These compounds were either used directly as substrates in ROMP experiments or as starting materials for the synthesis of other monomers.

2.4.1. 5-Methoxymethylbicyclo[2.2.1]hept-2-ene (*endo, exo* mixture) (12).

In a modification of the literature route,[2] a solution of 5-norbornene-2-methanol (2.8 g, 22.5 mmol, 70:30 mixture of *endo* and *exo* isomers) in 10 mL THF was added to an ice-cold suspension of NaH (0.84 g, 34.1 mmol) in 100 mL THF (100 mL) over a period of 30 min. The solution was stirred (0 °C) for 1 h, then treated with methyl iodide (2.8 mL, 45 mmol) in 10 mL THF. The solution was allowed to warm to RT overnight, then quenched with water (0 °C). The organic phase was extracted with Et_2O, dried ($MgSO_4$) and stripped of solvent. Vacuum distillation yielded 2.5 g (81%) of **12** as a clear, colourless liquid (70:30 mixture of *endo* and *exo* isomers.) The product was stored in the drybox over 4 Å molecular sieves. ^{1}H NMR ($CDCl_3$, δ) 5.93, 6.10 (m, 2 H, olefinic), 3.49 – 3.30 (m, 4 H), 3.25 – 2.61 (m, 3 H), 2.32 (m, 1 H), 1.88-1.53 (m, 1 H), 1.43-1.01 (m, 2 H), 0.54-0.38 (m, 1 H). ^{13}C{^{1}H} NMR ($CDCl_3$) δ 137.4, 136.9, 132.7, 77.9, 59.1, 49.8, 45.4, 44.2, 44, 42.5, 41.8, 39.2, 39.0, 30.0, 29.4. IR (neat) 3060 (m), 2965 (s), 2868 (s), 1448 (m), 1386 (w), 1346 (w), 1252 (w), 1112 (s), 957 (w), 927 (w), 720 (m) cm^{-1}. MS (EI) *m/z* (rel intens) 138 ([M+], 3), 106 (6), 91 (10), 79 (6), 77 (7), 71 (10), 66 (100) , 39 (6).

2.4.2. 5-Bromo-1-Cyclooctene (9)

1,5-Cyclooctadiene (25 mL, 0.20 mol) was added to a stirring solution of 30% HBr in glacial acetic acid (51 g, 0.19 mol). The mixture was stirred vigorously overnight (15 h) and the resulting orange solution was poured into an ice/water mixture (~150 mL). The product was extracted with petroleum ether, washed with 5% $NaHCO_{3(aq)}$ (3 × 20 mL), dried over $CaCl_2$, and the solvent removed under vacuum. The crude product was purified by vacuum distillation (43-54 °C, 0.3 mm Hg) to yield 24 g (63%) of crude bromide. This was chromatographed on silica gel with 20% benzene in hexane as eluant. Yield: 20.2 g (53%). Spectroscopic data agree with those reported.[3] ^{1}H NMR (δ, $CDCl_3$): 5.61 (m, 2 H, olefinic), 4.29 (m, 1 H, C*H*Br), 2.5 – 1.4 (m, 10 H, 5 × CH_2).

2.4.3. 5, 6-Epoxy-1-cyclooctene

A solution of *m*-chloroperbenzoic acid (38 g of 57-86% purity) in chloroform (450 mL) was added slowly, over a 5 h period, to stirring 1,5-cyclooctadiene (29 mL, 0.24 mol). The mixture was stirred at RT for 7 h and then filtered to remove solid salts. The filtrate was washed with aqueous $Na_2S_2O_4$ (5%, 200 mL) followed by $NaHCO_3$ (5%, 200 mL) and saturated $NaCl_{aq}$ (350 mL). The chloroform was removed under vacuum and the remaining crude product purified by vacuum distillation (55 °C, 0.9 mm Hg) to yield 12.9 g of clear, colourless oil (43%

yield). Spectroscopic data agree with those reported.[4] ^{1}H NMR (δ, $CDCl_3$): 5.56 (br m, 2 H, olefinic), 3.05 (br m, 2 H, 2 × C*H*O), 2..48 – 2.41 (m, 8 H, 4 × CH_2).

2.4.4. 5-Hydroxy-1-Cyclooctene

A slurry of LAH (1.8 g, 47 mmol) in THF (40 mL) was slowly added to a stirring solution of 5,6-epoxy-1-cyclooctene (*vide supra*) (10.8 g, 87 mmol) in THF (80 mL). The suspension was stirred at RT for 12 h, then cooled to 0 °C and quenched by dropwise addition of water. The mixture was allowed to warm to RT while stirring over 3 h. The salts were filtered off and washed with Et_2O (3 × 20 mL). The combined organic solvents were removed under vacuum and the remaining oily residue redissolved in Et_2O (100 mL), washed with H_2O (3 × 20 mL), and dried over $MgSO_4$. Solvent removal left a clear, colourless oil (9.0 g, 82%). Spectroscopic data agree with those reported.[4] ^{1}H NMR (δ, $CDCl_3$): 5.63 (m, 2 H, olefinic), 3.78 (m, 1 H, C*H*OH), 1.4 – 2.4 (m, 10 H, 5 × CH_2).

2.4.5. 5-Methoxy-1-cyclooctene (10)

A solution of 1.4 g of 5-hydroxy-1-cyclooctene (*vide supra*) (11.3 mmol) in dry THF (5 mL) was added to a suspension of 0.42 g of NaH (17.0 mmol) in dry THF (40 mL) at -10 °C over 10 min. A solution of 3.2 g methyl iodide (22.6 mmol) in dry THF (5 mL) was added over 10 min to the cooled (-20 °C) suspension. The reaction was allowed to warm to RT overnight, then

quenched with water and extracted with Et_2O. The organic layer was dried ($MgSO_4$), stripped and distilled under vacuum to yield 1.4 g (88%) of a clear, colorless oil. Spectroscopic data agree with those reported.[5] ^1H NMR (δ, $CDCl_3$): 5.62 (m, 2 H, olefinic), 3.29 (s, 3 H, OCH_3), 3.24 (m, 1 H, *CH*OMe), 2.4 – 1.5 (10 H, 5 × CH_2).

2.4.6. 5-Acetoxy-1-Cyclooctene (11)

Acetyl chloride (1.2 mL, 17 mmol) was slowly added, over a 5 min period, to a cold (0 °C) solution of 5-hydroxy-1-cyclooctene (1.0 g, 7.9 mmol) in pyridine (10 mL). The solution was allowed to warm to RT and stirred for an additional 1 h. The mixture was diluted with Et_2O (50 mL) and washed with saturated $NaHCO_{3(aq)}$ (2 × 20 mL) followed by water (2 × 20 mL). The organic phase was dried over $MgSO_4$ and concentrated to give 1.3 g (99%) of a spectroscopically clean pale-yellow oil, which was used without purification.[4] ^1H NMR (δ, $CDCl_3$): 5.63 (m, 2 H, olefinic), 4.79 (m, 1 H, *CH*O), 2.41 – 1.45 (m, 13 H, 5 × CH_2; s at 2.14 for CH_3).

2.5. Phosphines

2.5.1. 1,4-bis(dicyclohexylphosphino)butane (dcypb)

Cold (-35 °C) solution of $HPCy_2$ (2.0 mL, 11.4 mmol) in THF (20 mL) was stirred as a -35°C solution of n-BuLi (4.5 mL, 2.5 M in hexane) was added dropwise via syringe. The resulting yellow suspension was stirred while warming to RT over 1 h, at which point 1,4-

dibromobutane (681 μL, 5.7 mmol) was added dropwise via syringe. The resulting clear colourless solution was stirred for 1 h, then reduced to dryness. The white residue was suspended in methanol (10 mL) and stirred for 15 minutes to extract LiBr. The solids were then filtered off, washed with methanol (3 × 10 mL) and dried under vacuum. Yield 2.3 g (90 %). $^{31}P\{^1H\}$ NMR (δ, C_6D_6): -5.7. ^1H NMR (δ, C_6D_6): 2.22 – 0.95 (br, Cy, 4 × CH_2).

2.6. Aryloxide Salts.

2.6.1. $TlOC_6F_5$

The following preparation was adopted from a published procedure.[6] Thallium (I) ethoxide (320 μL, 5.5 mmol) was added to a stirring solution of pentafluorophenol (1.0 g, 5.5 mmol) in Et_2O (10 mL). A white precipitate gradually formed as the mixture was stirred at RT overnight (16 h). The suspension was cooled (-35 °C) and the white solid filtered off and washed with Et_2O (5 × 3 mL) followed by hexanes (2 × 2 mL), dried under vacuum, and used without further purification. Yield: 1.7 g (80%). $^{19}F\{^1H\}$ NMR (C_6D_6, δ): -84.41 (m, 2 F), -90.16 (t, 2 F, $^3J_{FF}$ = 45.2 Hz), -101.83 (m, 1F).

2.6.2. $KOCH_2Ph_2$

A solution of diphenylmethanol (300 mg, 1.63 mmol) in THF (10 mL) was stirred as a suspension of KH (65 mg, 1.63 mmol) in THF (5 mL) was slowly added, causing vigorous H_2

evolution. The solution was stirred at RT overnight (15 h) and the solvent removed under vacuum. The resulting yellow oil was suspended in hexanes (10 mL) and cooled to –35 °C to yield a white powder, which was filtered, washed with hexanes (3 × 2 mL), dried under vacuum, and used without further purification. Yield: 280 mg (77%). ^{1}H NMR (C_6D_6, δ): 7.40 - 7.11 (m, 10 H, Ph), 5.67 (s, 1 H, Ph_2CHOK).

2.7. Protic Acids

2.7.1. $[H(OEt_2)_2]^+$ $[(3,5\text{-}(CF_3)_2C_6H_3)_4B]^-$ ($HBAr^F_4$)

A solution of $NaBAr^f_4$ (1.5 g, 1.6 mmol) in Et_2O (30 mL) was allowed to stand over molecular sieves (4 Å) for 15 h then transferred to a Schlenk tube and cooled to 0 °C. The cold solution was stirred as HCl (1.6 mL of 2.0 M solution in Et_2O) was added via syringe. Stirring was continued at 0 °C for 15 min then the suspension was allowed to stand for 1 h to let the NaCl(s) settle. The supernatant was decanted and the solid washed with Et_2O (2 × 20 mL). The Et_2O washings were combined and the volume reduced to 5 mL, cooled to –75 °C, and hexanes (40 mL) added.The mixture was kept cold (-75 °C) for 1 h, then the supernatant was decanted off and the residue dried under vacuum. Yield: 1.5 g (96%). The product was stored under N_2 at –35 °C. Spectroscopic data agree with those reported.[7] ^{1}H NMR (δ, C_6D_6): 8.31 (br m, 8 H, 8 × *o*-H), 7.89 (br m, 4 H, 4 × *p*-H), 3.32 (br, 8 H, 4 × CH_2, $[H(OEt_2)_2]^+$), 1.24 (br, 12 H, CH_3, $[H(OEt_2)_2]^+$).

2.8. Pyrrole Ligand Precursors

2.8.1. 2-[(2, 6-Diisopropylphenyl)imino]pyrrole (HNN′)

A solution of 2,6-diisopropylaniline (5 mL, 26 mmol) and pyrrole-2-carboxaldehyde (2.5 g, 26 mmol) in MeOH (5 mL) was refluxed for 39 h, at which time conversion to the iminopyrrole product was determined to be only 46% (^{1}H NMR). Benzene (10 mL) was added to the solution and a distillation apparatus was attached. Heating (125 °C) was resumed with simultaneous distillation of volatile fractions; after heating thus for 40 h, conversion plateaued at 86%. The solution was cooled to RT, causing solidification of the mixture, and the product was precipitated as a pale pink powder on addition of MeOH (20 mL). It was filtered off, washed with MeOH (10 × 5 mL) and dried under vacuum. A second crop was isolated by reducing the filtrate volume to ~2 mL, cooling on ice, and filtering off the resulting pale pink powder, which was likewise washed with cold MeOH (3 × 5 mL) and dried under vacuum. The two crops were combined to yield 5.1 g (77%) of spectroscopically clean product which was used without further purification. NMR data agree with values reported.[8] ^{1}H NMR (δ, C_6D_6): 7.84 (br, 1 H, N=C*H*), 7.18 (br, 3 H, Ar), 6.45 (br m, 1 H, pyrrole), 6.05 (br m, 2 H, pyrrole), 3.24 (sept, 2 H, 2 × C(*H*)Me_2, $^3J_{CH}$ = 6.8 Hz), 1.12 (d, 12 H, 4 × CH_3, $^3J_{CH}$ = 6.8 Hz).

2.8.2. Lithium {2-[(2, 6-diisopropylphenyl)imino]pyrrolide}•Et_2O (LiNN′•Et_2O)

Based on a literature method,[9] a solution of 2-[(2, 6-diisopropylphenyl)imino]pyrrole (1.6 g, 6.3 mmol) in Et_2O (30 mL) was stirred vigorously at –80 °C as *n*-BuLi (2.5 mL of 2.5 M solution, 6.3 mmol) was added via cannula. The solution was stirred at –80 °C for 2 h, and the resulting white solid was filtered off, washed with Et_2O (8 × 10 mL), and dried under vacuum for 4 h. Yield: 1.55 g. Spectroscopic data agree with those reported,[9] but show, also, significant residual diethyl ether (reproducibly 1 mol equiv, based on ^{1}H NMR analysis), suggesting a solvated molecule of Et_2O, and implying a 73% yield of LiNN′•Et_2O. The product was stored at –35 °C under nitrogen. ^{1}H NMR (δ, C_6D_6): 8.02 (br, 1 H, N=C*H*), 7.40 - 7.15 (br m, 4 H, Ar + pyr), 6.89 (br m, 1 H, pyr), 6.42 (br m, 1 H, pyr), 3.42 (sept, 2 H, 2 × C(*H*)Me_2, $^3J_{CH}$ = 6.4 Hz), 2.95 (q, 4 H, 2 × CH_2, $^3J_{HH}$ = 9 Hz, Et_2O), 0.73 (t, 6 H, 2 × CH_3, $^3J_{HH}$ = 9 Hz, Et_2O).

2.9. Ruthenium Precursors

The following preparations were based on literature methods. These complexes were prepared for use as starting materials for the synthesis of derivatives of varied ligand frameworks and/or as *in situ* precursors in catalytic experiments.

2.9.1. $RuCl_2(PPh_3)_3$

A solution of $RuCl_3 \cdot xH_2O$ (2.0 g, 9.6 mmol) in MeOH (300 mL) was refluxed under N_2 for 1 hour, then allowed to cool. Solid PPh_3 (12.9 g,49.2 mmol) was added under a strong flow of N_2, and the mixture refluxed for an additional 3 hours. The resulting brown precipitate was filtered off, washed with MeOH (3 × 15 mL), then with hexanes (20 × 15 mL, or until the washings showed no trace of residual phosphine by TLC), and dried under vacuum. Yield 7.5 g (95%). ^1H and $^{31}P\{^1H\}$ NMR data are consistent with those reported.[10-12] $^{31}P\{^1H\}$ NMR (C_6D_6, δ): 61.08, 53.37 (br ABq, $[RuCl_2(PPh_3)_2]_2$, 14% of total integration), 42.85 (br s, $RuCl_2(PPh_3)_3$, 80%), -5.06 (s, PPh_3, 6%). ^1H NMR (C_6D_6, δ): 7.72 – 6.70 (m, Ph).

2.9.2. $Ru_2Cl_4(dcypb)_2(N_2)$ (16)

A green solution of $RuCl_2(PPh_3)_3$ (0.500 g, 0.521 mmol) and dcypb (0.235 g, 0.521 mmol) in toluene (10 mL) was stirred under N_2. Within 30 minutes the solution had become orange in colour and an orange precipitate had formed. After 24 h hexanes (10 mL) was added and the suspension cooled to –35 °C, precipitating more of the orange solid. The product was filtered off, washed with Et_2O (5 × 3 mL) followed by hexanes (5 × 5 mL) and dried under a flow of N_2 for 20 h. (Exposure to vacuum causes decomposition).[13] Yield 0.300 g (91%). Spectroscopic data have been previously reported.[13] ^1H NMR ($CDCl_3$): δ 0.7-3.1 (br, C*H*, C*H*$_2$). $^{31}P\{^1H\}$ NMR ($CDCl_3$): δ 57.5 (d, $^2J_{PP}$ = 39 Hz), 45.0 (d, $^2J_{PP}$ = 27 Hz), 44.6 (d, $^2J_{PP}$ = 39

Hz), 42.3 (d, $^2J_{PP}$ = 27 Hz); (C_6D_6): δ 60.1 (d, $^2J_{PP}$ = 39 Hz), 49.1 (d, $^2J_{PP}$ = 26 Hz), 45.3 (d, $^2J_{PP}$ = 39 Hz), 37.4 (d, $^2J_{PP}$ = 26 Hz).

2.9.3. $RuHCl(CO)(PCy_3)_2$ (13)

A suspension of $[RuCl_2(COD)]_x$ (0.250 g, 0.446 mmol) and PCy_3 (0.500 g, 1.8 mmol) in EtOH (10 mL) was sealed under N_2 (1 atm) in a Kontes flask and stirred at 70 °C for 3 days. The reaction mixture was cooled to RT and the crude product, an orange powder, was filtered off, washed with EtOH (5 × 3 mL) then Et_2O and dried under vacuum. This crude product was suspended in CH_2Cl_2 (15 mL) and filtered through Celite to remove a dark, insoluble impurity. The solvent was reduced to ~0.2 mL, then Et_2O (20 mL) was added and the suspension stirred at RT for 2 days in order to extract a soluble impurity (δ_P = 24.4 ppm (s)). The remaining bright yellow precipitate was filtered, washed with Et_2O (10 × 5 mL) and dried under vacuum to yield 120 mg (37%)* of spectroscopically clean $RuHCl(CO)(PCy_3)_2$. Characterization data agree with those reported.[14] $^{31}P\{^1H\}$ NMR (C_6D_6, δ): 46.87 (s). ^1H NMR (C_6D_6, δ): 2.72 – 1.15 (m, 66 H, Cy), -24.21 (t, 1 H, Ru*H*, $^2J_{HP}$ = 18.0 Hz). X-ray quality crystals were obtained by slow diffusion of acetone into a THF solution.

---

* A recent report describes a similar preparation, but at higher reaction temperatures, (90-95 °C vs 70 °C in this thesis). Higher yields of pure product (85%) are reported without the need for extensive purification steps.[14]

2.9.4. $RuCl_2(CO)(PCy_3)_2$ (14)

The literature route gives the complex in less than 35% yield.[15] In an alternative route, $RuHCl(CO)(PCy_3)_2$ (150 mg, 0.21 mmol) was treated with 3 mL $CHCl_3$. After 40 h at RT, the solution was concentrated to 0.5 mL and layered with acetone. The dark red, crystalline product was filtered off, washed with acetone (3 × 5 mL) and hexanes (3 × 5 mL), then dried under vacuum. Yield: 112 mg (70%). $^{31}P\{^1H\}$ NMR (C_6D_6, δ): 35.2 (s). ^1H NMR (C_6D_6, δ): 2.73 - 1.02 (m, Cy). IR (Nujol; cm^{-1}): ν(CO) 1934.

2.9.5. $RuCl_2(CO)(DMF)(PPh_3)_2$ (26)[16]

A brown suspension of $RuCl_2(PPh_3)_3$ (0.400 g, 0.417 mmol) in DMF (4 mL) was stirred under 1 atm CO at RT for 15 min while a yellow solid gradually precipitated. Et_2O (5 mL) was added to the stirring mixture and the product was filtered off, washed with Et_2O (5 × 4 mL) and dried under vacuum. Yield: 0.250 g (75%). $^{31}P\{^1H\}$ NMR ($CDCl_3$, δ): 34.51 (s). ^1H NMR ($CDCl_3$, δ): 8.12 (s, 1 H, $HCON(CH_3)_2$), 7.61-7.11 (m, 30 H, Ph), 2.76 (s, 3 H, $HCON(CH_3)_2$), 2.64 (s, 3 H, $HCON(CH_3)_2$). IR (Nujol; cm^{-1}): ν(CO) 1914; ν(CO, DMF) 1633.

2.9.6. $RuHCl(H_2)(PCy_3)_2$ (4)

This material was prepared by a variation on a literature method.[17] In a drybox, NEt_3 (199 μL, 1.43 mmol) was added to a stirred suspension of $[RuCl_2(COD)]_x$ (0.40 g, 1.43 mmol)

and PCy_3 (0.85 g, 3.0 mmol) in 2-propanol (20 mL). The mixture was sealed inside a glass-lined autoclave and removed from the drybox. The vessel was purged with $H_{2(g)}$ and pressurized to 200 psi. The reaction mixture was then stirred at 80 °C for 40 h. The vessel was allowed to cool to RT, depressurized, and reintroduced into the drybox where it was opened. The orange product was filtered off and washed with EtOH (3 × 3 mL) followed by hexanes (5 × 4 mL). A dark insoluble impurity was removed by stirring the product (under H_2) in 15 mL CH_2Cl_2 for 10 min and then filtering through Celite. The solvent was reduced to 0.2 mL under vacuum and the product precipitated by addition of cold hexanes (5 mL), under 1 atm H_2. The bright orange solid was filtered off and washed with hexanes (3 × 3 mL) and dried under vacuum. It was purified by reprecipitation from toluene/pentane under hydrogen. Yield: 0.511 g (73%). Spectroscopic data agree with those reported.[18] $^{31}P\{^1H\}$ NMR (C_6D_6, δ, Ar): 54.20 (s). ^1H NMR (C_6D_6, δ, Ar): 2.3 – 0.9 (m, 66 H, Cy), -16.3 (br, 3 H, Ru*H*(H_2); (δ, under H_2) : -14.0 (br s, Ru*H*(H_2)$_2$), 0.9-2.3 (m, Cy). Under $N_{2(g)}$, small amounts of $RuHCl(N_2)(PCy_3)_2$ are also observed (5 – 15%), based on the following spectroscopic data, which agree with a literature report.[19] $^{31}P\{^1H\}$ NMR (C_6D_6, δ, N_2): 43.7 (s). ^1H NMR (C_6D_6, δ, Ar): 2.59 –1.22 (m, 66 H, Cy), -27.26 (t, 1 H, Ru*H*, $^2J_{PH}$ = 18.3 Hz).

2.10. Hydrogenolysis of $RuCl_2(CHPh)(PCy_3)_2$ (1a)

2.10.1. Formation of $Ru(H)_2Cl_2(PCy_3)_2$ (2)

(a) A solution of **1a** (5 mg, 6.1 μmol) in CD_2Cl_2 (0.7 mL) showed clean, quantitative conversion to known Ru(IV) complex $Ru(H)_2Cl_2(PCy_3)_2$ (**2**)[20] and 1 equiv toluene after 24 h under H_2 (1 atm). $^{31}P\{^1H\}$ NMR (δ, CD_2Cl_2): 91.3 (s). ^1H NMR (δ, CD_2Cl_2): -12.4 (t, ^3J(H,P) = 31.6 Hz, 2 H, Ru*H*), 0.9-2.3 (m, 66 H, Cy), 2.4 (s, 3 H, toluene C*H*$_3$), 7.2 (m, 5 H, Ph).

2.10.2. Formation of $RuHCl(H_2)(PCy_3)_2$ (4)

A solution of **1a** (60 mg, 73 μmol) and P.S. (47 mg, 220 μmol) in CH_2Cl_2 (20 mL) was stirred under 1000 psi H_2 for 14 h. Removal of solvent under vacuum gave an orange solid, which was extracted with cold hexanes, filtered and washed with cold methanol and hexanes. Yield: 42 mg (82%). $^{31}P\{^1H\}$ NMR (δ, C_6D_6): 54.2 (s). ^1H NMR (δ, C_6D_6, Ar): -16.3 (br s, Ru*H*(H_2)), 0.9-2.3 (m, Cy). Under H_2: -14.0 (br s, Ru*H*(H_2)$_2$), 0.9-2.3 (m, Cy). A broad singlet for dihydrogen adduct **7** (δ_H -7.9)[18] is observed only on cooling to 193K (CD_2Cl_2).

2.10.3. Formation of $RuCl_2(H_2)(PCy_3)_2$ (3)

A suspension of **1a** (100 mg, 122 μmol) in hexanes (10 mL) was stirred under 1000 psi H_2 at 50°C for 40 h. The resulting pale yellow solid was filtered off and dried under vacuum. Yield 60 mg (67%). Solid state $^{31}P\{^1H\}$ NMR (δ): 47.5 ppm. $^{31}P\{^1H\}$ NMR (δ, C_6D_6, Ar): 91.3

(s, **2**), 54.2 (s, **4**). A third singlet appeared under H_2: 40.3 (s, **5**). In solution, signals due to trace impurities emerge in the $^{31}P\{^1H\}$ NMR spectrum. ^1H NMR (δ, C_6D_6, Ar): -16.2 (br s, Ru(H_2), **3**), -12.0 (t, $^3J_{HP}$ = 31.5 Hz, Ru(H)$_2$, **2**), 0.9-2.3 (m, Cy). Under H_2: -13.0 (br s, Ru(H_2), **3**), -12.0 (t, $^3J_{HP}$ = 31.5 Hz, Ru(H)$_2$, **2**), -9.8 (br s, Ru(H_2), **5**), 0.9-2.3 (m, Cy). No signal for **4**/**7** (δ_H -14.0) was observed. Hydride T_1 min for **3** (C_7D_8, H_2, 500 MHz, 268 K) 18.8 ms. Anal. Calcd. for $C_{36}H_{68}Cl_2P_2Ru$: C, 58.84; H, 9.33. Found: C, 58.91; H, 9.23.

2.10.4. Formation of $RuCl_2(H_2)(PCy_3)_2[O=C(NMe_2)Me]$ (6)

(a) A suspension of **1a** (100 mg, 122 μmol) in Et_2O-DMA (10:1, total volume 20 mL) was stirred under 1000 psi H_2 for 20 h. The resulting pale yellow solid was filtered off, washed with Et_2O and hexanes and dried. Yield: 70 mg (71%). Solid state $^{31}P\{^1H\}$ NMR (δ): 32.2 (s); a small peak at 47.5 ppm is assigned to **3**. $^{31}P\{^1H\}$ NMR (δ, C_6D_6, Ar): 91.3 (s, **2**), 54.2 (s, **3**). A third singlet appeared under H_2: 40.3 (s, **5**). In solution, trace impurities can be seen by $^{31}P\{^1H\}$ NMR analysis. ^1H NMR (δ, C_6D_6, Ar): -16.2 (br s, Ru(H_2), **3**), -12.0 (t, $^3J_{H,P}$ = 31.5 Hz, Ru(H)$_2$, 2), 0.9-2.6 (m, Cy, DMA). Integration vs. MeOH as internal standard: hydride (**2** + **3**) : aliphatics (Cy + DMA) = 2 : 75. Hydride T_1 min (C_7D_8, H_2, 500 MHz, 268K) 18.5 ms. IR (Nujol): ν(CO) 1630 cm^{-1}. Anal. Calcd. for $C_{40}H_{77}Cl_2NOP_2Ru$: C, 58.45; H, 9.44; N, 1.70. Found: C, 58.95; H, 9.67; N, 1.66.

(b) A solution of **1a** (50 mg, 61 μmol) and P.S. (13 mg, 61 μmol) in benzene-DMA (3:1, 20

mL total) was stirred under 1 atm H_2 for 16 h. Removal of benzene under vacuum gave a yellow suspension, which was filtered off, washed with methanol and cold hexanes, and dried. Yield: 20 mg (44%). Some P.S./DMA remained after this treatment. X-ray quality crystals of **6** slowly deposited from a C_6D_6 solution.

2.10.5. Formation of $Ru(H)(D)Cl_2(PCy_3)_2$ and $RuCl_2(HD)(PCy_3)_2$ (2_{HD}, 3_{HD})

A sample of **6** (10 mg, 12 μmol) in 1 mL C_6D_6 was freeze-thaw-degassed twice, then thawed under D_2. $^{31}P\{^1H\}$ NMR (δ, C_6D_6): 90.8, 90.6 (s, two isomers of 2_{HD}),[20] 54.2 (s, 3_{HD}), 40.1 (s, 5_{HD}). ^1H NMR (δ, C_6D_6): -11.86 (t, $^3J_{HP}$ = 31.5; 2_{HD}), -11.91 (t, $^3J_{HP}$ = 31.5; 2_{HD}), -13.1 (br t, $^1J_{HD}$ = 22.5; 3_{HD}).

2.10.6. Hydrogenolysis of $RuCl_2(CHPh)(PCy_3)_2$ (1a) in THF

A solution of **1a** (10 mg, 0.012 mmol) in THF-d_8 (1 mL) was degassed by three freeze-pump-thaw cycles and stirred under H_2 (1 atm) at RT for 40 h. NMR analyses (^{31}P, ^1H NMR, VT T_1 ^1H NMR) show a mixture of $RuHCl(H_2)(PCy_3)_2$ (**4**, 58%), $RuCl_2(H_2)(PCy_3)_2$ (**3**, 27%) and the bis-dihydrogen adduct of **3**, $RuCl_2(H_2)_2(PCy_3)_2$ (**5**, 15%). Spectroscopic data are provided above.

2.10.7. Hydrogenolysis of 1a in Presence of MeOH and Base.

A solution of **1a** (25 mg, 0.030 mmol) in a mixture of CH_2Cl_2/MeOH (2mL/0.5 mL) was treated with NEt_3 (21 μL, 0.152 mmol), purged with H_2, pressurized in an autoclave to 200 psi, and stirred at 60 °C for 24 h. The mixture was stripped to dryness and redissolved in C_6D_6 for NMR analysis. Majority products include $RuH_2Cl_2(PCy_3)_2$ (**2**, 11%),[20] $RuHCl(H_2)(PCy_3)_2$ (**4**, 27%),[18] and the hydridochloro carbonyl complex $RuHCl(CO)(PCy_3)_2$ (**13**, 22%),[21] relative yields based on ^{31}P NMR integrations. Spectroscopic data agree with reported values (provided above).

2.10.8. Regeneration of a Carbene Complex

(a) To a stirring solution of $RuHCl(H_2)(PCy_3)_2$ (**4**) (15 mg, 0.021 mmol) and NEt_3 (14.6 μL, 0.105 mmol) in CH_2Cl_2 (10 mL) was added 3-chloro-3-methyl-1-butyne (4.5 μL, 0.040 mmol), producing a deep red colour. ^{31}P NMR revealed exclusive formation of $RuCl_2(PCy_3)_2(CHCH{=}CMe)_2$ (**1b**, 100%, δ_P 36.4, s).[17]

(b) A solution of **1a** (43.6 mg, 0.053 mmol) in THF (10 mL) was stirred under 1000 psi H_2 for 48 h. To the resulting orange solution was added 3-chloro-3-methyl-1-butyne (18 μL, 0.159 mmol). Concentration and precipitation with hexanes gave **1b** as a deep red product (38 mg, 92%). NMR values correspond with those reported.[17]

(c) To a solution of **6** (20 mg, 0.024 mmol) and NEt_3 (8.6 μL, 0.12 mmol) in 2 mL CH_2Cl_2 was added 3-chloro-3-methyl-1-butyne (3.3 μL, 0.029 mmol), causing a color change from

orange to deep red. Yield of **1b**: 100% (NMR).

2.11. Catalytic Hydrogenation of Small-Molecule Olefins

2.11.1. General Procedure for Catalytic Hydrogenation of Allylbenzene.

In a drybox, 60 μL of a predissolved 11.49 mM solution of catalyst (0.69 μmol) in C_6D_6 was diluted with 1.0 mL C_6D_6. Excess allylbenzene (94 μL, 0.71 mmol) was added and the solution was placed inside a glass-lined autoclave, which was removed from the drybox, purged with H_2 and pressurized to 1000 psi with H_2. The solution was stirred at RT for 0.5 h. Relative product yields were determined by ^{1}H NMR, based on comparison with authentic samples of allylbenzene, *n*-propylbenzene, and 1-phenylpropene (chemical shifts reported below). An average of three trials is reported (± 3%). ^{1}H NMR (allylbenzene, C_6D_6, δ): 7.15 (br m, 5 H, Ar), 5.72 (br m, 1 H, C*H*=CH_2), 4.95 (m, 2 H, CH=CH_2), 3.18 (m, 2 H, CH_2); (*n*-propylbenzene, C_6D_6, δ): 7.08 (br m, 5 H, Ar), 2.35 (t, 2 H, $^2J_{HH}$ = 9 Hz, CH_2), 1.46 (m, 2 H, CH_2), 0.75 (t, 3 H, $^2J_{HH}$ = 9 Hz, CH_3); (mixture of *cis*- and *trans*-β-methylstyrene, C_6D_6, δ): 7.17 (br m, 5 H, Ar), 6.50 – 6.09 (br m, 2 H, C*H*=C*H*), 1.48 (m, 3 H, CH_3).

2.12. Tandem ROMP-Hydrogenation Catalysis

2.12.1. General Procedure for Tandem ROMP-Hydrogenation (Small Scale)

A representative procedure is given for cyclooctene monomer. A solution of **1a** (2 mg, 2.4 μmol) in CH_2Cl_2 (2 mL) was stirred rapidly as cyclooctene (64 μL, 490 μmol, [M]/[C] = 204) was added. Stirring was continued for 1.5 h, until ROMP was complete (0.5 h for norbornene monomer **12**), after which the solution was diluted (with CH_2Cl_2 or THF, then with MeOH) to 10 mL; base was added at this stage (where applicable). The solution was then purged with H_2 in a glass-lined autoclave, pressurized, and stirred at the stated temperature and pressure. After the stated reaction time, the solvent was removed under vacuum, and conversions determined by ^1H NMR ($CDCl_3$), based on the integration for the olefinic peak at δ_H 5.31, relative to the aliphatic peaks at δ_H 2.03 (br) and 1.33 (br). The average of 3 trials (± 3%) is reported. Spectroscopic data for all polymers are given in Appendix A.

2.12.2. ROMP-Hydrogenolysis-ROMP

A solution of **1a** (4 mg, 4.9 μmol) in 4 mL CH_2Cl_2 was stirred rapidly as monomer **12** (271 mg, 2.0 mmol) in CH_2Cl_2 (1 mL) was added. After 30 min, the reaction was treated with NEt_3 (3.5 μL, 25 μmol), and stirred under H_2 for 15 h, during which time the colour changed from pink to bright yellow. Addition of 3-chloro-3-methyl-1-butyne (1 μL, 7.2 μmol) restored the pink colour, following which a second portion of monomer **12** (68 mg, 0.49 mmol) in CH_2Cl_2 (1 mL) was added. The solution was stirred for 30 min, then quenched with ethyl vinyl ether. The polymer blend was isolated as a white powder by addition of the concentrated solution to

stirring MeOH. Yield: 278 mg (82%). ^{1}H NMR shows all characteristic peaks for poly-**12** (Appendix A). GPC: bimodal; M_n = 54 300 (PDI = 1.11); M_n = 19 000 (PDI = 1.11). Calcd M_n = 54 400 and 13 800.

2.12.3. ROMP-Hydrogenation-ROMP

A solution of **1a** (2 mg, 0.0024 mmol) in 3 mL CH_2Cl_2 was stirred as monomer **12** (35 μL, 0.18 mmol) was added. After 30 min, the solution was treated with NEt_3 (1.7 μL, 0.012 mmol), purged with H_2, pressurized to 250 psi H_2, and stirred at 50 °C for 24 h, after which an aliquot showed full reduction of poly-**12** (^{1}H NMR). The autoclave was depressurized and 3-chloro-3-methyl-1-butyne (2 μL, 0.018 mmol) added, followed by the second portion of monomer **12** (107 μL, 0.55 mmol). Complete polymerization was confirmed by ^{1}H NMR analysis after 2 h. Ethyl vinyl ether was then added, and the reaction stirred at RT for 1 h. GPC analysis of the solution exhibited a bimodal trace: M_n = 74 860 (PDI = 1.22); M_n = 12 190 (PDI = 1.10). The solvent was removed under vacuum to yield 125 mg (94%) of polymer. The presence of saturated and unsaturated poly-**12** was confirmed by ^{1}H NMR analysis (Appendix A).

2.12.4. Isolation of Saturated, Functionalized Polyethylenes

A general polymerization-hydrogenation procedure is described for the 5-bromo-1-cyclooctene monomer (**9**). A solution of **1a** (16 mg, 19.4 μmol) in CH_2Cl_2 (2 mL) was stirred

rapidly as monomer (732 mg, 3.88 mmol) in CH_2Cl_2 (1 mL) was added. The solution was stirred at RT for 4 h (time required for complete ROMP depends on the monomer: Table 3.3), then loaded into a glass-lined autoclave. The solution was diluted with additional solvent (8 mL) and NEt_3 (14.4 μL, 96 μmol) was added. The autoclave was removed from the drybox, purged with H_2, and pressurized to 1000 psi with H_2. The reaction was stirred at RT for 24 h. The solvent was removed under vacuum and complete reduction was confirmed by ^1H NMR analysis ($CDCl_3$).The polymer was precipitated by slow addition of a concentrated (0.5 mL) CH_2Cl_2 solution to rapidly-stirred MeOH, and dried under vacuum. Isolated yields average ~72%. Characterization data are listed in Appendix A.

2.13. Functionalized Poly(octenes)

Polymerizations were carried out as described above, a protocol analogous to a previous report.[4] Following ROMP, polymerization was terminated by addition of 2 drops ethyl vinyl ether and stirring was continued for 30 min. The polymer was isolated by dropwise addition of the concentrated CH_2Cl_2 solution (~0.2 mL) to rapidly-stirred MeOH. Isolated yields average ~70%. Characterization data are listed in Appendix A.

2.14. Vinylidene Complexes

2.14.1. Preparation of $Ru(OC_6F_5)_2(dcypb)[C{=}CH(Bu^t)]$ (18)

(a) A suspension of $Ru_2Cl_4(dcypb)_2(N_2)$ (**16**) (344 mg, 0.270 mmol) in chlorobenzene (10 mL) was stirred as a suspension of $TlOC_6F_5$ (418 mg, 1.08 mmol) in chlorobenzene (5 mL) was added. The suspension was stirred at RT for 18 h, over which time it changed colour from orange to brown. 3,3-Dimethyl-1-butyne (688 μL, 5.59 mmol) was added and atirring continued for 1 h at RT. The suspension was filtered through benzene-saturated Celite to remove the insoluble TlCl and the solvent volume was reduced to 1 mL under vacuum. The product was precipitated as an olive-green powder by addition of hexanes (15 mL). It was filtered, washed with MeOH (3 × 1 mL), Et_2O (2 × 2 mL), then hexanes (2 × 3 mL), and dried under vacuum prior to reprecipitation from CH_2Cl_2/hexanes. Yield: 410 mg (78%). X-ray quality crystals were obtained by slow evaporation of a CH_2Cl_2/C_6H_6 solution. $^{31}P\{^1H\}$ NMR (CD_2Cl_2, δ): 50.0 (s). ^1H NMR (CD_2Cl_2, δ): 3.57 (t, 1 H, Ru=C=C*H*, $^4J_{HP}$ = 3.3 Hz), 2.55 - 1.31(m, 64 H, Cy of dcypb, 4 × CH_2, $C(CH_3)_3$), 1.33 (s, $C(CH_3)_3$ within Cy envelope). $^{13}C\{^1H\}$ NMR (CD_2Cl_2, δ): 334.9 (t, Ru*C*, $^2J_{CP}$ = 21.4 Hz), 142.8 (br s,*ipso-C* of OC_6F_5), 141.3 (d, Ar, $^1J_{CF}$ = 237 Hz), 138.3 (d, Ar, $^1J_{CF}$ = 244 Hz), 130.9 (d, Ar, $^1J_{CF}$ = 236 Hz), 126.0 (s, RuC=*C*), 20 – 37 (aliphatic). $^{19}F\{^1H\}$ NMR (CD_2Cl_2, δ): -88.10 (m, 2 F), -95.30 (m, 2 F), -106.30 (m, 1 F). IR (nujol; cm^{-1}): υ(C=C) 1637. Anal. Calcd. for $C_{46}H_{62}F_{10}O_2P_2Ru$: C, 55.25; H, 6.25%. Found: C, 55.15; H, 6.50%.

(b) Reverse order of reagent addition (NMR scale). A suspension of **16** (15 mg, 0.012 mmol) in chlorobenzene (0.6 mL) was stirred as 3,3-dimethyl-1-butyne (30 μL, 0.24 mmol) was added. The orange suspension was stirred at RT for 20 h, at which time ^{31}P NMR analysis confirmed complete conversion to the known[22] complex RuCl(dcypb)(μ-Cl)$_3$Ru(dcypb)(C=CHBu^t) (**17a**). A solution of $TlOC_6F_5$ (18.6 mg, 0.048 mmol) in chlorobenzene was added, and the resulting mixture was stirred at RT. The progress of the reaction was monitored, *in situ*, on a daily basis by ^{31}P NMR spectroscopy. After 22 h, the following species were observed: [{Ru(C=CHBu^t)(dcypb)}$_2$(μ-Cl)$_3$]OC_6F_5 (**19•OC$_6$F$_5$**, 58%, δ_P 44.4, 43.2, ABq, $^2J_{PP}$ = 26 Hz), Ru(OC_6F_5)$_2$[C=CH(Bu^t)](dcypb) (**18**, 31%; δ_P 50.0, s), and Tl[{Ru(C≡CBu^t)(dcypb)}$_2$(μ-Cl)$_3$] (**20**, 11%, δ_P 55.96, br s, *vide infra*). A gradual decrease in **[19•OC$_6$F$_5$]** and **[20]** was noted, with a concomitant increase in **[18]**, until, after 19 d, the latter was the only species observed by ^{31}P NMR spectroscopy.

2.14.2. Preparation of [{Ru(C=CHBu^t) (dcypb)}$_2$(μ-Cl)$_3$]Cl (19•Cl)

Ethereal HCl (60 μL of a 2.0 M solution, 0.12 mmol) was added to a stirring solution of **18** (60 mg, 0.062 mmol) in CH_2Cl_2. The solution was stirred at RT for 30 min and the solvent reduced under vacuum to ca. 0.1 mL. The crude product was precipitated by addition of pentane (5 mL), the orange powder was filtered off, washed with pentane (3 × 3 mL), and dried under vacuum. The crude product was reprecipitated from CH_2Cl_2/pentane. Yield: 33 mg (75%).

Spectroscopic data are consistent with those reported below, for the PF_6 salt. The presence of residual HOC_6F_5 is indicated by an additional peak in the ^1H NMR spectrum (C_6D_6, δ): 9.62 (br, O*H*) and by peaks in the ^{19}F NMR spectrum (C_6D_6, δ): -84.62 (m, 2 F), -90.61 (t, 2 F, $^3J_{FF}$ = 41.5 Hz), -96.43 (m, 1 F). ESI-MS: calcd for $C_{68}H_{124}Cl_3P_4Ru_2$ (M^+) 1409; found *m/z* 1409.

2.14.3. [{Ru(C=CHBu^t)(dcypb)}$_2$(μ-Cl)$_3$]PF$_6$ (19•PF$_6$)

(a) From **16** via RuCl(dcypb)(μ-Cl)$_3$Ru(dcypb)(C=CHBu^t) (**17a**). 3,3-Dimethyl-1-butyne (232 μL, 1.88 mmol) was added to a stirring suspension of **16** (120 mg; 0.094 mmol) in chlorobenzene (5 mL). The bright orange suspension was stirred at RT for 18 h, at which time ^{31}P NMR confirmed complete conversion to the known neutral bimetallic complex **17a**.[22] $TlPF_6$ (33 mg, 0.094 mmol) was added and stirring continued for 3 h; complete conversion to the target product, **19•PF$_6$**, was confirmed by ^{31}P NMR analysis. The suspension was filtered through neutral alumina and the solvent reduced to 0.2 mL under vacuum. A first crop of pale yellow product was precipitated by addition of hexanes (10 mL), filtered off, washed with hexanes, and dried under vacuum. Yield: 80 mg (57%). A second crop (30 mg, 21%) was isolated by reducing the volume of filtrate to 0.1 mL and adding hexanes (5 mL). The combined crops were purified by dissolving in benzene (10 mL) and filtering through Celite. Solvent removal under vacuum left a yellow oil; the product crystallized on addition of toluene (0.5 mL). The supernatant was decanted off and the microcrystalline pale-yellow solid was washed with Et_2O (4 × 2 mL)

followed by hexanes (4 × 2 mL), and dried under vacuum. Yield: 99 mg (70%). $^{31}P\{^{1}H\}$ NMR (CD_2Cl_2, δ): 44.4, 43.2 (ABq, $^{2}J_{PP}$ = 26 Hz), -144.1 (sept, PF_6^-, $^{1}J_{PF}$ = 705 Hz). ^{1}H NMR (CD_2Cl_2, δ): 3.37 (t, 1 H, Ru=C=C*H*, $^{4}J_{HP}$ = 3.9 Hz), 2.71 - 1.17 (m, 64 H, Cy of dcypb, 4 × CH_2, $C(CH_3)_3$), 1.22 (s, $C(CH_3)_3$ within Cy envelope). $^{13}C\{^{1}H\}$ NMR (CD_2Cl_2, δ): 356.8 (t, Ru=*C*, $^{2}J_{CP}$ = 18.6 Hz), 120.8 (s, RuC=*C*), 40.5 – 20.6 (aliphatic). IR (nujol; cm^{-1}): υ(C=C) 1636. Anal. Calcd. for $C_{68}H_{124}Cl_3F_6P_5Ru_2$: C, 53.76; H, 8.23%. Found: C,53.48; H, 8.48%.

(b) From **18** via **19•Cl**. Ethereal HCl (150 μL of a 2.0 M solution; 0.30 mmol) was added to a stirring solution of **18** (150 mg, 0.15 mmol) in chlorobenzene (3 mL). The orange solution was stirred at RT for 2 h, then $TlPF_6$ (26 mg, 0.074 mmol) was added and the stirring continued for another 2 h. The suspension was filtered through benzene-saturated Celite and the volume reduced under vacuum to ca. 0.1 mL. Toluene (1 mL) and hexanes (5 mL) were added, causing precipitation of a yellow solid. The product was filtered off, and washed with Et_2O, dried under vacuum, and reprecipitated from CH_2Cl_2/hexanes. Yield: 85 mg (76%).

2.14.4. Carbonylation of [{Ru(C=CHBu^t)(dcypb)}$_2$(μ-Cl)$_3$]Cl (19•Cl, NMR Scale)

A solution of **19•Cl** (10.6 mg, 7.5 μmol) in chlorobenzene (2 mL) was refluxed under CO (1 atm) for 48 h. ^{31}P NMR showed a mixture of *ccc*-$RuCl_2$(dcypb)$(CO)_2$ (**22a**, 33%)[13] and the dinuclear salt Ru(CO)(dcypb)]$_2$(μ-Cl)$_3$}$^+${Cl}$^-$ (**21a**, 43%), identified by comparison with an

authentic sample (*vide infra*). Unidentified byproducts (several overlapping peaks at δ_P 20 ppm) were also observed in the ^{31}P NMR, accounting for 23% of the total integrated intensity.

2.14.5. Polymerization of Norbornene via Vinylidene Complexes

(a) Catalyzed by $Ru(OC_6F_5)_2[(C{=}CH(Bu^t)](dcypb)$ (**18**). A solution of norbornene (65 mg, 0.70 mmol) in CD_2Cl_2 (350 μL) was added to a rapidly stirred solution of **18** (7 mg, 7.0 μmol of Ru=C) in CD_2Cl_2 (350 μL). If required, $[H(OEt_2)_2]BAr^f_4$ (6.9 mg, 7.0 μmol) was first added to the Ru solution, and the resulting dark red mixture stirred for ca. 5 min prior to the addition of monomer. The polymerization was monitored by ^1H NMR spectroscopy.

(b) Catalyzed by $[\{Ru(C{=}CHBu^t)(dcypb)\}_2(\mu\text{-}Cl)_3]Cl$ (**19•Cl**). The precursor ionic complex was generated *in situ* by addition of HCl (7 μL of 2.0 M solution in Et_2O, 14 μmol) to a solution of **18** (7 mg, 7.0 μmol) in CH_2Cl_2 (350 uL). The resulting orange solution was stirred at RT for 30 min prior to addition of norbornene solution (65 mg, 0.70 mmol in 350 μL CH_2Cl_2). After 40 min, the solution had gelled into a thick mass. Addition of MeOH (4 mL) caused precipitation of the polymer as a wet solid which was separated from the solvent and dried under high vacuum for 24 h . Yield of insoluble polymer: 6 mg (9%).

(c) Catalyzed by $[\{Ru(C{=}CHBu^t)(dcypb)\}_2(\mu\text{-}Cl)_3]PF_6$ (**19•PF$_6$**). A solution of norbornene (65 mg, 0.70 mmol) in CH_2Cl_2 (350 μL) was added to a rapidly stirred solution of **19•PF$_6$** (5 mg, 7.0 μmol of Ru=C) in CH_2Cl_2 (350 μL). The solution was stirred at RT for 20 min, at which

point the high viscosity prevented further stirring, and addition of MeOH (4 mL) caused precipitation of the insoluble polymer. The cream-coloured solid was dried under high vacuum for 24 h. Yield of insoluble polymer: 6 mg (9%).

2.14.6. Preparation of $[\{Ru(C{=}CHBu^t)(dcypb)\}_2(\mu\text{-}Cl)_2]^{2+}\bullet 2\{BAr^F{}_4\}^-$ (23)

A solution of **19•PF$_6$** (15 mg, 10 μmol) in CH_2Cl_2 (0.7 mL) was stirred at RT as $NaBAr^F{}_4$ (19 mg, 20 μmol) was added. The reaction was monitored *in situ* by ^{31}P NMR spectroscopy. After 20 h, a new singlet was observed at δ_P 52.4 (20% of total integration) alongside the starting complex (80%). After 44 h, the proportion of product reached 30%, and after 6 d, dark brown, X-ray quality crystals had formed, with complete depletion of soluble phosphorus-containing species from the solution (^{31}P NMR). Single crystal X-ray analysis revealed the structure of edge-bridged species $[\{Ru(C{=}CHBu^t)(dcypb)\}_2(\mu\text{-}Cl)_2]^{2+}\bullet 2\{BAr^F{}_4\}^-$ (**23**). The crystals were finely ground for spectroscopic analysis. $^{31}P\{^1H\}$ NMR (CD_2Cl_2, δ): 52.4 (s, 50% of total integrated intensity), other peaks include starting material **19•PF$_6$** (44.4, 43.2, ABq), and several unidentified multiplets between 47 and 45 ppm. ^1H NMR (CD_2Cl_2, δ): 7.72 (br s, $BAr^F{}_4^-$), 7.57 (br s, $BAr^F{}_4^-$), 4.13 (t, 1 H, Ru=C=C*H*, $^4J_{HP}$ = 3 Hz, **23**), 3.37 (t, 1 H, Ru=C=C*H*, $^4J_{HP}$ = 3.9 Hz, **19•PF$_6$**), 1.17-2.85 (br, CH_2, Cy of dcypb , 4 × CH_2, C(CH_3)$_3$),), 1.27 (s, C(CH_3)$_3$ within Cy envelope). $^{19}F\{^1H\}$ NMR (CD_2Cl_2, δ): 12.56 (s, $BAr^F{}_4^-$). IR (CH_2Cl_2; cm^{-1}): ν(C=C) 1610 (**23**) and 1638 (**19•PF$_6$**).

2.15. (*tert*-Butyl)Acetylide Complexes

2.15.1. Preparation of Tl[{Ru(C≡CBu^t)(dcypb)}$_2$(μ-Cl)$_3$] (20)

(a) Via deprotonation of **19•PF$_6$** by TlOEt. TlOEt (20 μL, 0.34 mmol) was added to a stirring solution of **19•PF$_6$** (90 mg, 0.060 mmol) in toluene (3 mL). The resulting bright yellow solution was stirred at RT for 2 h and the insoluble salts were removed by filtering first through Celite then through neutral alumina. The solvent was reduced to ca. 0.1 mL under vacuum and the product precipitated as a bright yellow powder by addition of hexanes (5 mL). The solid was filtered off, washed with hexanes, and dried under vacuum. It was reprecipitated from THF / hexanes, yielding 38 mg (39%) of the bright yellow solid. $^{31}P\{^1H\}$ NMR (C_6D_6, δ): 56.0 (br s). ^1H NMR (C_6D_6 δ): 3.31 - 1.10 (m, Cy of dcypb, 4 × CH_2, $C(CH_3)_3$), 1.41 (s, $C(CH_3)_3$ within Cy envelope). $^{13}C\{^1H\}$ NMR (THF-d_8, δ): 129.1 (br s, Ru*C*≡CBu^t); (C_6D_6, δ): 66.0 (br s, RuC≡*C*Bu^t). IR (nujol; cm^{-1}): υ(C≡C) 2044.

(b) As an isolated by-product in the preparation of **18**. A mixture of $Ru_2Cl_4(dcypb)_2(N_2)$ (**16**, 100 mg, 0.079 mmol) and $TlOC_6F_5$ (61 mg, 0.16 mmol) in CH_2Cl_2 (10 mL) was stirred at RT for 10 min and the solvent removed under vacuum. The orange residue was redissolved in THF (25 mL) and stirred as 3,3-dimethyl-1-butyne (195 μL, 1.58 mmol) was added via syringe. The solution was stirred at RT for 15 h, filtered through Celite, and the volume reduced to ca. 0.2 mL under vacuum. A bright yellow solid was precipitated by addition of hexanes (5 mL). The solid was filtered off, washed with Et_2O followed by hexanes and dried under vacuum. Yield: 20 mg

(16%). Spectroscopic data agree with those reported above for **20**. An aliquot of the filtrate, dried and redissolved in C_6D_6, revealed a mixture of $Ru(OC_6F_5)_2[C{=}CH(Bu^t)](dcypb)$ (**18**, 39%), $[\{Ru(C{=}CHBu^t)(dcypb)\}_2(\mu\text{-}Cl)_3]Cl$ (**19•Cl**, 52%) and residual **20** (8%) by ^{31}P NMR analysis. X-ray quality crystals were obtained by slow evaporation of a benzene solution of the isolated acetylide complex.

2.15.2. Protonation of $Tl[\{Ru(C{\equiv}CBu^t)(dcypb)\}_2(\mu\text{-}Cl)_3]$ (20) by HOC_6F_5 (NMR scale)

Pentafluorophenol (24 mg, 0.13 mmol) was added to a stirring solution of **20** (15.5 mg, 0.010 mmol) in C_6H_6 (0.7 mL). The solution was stirred for 10 min at which time ^{31}P NMR analysis revealed complete conversion to **19•OC$_6$F$_5$** (δ_P = 44.4, 43.2, ABq, $^2J_{PP}$ = 26 Hz). After sitting at RT for 20 h, ^{31}P NMR analysis showed the presence of $Ru(OC_6F_5)_2[C{=}CH(Bu^t)](dcypb)$ (**18**, 18%; δ_P = 50.0 (s)) alongside **19•OC$_6$F$_5$** (82%).

2.16. Dcypb Carbonyl Complexes

2.16.1. $[Ru_2(\mu\text{-}Cl)_3(CO)_2(dcypb)_2]Cl$ (21a)

(a) From $RuCl_2(CO)(PPh_3)_2(DMF)$ (**26**). A solution of dcypb (520 mg, 1.15 mmol) in 10 mL CH_2Cl_2 was added to a suspension of **26** (925 mg, 1.16 mmol) in 35 mL CH_2Cl_2. The mixture was stirred at RT for 18 h, then stripped of solvent. Addition of benzene to the yellow oil caused deposition of X-ray quality crystals of **21a** over 2 h. The product was filtered, washed with C_6H_6

(2 mL), Et_2O (4 × 2 mL), then hexanes (5 × 2 mL), and dried under vacuum. Yield: 0.665 g (88%). $^{31}P\{^1H\}$ NMR ($CDCl_3$, δ): 50.8 (d, $^2J_{PP}$ = 23 Hz), 42.5 (d, $^2J_{PP}$ = 23 Hz). ^1H NMR ($CDCl_3$, δ): 1.10-2.53 (br m, CH_2, Cy of dcypb). $^{13}C\{^1H\}$ NMR ($CDCl_3$, δ): 200.3 (t, $^2J_{CP}$ = 15 Hz, *C*O). IR (Nujol; cm^{-1}): ν(CO) 1958. Anal. Calcd. for $C_{58}H_{104}Cl_4O_2P_4Ru_2$: C, 53.53; H, 8.06%. Found: C, 53.36; H, 7.89%. ESI-MS: calcd for $C_{58}H_{104}Cl_3O_2P_4Ru_2$ (M^+) 1266; found {M + H} *m/z* 1267.

(b) Via Decarbonylation of $RuCl_2$(dcypb)$(CO)_2$ (**22**). A solution of **22** (mixture of isomers: 95% *tcc* and 5% *ccc*) (42 mg, 0.062 mmol) in 20 mL MeOH was refluxed under N_2 for 16 h. The solvent was stripped off under vacuum to yield a yellow oil. Quantitative conversion to **21a** was indicated by ^{31}P NMR analysis. Clean **21a** crystallized on taking up the oil in benzene. Yield: 31 mg (78%).

(c) From Ru_2Cl_4(dcypb)$_2(N_2)$ (**16**). An orange suspension of **16** (50 mg, 0.039 mmol) in methanol (20 mL) was stirred under CO (1 atm) for 18 h, during which time the suspended solid turned pale yellow. ^{31}P NMR analysis of the reaction mixture confirmed complete conversion to **22** (80 % *tcc* isomer, 20 % *ccc*). The suspension was refluxed under N_2 for 16 h. The solvent was removed under vacuum, leaving a yellow oil which was then dissolved in benzene. The product, **21a**, crystallized at RT from the benzene solution. The precipitate was filtered off, washed with benzene (1 × 2 mL) followed by Et_2O (4 × 2 mL) and dried under vacuum. Yield: 42 mg (82 %).

2.16.2. Preparation of $RuCl_2(CO)_2$(dcypb) (22) via Carbonylation of 21a

(a) Predominantly *tcc*-**22**. Treatment of a stirred suspension of **21a** (50 mg, 0.039 mmol) in 20 mL EtOH with CO caused a colour change from orange to pale yellow over 18 h at RT. The reaction was cooled to -35 °C, and the precipitate filtered off and washed with EtOH, then Et_2O, and finally hexanes. Yield of clean *tcc*-**22** after drying under vacuum: 20 mg (38%). A second crop (9:1 mixture of *tcc:ccc* isomers) was obtained by concentration and addition of cold pentane. Yield after washing (cold pentane) and drying under vacuum: 29 mg (54%). Spectroscopic data agree with those reported.[13] $^{31}P\{^1H\}$ NMR (C_6D_6, δ): 13.8 (s).

(b) Predominantly *ccc*-**22**. A solution of **21a** (45 mg, 0.069 mmol Ru) in 10 mL $CHCl_3$ was stirred under 1 atm CO at RT. Complete conversion to **22** required 4 d (^{31}P NMR). Concentration and addition of cold pentane produced a pale yellow powder (mixture of isomers: 95% *ccc* and 5% *tcc*), which was filtered, washed with pentane and dried under vacuum. Yield: 42 mg (89%). Spectroscopic data agree with those reported.[13] $^{31}P\{^1H\}$ NMR (C_6D_6, δ): 39.4 (d, $^2J_{PP}$ = 23 Hz), 17.1 (d, $^2J_{PP}$ = 23 Hz).

2.16.3. Isomerization Behavior and Stability of Solvated $RuCl_2$(dcypb)$(CO)_2$ (22)

(a) A solution of **22** (mixture of isomers: 10% *ccc* and 90% *tcc*) in THF underwent complete isomerization to the *ccc* isomer over 28 h. Also present in the ^{31}P NMR spectrum: three overlapping singlets centered at 20 ppm (10% integrated intensity) assigned to unknown

complex(es) **27**. By contrast, in $CHCl_3$ solvent, neither isomerization nor decompositon was observed.

(b) Dissolving clean *tcc* –**22** in C_6D_6 (20 mg in 0.7 mL) caused 10% isomerization to the *ccc*–**22** after 18 h at RT, and 17% conversion to **27**. After 48 h, the amount of *ccc*–**22** was virtually unchanged (13% of total ^{31}P NMR integration), but peaks assigned to **27** accounted for 40% of the total integrated intensity.

(c) Bubbling N_2 through an ethanol solution of *tcc*-**22** at 60 °C for 3.5 h gave a mixture of the dimerized decarbonylation product, **21a** (50%, ^{31}P NMR) and **27**. Higher stability was found in MeOH, EtOH, and $CHCl_3$ than in benzene, toluene, or THF.

2.16.4. Solution Behavior of $Ru_2Cl_4(dcypb)_2(CO)_2$ (21)

The isomeric form of **21** is solvent-dependent: (i) $CDCl_3$: $^{31}P\{^1H\}$ NMR ($CDCl_3$, δ): 50.8 (d, $^2J_{PP}$ = 23 Hz, **21a**), 42.5 (d, $^2J_{PP}$ = 23 Hz, **21a**). $^{13}C\{^1H\}$ NMR ($CDCl_3$, δ): 200.3 (t, $^2J_{PC}$ = 15 Hz, *C*O, **21a**). ^1H NMR ($CDCl_3$, δ): 1.10-2.53 (br m, CH_2, Cy of dcypb). IR (Nujol, cm^{-1}): ν(CO) 1958. (ii) C_6D_6: $^{31}P\{^1H\}$ NMR (C_6D_6, δ): 55.3 (d, **21a**, $^2J_{PP}$ = 23 Hz), 42.3 (d, **21a**, $^2J_{PP}$ = 23 Hz), 40.6 (s, **21b** or **21c**), 34.4 (s, **21b** or **21c**). ^1H NMR and IR spectra are indistinguishable from those in $CDCl_3$. In benzene, the concentration of solute is rapidly depleted by crystallization of **21a** (identified by X-ray diffraction), precluding measurement of the $^{13}C\{^1H\}$ NMR spectrum.

(iii) Chlorobenzene: $^{31}P\{^{1}H\}$ NMR (C_6H_5Cl, δ): 52.2 (d, **21a**, $^{2}J_{PP}$ = 25 Hz), 42.5 (d, **21a**, $^{2}J_{PP}$ = 25 Hz), 39.0 (s, **21b** or **21c**), 32.7 (s, **21b** or **21c**); ratio **21b**: **21c** : **21a** is 1:1:10.

2.16.5. Preparation of $[\{Ru(dcypb)(CO)\}_2(\mu\text{-}Cl)_3]^+PF_6^-$ (21a•PF_6)

A solution of $TlPF_6$ (20 mg, 0.059 mmol) in 2 mL THF was added to a suspension of $[Ru_2(\mu\text{-}Cl)_3(CO)_2(dcypb)_2]Cl$ (75 mg, 0.12 mmol Ru) in 6 mL THF. The suspension was stirred for 16 h, then filtered first through Celite and then through neutral alumina. The filtrate was concentrated, and Et_2O added to precipitate a yellow solid. This was filtered off, washed with Et_2O and hexanes, and dried under vacuum. The product was recrystallization from THF/Et_2O. Yield: 66 mg (81%). $^{31}P\{^{1}H\}$ NMR (acetone-d_6, δ): 52.7 (d, $^{2}J_{PP}$ = 24 Hz), 41.6 (d, $^{2}J_{PP}$ = 24 Hz), -146.3 (sept, $^{1}J_{PF}$ = 708 Hz). ^{1}H NMR (acetone-d_6, δ): 1.10 - 2.59 (br m, CH_2, Cy of dcypb). IR (Nujol, cm^{-1}): ν(CO) 1954 (s). Anal. Calcd. for $C_{58}H_{104}O_2Cl_3P_5F_6Ru_2$: C, 49.38; H, 7.43 %. Found: C, 49.63; H, 7.53 %.

2.16.6. Preparation of $K[RuH_3(CO)(dcypb)]$•KBH^sBu_3 (28)

A suspension of **21** (0.300 g, 0.46 mmol Ru) in 15 mL C_6H_6 was stirred as potassium tri-*sec*-butylborohydride (1.84 mL of 1.0 M solution) was injected. The yellow solution was stirred at RT for 15 h, then stripped of solvent. The resulting oil was taken up in pentane. Cooling the solution to -35 °C gave small amounts (14 mg) of **28** as a pale yellow powder. Attempts to dry

the precipitate under vacuum for microanalysis caused decomposition to many ^{31}P-containing species (NMR). The filtrate was stripped to a yellow oil, which could not be purified. X-ray quality crystals were obtained from a sample of the oil that was subsequently dissolved in toluene, then stripped again. Crystals of **28** (as a toluene solvate) deposited from the oil over 2 days at RT. Spectroscopic characterization was carried out on the mixture of crystals and oil. $^{31}P\{^{1}H\}$ NMR (C_7D_8, δ): 54.7 (s). ^{1}H NMR (C_7D_8, δ): 0.21 - 2.04 (br, CH_2, Cy of dcypb; ^{s}Bu), -1.01 (br, 1 H, B*H*), -9.29 (br t, 1 H, Ru*H*, $^{2}J_{HPcis}$ = 22 Hz), -10.32 (m, 2 H, Ru*H*). $^{1}H\{^{31}P\}$ NMR: -9.2 (t, Ru*H*, $^{2}J_{HH}$ = 4.8 Hz), -10.31 (br s). Hydride T_1 (min, 263 K, 300 MHz): (δ -9.29) 208 msec; (δ -10.32) 279 msec. $^{13}C\{^{1}H\}$ NMR (C_6D_6, δ): 213.7 (t, *C*O $^{2}J_{CP}$ = 7.7 Hz). IR (neat; cm^{-1}): ν(CO) 1916 (m), ν(BH) 1901 (m), ν(RuH) 1834 (s).

2.16.7. Preparation of RuH[OC(Ph)(C_6H_4)](CO)(dcypb) (30) via 28

A suspension of **21a** (100 mg, 0.15 mmol Ru) in 4 mL C_6H_6 was stirred as potassium tri-*sec*-butylborohydride (0.616 mL of 1.0 M solution) was added quickly via syringe. The yellow solution was stirred at RT for 15 h, following which benzophenone (84.2 mg, 0.46 mmol) was added to give a red solution. After a further 5 h, the solvent was reduced to 0.5 mL under vacuum and diethyl ether (10 mL) was added. The solution was filtered through neutral alumina, then concentrated to 2 mL. Microcrystalline **30** precipitated on cooling to -35 °C over 15 h. The dark red crystals were filtered and washed with cold Et_2O (2 × 1 mL), followed by cold pentane

(4 × 1 mL). Isolated yield of spectroscopically clean **30**: 60 mg (51%); the low yield is incurred by the solubility of **30**. The product was recrystallized from benzene/pentane. Experiments carried out on NMR scale in C_6D_6 showed a ^1H NMR singlet (5.67 ppm) for $KOCHPh_2$; no benzhydrol was observed by NMR or IR. $^{31}P\{^1H\}$ NMR (C_6D_6, δ): 25.7 (d, $^2J_{PP}$ = 20 Hz), 30.5 (d, $^2J_{PP}$ = 20 Hz). ^1H NMR (C_6D_6, δ): 9.00 (dd, 1 H, *o*-C*H* of *ortho*-metallated ring, $^3J_{HH}$ = 7.7 Hz, $^4J_{HP}$ = 4.1 Hz), 7.85 (d, 1 H, Ph, J_{HH} = 8.1 Hz), 7.65 (m, 2 H, Ph), 7.09 (m, 4 H, Ph), 6.79 (t, 1 H, Ph, J_{HH} = 7.5 Hz), 0.53 – 2.60 (m, 52 H CH_2, Cy of dcypb), -6.32 (dd, 1 H, Ru*H*, $^2J_{HP_{trans}}$ = 86.7 Hz, $^2J_{HPcis}$ = 24.3 Hz). $^{13}C\{^1H\}$ NMR (C_6D_6, δ): 215.4 (dd, Ru*C*, $^2J_{CPtrans}$ = 66 Hz, $^2J_{CPcis}$ = 6.5 Hz), 212.1 (t, Ru*C*O, $^2J_{CP}$ = 8.1 Hz), 205.3 (dd, Ru-O=*C*, $^3J_{CP}$ = 7.4 Hz, $^3J_{CP}$ = 3.1 Hz). IR (Nujol; cm^{-1}): ν(CO) 1900 (s), ν(RuH) 1859 (m), ν(CO; ketonic) 1580 (w). Anal. Calcd. for $C_{42}H_{62}O_2P_2Ru$: C, 66.20; H, 8.20%. Found: C, 66.67; H, 7.94%.

2.16.8. Preparation of RuH[OC(Ph)(C_6H_4)](CO)(dcypb) (30) from 21 (NMR scale)

Addition of $KOCHPh_2$ (14 mg, 0.061 mmol) in 0.3 mL C_6D_6 to a stirred suspension of **21** (20 mg, 0.031 mmol Ru) in 0.4 mL C_6D_6 caused immediate dissolution and a colour change from pale yellow to dark red. Stirring was continued for 1 h, after which PPh_3 (8.1 mg, 0.031 mmol) was added as integration standard. ^{31}P NMR: **30** (100%). ^1H NMR: **30** + Ph_2CHOH (1:1 ratio). δ

Ph_2CHOH: 7.60-7.15 (m, 10 H, Ph), 5.49 (d, 1 H, C*H*, J_{HH} = 3.6 Hz). The presumed hydroxyl O*H* peak (δ ~ 1.76) is obscured by the cyclohexyl resonances of **30**.

2.16.9. Preparation of RuCl(OC(C_6H_4)(Ph))(CO)(dcypb) (32)

A solution of **21a** (100 mg, 0.154 mmol) in benzene (10 mL) was stirred as a solution of KBH^sBu_3 (615 μL of a 1.0 M solution, 0.615 mmol) was added via syringe. The solution was stirred at RT for 15 h. Benzophenone (112 mg, 0.615 mmol) was added and the solution was stirred at RT for 10 h, turning dark red. The solution was filtered through neutral alumina and the solvent removed under vacuum, leaving a red oil. On dissolution in $CHCl_3$ (5 mL), the colour turned bright orange; the solution was stirred at RT for 15 h, then stripped of solvent. The orange oil was redissolved in a minimum of Et_2O, and pentane added to precipitate a bright orange solid, which was filtered off and washed with pentane. Recrystallization from CH_2Cl_2/hexanes gave 88 mg (72%) of a bright orange microcrystalline solid. $^{31}P\{^1H\}$ NMR (C_6D_6, δ): 46.0 (d, $^2J_{PP}$ = 17 Hz), 6.2 (d, $^2J_{PP}$ = 17 Hz). ^1H NMR (C_6D_6, δ): 8.62 (dd, 1 H, *o*-C*H* of *ortho*-metallated ring, $^3J_{HH}$ = 7.4 Hz, $^4J_{HP}$ = 5.1 Hz), 7.52 (m, 2 H, Ph), 7.12 (m, 2 H, Ph), 6.79 (m, 4 H, Ph), 0.78 – 2.95 (m, 52 H, CH_2, Cy of dcypb). $^{13}C\{^1H\}$ NMR (C_6D_6, δ): 210.6 (dd, RuCO, $^2J_{CP}$ = 15.9 Hz, $^2J_{CP'}$ = 7.4 Hz), 209.8 (d, Ru-O=*C*, $^3J_{CP}$ = 6.9 Hz), 204.1 (dd, Ru*C*, $^3J_{CPcis}$ = 10.0 Hz, $^3J_{CPtrans}$ = 78.4 Hz). IR

(C_6D_6; cm^{-1}): ν(CO) 1926 (s), ν(CO; ketonic) 1579 (w). Anal. Calcd. for $C_{42}H_{61}ClO_2P_2Ru$: C, 63.34; H, 7.72%. Found: C, 63.35; H, 8.19%.

2.16.10. Preparation of 28-d_3 and its Reaction with Benzophenone

A suspension of **21** (20 mg, 0.031 mmol) in C_6D_6 (0.7 mL) was stirred as Super-Deuteride® (120 μL of a 1.0 M solution) was added. The yellow solution was stirred at RT for 15 h. ^{31}P NMR showed the expected singlet at 54.3 ppm; an unidentified byproduct (<10% of total integrated intensity) was also apparent at 61.1 ppm. ^1H NMR confirmed formation of **28**-d_3. Benzophenone was added (22 mg, 0.12 mmol), and the reaction was stirred at RT. ^{31}P NMR analysis after 2 h confirmed formation of **30**. ^1H NMR analysis showed a spectrum identical to that reported for **30** above, in which the hydride signal at -6.32 ppm integrated 1:1 vs. an isolated, *ortho* aromatic proton at 9.00 ppm.

2.16.11. Reaction of $RuCl_2(CO)(PCy_3)_2$ (14) with $KOCHPh_2$

A solution of **14** (10 mg, 0.0131 mmol) in 0.7 mL C_6D_6 was stirred with $KOCHPh_2$ (6 mg, 0.027 mmol). After 1 h, $RuHCl(CO)(PCy_3)_2$ (**13**)[14] was evident as the major product by NMR analysis (^1H, ^{31}P; < 50% of total ^{31}P NMR integration), along with residual **14**, free PCy_3, and unidentified byproducts. Further decomposition is evident on prolonged reaction time (20 h).

2.16.12. Reaction of $RuCl_2(CO)(PPh_3)_2(DMF)$ (26) with $KOCHPh_2$.

A solution of **26** (30 mg, 0.038 mmol) in 0.7 mL C_6D_6 was stirred with $KOCHPh_2$ (34 mg, 0.15 mmol). After 20 h, ^1H and ^{31}P NMR analysis showed the characteristic[23] hydride and ^{31}P signals for $RuH_2(CO)(PPh_3)_3$ (22% of total ^{31}P NMR integration). $^{31}P\{^1H\}$ NMR (δ, C_6D_6): 55.6 (d, $^2J_{PP}$ = 18 Hz), 43.41 (t, $^2J_{PP}$ = 18 Hz). Several unidentified products and free PPh_3 were also observed.

2.16.13. Catalytic Hydrogenation of Benzophenone by 28

Potassium tri-*sec*-butylborohydride (62 μl of 1.0 M solution) was added to a stirred suspension of **21** (10 mg, 0.015 mmol Ru) in 1 mL C_6H_6, and the resulting solution was stirred at RT for 15 h. An aliquot (160 μL, 0.0024 mmol Ru) of this standard solution was then added to benzophenone (1.31 g, 7.19 mmol) in 7 mL isopropanol or benzene. For reactions at atmospheric pressure, the resulting pink solution was degassed by three freeze-pump-thaw cycles, then placed under 1 atm H_2 and stirred at 60 °C for 24 h. For reactions at higher pressures, the solution was loaded into a glass-lined autoclave, purged with H_2, pressurized to the designated pressure, and heated to the desired temperature for 18 or 24 h. Conversions, determined by ^1H NMR, are listed in Table 2 (reactions in duplicate, ±2%). Control experiments indicated 55% conversion on carrying out the above experiment in isopropanol under N_2 atmosphere.

2.16.14. Catalytic Hydrogenation of Benzophenone by 30

(a) *In situ* preparation of **30** via **28**. Potassium tri-*sec*-butylborohydride (62 μl of 1.0 M solution) was added to a stirred suspension of **21** (10 mg, 0.015 mmol Ru) in 1 mL C_6H_6, and the resulting solution was stirred at RT for 15 h. Benzophenone (27 mg, 0.15 mmol) was added to the yellow solution, causing a color change to dark red. After stirring at RT for 5 h, complete conversion to **30** was confirmed by ^{31}P NMR. An aliquot (160 μL, 0.0024 mmol Ru) of this standard solution was then added to benzophenone (1.31 g, 7.19 mmol) in 7 mL isopropanol. The resulting pink solution was degassed by three freeze-pump-thaw cycles, then placed under 1 atm H_2 and stirred at 60 °C for 24 h. Conversion determined by ^1H NMR: 96% Ph_2CHOH (reactions in duplicate, ±2%)

(b) *In situ* preparation of **30** via **21**. To a stirred suspension of **21** (10 mg, 0.015 mmol Ru) in 1 mL C_6H_6 was added $KOCHPh_2$ (7 mg, 0.031 mmol). The resulting dark red solution was stirred at RT for 1 h. Complete conversion to **30** was confirmed by ^{31}P NMR. An aliquot (160 μL, 0.0024 mmol Ru) of this standard solution was then added to benzophenone (1.31 g, 7.19 mmol) in 7 mL isopropanol. The resulting pink solution was degassed by three freeze-pump-thaw cycles, then placed under 1 atm H_2 and stirred at 60 °C for 24 h. Conversion determined by ^1H NMR: 95% Ph_2CHOH (reactions in duplicate, ±2%).

(c) Large scale reduction. Potassium tri-*sec*-butylborohydride (110 μl of 1.0 M solution) was added to a stirred suspension of **21** (17.5 mg, 0.0275 mmol Ru) in 3 mL C_6H_6, and the

resulting solution was stirred at RT for 15 h. Benzophenone (200 mg, 1.10 mmol) was added to the yellow solution, causing a color change to dark red. After stirring at RT for 5 h, complete conversion to **30** was confirmed by ^{31}P NMR analysis. The red catalyst solution was added to a solution of benzophenone (99.8 g) in 200 mL isopropanol, and the reaction was refluxed under 1 atm H_2. An aliquot withdrawn for ^{1}H NMR analysis showed 48% conversion within 1 h. A distillation apparatus was attached to the reaction vessel and heating was continued. After a further 2 h of heating, conversion reached 90% (done in duplicate ± 2%).

2.16.15. Murai Coupling of Ethylene and Benzophenone via 28

Potassium tri-*sec*-butylborohydride (62 μl of 1.0 M solution) was added to a stirred suspension of **21a** (10 mg, 0.015 mmol Ru) in 1 mL C_6H_6, and the resulting solution was stirred at RT for 15 h. An aliquot (300 μL, 0.0045 mmol) was withdrawn and diluted with 3 mL C_6H_6. Benzophenone (13 mg, 0.071 mmol) was added, causing an immediate color change from yellow to pink. The solution was loaded into a glass-lined autoclave, purged with ethylene, pressurized to 260 psi and stirred at 60 °C for 22 h. The monoinsertion product, 2-ethylbenzophenone,[24] was identified by ^{1}H NMR analysis ($CDCl_3$): 58% conversion. The average of 2 trials (± 2%) is reported. Reactions at higher temperatures (90 °C) produced mixtures of the mono- and disubstituted (2, 2'-diethylbenzophenone[24]) products.

2.16.16. Murai Coupling of Ethylene and Benzophenone via 30

Potassium tri-*sec*-butylborohydride (62 μL of 1.0 M solution) was added to a stirred suspension of **21** (10 mg, 0.015 mmol Ru) in 1 mL C_6H_6, and the resulting solution was stirred at RT for 15 h. Benzophenone (40 mg, 0.22 mmol) was added, and stirring continued at RT for 5 h, after which complete conversion to **30** was confirmed by ^{31}P NMR analysis. An aliquot (300 μL, 0.0045 mmol **30**) was withdrawn and diluted with 3 mL C_6H_6. Benzophenone (12.6 mg, 0.069 mmol) was added. The solution was loaded into a glass-lined autoclave, purged with ethylene, pressurized to 260 psi and stirred at 60 °C for 22 h. The monoinsertion product, 2-ethylbenzophenone,[24] was identified by ^1H NMR analysis: 26% conversion. The average of 2 trials (± 3%) is reported.

2.17. Iminopyrrolato Derivatives of Ruthenium

2.17.1. RuCl{2-[(2, 6-^{i}Pr$_2$C$_6$H$_3$)-N=CH]C$_4$H$_3$N}(PCy$_3$)(CHPh) (34)

(a) Preparative Scale. A solution of $RuCl_2(PCy_3)_2(CHPh)$ (**1a**, 0.30 g, 0.36 mmol) in C_6H_6 (6 mL) was stirred as lithium[2-{(2, 6-diisopropylphenyl)imino}pyrrolide]•Et_2O (LiNN′•Et_2O, 0.19 g, 0.57 mmol) in C_6H_6 (6 mL) was added. The dark purple solution was stirred at RT for 18 h, turning dark brown. ^{31}P NMR confirmed the disappearance of all **1a**. The mixture was filtered through a plug of neutral alumina and the volume reduced to an oil under high vacuum. A crude crop of product (red-brown powder) was isolated by addition of pentane (10 mL). The crude

product was filtered-off, washed with pentane (5 × 3 mL) and dried under high vacuum. Yield: 183 mg (66%). It was purified by reprecipitation as follows. Dissolved in a 1:1 mixture of Et_2O:C_6H_6 (10 mL), it was filtered through neutral alumina, and the volume reduced to ~0.2 mL under vacuum. The product slowly precipitated on addition of cold (-35 °C) pentane (8 mL). After further cooling (-35 °C, 24 h), the product was isolated via filtration; the dark brown powder was washed with pentane (6 × 2 mL) and dried under vacuum. Yield: 102 mg (37%). Low yields are incurred by the high solubility in hydrocarbon solvents, including pentane. Crystals suitable for X-ray analysis were grown at RT by slow evaporation of a toluene solution. $^{31}P\{^1H\}$ NMR ($CDCl_3$, δ): 49.20 (s); (C_6D_6, δ): 49.97 (s). ^1H NMR ($CDCl_3$, δ): 19.65 (d, 1 H, Ru=C*H*, $^3J_{HP}$ = 11.0 Hz), 7.84 (d, 1 H, C(*H*)=N, $^4J_{HP}$ = 3.9 Hz), 7.50 (m, 1 H, Ar), 7.38 (m, 2 H, Ar), 7.18 (m, 2 H, Ar), 7.09 – 7.01 (m, 3 H, Ar + 3-pyr), 6.88 (m, 1 H, *m*-C*H* of Ar-N), 6.51 (br s, 1 H, 5-pyr), 6.18 (m, 1 H, 4-pyr), 3.05 (sept, 1 H, C*H*Me$_2$, $^3J_{HH}$ = 6.8 Hz), 2.50 (br m, 4 H, C*H*Me$_2$ + 3 × *ipso*-Cy), 1.91 – 1.10 (m, 36 H, 15 × CH_2 + 2 × CH_3) including CH_3 doublets at δ 1.28 (d,$^3J_{HH}$ = 6.7 Hz), and 1.19 (d, $^3J_{HH}$ = 6.7 Hz), 0.66 (d, 3 H, CH_3, $^3J_{HH}$ = 6.8 Hz), 0.45 (d, 3 H, CH_3, $^3J_{HH}$ = 6.8 Hz); (C_6D_6, δ): 20.00 (d, 1 H, Ru=C*H*, $^3J_{HP}$= 11.6 Hz), 7.70 (d, 1 H, C(*H*)=N, $^4J_{HP}$ = 3.9 Hz), 7.55 (m, 2 H, *o*-CH × 2), 7.23 – 6.97 (m, 6 H, Ar + 3-pyr), 6.79 (br, 1 H, 5-pyr), 6.45 (br m, 1 H, 4-pyr), 3.35 (sept, 1 H, C*H*Me$_2$, $^3J_{HH}$ = 6.7 Hz), 2.86 (sept, 1 H, C*H*Me$_2$, $^3J_{HH}$ = 6.8 Hz), 2.60 (br m, 3 H, *ipso*-Cy), 2.02 – 0.60 (m, 42 H, Cy + CH(CH_3)$_2$) including δ 1.52 (d, CH_3, $^3J_{HH}$ = 6.7 Hz), 1.30 (d, CH_3, $^3J_{HH}$ = 6.7 Hz), 0.89 (d, CH_3, $^3J_{HH}$ = 6.8 Hz), 0.68 (d, CH_3, $^3J_{HH}$

= 6.8 Hz). $^{13}C\{^{1}H\}$ NMR ($CDCl_3$, δ): 303.7 (d, Ru=*C*, $^{2}J_{CP}$ = 14.1 Hz), 163.0 (s, *C*H=N), 153.6 (d, *ipso*-C_6H_5, $^{3}J_{CP}$ = 1.9 Hz), 146.1 (s, *ipso*-2,6-diisopropylphenyl), 142.9 (s, *C*-$CHMe_2$), 142.8 (d, 2-pyr, $^{3}J_{CP}$ = 2.0 Hz), 142.0 (s, *C*-$CHMe_2$), 141.7 (s, 5-pyr), 129.3 (*o*-C_6H_5), 129.0 (*m*- or *p*-C_6H_5), 128.9 (*m*- or *p*-C_6H_5), 125.8 (*p*-*C* of Ar-N), 122.5 (br, 2 × *o*–*C* of Ar-N), 114.0 (s, 4-pyr), 33.5 (d, ipso-Cy, $^{1}J_{CP}$ = 20 Hz), 30.3, 29.4, 29.3, 27.8, 27.7, 27.6, 26.8, 26.4, 25.4, 24.2, 23.3, 21.9. IR (CH_2Cl_2; cm^{-1}): 1569 (s), 1445 (s), 1390 (m), 1173 (w), 1038 (m), 894 (w). Anal. Calcd. for $C_{42}H_{60}ClN_2PRu$: C, 66.34; H, 7.95%. Found: C, 66.73; H, 8.27%.

(b) NMR Scale. A solution of LiNN′•Et_2O (17.2 mg, 66 μmol) in C_6D_6 (0.4 mL) was added to a stirring solution of **1a** (30 mg, 36 μmol) in C_6D_6 (0.3 mL). The solution was stirred at RT for 20 h, turning dark brown, and 1,2-dichloroethane (10 μL of a 2.0 M solution in C_6D_6) was added as an internal standard for ^{1}H NMR analysis. ^{1}H NMR shows the characteristic peaks for **34** (28 μmol or a 78% yield, determined by the relative integrations of the alkylidene resonance at δ_H 20.00 (d) and the singlet for 1,2-dichloroethane at δ_H 2.87). Also present was 2-[(2, 6-diisopropylphenyl)imino]pyrrole (HNN′, 32 μmol), for which the characteristic peaks at the following locations were consistent with an authentic sample: 7.84 (s, 1 H, *H*C=N), 6.45 (br m, 1 H, pyr), 6.05 (br m, 2 H, pyr), 3.24 (sept, 2 H, 2 × C*H*Me_2, $^{3}J_{HH}$ = 6.8 Hz), and 1.12 (d, 12 H, 4 × CH_3, $^{3}J_{HH}$ = 6.8 Hz). There was no evidence of residual LiNN′ starting material. $^{31}P\{^{1}H\}$ NMR reveals **34** (δ 49.97, s, 52% of total integration), free PCy_3 (δ 10.58, 31% of total), and unidentified species at δ_P 75.96 (s, 1%), 54.60 (s, 7%), 25.67 (s, 9%).

2.17.2. Control Experiments involving LiNN^{t}•Et_2O

(a) With PCy_3 . A suspension of lithium LiNN^{t}•Et_2O (20 mg, 60 μmol) in C_6D_6 (0.7 mL) was added to PCy_3 (22 mg, 1.3 equiv) and the solution stirred at RT for 20 h. ^{31}P and ^{1}H NMR analyses showed no evidence of reaction.

(b) With RuCl{2-[(2, 6-$^{i}Pr_2C_6H_3$)-N=CH]C_4H_3N}(PCy_3)(CHPh) (**34**). A solution of **34** (15 mg, 20 μmol) was added to LiNN^{t}•Et_2O (7 mg, 1 equiv) in C_6D_6 (0.7 mL). The solution was stirred at RT for 20 h and 1,2-dichloroethane (10 μL of 2.0 M solution in C_6D_6) was added as an internal standard. ^{31}P and ^{1}H NMR analysis showed no evidence of reaction.

2.17.3. Evaluating the Stability of 34 to Air.

Complex **34** was dissolved in $CDCl_3$ (0.7 mL, non-distilled, non-degassed) under air, and triphenylmethane (4.8 mg, 1 equiv) was added as an internal standard. The mixture was analyzed periodically by ^{31}P and ^{1}H NMR. After 72 h, there was still no evidence of decomposition: the characteristic doublet at δ_H 19.65 (Ru=C*H*Ph, **34**) integrated in a 1:1 ratio with the singlet at δ_H 5.57 (C*H*Ph_3, triphenylmethane).

2.17.4. RuCl{2-[(2, 6-$^{i}Pr_2C_6H_3$)-N=CH]C_4H_3N}$(py)_2$(CHPh) (35)

A solution of **1a** (0.50 g, 0.61 mmol) in C_6H_6 (5 mL) was stirred as LiNN^{t}•Et_2O (0.32 g, 1.0 mmol) in C_6H_6 (5 mL) was added. The dark purple solution was stirred at RT for 18 h,

turning dark brown. The mixture was filtered through a plug of neutral alumina and the solvent removed under vacuum to give a brown oil. The oil was redissolved in a mixture of Et_2O/hexanes (1:1, total volume: 10 mL) and stirred as pyridine was added (2 mL, excess). The mixture was stirred at RT for 20 h, resulting in a yellow-green suspension. The crude product was isolated by filtration, washed with hexanes and dried under vacuum. It was reprecipitated twice from CH_2Cl_2/hexanes. The purified product, a green microcrystalline solid, was filtered, washed with hexanes (10 × 3 mL), and dried under high vacuum for 20 h yielding 195 mg (50%) of analytically pure product. ^{1}H NMR ($CDCl_3$, δ): 20.51 (s, 1 H, Ru=C*H*), 8.59 – 6.91 (m, 20 H, Ar), 6.46 (br s, 1 H, 5-pyr), 6.20 (m, 1 H, 4-pyr), 4.41 (br m, 1 H, C*H*Me_2), 2.83 (br m, 1 H, C*H*Me_2), 0.99 (d, 3 H, C*H*$_3$, $^3J_{HH}$ = 6.0 Hz), 0.79 (d, 6 H, 2 × C*H*$_3$, $^3J_{HH}$ = 6.0 Hz), 0.62 (d, 3 H, C*H*$_3$, $^3J_{HH}$ = 6.0 Hz). ^{13}C{^{1}H} NMR ($CDCl_3$, δ): 316.6 (d, Ru=*C*, $^2J_{CP}$ = 14.1 Hz), 164.0, 156.9, 155.3, 155.1, 154.9, 148.0, 146.6, 145.5, 143.3, 137.0, 136.5, 136.0, 131.3, 129.8, 126.9, 124.2, 123.9, 123.8, 122.8, 118.5, 112.6, 29.6, 27.9, 27.5, 26.0, 23.5, 22.4. IR (CH_2Cl_2; cm^{-1}): 1593 (m), 1567 (s), 1445 (s), 1389 (m), 1299 (w), 1040 (m). Anal. Calcd. for $C_{34}H_{37}ClN_4Ru$: C, 63.99; H, 5.84%. Found: C, 64.27; H, 6.21%.

2.17.5. General Procedure for RCM of Diethyl Diallylmalonate

(a) **In C_6D_6.** Diethyl diallylmalonate (28 μL, 0.12 mmol) was added to a solution of Ru catalyst **34** or **35** (6 μmol) in C_6D_6 (0.75 mL). If required, one of the following compounds was

added: $TlPF_6$ (10 mg, 29 μmol, 5 equiv or 2 mg, 1 equiv), PCy_3 (20 μL of a 0.30 M solution in C_6D_6, 1 equiv), or CuCl (6 mg, 60 μmol, 10 equiv). If required, the mixture was warmed in an oil bath, stirring under air or nitrogen atmosphere for the stated reaction time. Conversions were determined based on the relative integrations for the ^1H NMR signals at δ 3.21 ppm (CH_2, 4,4-dicarbethoxycyclopent-1-ene, vs) and δ 2.89 (CH_2, diethyl diallylmalonate, d). The identity of the RCM product 4,4-dicarbethoxycyclopent-1-ene, was verified by GC-MS after filtering the solution through benzene-saturated silica gel to remove catalytic contaminants. M^+ calcd for $C_{11}H_{16}O_4$ = 212, found 212 (EI-MS).

(b) **In Neat Substrate**. Under an atmosphere of air, **34** (13 μmol) was added to diethyl diallylmalonate (500 μL, 2.1 mmol) and the reaction vessel (small vial) was capped loosely. The mixture was stirred at 70 °C and aliquots withdrawn periodically for ^1H NMR analysis.

2.18. References

(1) Genet, J. P.; Pinel, C.; Ratovelomanana-Vidal, V.; Mallard, S.; Pfister, X.; Andrade, M. C. C. D.; Laffitte, J. A. *Tetrahedron: Assymmetry* **1994**, *5*, 665.

(2) Ivin, K. J.; Lam, L.-M.; Rooney, J. J. *Macromol. Chem. Phys.* **1994**, *195*, 1189.

(3) Ashby, E. C.; Coleman, D. *J. Org. Chem.* **1987**, *52*, 4554.

(4) Hillmyer, M. A.; Laredo, W. R.; Grubbs, R. H. *Macromolecules* **1995**, *28*, 6311.

(5) Demonceau, A.; Stumpf, A. W.; Saive, E.; Noels, A. F. *Macromolecules* **1997**, *30*, 3127.

(6) Hughes, R. P.; Zheng, X.; Morse, C. A.; Curnow, O. J.; Lomprey, J. R.; Rheingold, A. L.; Yap, G. P. A. *Organometallics* **1998**, *17*, 457.

(7) Brookhart, M.; Grant, B.; Volpe, A. F. J. *Organometallics* **1992**, *11*, 3920.

(8) Matsuo, Y.; Mashima, K.; Tani, K. *Chem. Lett.* **2000**, 1114.

(9) Dawson, D. M.; Walker, D. A.; Thornton-Pett, M.; Bochmann, M. *J. Chem. Soc., Dalton Trans.* **2000**, 459.

(10) Hallman, P. S.; Stephenson, T. A.; Wilkinson, G. *Inorg. Synth.* **1970**, *12*, 237.

(11) Hoffman, P. R.; Caulton, K. G. *J. Am. Chem. Soc.* **1975**, *97*, 237.

(12) Stephenson, T. A.; Wilkinson, G. *J. Inorg. Nucl. Chem.* **1966**, *28*, 945.

(13) Amoroso, D.; Yap, G. P. A.; Fogg, D. E. *Can. J. Chem.* **2001**, *79*, 958.

(14) Yi, C. S.; Lee, D. W.; Chen, Y. *Organometallics* **1999**, *18*, 2043.

(15) Moers, F. G.; Hoedt, R. W. M. T.; Langhout, J. P. *J. Organomet. Chem.* **1974**, *65*, 93.

(16) James, B. R.; Markham, L. D.; Hui, B. C.; Rempel, G. L. *J. Chem. Soc., Dalton Trans.* **1973**, 2247.

(17) Wilhelm, T. E.; Belderrain, T. R.; Brown, S. N.; Grubbs, R. H. *Organometallics* **1997**, *16*, 3867.

(18) Christ, M. L.; Sabo-Etienne, S.; Chaudret, B. *Organometallics* **1994**, *13*, 3800.

(19) Olivan, M.; Caulton, K. G. *Inorg. Chem.* **1999**, *38*, 566.

(20) Rodriguez, V.; Sabo-Etienne, S.; Chaudret, B.; Thoburn, J.; Ulrich, S.; Limbach, H.-H.; Eckert, J.; Barthelat, J.-C.; Hussein, K.; Marsden, C. J. *Inorg. Chem.* **1998**, *37*, 3475.

(21) Yi, C. S.; Lee, D. Y. *Organometallics* **1999**, *18*, 5152.

(22) Amoroso, D.; Yap, G. P. A.; Fogg, D. E. *Organometallics* **2002**, *21*, 3335.

(23) Ahmad, N.; Levison, J. J.; Robinson, S. D.; Uttley, M. F. In *Inorg. Synth.*; Parshall, G. W., Ed.; McGraw-Hill: New York, 1974; Vol. 15; pp 45.

(24) DeRoos, A. M. *Recl. Trav. Chim. Pays-Bas* **1968**, *87*, 1381.

CHAPTER 3

Tandem ROMP-Hydrogenation: Reversible Cycling Between Metathesis and Hydrogenation Catalysis

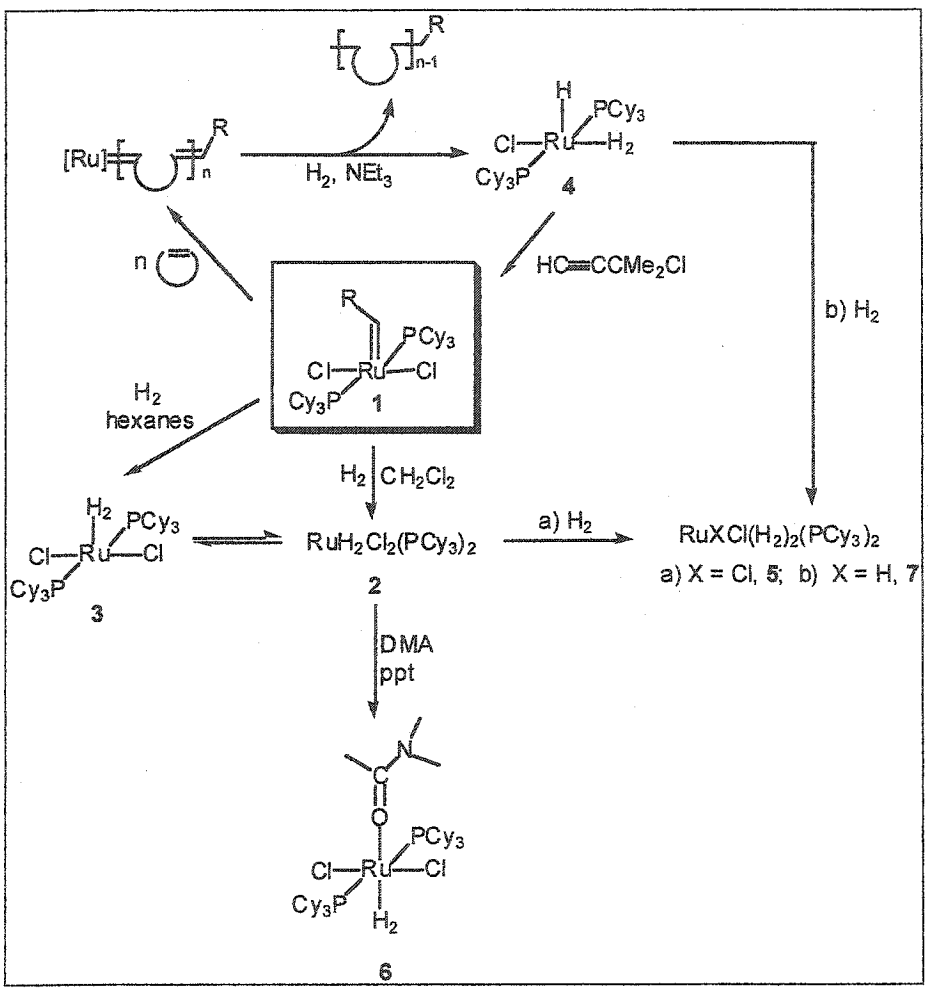

Figure 3.1 Pictorial summary of Chapter 3.

Parts of this chapter have been published:

(a) Drouin, S. D.; Yap, G. P. A.; Fogg, D. E. *Inorg. Chem.* **2000**, *39*, 5412.

(b) Drouin, S. D.; Zamanian, F.; Fogg, D. E. *Organometallics*, **2001**, *20*, 5495.

(c) Fogg, D. E.; Amoroso, D.; Drouin, S. D.; Snelgrove, J. L; Conrad, J. C.; Zamanian, F. *J. Mol. Catal.* **2003**, *190*, 177.

Chapter 3 References: p 105

3.1. Introduction

Increasing demand for synthetic efficiency has spurred the development of tandem catalytic methodologies, wherein two or more transformations are carried out in series within a single reaction vessel.[1] In the current literature, the term "tandem catalysis" loosely describes any system in which two or more mechanistically distinct catalytic transformations are carried out sequentially, without isolation of intermediates. A subset of this category is "orthogonal catalysis", in which two or more different catalytic precursors are added to a reaction mixture, each enabling a different step of a reaction cascade (Figure 3.2).[2] Less common is "multifunctional catalysis", in which a *single* catalyst precursor mediates different types of catalytic transformations in series (Figure 3.3).[3] In this thesis, the term "tandem catalysis" is reserved for the latter category, implying a highly efficient approach to catalytic reactions. The ability to selectively toggle between different modes of catalysis is particularly attractive for a range of applications, including combinatorial organic synthesis.[4] Such selective control over catalyst function is demonstrated herein, where a single catalyst precursor is reversibly activated for metathesis and hydrogenation catalysis (eq 1).

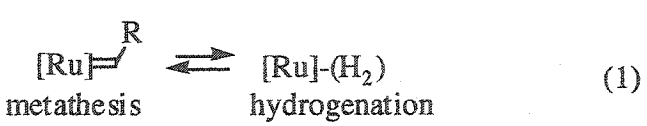

(1)

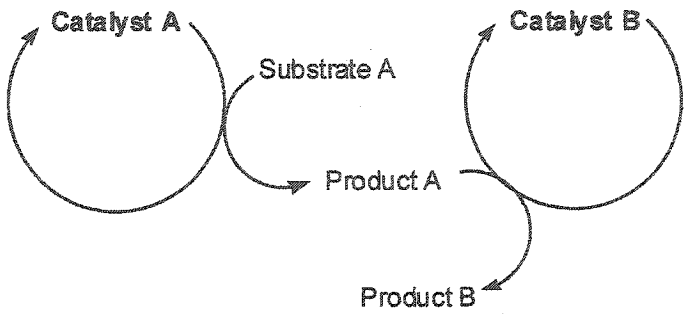

Figure 3.2 Schematic illustration of orthogonal catalysis.

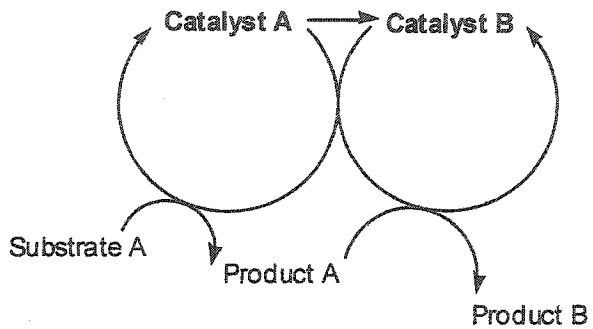

Figure 3.3 Schematic illustration of multifunctional tandem catalysis.

The products of metathesis reactions are synthetically versatile by virtue of their unsaturation, which allows for post-metathesis functionalization. This possibility has inspired elegant retrosynthetic strategies, including domino processes involving sequential metathesis events.[5,6] Depending on the intended application, however, it may be desirable to hydrogenate the products of RCM or CM.[5f] Reduction is conventionally accomplished in a two-step process in which the metathesis product is first isolated and

then hydrogenated in a separate procedure using the heterogeneous catalyst Pd/C.[5f,7] The development of more efficient hydrogenation strategies, particularly tandem methods, is relevant to a growing number of applications, including the commercialization of ROMP polymers (*vide infra*).[5] At the outset of this project, there were no literature reports on "tandem metathesis-hydrogenation". Subsequently, and concurrent with the present work, there appeared several reports describing the empirical utility of tandem metathesis-hydrogenation methodologies.[3c-h]

Hydrogenation expands the range of applications open to ROMP materials by eliminating the inherent susceptibility of olefinic linkages to oxidative and thermal degradation.[5,8-10] Interest in the hydrogenation of ROMP polymers was originally fuelled by industrial demand for lightweight, moldable polymers with desirable optical characteristics.[11] For example, hydrogenation of ROMP-derived poly(norbornene) affords a thermally stable material which has been applied in the commercial fabrication of lenses and other optical devices.[11c] Other work suggests that the hydrogenation of ROMP polymers will significantly expand their applicability as solution phase (ROMPgel) supports for parallel synthesis,[5a] and as model substrates for molecular theories and rheology.[12]

Hydrogenation of internal olefins is a challenging problem, exacerbated in the case of polymer substrates by steric constraints imposed by the random coil.* ROMP polymers obtained via ruthenium catalysis are particularly difficult to hydrogenate due to the predominance of trans olefinic groups (generally ~80%) in the polymer backbone.[10,13]

A successful methodology for the catalytic hydrogenation of ROMP products will also be applicable to small-molecule products of RCM or CM, which undergo reduction more readily. Though the reduction of unsaturated polymers can be accomplished stoichiometrically using diimide,[9,14] the utility of this approach is limited by the occurrence of side reactions in which residual hydrazide fragments attach to the polymer chains.[15] Catalytic methods are cleaner and more efficient, and a large body of work details the effectiveness of transition metal catalysts for the reduction of polymeric olefins.[8a] A recent report describes tandem catalytic ROMP-hydrogenation, in which the hydrogenation step is effected heterogeneously on a silica support.[3e] However, this approach is limited to soluble polymers, owing to the difficulty of separating the reduced polymer from the support. Homogeneous catalysts offer distinct advantages for ROMP-hydrogenation, including a better chance of realizing quantitative hydrogenation, because the catalyst can diffuse to the olefinic sites on the chain.[16] Homogeneous nickel and

---

* 1,2-Olefins in polybutadiene are reduced faster than 1,4-olefins and cis-1,4 units faster than trans- 1,4 units.[8a]

rhodium complexes catalyze reduction of ROMP polymers at 100-135 °C and 300 psi.[17] At the beginning of this work, the available evidence suggested that more forcing conditions were required for Ru-catalyzed reduction;[11b] it was nevertheless attractive for the possibility of tandem ROMP-hydrogenation (Figure 3.4).

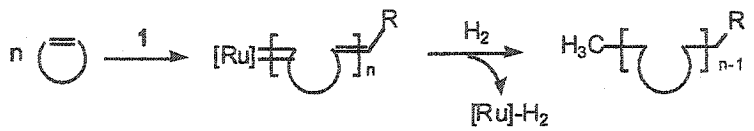

1a = $RuCl_2(PCy_3)_2(CHPh)$
1b = $RuCl_2(PCy_3)_2(CHCMe_2)$

Figure 3.4 Tandem, catalytic ROMP-hydrogenation of cycloolefins by Ru-precursors.

This chapter describes the transformation of ROMP catalyst $RuCl_2(PCy_3)_2(CHPh)$ (**1a**) into dihydride, dihydrogen, and hydride species, and the application of these species in tandem metathesis-hydrogenation processes. The tandem protocol is also expanded to include reversible cycling between hydrogenation and metathesis chemistry (Figure 3.5). Use of methanol in the hydrogenation step permits complete polymer hydrogenation under very mild conditions, under one atmosphere of H_2, in comparison to pressures ranging from 7 to 114 atm in the related literature.[3c,e,8a] This work also represents

fundamental groundwork toward the development of efficient *asymmetric* tandem processes.

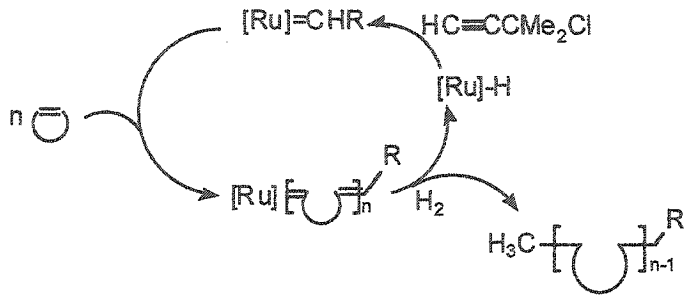

Figure 3.5 Schematic illustration of reversible cycling between ROMP and hydrogenation catalysis.

3.2. Hydrogenolysis of $RuCl_2(PCy_3)_2(CHPh)$ (1a)

Hydrogenolysis of the Grubbs catalyst **1a** in CD_2Cl_2 at RT effects clean conversion into a single phosphorus-containing species, which was identified as the Ru(IV) complex $Ru(H)_2Cl_2(PCy_3)_2$ (**2**, Figure 3.6) based on its characteristic NMR features.[18] The latter include a ^{31}P NMR singlet at δ_P 91.3, and a triplet at δ_H –12.4 ($^3J_{HP}$ 31.6 Hz) in the ^1H NMR spectrum. One equivalent of toluene is also observed.

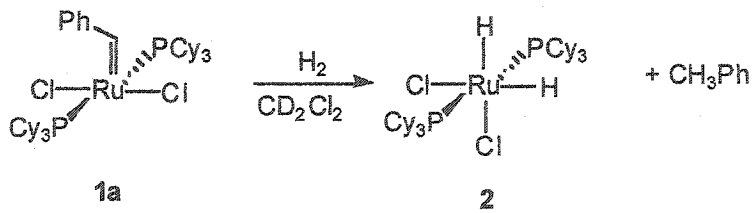

Figure 3.6 Hydrogenolysis of $RuCl_2(PCy_3)_2(CHPh)$ (**1a**) in CD_2Cl_2.

Hydrogenolysis of **1a** in hexanes yields a dark yellow precipitate, which is compositionally identical to **2** (microanalysis), but is identified as the dihydrogen tautomer, $RuCl_2(H_2)(PCy_3)_2$ (**3**, Figure 3.7), on the basis of the NMR data discussed below. Complicating isolation of **3** from "better" solvents is its instability toward slow loss of HCl to yield a hydridochloro derivative (Section 3.3). It also undergoes tautomerism in solution to form mixtures of **2/3** , as described below.

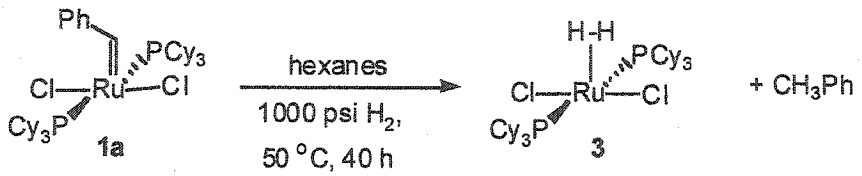

Figure 3.7 Hydrogenolysis of $RuCl_2(PCy_3)_2(CHPh)$ (**1a**) in hexanes.

Solid state $^{31}P\{^1H\}$ NMR spectra of **3** show a single peak at 47.5 ppm, a location far upfield of the corresponding solution value for **2** (91.3 ppm).* Dissolution of this sample in C_6D_6 under Ar reveals a mixture of **3** and **2** in a ratio of ca. 1:2 (^{31}P, ^1H NMR). The spectra show the following characteristic peaks for **3**: a singlet at δ_P 54.2 and a broad

---

* While chemical shift differences between solid state and solution NMR data are common, structures are considered qualitatively different when the chemical shift difference is greater than ca. 6 ppm.[19]

peak at δ_H –16.2, the latter representing a η^2-dihydrogen ligand. These data were initially puzzling because they coincide with those of the known[20] *hydridochloro* complex $RuHCl(H_2)(PCy_3)_2$ (**4**). Unequivocal characterization as **3** is based on T_1 and J_{HD} data. The T_1 minimum value (18.8 ms at 268K and 500 MHz), corresponding to an H-H distance of 0.84 Å for fast-spinning H_2,[21a] is significantly shorter than that for **4** (30 ms at 243K, 250 MHz; 60 ms at 500 MHz).[20] The comparatively long relaxation time for **4** is characteristic of η^2-H_2 perturbed by interaction with cis-hydride.[21b] The HD derivative of **4** exhibits a coupling constant of 22.5 Hz, corresponding to an H-H distance of 1.04 Å.[21c] The discrepancy with the T_1-derived value may reflect the intermediacy between fast and slow spinning of the dihydrogen ligand (the H-H distance calculated for non-spinning H_2 is 1.06 Å).[21a]

Solutions of **3** under H_2 reveal new $^{31}P\{^1H\}$ and ^1H NMR singlets (δ_P 40; δ_H -9.8), both of which disappear on evacuation and backfilling with Ar. ^{31}P EXSY experiments indicate a correlation between the peaks at δ_P 54 and 40, consistent with chemical exchange between coordinatively unsaturated **3** and its bis(H_2) derivative **5** (Figure 3.8). ^1H EXSY experiments likewise correlate the hydride peaks at -9.8 and –13.0 ppm. The latter is assigned to **3**, its downfield shift relative to the value under Ar (-16.2 ppm) arising from exchange averaging with **5**.

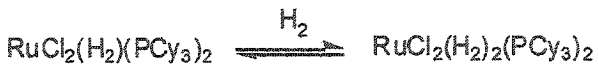

3 5

Figure 3.8 Reversible coordination of H_2 to $RuCl_2(H_2)(PCy_3)_2$ (**3**).

Whereas dissolving **3** in benzene or toluene gives a mixture of these dihydride and dihydrogen species, solely **2** is observed in CH_2Cl_2. The **3**→**2** conversion is clearly due to tautomerism, rather than reaction with chlorinated solvent,[22a] as dissolving **3** in CD_2Cl_2 does not effect incorporation of deuterium (^1H and ^2H evidence). The barrier to interconversion is presumably due to movement of the heavy atoms, possibly involving compression of the P-Ru-P angle in **2** relative to **3**. An iodo analog of **4** exhibits a P-Ru-P angle of 175°,[23] vs. angles of ~112° determined computationally for **2**,[18] and crystallographically for $[Ru(H)_2Cl_2(P^iPr_3)_2]$.[24] Dihydrogen-dihydride tautomeric equilibria have been spectroscopically observed in other systems, and solvent effects on the position of equilibrium have been described.[21b]

3.3. Hydrogenolysis of 1a in the Presence of Base

When hydrogenolysis of **1a** is carried out in benzene-dimethylacetamide (DMA), in the presence or absence of the strong base Proton Sponge (1,8-bis(dimethylamino)naphthalene), a pale yellow solid precipitates from solution. By analogy with related work,[22] hydridochloro complex **4**[20] was expected. Heterolytic activation of dihydrogen is well known to give such species. Indeed, the generally-accepted role of base in promoting catalytic hydrogenation via transition-metal dihalides involves abstraction of HX to give hydridohalo intermediates that afford entry into the catalytic cycle.[25-27] Surprisingly, the kinetically favored reaction path *did not* involve loss of HCl, but rather conversion into previously unreported dichloro complex $RuCl_2(H_2)(PCy_3)_2(\eta^1\text{-}O{=}C(NMe_2)Me)$ (**6**, Figure 3.9), which precipitates preferentially from a DMA/Et_2O solution, and is isolated in ca. 70% yield. Its identity is supported by spectroscopic data, microanalysis, and X-ray crystallography.

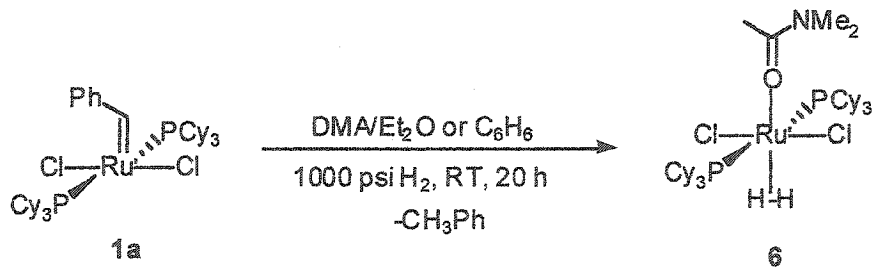

Figure 3.9 Preparation of $RuCl_2(H_2)(PCy_3)_2(\eta^1\text{-}O{=}C(NMe_2)Me)$ (**6**).

In solution, a five-coordinate structure resulting from dissociation of DMA (i.e. **3**, rather than **6**) is probable, given the spectroscopic resemblance to base-free **3**. ^{31}P and ^{1}H NMR spectra for **6** in C_6D_6 are identical to those for **3** (disregarding peaks for free DMA in the case of **6**), and the dihydrogen T_1 values are also identical within experimental error, differing by only 0.3 ms. A structural difference between the solid and solution state is manifested in $^{31}P\{^{1}H\}$ NMR spectra of **6**: the solid-state spectrum reveals a signal at 32 ppm, whereas the corresponding solution spectrum exhibits only the singlets for **3** and **2** (δ_P 54 and 91, respectively).* While formation of **6** may occur via the five-coordinate precursor **3**, the intermediacy of **2** is also plausible, based on a related report which describes the reaction of the osmium(IV) dihydride $Os(H)_2Cl_2(P^iPr_3)_2$ with pyrazole to give a dihydrogen complex as a base adduct (Figure 3.10).[28]

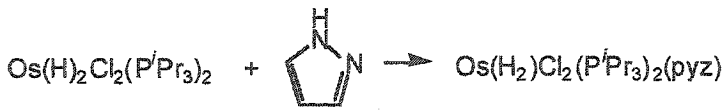

Figure 3.10 Base-assisted transformation of a dihydride complex into a dihydrogen derivative.[28]

In CH_2Cl_2 solvent, hydrogenolysis of **1a** in the presence of strong base such as Proton Sponge effects abstraction of HCl to afford **4**,[20] which can be isolated in >80%

* Differences between solution and solid state chemical shifts are addressed in Section 3.2.

yield by this route (Figure 3.11). When dissolved in C_6D_6 under argon, complex **4** is spectroscopically indistinguishable from **3**. The hydride signals can, however, be distinguished under H_2 atmosphere: the dihydrogen resonance for **4** appears at –14.5 ppm (RT, C_6D_6, 200 MHz), owing to dynamic averaging with its bis-dihydrogen adduct, **7**.[20] Under the same conditions, the dihydrogen resonance for **3** appears as a broad peak at δ_H –13.0. Solutions containing mixtures of **3** and **4** under H_2 show both peaks, side by side, in the hydride region of the ^1H NMR spectrum.

It is likely that the formation of **4** proceeds via intermediate **2**, based on reports which describe the facile dehydrohalogenation of **2**[22b] and analogues $RuCl_2H_2(P^iPr_3)_2$[29a] and $RuCl_2H_2(P^tBu_2Me)_2$.[29b] Reaction via dihydrogen tautomer **3** is also plausible, however, and is consistent with the documented acidity of coordinated η^2-H_2 ligands.[21b]

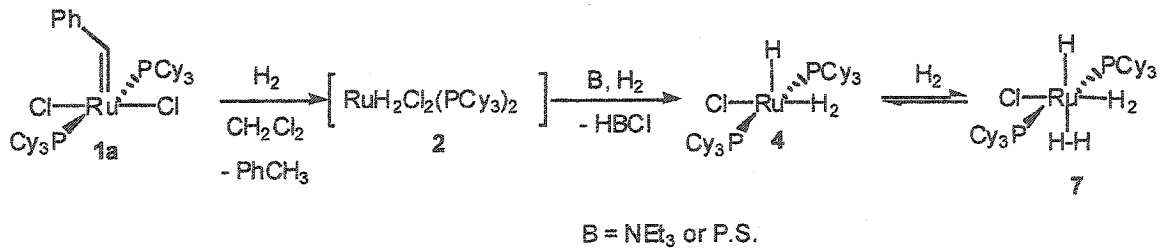

Figure 3.11 Formation of $RuHCl(H_2)(PCy_3)_2$ (**4**) from $RuCl_2(PCy_3)_2(CHPh)$ (**1a**).

3.4. Molecular Structure of $RuCl_2(H_2)(PCy_3)_2$(DMA) (6)

Crystals of **6** were grown from a benzene/DMA solution. Single-crystal X-ray analysis of **6** was carried out; the ORTEP is shown in Figure 3.12, selected bond lengths and angles in Table 3.1. The structure confirms retention of both chloride ligands. In this regard, it is worth noting that omission of chlorinated solvents from the crystallizing system eliminated the possibility of "shuttling" between hydridochloro and dichloro species.[22a] Though the dihydrogen ligand was not located, its existence is supported by spectroscopic data (Section 3.3); it is presumed to occupy the site trans to coordinated DMA within the octahedral coordination geometry. The positions of the mutually trans phosphines in the basal plane reflect a slight distortion from the ideal value of 90°, owing to the steric demand of the PCy_3 ligands: both Ru-P bonds are angled at 97.78(4)° from the Ru-O axis. The weak interaction implied by the long Ru-O bond in **6** is consistent with minimal perturbation of the ν(CO) IR resonance (1630 cm^{-1}, vs. 1640 cm^{-1} for free DMA). Ru-P and Ru-Cl bond lengths are comparable to those in related $RuCl_2(PCy_3)_2(L)$ complexes, including alkylidene (L = CH-*p*-C_6H_4Cl)[13] and vinylidene (L = C=CHPh)[30] complexes.

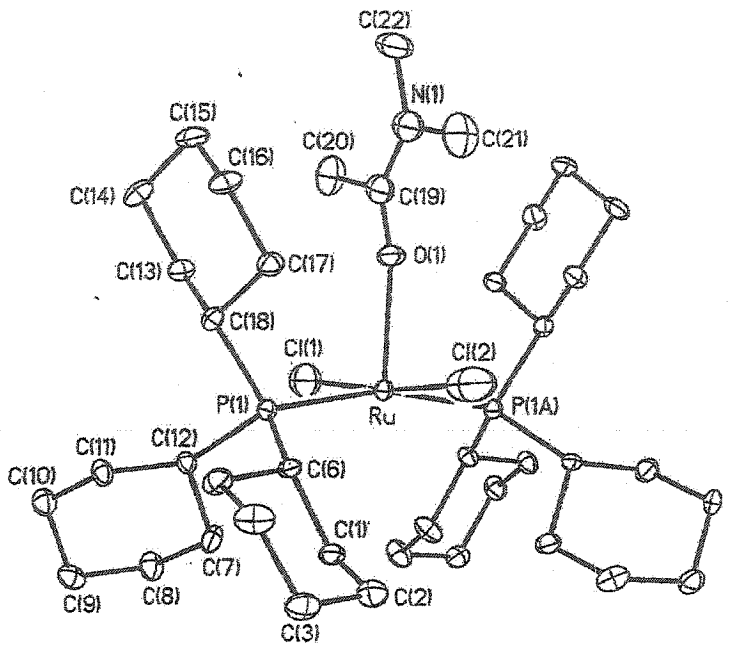

Figure 3.12 ORTEP diagram of $RuCl_2(H_2)(PCy_3)_2(DMA)$ (**6**). Thermal ellipsoids shown at 30% probability level. Hydrogen atoms are omitted for clarity.

Table 3.1 Selected bond lengths (Å) and angles (deg) for $RuCl_2(H_2)(PCy_3)_2(DMA)$ (**6**)

Bond Distances (Å)		Bond Angles (deg)	
Ru-O(1)	2.323(7)	O(1)-Ru-P(1)	97.78(4)
Ru-P(1)	2.3707(16)	P(1)-Ru-P(1A)	164.29(8)
Ru-Cl(1)	2.423(4)	O(1)-Ru-Cl(1)	90.21(19)
Ru-Cl(2)	2.428(6)	O(1)-Ru-Cl(2)	83.35(19)
O(1)-C(19)	1.212(13)	Cl(1)-Ru-Cl(2)	173.55(13)

3.5. Tandem ROMP-Hydrogenation Catalysis

Facile formation of the known[31] hydrogenation catalyst $RuHCl(H_2)(PCy_3)_2$ (**4**) via hydrogenolysis of metathesis precursor **1a** suggested that a protocol for tandem metathesis-hydrogenation would be feasible. Given the potential utility and versatility of such an approach (Section 3.1), investigations were undertaken to probe catalytic ROMP-hydrogenation chemistry. For the purpose of optimization, cyclooctene (**8**) was chosen as a model substrate. This monomer is easily purified and readily undergoes ROMP by catalysts of type **1** (Figure 3.13).[32] The extent of reduction is easily monitored by ^1H NMR analysis of the product mixture (Figure 3.14).

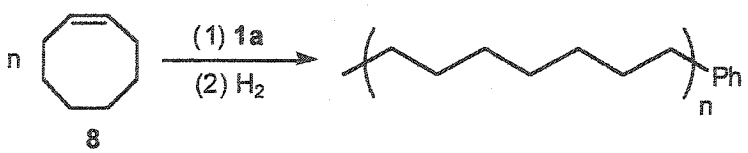

8

1a = $RuCl_2(PCy_3)_2(CHPh)$

Figure 3.13 Tandem ROMP-hydrogenation of cyclooctene (**8**).

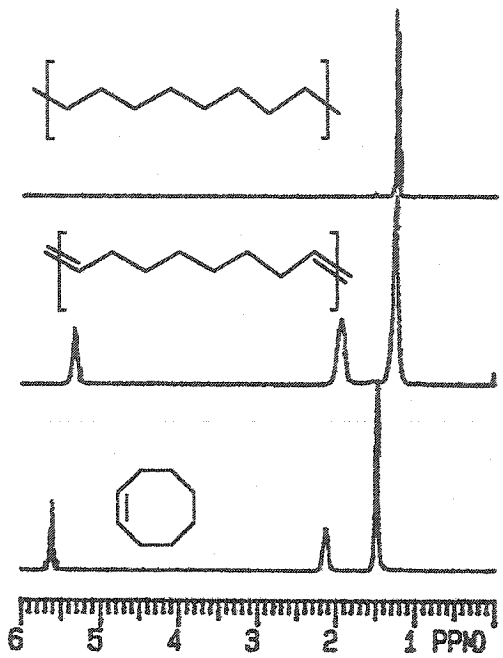

Figure 3.14 ^{1}H NMR spectra showing the sequential transformation of cyclooctene (**8**) into polyethylene via ROMP-hydrogenation.

Initial experiments were carried out in CH_2Cl_2 solvent. Low hydrogenation activity even at 1000 psi (Table 3.2, entry 1) is attributed to the predominance of octahedral $RuH_2Cl_2(PCy_3)_2$ (**2**), the sole spectroscopically observable species in CD_2Cl_2 (Section 3.2). Reduction is faster in neat THF, in which both $RuCl_2(H_2)_2(PCy_3)_2$ (**5**) and five-coordinate, mono-H_2 derivative **3** are present. As ROMP is slow in THF,[32,33] however, the polymerization step was carried out in CH_2Cl_2, followed by dilution with THF (3:1) for subsequent hydrogenation. Complete reduction of poly(octene) is then effected within 24 h at 1000 psi H_2 (entry 2), though conversions drop sharply at lower pressures.

Table 3.2 ROMP-Hydrogenation of Cyclooctene (**8**) in CH_2Cl_2 and THF/CH_2Cl_2 [a]

Entry	cosolvent	Additive[b]	pH_2 (psi)	Time (h)	Conversion (%)
1	-	-	1000	24	32
2	75% THF	-	1000	24	>99
3	75% THF	-	100	24	9
4	-	NEt_3	100	24	85
5	-	P.S.[c]	100	24	31
6	75% THF	NEt_3	100	24	55

[a] General conditions: ROMP at RT under N_2 in CH_2Cl_2 (2 mL); 1.5 h, 1.2 mM **1a**, 204 equiv **8**. Diluted as indicated for hydrogenation (total volume 10 mL). Conversions determined by ^1H NMR; average of 3 trials (± 3%).[b] NEt_3 or Proton Sponge, 12 μmol, added immediately prior to hydrogenation. [c] P.S. = Proton Sponge.

Transformation of **3/5** into **4** by addition of NEt_3 dramatically increases catalytic activity, giving 85% reduction at 100 psi (entry 4). Indeed, base is well known to accelerate reduction via transition-metal dichlorides, promoting heterolytic activation of H_2 by abstraction of HCl and formation of catalytically active hydridochloro species.[25-27] When NEt_3 is used, THF cosolvent is no longer beneficial, but is actually detrimental to overall hydrogenation activity. The role of THF in promoting tautomerism to **3** is clearly redundant under these conditions; its lower dielectric constant vs. CH_2Cl_2 (ε_{THF} = 7 vs. 9

for CH_2Cl_2), or its coordination to the metal centre, may also hinder hydrogenation.[34] The hydrogenation activity exhibits an unexpected, non-stoichiometric dependence on [NEt_3] (Figure 3.15). This may be due to chlorination of **4** by CH_2Cl_2, and thus regeneration of **2**, over the timescale of hydrogenation.* Further base would then be required to restore **4**.

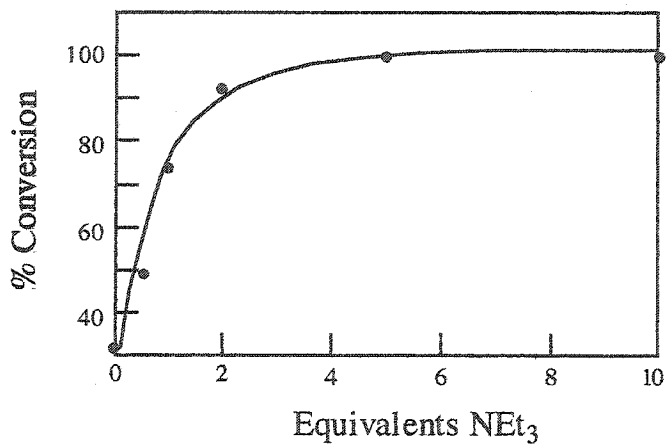

Figure 3.15 Effect of base on hydrogenation activity in tandem ROMP-hydrogenation of cyclooctene. Reaction conditions: 490 μmol cyclooctene; 2.4 μmol of catalyst **1a**; CH_2Cl_2 solvent. Polymerization at RT over 1.5 h; hydrogenation at RT, 1000 psi H_2, 24 h.

---

* Exchange of hydride for chloride is common in $CHCl_3$ or CH_2Cl_2, and such solvents are often avoided in small-molecule reduction.[25] However, their use in polymer hydrogenation - as in the present case - can be dictated by solubility and reactivity considerations. Of the common solvents, only CH_2Cl_2 and THF fully dissolve these polymer substrates. The limitations of THF are discussed above. While nucleophilic attack on CH_2Cl_2 is, in principle, also possible, NEt_3 is rather unreactive toward methylene chloride, though Pt complexes can promote amine chloromethylation.[35,36] If a CH_2Cl_2-NEt_3 reaction does occur, however, it clearly does not compete with initial abstraction of HCl from **2/3** to yield **4**. The latter reaction is immediate and quantitative.

The strong, non-nucleophilic base Proton Sponge (pKa 12.3) affords lower conversions (entry 5) than NEt_3 (pKa 10.8), suggesting a steric constraint on the rate of dehydrohalogenation, though the precise origins of this difference have not yet been elucidated.

3.6. Structural Integrity of the ROMP Polymers: Molecular Weights and PDIs

Gel permeation chromatography (GPC) analyses were carried out in order to evaluate any potential effect of hydrogenation on molecular weights and polydispersities. Poly(octene) was fully soluble in methylene chloride; GPC analyses revealed PDI and M_n values averaging 1.42 and 5.3×10^4, respectively, although molecular weights show considerable variability ($\pm 1.4 \times 10^4$). They are significantly higher than those predicted from the monomer-to-catalyst ratio (calculated M_n = 22 000), as typical for non-living ROMP of low-strain monomers, in which chain transfer processes compete effectively with initiation and propagation steps.[37] Attempts to acquire the corresponding molecular weight data on the reduced product (polyethylene) were frustrated by the low solubility of the latter. Soluble polyethylenes were obtained, instead, via ROMP-hydrogenation of functionalized cyclooctenes (Figure 3.16, Table 3.3). M_n and PDI values for the reduced polymers of **9** and **10** agree with data for their parent materials,[38] suggesting that the hydrogenation step is not attended by adverse effects, such as chain scission processes.

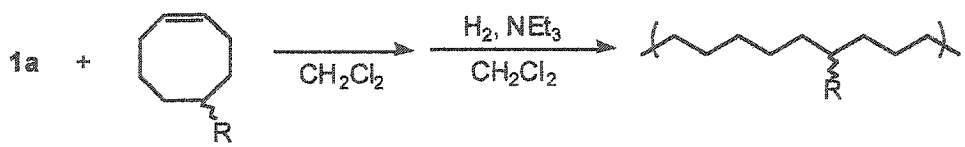

Figure 3.16 Preparation of functionalized polyethylenes via tandem ROMP-hydrogenation.

Table 3.3 Tandem ROMP-Hydrogenation of Functionalized Cyclooctenes[a]

entry	monomer	ROMP time (h)[b]	reduction (%)[c]	reduced polyoctenes		
				Yield (%)[d]	10^{-3} M_n[e]	PDI[e]
1	**8**	1.5	100	86	*f*	*f*
2	**9**	4	100	68[g]	45.3	1.38
3	**10**	4	100	69[g]	62.7	1.40
4	**11**	24	54	60[g]	61.2	1.23

[a] Reaction conditions: CH_2Cl_2 solvent, RT, monomer : **1a** = 204 : **1a**, [**1a**] = 1.2 mM; diluted with CH_2Cl_2 for hydrogenation ([**1a**] = 0.24 mM) under 1000 psi H_2, over 24 h, RT, with added NEt_3 (5 equiv relative to **1a**). [b] ROMP time required for complete polymerization determined by ^{1}H NMR. [c] Determined by ^{1}H NMR of the crude product mixture. [d] Polymer isolated by precipitation from MeOH; average values are reported (± 5%) [e] Determined by GPC in CH_2Cl_2 using polystyrene standards; average values are reported (Appendix A). [f] Insufficient solubility at RT. [g] Isolated yields are limited by the high solubility of the functionalized poly(octenes).

The very slow rate of polymerization of the ester-substituted cyclooctene **11** (entry 4), noted in previous work,[37] may reflect inhibition via chelation (Figure 3.17).

Stable chelate complexes,[39] which can sequester a metathesis catalyst in unproductive forms, have been invoked to explain the inhibition of **1a** by carbonyl groups located in the vicinity of the olefin.* Interference via *inter*molecular interactions can be ruled out, based on control experiments which show no inhibition on addition of ethyl acetate (Section 3.7). The poor hydrogenation performance noted for the **1a/11** combination (entry 4) may be due to decomposition incurred over the prolonged polymerization period.

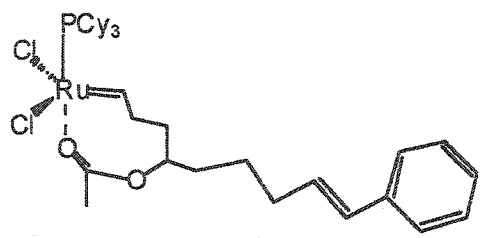

Figure 3.17 Chelation of monomer **11**, illustrated for the monoinsertion product.

In contrast with cyclooctenes, high-strain bicyclic monomers generally yield living polymers, affording greater control over molecular weights and polydispersities.

* The available evidence suggests that formation of 5- and 6-membered metallacycles is particularly facile. Though less common, the formation of larger chelate rings is also plausible.[39]

Use of such monomers in tandem ROMP-hydrogenation experiments would permit more rigorous examination of polymer structure and, specifically, of any changes incurred during the hydrogenation step. Ether-functionalized norbornene **12** (Figure 3.18) was chosen as a model substrate for tandem ROMP-hydrogenation experiments in view of the solubility of its reduced ROMP polymer. GPC analyses of the material obtained via ROMP-hydrogenation of **12** revealed near-monodisperse polyolefin (10^{-4} M_n = 3.0, PDI = 1.04); molecular weights and PDI values were unchanged following reduction of poly(**12**), confirming the earlier suggestion that the hydrogenation step has no adverse effect on the structural integrity of ROMP polymers.

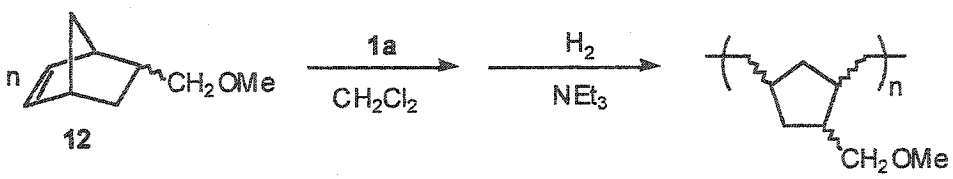

Figure 3.18 Tandem ROMP-hydrogenation of ether-functionalized norbornene **12**.

3.7. Functional Groups

In order for the tandem ROMP-hydrogenation process to be versatile and broadly applicable, it must tolerate a range of functionalized monomers. Thus, screening experiments were carried out in order to determine whether particular functional groups

interfere with the catalysis. In these experiments, both ROMP and hydrogenation were carried out in presence of one or more different additives (Table 3.4). The results suggest that on the ROMP timescale, the process is tolerant toward tertiary amines, alcohols, and esters (entries 1–3). The presence of *tert*-butylacetic acid resulted in low yields of polymer, possibly owing to competitive decomposition of the ROMP catalyst **1a**. A related report has noted poor conversions for the polymerization of acid-functionalized monomers via **1a**, suggesting that the catalyst may undergo decomposition via protonation of a phosphine ligand.[40] However, it is worth noting that this effect is not general, as the presence of acid can sometimes enhance the activity of Ru-based metathesis and hydrogenation catalysts (Section 3.9).

Table 3.4 Tandem ROMP-Hydrogenation of **12** in the Presence of Additives[a]

entry	additive[b]	yield (%)[c]	10^{-3} M_n[d]	PDI[d]
1	NEt_3	85	25.0	1.04
2	MeOH	80	29.4	1.03
3	$CH_3COOCH_2CH_3$	83	35.1	1.02
4	$(CH_3)_3CCOOH$	24	18.0	1.14

[a] Reaction conditions: 980 μmol **12**; 4.8 μmol **1a**. Polymerization in 10 mL solvent (CH_2Cl_2 + additive) at RT over 30 min. In all cases, 20% MeOH added prior to hydrogenation carried out at 1000 psi H_2, RT, over 24 h. Complete reduction confirmed by ^1H NMR. [b] Amount of additive: NEt_3 = 3.6 μL (26 μmol); MeOH = 2 mL (cosolvent, 20%); $CH_3CO_2C_2H_5$ = 88 μL (980 μmol); $(CH_3)_3CCO_2H$ = 125 μL (980 μmol). [c] Isolated yield. [d] Determined by GPC in CH_2Cl_2 using polystyrene standards.

3.8. Cycling Between ROMP and Hydrogenation

Extension of the tandem ROMP-hydrogenation methodology to multiple catalytic cycles could give access to "tailored" polymer blends in which the molecular weight and structure of each component was specified. Such materials offer precise models for investigation of the rheological properties of narrow-polydispersity polyolefin blends; they also have the broader potential to address processing difficulties inherent to narrow-PDI ROMP polymers. Use of polymer blends to modulate melt and flow properties has emerged as a key solution to processing problems in metallocene-derived polyolefins.[41]

An influential report by the Grubbs group describes facile and clean generation of metathesis precursor **1b** via reaction of **4** with 3-chloro-3-methyl-1-butyne.[42] In the present work, this methodology was exploited to effect reinstallation of alkylidene following hydrogenation. Deployment of this chemistry within the context of multiple cycles of ROMP and hydrogenation requires that it be tolerant to the presence of base. Therefore, model studies were performed to ensure that the presence of excess base would not hamper clean regeneration of metathesis catalyst **1b** from **4**. NMR experiments confirmed that **1b** is formed cleanly in the presence of excess triethylamine. Related experiments demonstrated that hydrogenolysis products **2** and **4** also converge cleanly to product **1b** (Figure 3.19). The reaction can be carried out in CH_2Cl_2 or THF; the presence of NEt_3 has no effect.

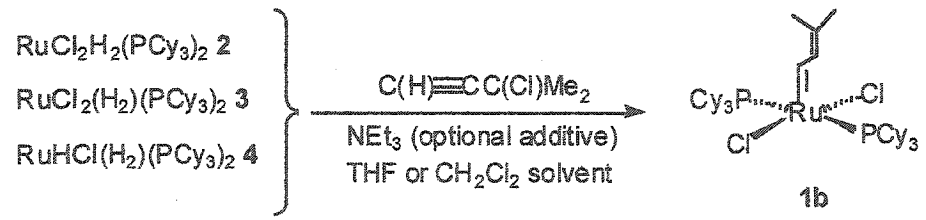

Figure 3.19 Clean formation of metathesis catalyst **1b** by reaction of complexes **2**, **3**, or **4** with 3-chloro-3-methyl-1-butyne.

Initial experiments involved the ROMP-hydrogenolysis-ROMP sequence illustrated in Figure 3.20. ROMP of **12** (400 equiv) was followed by hydrogenolysis (1 atm H_2; NEt_3 added), then transformation of the catalyst to **1b** by addition of 3-chloro-3-methyl-1-butyne, and finally addition of a second portion of **12** (100 equiv). GPC analysis of the isolated product confirmed the presence of a bimodal molecular weight distribution, in which the molecular weights of the two fractions were in good agreement with predicted values. For the first fraction , M_n (found) was 54 000 vs. 55 200 (calcd); for the second, M_n(found) was 19 000, vs. 14 000 (calcd). ROMP-hydrogenation-ROMP was carried out likewise, using H_2 pressures of 250 psi in the second step. A representative gel permeation chromatograph (GPC) trace is shown in Figure 3.21.

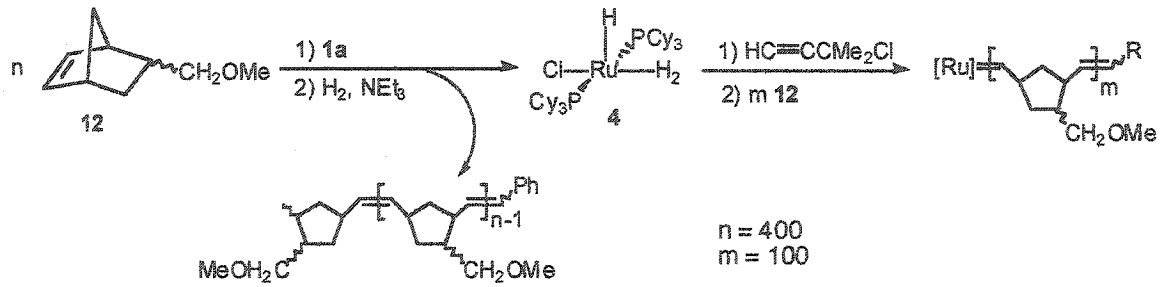

Figure 3.20 Schematic illustration of a ROMP-hydrogenolysis-ROMP application.

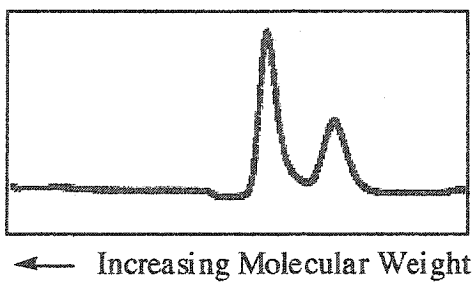

Figure 3.21 Representative GPC trace for a polymer blend obtained via tandem ROMP-hydrogenation-ROMP of **12**.

3.9. Alcohol Cosolvents

Solvents employed in catalytic reactions can have dramatic and unpredictable effects on reactivity.[43] While methanol inhibits the hydrogenation performance of some rhodium and iridium precursors,[26] it can enhance the activity of some ruthenium systems.[44] With the goal of optimizing the conditions for tandem ROMP-hydrogenation, methanol cosolvent was introduced prior to the hydrogenation of poly(octene). A

powerful rate acceleration resulted, allowing reduction at drastically lower pressures of H_2 (Table 3.5).

Table 3.5 Tandem ROMP-Hydrogenation of Cyclooctene (**8**) in Alcohol Cosolvents.[a]

entry	cosolvent	additive[b]	pH_2 (psi)	time (h)	conversion (%)
1	10% MeOH	-	100	4	51
2	20% MeOH	-	100	4	83
3	20% MeOH	HBF_4	100	4	89
4	20% MeOH	PCy_3	100	4	0
5	90% MeOH	-	100	4	51
6	20% MeOH	-	50	24	>99[c]
7	20% MeOH	NEt_3	15	4	43[d]
8	20% MeOH	NaOMe	15	4	63[d]
9	20% MeOH	NEt_3	15	24	>99[d]
10	20% ^{i}PrOH	-	100	4	54

[a] General conditions: ROMP at RT under N_2 in CH_2Cl_2 (2 mL); 1.5 h, 1.2 mM **1a**, 204 equiv **8**. Diluted as indicated immediately prior to hydrogenation (total volume 10 mL); dilution with CH_2Cl_2 must precede addition of alcohol, to prevent polymer precipitation. Conversions determined by ^{1}H NMR; average of 3 trials (± 3%).[b] NEt_3, PCy_3, NaOMe (12 μmol, 5 equiv) or HBF_4 (2.6 mmol, 1.1 equiv) added, if applicable, prior to cosolvent. [c] Hydrogenation at 50 °C. [d] Hydrogenation at 60 °C.

Rates increased with increased MeOH concentration, with an upper limit of ~20% being imposed by the solubility of polyethylene: at higher MeOH concentrations, incompletely reduced polymer precipitated from solution (entry 5). Such insolubility is usual for hydrocarbon polymers, and MeOH is in fact normally used for isolation of such materials. The unorthodox expedient of using methanol as the reaction medium resulted in >99% reduction at 50 psi H_2 (50 °C, 24 h). Quantitative polymer reduction was achieved at the unprecedentedly low pressure of 1 atm H_2 when NEt_3 was also used (entry 9).

Addition of the acid HBF_4 (entry 3) enhanced conversions, possibly owing to phosphine dissociation. Protic acids are sometimes used as phosphine scavengers to enhance the performance of metathesis[45] and hydrogenation[46b,c] catalysts by assisting in the creation of a vacant coordination site at the metal. The corollary, inhibition of activity by excess free phosphine, was confirmed (entry 4).

High conversions observed for the MeOH/NEt_3 systems may be due, in part, to formation of the known,[46] highly active hydrogenation catalyst $RuHCl(CO)(PCy_3)_2$ (**13**, Figure 3.22). The latter was observed by ^1H and ^{31}P NMR spectroscopy, along with **2**, **4**, and several minor unidentified products, in independent hydrogenolysis experiments.

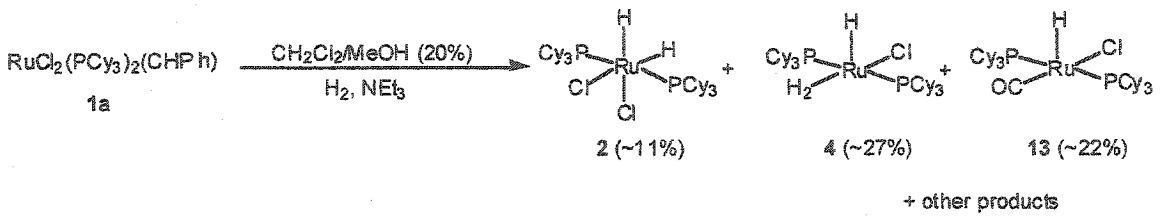

Figure 3.22 Hydrogenolysis of $RuCl_2(PCy_3)_2(CHPh)$ (**1a**) in presence of MeOH and NEt_3.

Facile decarbonylation of methanol by Ru(II) complexes is well established in the literature,[47,48,49] and, subsequent to publication of the present work, a report suggested that exposure of **4** to even trace amounts of methanol results in formation of **13**.[50] Interestingly, a very recent publication describes formation of **13** on reaction of **1a** with 1-propanol and NEt_3, showing that other alcohols are also suitable for this transformation, and that the presence of H_2 may not be essential.[48] A related report describes **13** as the sole product on thermolysis of the carbene complex $RuCl_2(PCy_3)(CHOEt)$ in benzene (Figure 3.23).[51]

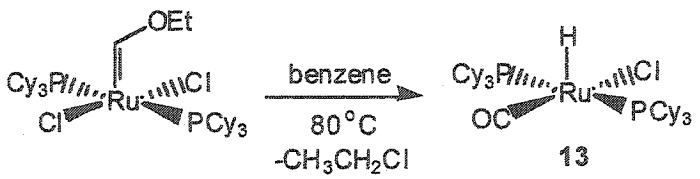

Figure 3.23 Thermal decomposition of $RuCl_2(PCy_3)_2[=CH(OEt)]$.[51]

Independent experiments were carried out in order to determine the relative hydrogenation activities of **13** and **4**. The results indicate that olefin hydrogenation is

more efficient via **13** (Section 3.9, below). In tandem catalysis, hydrogenation rates increase on use of NaOMe in place of NEt_3 (entries 7 and 8, Table 3.5), possibly owing to faster Ru-carbonylation to form **13**. Such reactivity is consistent with related literature, which suggests that a ruthenium methoxide intermediate is implicated in the decarbonylation mechanism.[48,49] Importantly, however, observation of an accelerating effect for isopropanol (entry 10, Table 3.5 vs. entry 1 Table 3.2), which is *not* subject to decarbonylation, points to an additional role for alcohol in the hydrogenation catalysis.*

3.10. Comparative Hydrogenation Activities of 4 and 13

Hydridocarbonyl complex **13** has emerged as a highly active catalyst for hydrogenation of both molecular[46a,c] and polymeric[8a] olefins. In order to compare the hydrogenation activities of **13** and **4**, these complexes were independently isolated and applied in the catalytic reduction of allylbenzene (Table 3.6). The activity of $RuCl_2(CO)(PCy_3)_2$ (**14**), which is itself a patented hydrogenation catalyst,[52] and which may act as a precursor[25] to the more active hydridochloro derivative **13**, is included for comparison.

---

* In hydrogenation catalysis, weakly-coordinating alcohol solvents can activate otherwise unreactive trichloride-bridged dinuclear species by assisting in the cleavage of a bridging unit (Chapter 5). In this regard, it is worth noting that $Ru_2(\mu\text{-}Cl)_3$ species are very common in the chemistry of ruthenium, and their facile formation may represent a general deactivation pathway in the catalytic chemsitry of ruthenium (Chapters 4 and 5).

Table 3.6 Hydrogenation of allylbenzene to *n*-propylbenzene.[a]

entry	catalyst	time (h)	% conv.[b]	turnover rate (h^{-1})[b,c]
1	$RuHCl(CO)(PCy_3)_2$ (**13**)	0.5	80 (5)	1605 (103)
2	$RuCl_2(CO)(PCy_3)_2$ (**14**)	0.5	44 (3)	885 (62)
3	$RuHCl(H_2)(PCy_3)_2$ (**4**)	0.5	31 (1)	617 (21)

[a] Reaction conditions: 0.71 mmol alkene (0.71 M); 0.69 μmol of catalyst (0.69 mM; catalyst : alkene = 1 : 1029); 1 mL C_6D_6; 1000 psi H_2; room temperature. [b] Conversions determined by ^1H NMR. Each value represents an average of three trials (± 3%). The values in parentheses correspond to isomerization turnovers for formation of *β*-methylstyrene (^1H NMR). [c] Turnover rate = (mol of product)(mol of catalyst)$^{-1}h^{-1}$.

Carbonyl complexes **13** and **14** are both more active than **4** for H_2-hydrogenation of allylbenzene, suggesting that the CO ligand may have an activating effect on the catalysis. These results are discussed in more detail in the next section, where they are placed within a broader context of ligand electronic effects in olefin hydrogenation catalysis. The lower activity of the dichloro complex **14** relative to **13** may reflect an induction period; if the former undergoes *in situ* heterolytic activation of H_2 (Figure 3.24),[27] then it effectively functions as a precursor to **13**.

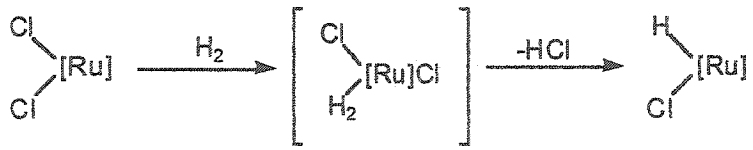

Figure 3.24 General scheme illustrating the heterolytic activation of H_2 by a Ru(II) dichloro precursor, to generate a Ru-monohydride derivative.[27]

3.11. Ligand Electronic Effects in Hydrogenation Catalysis

Effects of ligand properties on activity are difficult to assess, because the kinetic profile of a catalytic transformation usually represents the combined effects of several energetic relationships and equilibria. Small changes in ligand parameters may lead to mechanistic differences between related systems, which hampers comparison.[25] Despite these complexities, some trends have emerged from the extensive body of work in Ru- and Rh-based olefin hydrogenation catalysis.[25,43] Some of these, summarized herein, offer indirect mechanistic insight into the relative hydrogenation activities of **13** and **4**.

In hydrogenation of olefins or alkynes by Ru(II) catalysts, catalytic activity generally correlates with the basicity of coordinated phosphine ligands. For example, the activity of $RuCl_2[(p\text{-}XC_6H_4)_3P]_3$ (X = H, CH_3, OCH_3) for reduction of olefins is ranked as follows: X = H < CH_3 < OCH_3.[53] Similarly, activity for alkyne hydrogenation increases with the basicity of the phosphine ligands for precursors of type $[RuH(PR_3)_5]^+$,[44a] while

$RuHCl(CO)(PCy_3)_2$ (**13**) is substantially more active for hydrogenation of polymeric olefins than the corresponding arylphosphine derivative $RuHCl(CO)(PPh_3)_3$.[8a] While relatively few investigations have studied the mechanism and activity of Ru-alkylphosphine hydrogenation catalysts, some evidence suggests that the activity of **13** is mediated by a monophosphine active species (Figure 3.25).[46a] Interestingly, replacement of one PCy_3 ligand of **13** by the more basic ligand IMes (IMes = bis(1,3-(2,4,6-trimethylphenyl)imidazol-2-ylidene) causes a significant *decrease* in activity: at ambient temperature: the hydrogenation activity of **13** is four times that of the IMes derivative $RuHCl(CO)(IMes)(PCy_3)$ (**15**).[46c] By analogy with the hydrogenation behaviour of **13**,[46a] and the metathesis activity of $RuCl_2(IMes)(PCy_3)(CHPh)$,[54] catalysis via **15** is almost certainly initiated by phosphine dissociation. The strongly basic IMes ligand may stabilize the putative Ru(IV) intermediate, $Ru(H)_2Cl(alkyl)(CO)(IMes)$, transforming it into a catalytic sink.*

*The mechanistic picture is almost certainly more complicated in alcohol solvents: results by Ureshini Dharmasena of the Fogg group suggest that substitution of a tricyclohexylphosphine ligand by IMES *can* result in enhanced hydrogenation activity in situations where MeOH cosolvent and NEt_3 are both present.

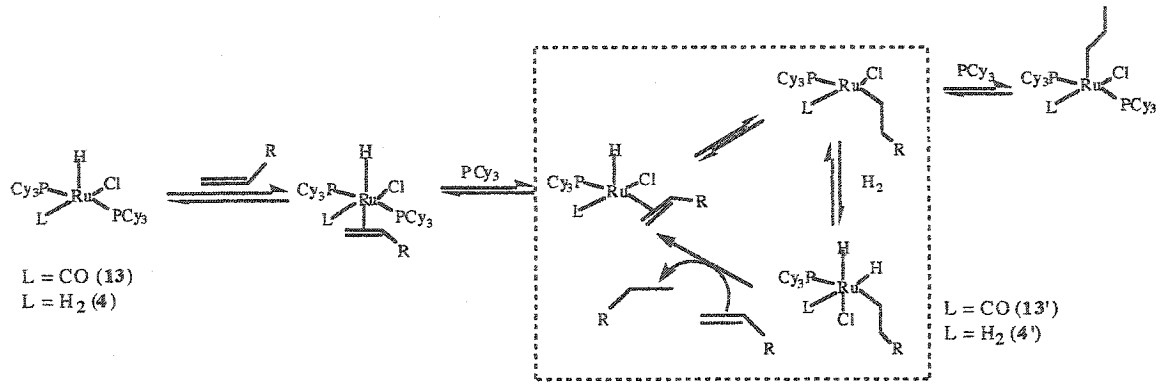

Figure 3.25 Proposed mechanism for catalytic hydrogenation of olefins by **13**,[46a] which may also be applicable to 4.

Wilkinson's-type catalysts $RhCl(PAr_3)_3$, like the Ru-arylphosphine systems, show a positive correlation between arylphosphine basicity and activity for hydrogenation of simple alkenes. Activity increases in the order Ar = C_6H_5 < *p*-C_6H_4Me < *p*-C_6H_4OMe.[55] It falls dramatically, however, on use of highly basic alkylphosphines.* Thus, $RhCl(PEtPh_2)_3$ and $RhCl(PCy_3)_2$ have only half and 1/40 the activity of $RhCl(PPh_3)_3$, respectively.[56] This trend may reflect a balance between the energetics of oxidative addition and reductive elimination: while electron-donating ligands tend to facilitate

* Use of basic alkylphosphine ligands in $[Rh(PP)(diene)]^+$ systems yields highly active hydrogenation catalysts, as exemplified by Rh-DuPHOS systems (PP = chelating diphosphine).[34] Increased hydrogenation activity for these catalysts relative to the related arylphosphine systems can be attributed to operation via an unsaturate mechanism, where formation of hydrido intermediates, if any, does not significantly influence the reaction kinetics.[25] Mechanistic work suggests concerted addition of H_2 in hydrogenation of enamides by these cationic precursors,[57] and indeed this accounts for the observed enantioselectivity in the reduction of prochiral enamides.[58] However, the lack of consensus on this issue is underscored by recent experimental[58] and theoretical work,[60] which postulate involvement of Rh(III) dihydride intermediates in such systems.

oxidative addition of H_2 to the Rh(I) precursor, excessive ligand basicity can stabilize the Rh(III) intermediate to the point that it becomes a catalytic sink (Figure 3.26).[56] In this context, it is worth noting that the Rh(III) dihydride species $RhH_2Cl(PCy_3)_2$ is sufficiently stable to be isolated,[61] while its bis(triphenylphosphine) analog has thus far eluded isolation.[26]

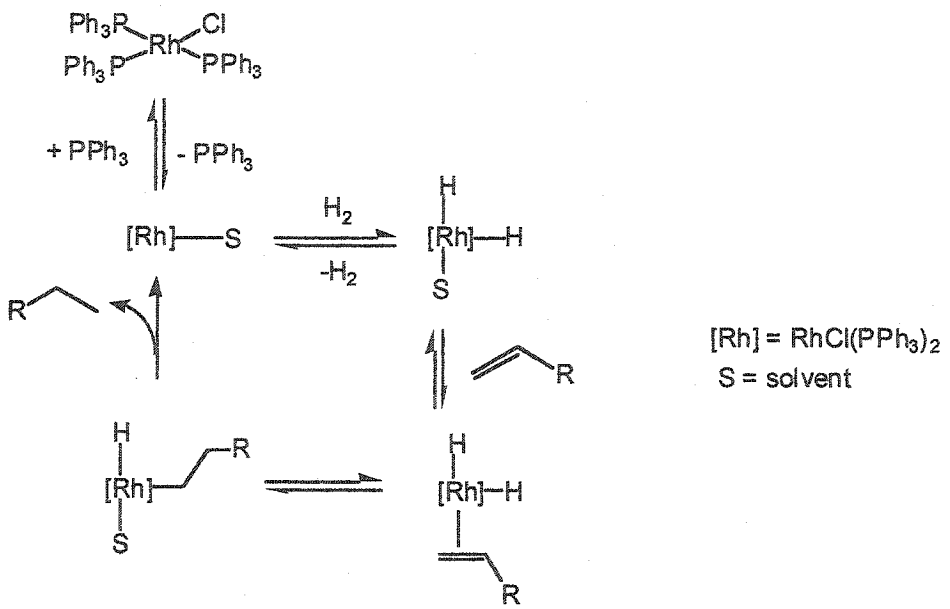

Figure 3.26 Dominant catalytic cycle for hydrogenation of simple olefins via Wilkinsons' catalyst.[26]

The observed rate enhancement associated with the presence of the CO ligand in **13** is more difficult to rationalize. Rates of olefin hydrogenation via Rh and Ir arylphosphine complexes are lowered where π-acid ligands such as CO are present.[25,43]

Proposed causes include an increased activation barrier for oxidative addition of H_2 and/or decreased lability of the phosphine ligands.[25,43] The comparatively low activity of $RuHCl(CO)(PPh_3)_3$ vs. $RuHCl(PPh_3)_3$ for olefin hydrogenation, however, may simply reflect its kinetic stability.[25] In these systems, catalysis is likely initiated by a four-coordinate precursor (Figure 3.27)[26,62] and, in this context, $RuHCl(CO)(PPh_3)_3$ is kinetically disadvantaged by its coordinative saturation.

$$[RuHCl(PPh_3)_3] \rightleftharpoons [RuHCl(PPh_3)_2] + PPh_3$$

$$[RuHCl(PPh_3)_2] + \text{alkene} \rightleftharpoons [Ru(\text{alkyl})Cl(PPh_3)_2]$$

$$[Ru(\text{alkyl})Cl(PPh_3)_2] + H_2 \longrightarrow [RuHCl(PPh_3)_2] + \text{alkane}$$

Figure 3.27. Mechanism for the catalytic hydrogenation of olefins by $RuHCl(PPh_3)_3$.[26,62]

In contrast with $RuHCl(PPh_3)_3$, alkylphosphine complex **13** operates via a monophosphine intermediate (Figure 3.25). This mechanism is invoked to tentatively rationalize the superior activity of **13** vs. **4**. In the case of **4**, the absence of the π-acid CO ligand may yield an excessively stable Ru(IV) intermediate (**4'**, Figure 3.25), which would slow catalysis at the reductive elimination step. Reports of the Ru(IV) dihydride $RuH_2Cl_2(PCy_3)_2$ (**2**, Section 3.2)[18] hint at the thermodynamic stability of such complexes. In the case of the postulated intermediate **4'**, the potential exists for a stabilizing

interaction between the cis-disposed hydride and dihydrogen ligands.[21b] More work on the Ru-PCy_3 systems, including theoretical modeling and kinetic studies, is needed to adequately rationalize the superior catalytic performance of **13** over that of **4**.

3.12 Conclusions

The foregoing describes the facile transformation of metathesis catalyst **1a** into interconvertible dihydride, dihydrogen, and hydridochloro species. Hydrogenolysis of **1a** in hexanes yields the novel dihydrogen complex $RuCl_2(H_2)(PCy_3)_2$ (**3**), which spontaneously precipitates from the reaction mixture, thus circumventing potential complications arising from its thermodynamic instability in solution. This instability includes a tendency to undergo tautomerism to form variable amount of $Ru(H)_2Cl_2(PCy_3)_2$ (**2**), and loss of HCl to afford $RuHCl(H_2)(PCy_3)_2$ (**4**) as the thermodynamic product from H_2/base treatment. Complex **3** is almost certainly implicated in other chemistry of **4**, possibly including catalytic dechlorination of aryl chlorides,[63] but its presence has gone unrecognized, owing to its ^{31}P NMR equivalence with **4**.[20] The stoichiometric chemistry was applied toward the development of a protocol for the catalytic, tandem ROMP / hydrogenation of cycloolefins, demonstrating the use of simple chemical switches to "toggle" between metathesis and hydrogenation catalysis. In the hydrogenation step, the combined effect of methanol cosolvent and base allows

quantitative reduction at one atmosphere H_2. This optimized activity is attributed, in part, to the presence of the active hydrogenation catalyst $RuHCl(CO)(PCy_3)_2$ (**13**). The ability to carry out this hitherto demanding transformation at atmospheric pressures, without specialized equipment, has important implications not only for hydrogenation of unsaturated polymers, but also for the broader field of metathesis chemistry, in which tandem transformations may likewise be carried out on small molecules with great simplicity. The superior hydrogenation activity of complex **13** vs. that of dihydrogen analog $RuHCl(H_2)(PCy_3)_2$ (**4**) is a surprising development in the catalytic chemistry, which will undoubtedly inspire future efforts in the design and optimization of novel Ru hydrogenation catalysts.

Chapter 3 References: p 105

3.13 References

(1) For recent reviews on tandem reactions see: (a) Winkler, J. D. *Chem. Rev.* **1996**, *96*, 167. (b) Parsons, P. J.; Penkett, C. S.; Shell, A. J. *Chem. Rev.* **1996**, *96*, 195. (c) Tietze, L. F. *Chem. Rev.* **1996**, *96*, 115. (d) Denmark, S. E.; Thorarensen, A. *Chem. Rev.* **1996**, *96*, 137.

(2) For recent examples of orthogonal catalysis see: (a) Cossy, J.; Bargiggia, F.; BouzBouz, S. *Org. Lett.* **2003**, *5*, 459. (b) Jeong, N.; Sung, B. K.; Kim, J. S.; Park, S. B.; Seo, S. D.; Shin, J. Y.; In, K. Y.; Choi, Y. K. Pure Appl. Chem. 2002, 74, 85. (c) Cossy, J.; Bargiggia, F. C.; BouzBouz, S. *Tet. Lett.* **2002**, *43*, 6715. (d) Son, S. U.; Park, K. H.; Chung, Y. K. *J. Am. Chem. Soc.* **2002**, *124*, 6838. (e) Komon, Z. J. A.; Diamond, G. M.; Leclerc, M. K.; Murphy, V.; Okazaki, M.; Bazan, G. C. *J. Am. Chem. Soc.* **2002**, *124*, 15280. (f) Yu, H.-B.; Hu, Q.-S.; Pu, L. *J. Am. Chem. Soc.* **2000**, *122*, 6500. (g) Jeong, N.; Seo, S. D.; Shin, J. Y. *J. Am. Chem. Soc.* **2000**, *122*, 10220. (h) Barnhart, R. W.; Bazan, G. C. *J. Am. Chem. Soc.* **1998**, *120*, 1082.

(3) For recent examples of multifunctional tandem catalysis see: (a) Sutton, A. E.; Seigal, B. A.; Finnegan, D. F.; Snapper, M. L. *J. Am. Chem. Soc.* **2002**, *124*, 13390. (b) Motherwell, W. B. *Pure Appl. Chem.* **2002**, *74*, 135. (c) Bielawski, C. W.; Louie, J.; Grubbs, R. H. *J. Am. Chem. Soc.* **2000**, *122*, 12872. (d) Louie, J.; Bielawski, C. W.; Grubbs, R. H. *J. Am. Chem. Soc.* **2001**, *123*, 11312. (e) Watson, M. D.; Wagener, K. B. *Macromolecules* **2000**, *33*, 3196. (f) Wagener, K. B.; Watson, M. D. U.S. Patent 6,107,237, 2000. (g) Chen, Y.; Dujardin, R.; Pielarzik, H.; Franz, U. U. S. Patent 5,932,664, 1997. (h) McLain, S. J.; McCord, E. F.; Arthur, S. D.; Hauptman, E.; Feldman, J.; Nugent, W. A.; Johnson, L. K.; Mecking, S.; Brookhart, M. *Polym. Mater. Sci. Eng.* **1997**, *76*, 246.(i) Borstin, P.; Nielsen, P. *Chem. Commun.* **2002**, 2140.(j) Thadani, A. N.; Rawal, V. H. *Org. Lett.* **2002**, *4*, 4317. (k) Thadani, A. N.; Rawal, V. H. *Org. Lett.* **2002**, *4*, 4321. (l) Choudary, B. M.; Chowdari, N. S.; Jyothi, K.; Kumar, N. S.; Kantam, M. L. *Chem. Commun.* **2002**, 586. (m) Teoh, E.; Campi, E. M.; Jackson, W. R., Robinson, A. J. *Chem. Commun.* **2002**, 978. (n) Evans, P. A.; Robinson, J. E. *J. Am. Chem. Soc.* **2001**, *123*, 4609. (o) Ikeda, S.-I. *Acc. Chem. Res.* **2000**, *33*, 511. (p) Eilbracht, P.; Bärfacker, L.; Buss, C.; Hollmann, C.; Kitsos-Rzychon, B. E.;

Kranemann, C. L.; Rische, T.; Roggenbuck, R.; Schmidt, A. *Chem. Rev.* **1999**, *99*, 3329. (q) Molander, G. A.; Harris, C. R. *Chem. Rev.* **1996**, *96*, 307.

(4) Thompson, L. A.; Ellmann, J. A. *Chem. Rev.* **1996**, *96*, 555.

(5) For recent reviews on olefin metathesis, see: (a) Barrett, A. G. M.; Hopkins, B. T.; Köbberling, J. *Chem. Rev.* **2002**, *102*, 3301. (b) Frenzel, U.; Nuyken, O. *J. Polym. Sci. Part A: Polym. Chem.* **2002**, *40*, 2895. (c) Trnka, T. M.; Grubbs, R. H. *Acc. Chem. Res.* **2001**, *34*, 18. (d) Dragutan, V.; Dragutan, I. *Platinum Metals Rev.* **2001**, *45*, 155. (e) Buchmeiser, M. R. *Chem. Rev.* **2000**, *100*, 1565.(f) Fürstner, A. *Angew. Chem. Int. Ed.* **2000**, *39*, 3012. (g) Schuster, M.; Blechert, S. *Angew. Chem. Int. Ed. Engl.* **1997**, *36*, 2036. (h) Armstrong, S. K. *J. Chem. Soc., Perkin Trans. 1* **1998**, 371.

(6) Zuercher, W. J.; Hashimoto, M.; Grubbs, R. H. *J. Am. Chem. Soc.* **1996**, *118*, 6634.

(7) For examples, see: (a) Creighton, C. J.; Reitz, A. B. *Org. Lett.* **2001**, *3*, 893. (b) Wallace, D. J.; Goodman, J. M.; Kennedy, D. J.; Davies, A. J.; Cowden, C. J.; Ashwood, M. S.; Cottrell, I. F.; Dolling, U.-H.; Reider, P. J. *Org. Lett.* **2001**, *3*, 671. (c) Fürstner, A.; Thiel, O. R.; Kindler, N.; Bartkowska, B. *J. Org. Chem.* **2000**, *65*, 7990.

(8) (a) McManus, N. T.; Rempel, G. L. *J. Macromol. Sci., Rev. Macromol. Chem. Phys.* **1995**, *C35*, 239. (b) Maréchal, E. In *Comprehensive Polymer Science*; Eastmond, G. C., Ledwith, A., Russo, S., Sigwalt, P., Eds.; Pergamon: Toronto, 1989; Vol. 6.

(9) (a) Sohn, B. H.; Gratt, J. A.; Lee, J. K.; Cohen, R. E. *J. Appl. Polym. Sci.* **1995**, *58*, 1041. (b) Yoshida, Y.; Yoshinari, M.; Iko, A.; Komiya, Z. *Polymer J.* **1998**, *30*, 819. (c) Kohara, T. *Macromol. Symp.* **1996**, *101*, 571.

(10) Ivin, K. J.; Mol, J. C. *Olefin Metathesis and Metathesis Polymerization*; Academic Press: San Diego, 1997.

(11) (a)Yamamoto, Y. S., Tadahiro; Takao, T.; Ikeda, K.; Fukuda, T. Japan. Patent 2001027803, 2001. (b) Sunaga, T.; Okita, M.; Asanuma, T. U.S. Patent

6,197,894, 2001. (c) Kamijima, T.; Otsuki, T. Japan. Patent 2001064367, 2001. (d) Bansleben, D. A.; Huynh-Tran, T.-C.; Blanski, R. L.; Hughes, P. A.; Roberts, W. P.; Grubbs, R. H.; Hatfield, G. R. PCT Int. Appl. WO 2000018579, 2000. (e) Suzuki, T.; Obuchi, K.; Tokoro, M. Japan. Patent 11130846, 1999. (f) Sekiguchi, M.; Otsuki, T.; Ishigaki, T. Japan. Patent 2001031744, 2001. (g) Murakami, T.; Tada, M.; Tsunogae, Y. U.S. Patent 5,905,129, 1999. (h) Chen, Y.; Dujardin, R.; Bruder, F.-K.; Rechner, J. U.S. Patent 5,990,246, 1999.

(12) Schulz, D. N. In *Encyclopedia of Polymer Science and Engineering*, Mark, H. F., Bikales, N. M., Overberger, C. G., Menges, G., Kroschwitz, J. I., Eds.; Wiley-Interscience: New York, 1987; Vol. 7.

(13) Schwab, P.; Grubbs, R. H.; Ziller, J. W. *J. Am. Chem. Soc.* **1996**, *118*, 100.

(14) Al-Samak, B.; Amir-Ebrahimi, V.; Carvill, A. G.; Hamilton, J. G.; Rooney, J. J. *Polymer Intl.* **1996**, *41*, 85.

(15) Edwards, H. G. M.; Farrell, D. W.; Johnson, A. F.; Lewis, I. R.; Ward, N. J.; Webb, N. *Macromolecules* **1992**, *25*, 525.

(16) Parshall, G. W.; Ittel, S. D. *Homogeneous Catalysis*; 2nd ed.; Wiley-Interscience: Toronto, 1992.

(17) (a) Kodemura, J.; Natsuume, T. *Polym. J.* **1995**, *27*, 1167. (b) Yi, K. S.; Tenney, L. P.; Lane, P. C.; Wessel, J. V.; Marchant, N. S. US Patent 5,705,572, 1998.

(18) Rodriguez, V.; Sabo-Etienne, S.; Chaudret, B.; Thoburn, J.; Ulrich, S.; Limbach, H.-H.; Eckert, J.; Barthelat, J.-C.; Hussein, K.; Marsden, C. J. *Inorg. Chem.* **1998**, *37*, 3475.

(19) Bemi, L.; Clark, H. C.; Davies, J. A.; Fyfe, C. A.; Wasylishen, R. E. *J. Am. Chem. Soc.* **1982**, *104*, 438.

(20) Christ, M. L.; Sabo-Etienne, S.; Chaudret, B. *Organometallics* **1994**, *13*, 3800.

(21) (a) Bautista, M. T.; Cappellani, E. P.; Drouin, S. D.; Morris, R. H.; Schweitzer, C. T.; Sella, A.; Zubkowski, J. *J. Am. Chem. Soc.* **1991**, *113*, 4876; (b) Jessop, P. G.;

Morris, R. H. *Coord. Chem. Rev.* **1992**, *121*, 155; (c) Maltby, P. A.; Schlaf, M.; Steinbeck, M.; Lough, A. J.; Morris, R. H.; Klooster, W. T.; Koetzle, T. F.; Srivastava, R. C. *J. Am. Chem. Soc.* **1996**, *118*, 5396.

(22) (a) Olivan, M.; Caulton, K. G. *Inorg. Chem.* **1999**, *38*, 566. (b) Wolf, J.; Stüer, W.; Grunwald, C.; Gevert, O.; Laubender, M.; Werner, H. *Eur. J. Inorg. Chem.* **1998**, 1827.

(23) Chaudret, B.; Chung, G.; Eisenstein, O.; Jackson, S. A.; Lahoz, F. J.; Lopez, J. A. *J. Am. Chem. Soc* **1991**, *113*, 2314.

(24) Grunwald, C.; Gevert, O.; Wolf, J.; Gonzalez-Herrero, P.; Werner, H. *Organometallics* **1996**, *15*, 1960.

(25) James, B. R. In *Comprehensive Organometallic Chemistry*; Wilkinson, G., Ed.; Pergamon Press: New York, 1982; Vol. 8, Chapter 51, and references therein.

(26) Chaloner, P. A.; Esteruelas, M. A.; Joo, F.; Oro, L. A. *Homogeneous Hydrogenation*; Kluwer: Boston, 1994.

(27) Crabtree, R. H. *The Organometallic Chemistry of the Transition Metals*; 3rd ed.; Wiley-Interscience: Toronto, 1994.

(28) Esteruelas, M. A.; Lahoz, F. J.; Oro, L. A.; Onate, E.; Ruiz, N. *Inorg. Chem.* **1994**, *33*, 787.

(29) (a) Coalter, J. N.; Bollinger, J. C.; Huffman, J. C.; Werner-Zwanziger, U.; Caulton, K. G.; Davidson, E. R.; Gérard, H.; Clot, E.; Eisenstein, O. *New J. Chem.* **2000**, *24*, 9. (b) Olivan, M.; Clot, E.; Eisenstein, O.; Caulton, K. G. *Organometallics*, **1998**, *17*, 3091.

(30) Katayama, H.; Ozawa, F. *Organometallics* **1998**, *17*, 5190.

(31) Beatty, R. P.; Paciello, R. A., U. S. Patent 5,554,778, 1996.

(32) Nguyen, S. T.; Grubbs, R. H.; Ziller, J. W. *J. Am. Chem. Soc* **1993**, *115*, 9858.

(33) Sanford, M. S.; Ulman, M.; Grubbs, R. H. *J. Am. Chem. Soc.* **2001**, *123*, 749.

(34) Burk, M. J.; Martinez, J. P.; Feaster, J. E.; Cosford, N. *Tetrahedron* **1994**, *50*, 4399.

(35) Nevstad, G. O.; Sontad, J. *J. Acta. Chem. Scand.* **1984**, *B 38*, 469.

(36) Mas, M.; Sola, J.; Solans, X.; Aguilo, M. *Inorg. Chim. Acta* **1987**, *133*, 217.

(37) Hillmyer, M. A.; Laredo, W. R.; Grubbs, R. H. *Macromolecules* **1995**, *28*, 6311.

(38) Polymer characterization data are summarized in Appendix A.

(39) Fürstner, A.; Thiel, O. R.; Lehmann, C. W. *Organometallics* **2002**, *21*, 331, and references threrein.

(40) Maughon, B. R.; Grubbs, R. H. *Macromolecules* **1997**, *30*, 3459.

(41) (a) Böhm, L. L.; Enderle, H. F.; Fleissner, M. In *Catalyst Design for Tailor-Made Polyolefins*; Elsevier: Amsterdam, 1994; p. 351. (b) Marechal, P. EP 1083183, 2001.

(42) Wilhelm, T. E.; Belderrain, T. R.; Brown, S. N.; Grubbs, R. H. *Organometallics* **1997**, *16*, 3867.

(43) James, B. R. *Homogeneous Hydrogenation*; John Wiley & Sons: Toronto, 1973.

(44) See, for example: (a) Nkosi, B. S.; Coville, H. J.; Albers, M. O.; Gordon, C.; Viney, M.; Singleton, E. *J. Organomet. Chem.* **1990**, *386*, 111. (b) Fogg, D. E.; James, B. R.; Kilner, M. *Inorg. Chim. Acta* **1994**, *222*, 85. (c) Zanetti, N. C.; Spindler, F.; Spencer, J.; Togni, A.; Rihs, G. *Organometallics* **1996**, *15*, 860. (d) Bianchini, C.; Barbaro, P.; Scapacci, G.; Zanobini, F. *Organometallics* **2000**, *19*, 2450.

(45) (a) Lynn, D. M.; Mohr, B.; Grubbs, R. H. *J. Am. Chem. Soc.* **1998**, *120*, 1627. (b) Dias, E. L. Ph. D. Thesis, California Institute of Technology, 1998.

(46) (a) Yi, C. S.; Lee, D. Y. *Organometallics* **1999**, *18*, 5152. (b) Yi, C. S.; Lee, D. W.; He, Z. *Organometallics* **2000**, *19*, 2909. (c) Lee, H. M.; Smith, D. C.; He, Z.; Stevens, E. D.; Yi, C. S.; Nolan, S. P. *Organometallics* **2001**, *20*, 794. (d) Yi, C. S.; Lee, D. W.; Chen, Y. *Organometallics* **1999**, *18*, 2043.

(47) *Inorganic Reactions and Methods*; Zuckerman, J. J., Ed.; VCH, 1987; Vol. 2.

(48) Dinger, M. B.; Mol, J. C. *Organometallics* **2003**, *22*, 1089.

(49) (a) Chen, Y.; Chan, W. C.; Lau, C. P.; Chu, H. S.; Lee, H. L.; Jia, G.*Organometallics*, **1997**, *16*, 1241. (b) Coalter, J. N.; Huffman, J. C.; Caulton, K. G. *Organometallics*, **2000**, *19*, 3569. (c) Marchenko, A. V.; Huffman, J. C.; Valerga, P.; Tenorio, M. J.; Puerta, M. C.; Caulton, K. G. *Inorg. Chem.*, **2001**, *40*, 6444. (d) Chaudret B. N.; Cole-Hamilton, D. J.; Nohr, R. S.; Wilkinson, G. *J. Chem. Soc., Dalton Trans.*, **1977**, 1546. (e) Van Der Sluys, L. S.; Kubas, G. J.; Caulton, K. G. *Organometallics*, **1991**, *10*, 1033.

(50) Coalter, J. N.; Caulton, K. G. *New J. Chem.* **2001**, *25*, 679.

(51) Louie, J.; Grubbs, R. H. *Organometallics* **2002**, *21*, 2153.

(52) Rempel, G. L.; McManus, N. T.; Mohammadi, N., EP 455154, 1991.

(53) James, B. R. In *Adv. Organomet. Chem.*; Stone, F. G. A., West, R., Eds.; Academic Press: New York, 1979; Vol. 17.

(54) Sanford, M. S.; Love, J. A.; Grubbs, R. H. *J. Am. Chem. Soc.* **2001**, *123*, 6543.

(55) O'Connor, C.; Wilkinson, G. *Tet. Lett.* **1969**, *18*, 1375.

(56) Simpson, M. C.; Cole-Hamilton, D. J. *Coord. Chem. Rev.* **1996**, *155*, 163.

(57) Halpern, J.; Riley, D. P.; Chan, A. S.; Pluth, J. J. *J. Am. Chem. Soc.* **1977**, *99*, 8055.

(58) Brown, J. M.; Chaloner, P. A.; Parker, D. In *Catalytic Aspects of Metal Phosphine Complexes*; Alyea, E. C., Meek, D. W., Eds.; American Chemical Society: Washington, D. C., 1982; Vol. 196.

(59) Brown, J. M.; Giernoth, R. *Current Opinion in Drug Discovery & Development* **2000**, *3*, 825, and references therein.

(60) Landis, C. R.; Feldgus, S. *Angew. Chem. Int. Ed.* **2000**, *39*, 2863.

(61) Van Gaal, H. L. M.; Moers, F. G.; Steggerda, J. J. *J. Organomet. Chem.* **1974**, *65*, C43.

(62) James, B. R. *Inorg. Chim. Acta Rev.* **1970**, 73.

(63) Cucullu, M. E.; Nolan, S. P.; Belderrain, T. R.; Grubbs, R. H. *Organometallics* **1999**, *18*, 1299.

CHAPTER 4

Reactions of Electron-Rich Chlororuthenium Vinylidenes with Perfluorophenoxide

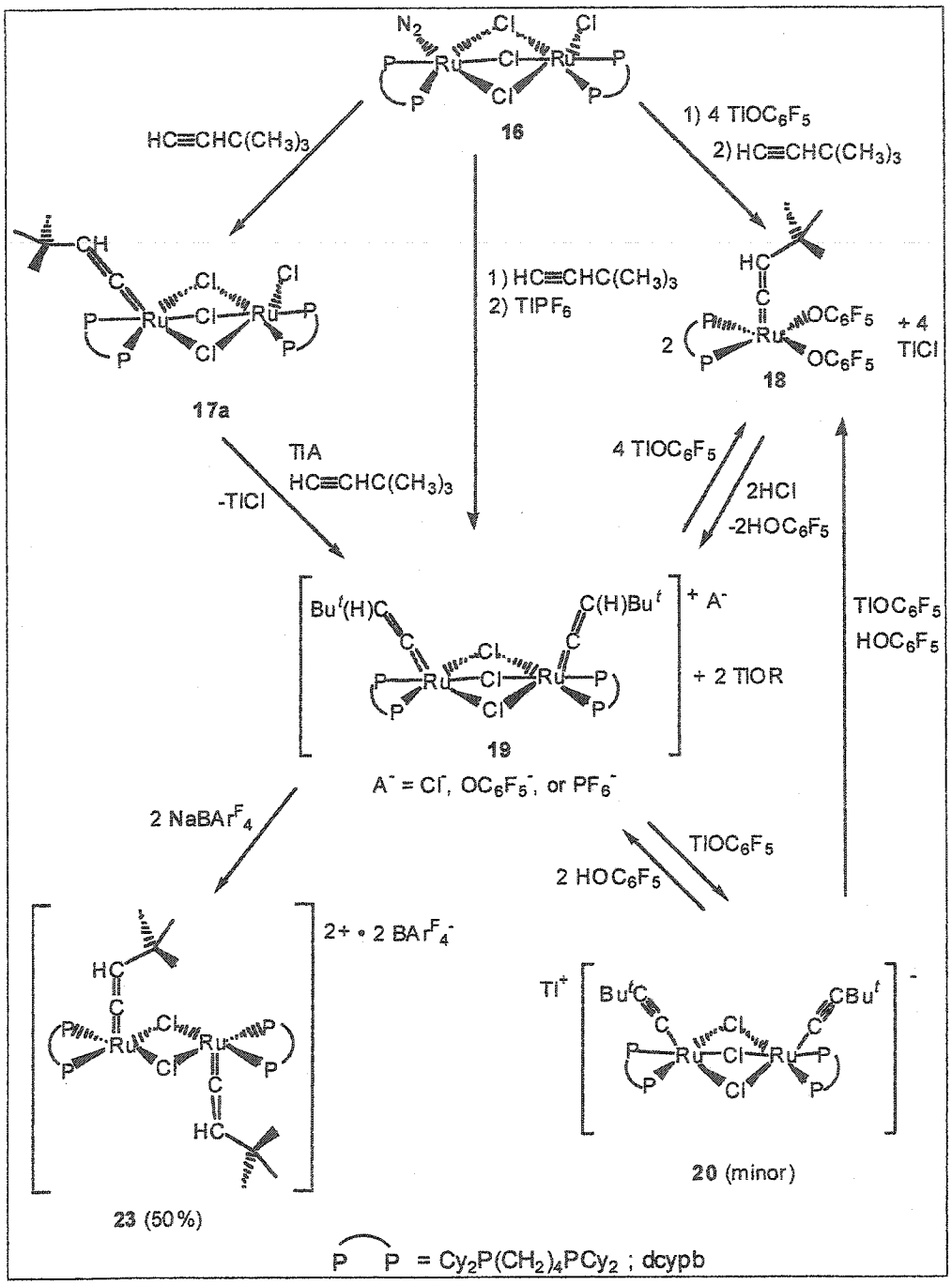

Figure 4.1. Pictorial summary of Chapter 4.

4.1. Introduction and Background

The susceptibility of choloruthenium metathesis catalysts to dimerization, forming very stable $Ru_2(\mu\text{-}Cl)_3$ structures, was outlined in Section 1.5. Related work shows that trichloride-bridged monovinylidene complexes **17a** and **17b** (Figure 4.2) are the sole products from reaction of **16** with terminal alkynes.[1] The absence of either mononuclear or the *disubstituted* dinuclear derivatives may be a function of the low solubility of **16**, or, alternatively, it may reflect bimolecular deactivation. This chapter describes an effort to drive this chemistry beyond the $Ru_2(\mu\text{-}Cl)_3$ motif, by replacing the chloride ligands by "pseudohalide" aryloxides.

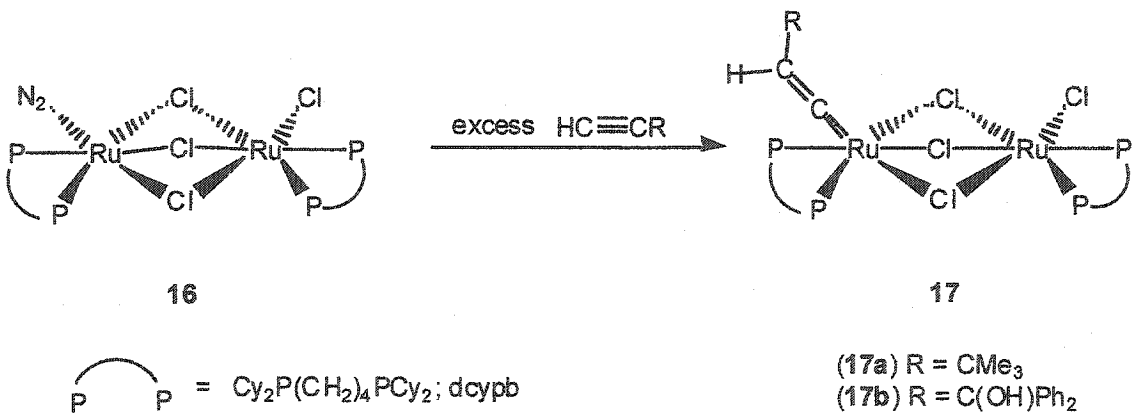

Figure 4.2 Preparation of the monovinylidene dinuclear complexes **17a**, **17b**.[1]

4.1.1. Pseudohalide Ligands

Alkoxide groups have been used (albeit rarely) as pseudohalide ligands in the design of novel Ru-alkylidenes.[2] Recent reports describe the replacement of both chlorides in $RuCl_2(CHPh)(PCy_3)_2$ (**1a**) to yield four-coordinate bis(alkoxide) species

$Ru(OR)_2(CHPh)(PCy_3)$ (R = Bu^t, Ad;[2a] R = $C(CF_3)_3$, $C(CF_3)_2(CH_3)$[2b]), all with a nominal 14-valence electron count. Despite the coordinative unsaturation of these complexes, metathesis activity was near zero, probably owing to the substantial three-dimensional bulk of the alkoxide ligands. While aryloxide ligands are attractive for their attenuated (and tunable) steric bulk, their tendency to bind to ruthenium in an η^5-ArO fashion[3] may limit their ability to function as pseudohalide ligands. Perfluorophenoxides represent a promising and little explored variant on the aryloxide motif: their attenuated π-donor capacity appears to permit σ–bonding to Ru(II), even within coordinatively unsaturated species.[4,5] Use of pentafluorophenoxide ligands in the design of novel ruthenium metathesis catalysts is explored herein. Vinylidene complexes are targeted in lieu of alkylidenes, because preliminary evidence suggested that the latter can be susceptible to deprotonation by phenoxide ligands. For example, the short-lived phenoxo benzylidene species $Ru(OPh)_2(P^iPr_3)_2(CHPh)$, spontaneously extrudes phenol to yield the carbyne derivative $Ru(OPh)(P^iPr_3)_2(\equiv CPh)$.[2a,6]

4.1.2. Ru Vinylidene Complexes

Recent work on Ru-based catalysts has exploited the stability, accessibility, and versatility of vinylidene complexes, which catalyze a range of organic transformations, including olefin metathesis and alkyne coupling reactions.[7] Single-component ruthenium

metathesis catalysts bearing a vinylidene ligand show activity under aerobic conditions[8a] and in the presence of polar functional groups, including water.[8b] Initiation is invariably slower than for their alkylidene counterparts; in the context of ROMP, this difference is manifested by high molecular weights and broad polydispersities (PDIs).[1,8c-f] It is worth noting that this kinetic profile need not disqualify Ru-vinylidenes from the arena of useful ROMP catalysts, as control over molecular weights can be achieved by addition of chain-transfer agents (CTA).[9] Moreover, broad or polymodal PDIs are sometimes desirable for ease of processing.[10]

The convenience of terminal alkynes for installation of vinylidene ligands is well documented in the literature,[7] and has proven particularly useful in the efficient preparation of novel Ru metathesis catalysts.[8] Reaction involves initial formation of a π-alkyne intermediate and subsequent tautomerization to the vinylidene structure, which, for Ru(II) complexes, most likely occurs via a 1,2-hydrogen shift (Figure 4.3).[7b,11]

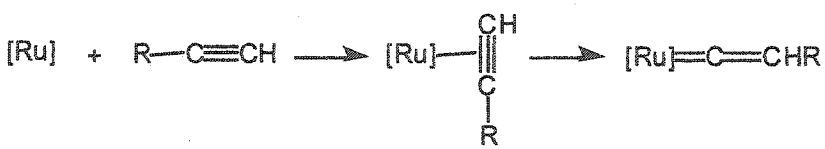

Figure 4.3 Formation of Ru(II) vinylidene complexes from terminal alkynes.

This chapter describes the synthesis and characterization of a Ru-vinylidene ROMP initiator bearing dcypb and two perfluorophenoxide ligands; the latter act as σ-

binding pseudohalides, affording access to a mononuclear structure which is inaccessible for the dichloro analogue. Stoichiometric protonolysis of coordinated perfluorophenoxide is described, as well as ROMP activity of selected, catalytically-relevant complexes.

4.2. $Ru(OC_6F_5)_2[C{=}CH(Bu^t)](dcypb)$ (18)

In chlorobenzene solution, sequential treatment of **16** with 4 equiv $TlOC_6F_5$ and excess 3,3-dimethyl-1-butyne affords mononuclear vinylidene complex $Ru(OC_6F_5)_2[=C=CH(Bu^t)](dcypb)$ (**18**, Figure 4.4) in ~80% isolated yield. The order of reagent addition can be reversed without sacrificing product yield or purity, though reaction is much slower (19 d vs. 19 h) owing to formation of a particularly stable face-bridged dinuclear intermediate (Section 4.4). Attempts to cleanly generate a *mono*perfluorophenoxide vinylidene complex by use of two equiv $TlOC_6F_5$ instead of four were unsuccessful: disproportionation resulted, with low yields of product **18** (< 30%, isolated).

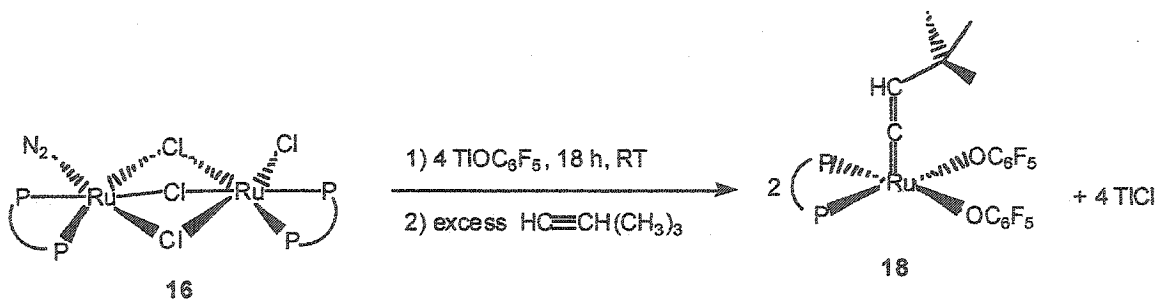

Figure 4.4 One-pot preparation of $Ru(OC_6F_5)_2[=C=CH(Bu^t)](dcypb)$ (**18**).

The identity of **18** is supported by microanalysis, detailed spectroscopic data, and X-ray crystallography. The IR spectrum shows a strong C=C stretching band at 1637 cm^{-1}, and the vinylidene ligand also gives rise to a $^{13}C\{^1H\}$ NMR triplet at δ_C 334.9. In the ^1H NMR spectrum, the vinylidene proton is seen as a triplet at 3.57 ppm ($^4J_{HP}$ = 3.3 Hz), which collapses to a singlet in the $^1H\{^{31}P\}$ NMR spectrum. The singlet at 50.0 ppm in the ^{31}P NMR spectrum suggests the chemical equivalence of both phosphorus nuclei, each trans to a perfluorophenoxide ligand.

4.3. Molecular structure of Ru(OC$_6$F$_5$)$_2$[=C=CH(Bu^t)](dcypb) (18)

X-ray quality crystals of **18** were obtained by slow evaporation of a CH_2Cl_2/C_6H_6 solution. The structure is a distorted square pyramid with the vinylidene ligand in the apical position (Figure 4.5). Selected bond distances and angles are listed in Table 4.1.

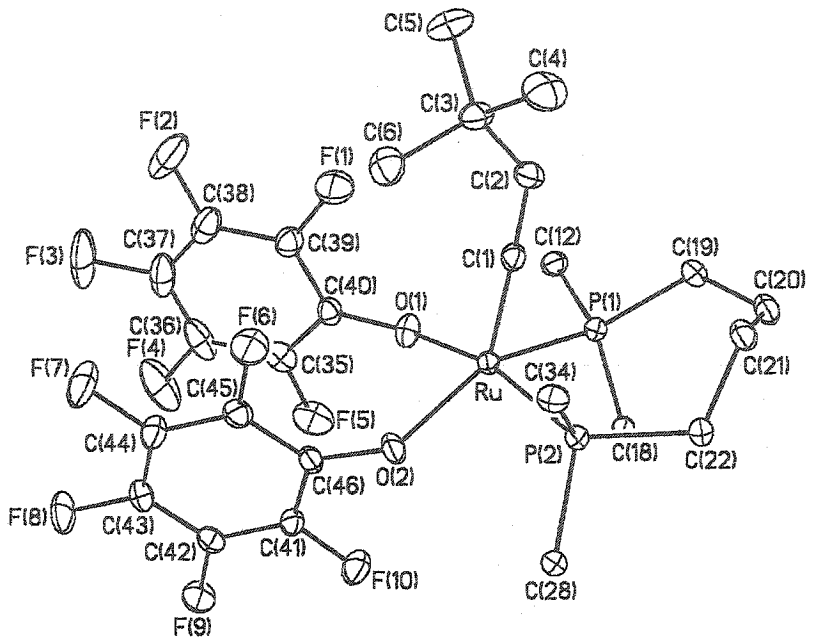

Figure 4.5 ORTEP diagram for $Ru(OC_6F_5)_2[=C=CH(Bu^t)](dcypb)$ (**18**). Thermal ellipsoids are shown at the 30% probability level. For clarity, each cyclohexyl group is abbreviated to a single carbon and hydrogen atoms are omitted.

The wide P(1)-Ru-P(2) bite angle (98.45(2)°) is consistent with that found in other Ru-dcypb complexes, and attests to the steric demand of the dcypb ligand.[1,12,13] Both Ru-O bonds tilt toward the vacant site, and the O atoms are displaced by 14° and 34° out of the sterically congested P-Ru-P plane. Alignment of the two perfluorophenoxide groups deviates only slightly from coplanarity, by 9.3°, while the centroid-to-centroid distance of 3.28 Å suggests a π-stacking interaction, by comparison with the interlamellar distance in graphite (3.354 Å).[14] The Ru-C(1) bond distance of 1.793(2) Å is comparable to other

Ru-vinylidene complexes, including $RuBr_2[=C=C(H)Bu^t](PPh_3)_2$ (1.768(17) Å),[11] and $\{RuCl[=C=C(H)Ph][\kappa^2(P,O)\text{-}Pr^i_2PCH_2CH_2OMe]_2\}^+OTf^-$ (1.7903 Å).[15] The Ru-O bond lengths (2.1260(18) and 2.0342(16) Å) are similar to values for the *p*-methylphenoxide complexes $Ru(H)(OC_6H_4\text{-}p\text{-}Me)(CO)(PMe_3)_3$ (2.108(6) Å)[16a] and cis-$Ru(H)(OC_6H_4\text{-}p\text{-}Me)(PMe_3)_4$ (2.145(6) Å),[16b] as are the Ru-O-C angles (average 133.7°).

Table 4.1 Selected bond lengths (Å) and angles (deg) for $Ru(OC_6F_5)_2[=C=CH(Bu^t)](dcypb)$ (**18**).

Bond Distances (Å)		Bond Angles (deg)	
Ru-P(1)	2.3309(7)	P(1)-Ru-P(2)	98.45(2)
Ru-P(2)	2.3143(6)	O(1)-Ru-O(2)	88.21(7)
Ru-C(1)	1.793(2)	O(2)-Ru-P(1)	150.38(6)
Ru-O(1)	2.1260(18)	O(1)-Ru-P(1)	84.85(5)
Ru-O(2)	2.0342(16)	O(2)-Ru-P(2)	82.31(5)
C(1)-C(2)	1.316(3)	O(1)-Ru-P(2)	166.16(6)
O(1)-C(40)	1.305(3)	C(1)-Ru-P(1)	85.49(7)
O(2)-C(46)	1.326(3)	C(1)-Ru-P(2)	90.19(8)
		C(2)-C(1)-Ru	177.6(2)
		Ru-O(1)-C(40)	134.59(17)
		Ru-O(2)-C(46)	132.81(15)
		C(1)-C(2)-C(3)	130.2(2)

4.4. Protonolysis of $Ru(OC_6F_5)_2[=C=CH(Bu^t)](dcypb)$ (18)

Attempts to generate a monochloro complex from **18** by protonolysis with stoichiometric amounts of HCl resulted in disproportionation. ^{31}P NMR analysis revealed 50% conversion to a new chlorinated species, $[\{Ru[=C=C(H)Bu^t](dcypb)\}_2(\mu\text{-}Cl)_3]Cl$

(**19•Cl**) (δ_P 44.4, 43.2, ABq, J_{PP} = 26 Hz). Addition of a second equivalent of HCl completed transformation into **19•Cl** (Figure 4.6, Route A). These experiments gave no evidence of competitive protonation of the vinylidene ligands in **18** or **19•Cl**; reactivity in related work yields cationic carbyne derivatives.[7b,17b] The structure of **19•Cl** is assigned on the basis of spectroscopic evidence, buttressed by microanalytical data for its PF_6 salt. Thus, exchange of the chloride counterion in **19•Cl** by $TlPF_6$ yields an insoluble precipitate (TlCl) and **19•PF$_6$**, with no change in the characteristic ^{31}P NMR resonance. Complex **19•PF$_6$** can also be prepared by addition of $TlPF_6$ to a solution containing **17a** and excess 3,3-dimethyl-1-butyne (Figure 4.6, Route B).

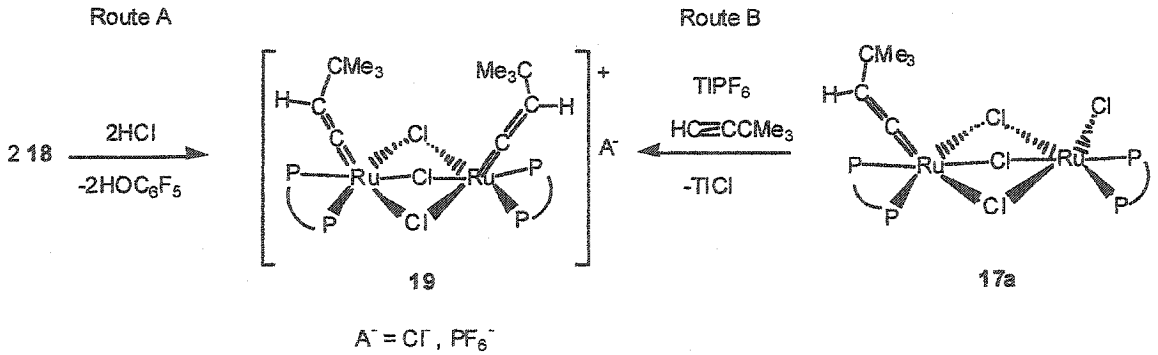

Figure 4.6 Preparation of [{Ru[=C=C(H)Bu^t](dcypb)}$_2$(μ-Cl)$_3$]$^+$ (**19**) via two different routes.

Complexes **19•Cl** and **19•PF$_6$** are essentially identical by IR and NMR spectrosopy, neglecting counter-ion resonances. Infrared analysis shows a strong C=C stretching vibration at 1636 cm^{-1}. ^{1}H NMR analysis reveals a triplet for the vinylidene

proton at δ_H 3.37 ($^4J_{HP}$ = 3.9 Hz), which collapses to a singlet following ^{31}P decoupling. A sharp singlet due to the *tert*-butyl protons, at δ_H 1.22, is visible above the broad, unresolved dcypb peaks (1.17 – 2.71 ppm). In the $^{13}C\{^1H\}$ NMR spectrum, the vinylidene α-carbon is represented by a characteristically low-field triplet at δ_C 356.8 ($^2J_{CP}$ = 19 Hz), and C_β is observed at δ_c 120. In the $^{31}P\{^1H\}$ NMR spectrum, two mutually coupled, inequivalent phosphorus centres appear as an AB quartet at δ_P 44.3 and 43.2 ($^2J_{PP}$ = 26 Hz); this type of ^{31}P NMR pattern is common for trichloride-bridged Ru complexes bearing chelating diphosphine ligands (Chapter 5). A high field septet for the PF_6 counter-ion is also observed at δ_P -144.1 (J_{PF} = 705 Hz) for **19•PF$_6$**. Formulation as a dinuclear species is supported by electrospray mass spectrometric data for **19•Cl**, which shows the molecular ion peak for the cation at *m/z* 1409. Attempts to confirm the presence of the presumed chloride counterion of **19•Cl** by microanalysis were frustrated by the presence of variable amounts of residual pentafluorophenol, observed by ^1H (δ_H 9.62, br, O*H*) and ^{19}F NMR (δ_F -84.62, -90.61, -96.43) analysis, despite repeated recrystallizations. Retention of perfluorophenol is attributed to hydrogen-bonding a very common feature in phenol coordination chemistry.[18a,19]

Cation **19** is also observed with an aryloxide counterion in the one-pot preparation of **18** from **16** involving addition of alkyne prior to $TlOC_6F_5$ (Figure 4.7). Indeed, the slow rate of formation of **18** by this route (~8 d for complete conversion at RT) is

attributed to the relative inertness of the $Ru_2(\mu\text{-}Cl)_3$ entity in **19**, as discussed further in the next section. Identification of **19**•OC_6F_5 is based on observation of the characteristic ^{31}P NMR resonance for **19**. Small amounts of alkynyl complex **20** (~ 11%, δ_P 55, Section 4.7), a conjugate base of **19**, are also observed during the reaction. When the reaction mixture is stirred for prolonged periods (~ 19 d at RT), **19** and **20** are replaced entirely by mononuclear **18** (δ_P 50.0). Formation of **19**•OC_6F_5 is attributed to thallium-induced abstraction of the terminal chloride from intermediate **17a**, and subsequent coordination/rearrangement of the alkyne.

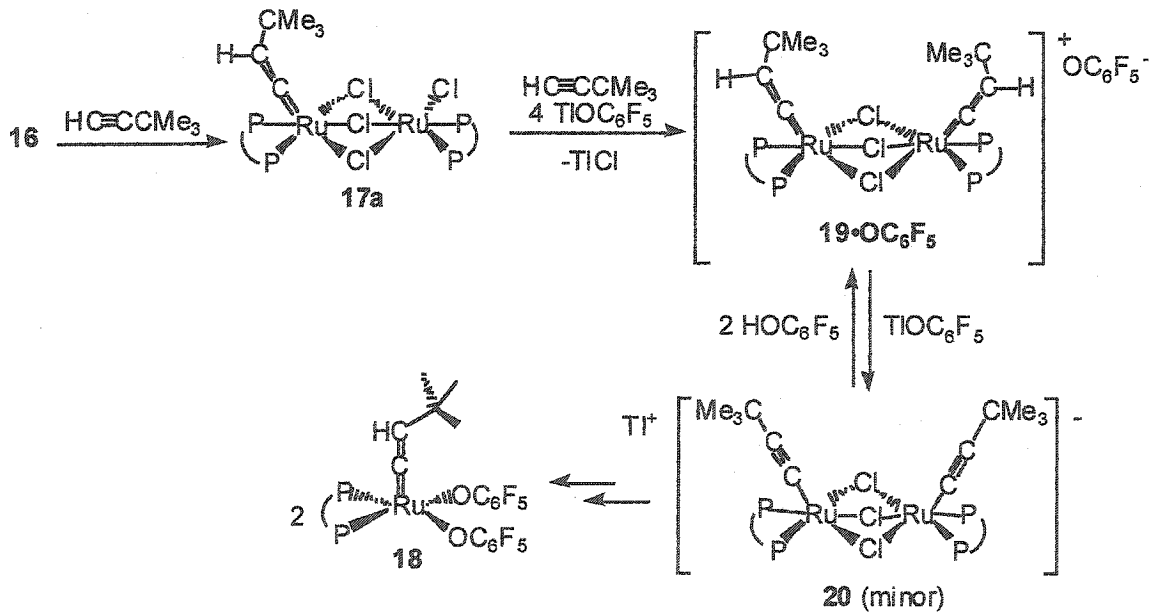

Figure 4.7 Dinuclear species **19**•OC_6F_5: an intermediate in the preparation of **18**.

4.5. Robustness of the Trichloride Bridging Unit

4.5.1. Carbonylation of [{Ru[C=C(H)Bu^t](dcypb)}$_2$(μ-Cl)$_3$]Cl (19)

The vinylidene ligand in **19•Cl** can be displaced by CO (Figure 4.8), as found for other vinylidene complexes.[7,8b,20] The substitution is thought to occure via vinylidene to *t*-butylacetylene retrotautomerization, and decoordination of alkyne.[8b] Thus, refluxing **19•Cl** under CO in chlorobenzene produced, as the major product, dinuclear carbonyl complex [{Ru(dcypb)(CO)}$_2$(μ-Cl)$_3$]$^+$Cl$^-$ (**21a**, 43% by ^{31}P NMR analysis). Full characterization of **21a**, which is isostructural with **19•Cl**, is detailed in Chapter 5. It is surprising, given the abundance of CO and the prolonged reaction time (48 h), that bis-CO complex[12] RuCl$_2$(CO)$_2$(dcypb) (**22**, 33%) is but a *minor* product under these reaction conditions. This contrasts with the extensive body of literature describing the preferential and irreversible formation of mononuclear bis-carbonyl complexes on treatment of Ru(II)-phosphine complexes with CO.[21] Examples from arylphosphine chemistry include carbonylation of dinuclear trichloride bridged structures.[22c] Chapter 5 of this thesis discusses the relationship between products **21a** and **22**.

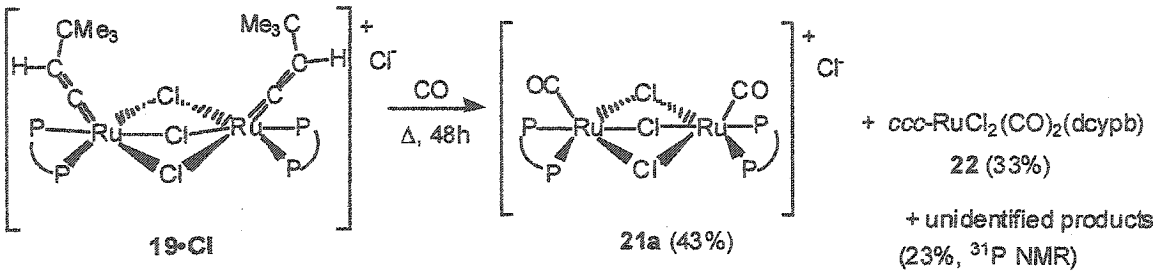

Figure 4.8 Carbonylation of $[\{Ru[C{=}C(H)Bu^t](dcypb)\}_2(\mu\text{-}Cl)_3]^+Cl^-$ (**19•Cl**).

4.5.2. Slow Chloride Abstraction from 19

The stability of the trichloride bridging unit in **19** is manifested in its low reactivity toward chloride-abstracting agents such as $TlPF_6$ or $NaBAr^F_4$. For example, preparation of **19•PF$_6$** by the anion-exchange reaction between **19•Cl** and $TlPF_6$ (Section 4.4) proceeds cleanly, with no evidence of byproducts, even on use of excess $TlPF_6$ (4 h, RT, chlorobenzene). Chloride abstraction does occur, albeit slowly, on prolonged reaction of **19•PF$_6$** with 2 equiv $NaBAr^F_4$. Conversion to a single product (30% after 44 h at RT) is indicated by appearance of a sharp singlet at δ_P 52.4 in the ^{31}P NMR spectrum. The product is identified as edge-bridged **23** (Figure 4.9) on the basis of spectroscopic and X-ray analysis of crystals that deposited from CH_2Cl_2 solution. Attempts to purify the product for microanalysis via reprecipitation were hindered by poor solubility in common solvents.

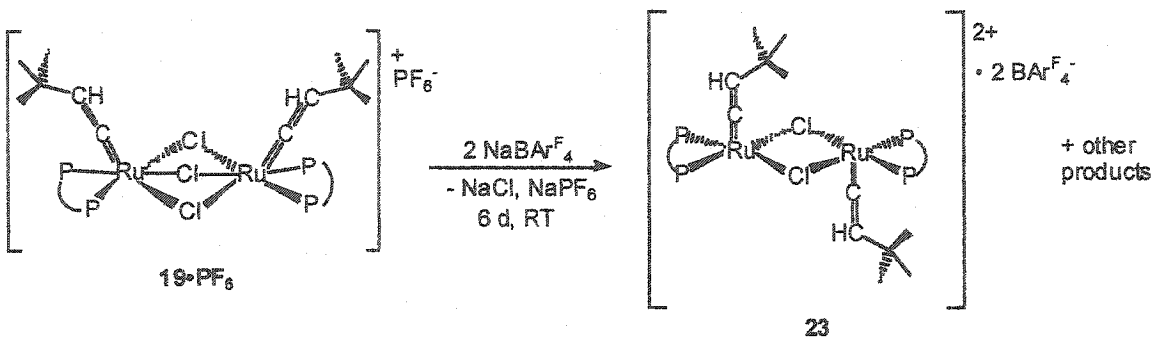

Figure 4.9 Slow chloride abstraction from **19•PF$_6$**.

Crystals of **23** were isolated, dried and crushed to a powder for further spectroscopic analysis. Infrared spectroscopy of the crude product shows a new C=C stretching band at 1610 cm^{-1} alongside that for the starting material ($\nu_{C=C}$ for **19•PF$_6$**: 1638 cm^{-1}). The presence of residual **19•PF$_6$** is confirmed by ^{31}P NMR analysis (ca. 30%) which also shows several unassigned peaks (δ_P 45-47) accompanying the singlet for the dication of **23** at δ_P 52.4 (50% of total integrated intensity). Observation of a singlet for **23** is consistent with crystallographic data, which reveal two cis-disposed, equivalent phosphine ligands. In the ^{1}H NMR spectrum, the vinylidene proton of **23** appears as a broad triplet at 4.13 ppm (J_{HP} = 3 Hz) and the presence of residual **19•PF$_6$** is evidenced by its characteristic triplet at δ_H 3.37. Poor solubility precluded ^{31}C NMR analysis.

4.6. Molecular Structure of $[\{Ru[C=C(H)Bu^t](dcypb)\}_2(\mu\text{-}Cl)_2]^{2+} \cdot 2\{BAr^F{}_4\}^-$ (23).

Single crystal X-ray analysis of **23** confirms the dinuclear structure. An ORTEP diagram is shown in Figure 4.10, selected bond lengths and angles in Table 4.2. The structure contains a C_2 axis, which relates the two metal centres. two symmetry-related metal centres. Each occupies a square pyramidal coordination environment, with apical vinylidene ligands in a transoid relationship. The vacant sites are unhindered by agostic interactions. The Cl-Ru-Cl bond angle of 76.28(4)° manifests compression of the bridging edge, opposite the expanded bite angle of the diphosphine ligand (P-Ru-P = 98.76(4)°), the latter feature being common for the bulky ligand dcypb (*vide supra*). The Ru-C(1) bond length (1.798(4) Å) is typical of Ru-vinylidenes, as is the C(1)-C(2) bond distance of 1.308(6) Å (*vide supra*).The average Ru-Cl (2.48 Å) and Ru-P (2.34 Å) bond lengths are consistent with those in the dicationic alkylidene dimer $[\{Ru(=CH\text{-}CH=CMe_2)(\kappa^2\text{-}dtbpm)\}_2(\mu\text{-}Cl)_2]^{2+}$ (2.49 Å and 2.33 Å, respectively).[23]

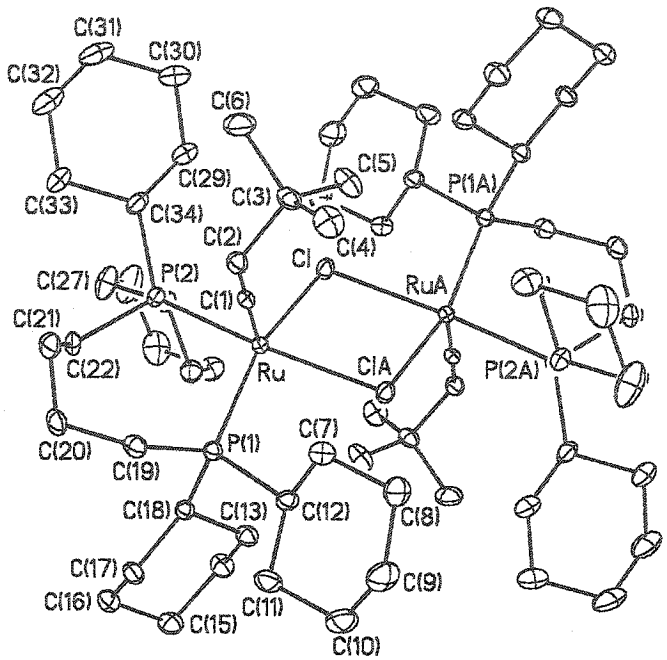

Figure 4.10 ORTEP diagram of $[\{Ru(C{=}CH^tBu)(dcypb)\}_2(\mu\text{-}Cl)_2]^{2+}$ ($\mathbf{23}^{2+}$). Thermal ellipsoids shown at 30% probability level. For clarity, hydrogen atoms and $BAr^F{}_4^-$ counterions are omitted.

Table 4.2 Selected bond lengths (Å) and angles (deg) for **23**.

Bond Distances (Å)		Bond Angles (deg)	
Ru-C(1)	1.798(4)	C(1)-Ru-P(2)	89.06(13)
Ru-P(2)	2.3210(12)	C(1)-Ru-P(1)	86.98(13)
Ru-P(1)	2.3594(12)	P(2)-Ru-P(1)	98.76(4)
Ru-Cl	2.4500(12)	C(1)-Ru-Cl	108.66(13)
Ru-Cl#1	2.5159(11)	P(2)-Ru-Cl	90.70(4)
C(1)-C(2)	1.308(6)	P(1)-Ru-Cl	161.94(4)
		C(1)-Ru-Cl#1	104.01(14)
		P(2)-Ru-Cl#1	163.85(4)
		P(1)-Ru-Cl#1	91.46(4)
		C(2)-C(1)-Ru	178.4(4)
		Cl-Ru-Cl#1	76.28(4)

4.7. Isolation of a σ-acetylide Intermediate Complex

As briefly noted in Section 4.4, σ-acetylide Tl[{Ru(C≡CBu^t)(dcypb)}$_2$(μ-Cl)$_3$] (**20**) can form as an intermediate in the preparation of **18**. On reaction of **19** with < 4 equiv $TlOC_6F_5$ in THF solvent, **20** was isolated in low yield (ca. 16%) and characterized by spectroscopy and X-ray crystallography.

The C≡C group gives rise to a sharp IR band at 2044 cm^{-1}. In the ^{13}C NMR spectrum, a broad singlet for the α-C is observed at 129 ppm. Phosphine fluxionality is implied by the breadth of the ^{31}P NMR singlet at δ_P 56.0. Such dynamic behaviour is common for solvated Ru$_2$(μ-Cl)$_3$ structures bearing a chelating diphosphine ligand (Chapter 5). The *tert*-butyl CH_3 groups appear as a characteristically sharp singlet at 1.41 ppm rising above the cyclohexyl envelope in the ^{1}H NMR spectrum.

Formation of **20** is attributed to deprotonation of **19** by $TlOC_6F_5$ (Figure 4.11). This type of reaction is common in the chemistry of vinylidene complexes;[7b] recent work suggests that deprotonation at the β-carbon is an essential step in the activation of Ru-vinylidene complexes toward catalytic coupling[24] and stoichiometric hydration[25] of terminal alkynes. Yields of **20** are limited by reprotonation of **19** by the perfluorophenol co-product, and nucleophilic substitution, to form Ru(OC$_6$F$_5$)$_2$(dcypb)[C=CH(Bu^t)] (**18**, Figure 4.11, R = C_6F_5), and insoluble TlCl coproduct.

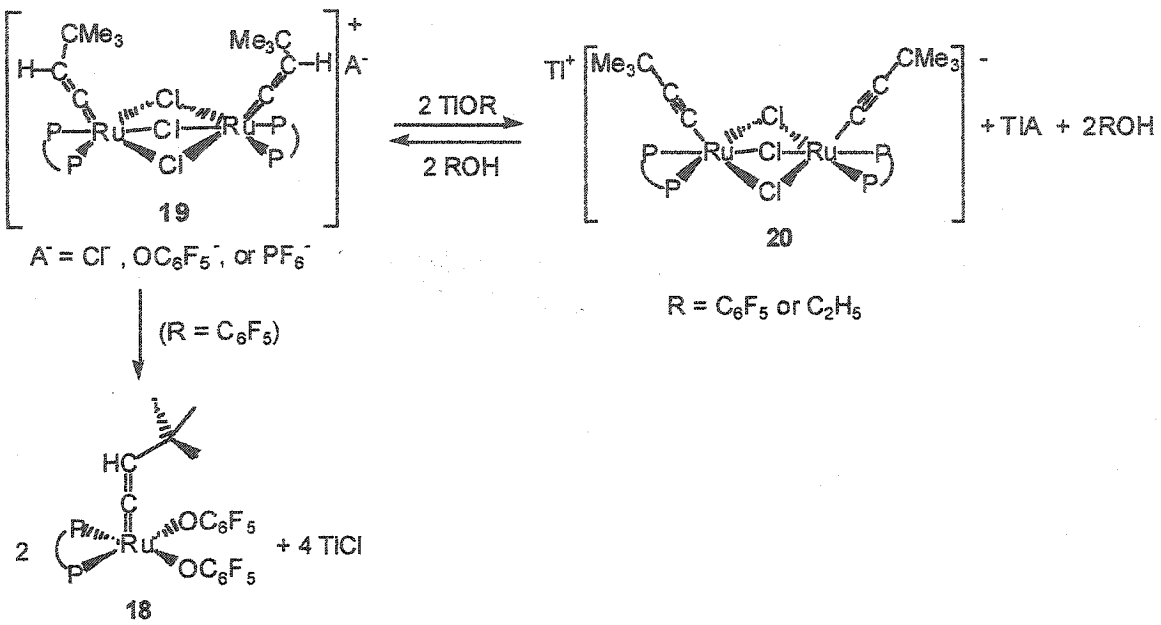

Figure 4.11 Formation of Tl[{Ru(C≡CBu^t)(dcypb)}$_2$(μ-Cl)$_3$] (**20**).

Reversibility of the deprotonation was confirmed in separate NMR experiments: rapid reaction of isolated **20** with excess perfluorophenol gave **19**•OC_6F_5 quantitatively within 10 min (^{31}P NMR), attesting to the acidic character of the perfluorophenol (pKa 5.3).[26] After 20 h at RT, **18** was evident (18%; δ_P = 50.0 (s)) accompanying **19** (82%). The former presumably forms by chloride metathesis of **19** with the $TlOC_6F_5$ coproduct. This observation prompted us to attempt synthesis of **20** via treatment of **19**•PF_6 with TlOEt, which generates a much weaker conjugate acid in this reaction (EtOH, pKa 18). Isolated yields of **20** were improved to 39%. Throughout this work, the extreme sensitivity of **20** to air and to protic solvents hampered its isolation and purification.

4.8. Molecular Structure of $Tl[\{Ru(C{\equiv}CBu^t)(dcypb)\}_2(\mu\text{-}Cl)_3]$ (20).

Crystals of **20** suitable for X-ray analysis were grown by slow evaporation of a benzene solution. The ORTEP diagram of **20** is shown in Figure 4.12 and selected bond lengths and angles are listed in Table 4.3. The structure is a cofacial bioctahedron with a C_2 through a Cl atom (Cl(2), Figure 4.12) such that only half of the polyhedron is symmetry independent. Bonding interactions exist between the thallium "counterion" and two bridging chlorides (Tl-Cl = 2.9157(13) Å), placing the thallium atom equidistant between the Ru centres (Tl-Ru = 3.437(14) Å). The Ru-C and C(1)-C(2) bond distances (1.989(5) and 1.211(7) Å, respectively) are very close to those in $Ru(\eta^5\text{-}C_5Me_5)(PPh_3)_2(C{\equiv}CSiMe_3)$ (2.004(4) and 1.213(5) Å)[27a] and *ttt*-$Ru\text{-}(CO)_2(PEt_3)_2(C{\equiv}CSiMe_3)_2$ (2.062(2) and 1.221(2) Å),[27b] showing little sensitivity to changes in the ligand environment. The Ru-Ru separation of 3.467(14) Å, similar to that found in the trichloro-bridged structure $[Ru_2(\mu\text{-}Cl)_3(PEt_2Ph)_6]^+$ (3.443(4) Å),[28] suggests a repulsive rather than an attractive metal-metal interaction.[29] The Ru-Cl bond distances (2.5211(13) – 2.5506(14) Å) agree well with those in other chloride-bridged structures,[22] including $[\{Ru(CO)(dcypb)\}_2(\mu\text{-}Cl)_3]Cl$ (**21a**, Chapter 5)

The acetylide ligand is nearly linear, with Ru-C(1)-C(2) and C(1)-C(2)-C(3) bond angles of 172.9(5)°, and 170.9(6)°, respectively, the former comparing closely to the Ru-C(1)-C(2) angle of 173.8(4)° in $Ru(\eta^5\text{-}C_5Me_5)(PPh_3)_2(C{\equiv}CSiMe_3)$.[30] The Cl-Ru-Cl bond

angles (77.73(4) – 79.61(5)°) manifest compression of the bridging face, a common feature in $Ru_2(\mu\text{-}Cl)_3$ structures,[22] while the steric effect of the dcypb ligand is observed in the slightly wide P-Ru-P bite angle (92.62(5)°), which is comparable to those in other Ru-dcypb dinuclear structures, including $[\{Ru(CO)(dcypb)\}_2(\mu\text{-}Cl)_3]Cl$ (average 92.7°).[22d]

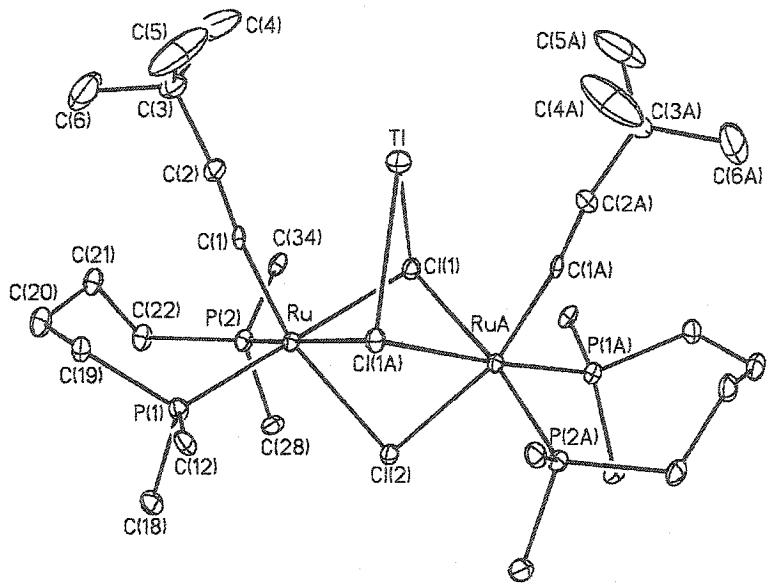

Figure 4.12 ORTEP diagram of $Tl[\{Ru(C{\equiv}CBu^t)(dcypb)\}_2(\mu\text{-}Cl)_3]$ (**20**). Thermal ellipsoids shown at 30% probability level. For clarity, each cyclohexyl group is abbreviated to a single carbon and hydrogen atoms are omitted.

Table 4.3 Selected bond lengths (Å) and angles (deg) for **20**.

Bond Distances (Å)		Bond Angles (deg)	
Ru-C(1)	1.989(5)	P(1)-Ru-P(2)	92.62(5)
Ru-P(1)	2.2865(14)	P(1)-Ru-Cl(1)	175.53(5)
Ru-P(2)	2.2699(15)	P(2)-Ru-Cl(1A)	170.48(5)
Ru-Cl(1)	2.5211(13)	C(1)-Ru-Cl(2)	164.05(14)
Ru-Cl(2)	2.5506(14)	C(2)-C(1)-Ru	172.9(5)
Ru-Cl(1A)	2.5459(13)	Cl(1)-Ru-Cl(1A)	79.61(5)
C(1)-C(2)	1.211(7)	Cl(1)-Ru-Cl(2)	78.18(4)
Tl-Cl(1)	2.9157(13)	Cl(1A)-Ru-Cl(2)	77.73(4)

4.9. ROMP via Vinylidene Complexes

Bis(perfluorophenoxide) complex **18** is an active catalyst for the ring opening metathesis polymerization of norbornene (Table 4.4). The resulting poly(norbornene) manifests a cis content of 25% at complete conversion, slightly higher than that obtained from the related monophosphine catalyst $RuCl_2(C{=}CH^tBu)(PCy_3)_2$ (**24**, 10% cis),[8d]. This difference may be due to enhanced steric definition at the active site, which can attenuate the usual steric preference for trans linkages in the growing chain.[31]

Table 4.4 Ru-Catalyzed ROMP of norbornene (NBE)[a]

Entry	Catalyst	Additive[b]	Time (min)	% conv.
1	**18**	-	270	11
2	**18**	-	1200	44
3	**18**	$[H(OEt_2)_2]BAr^F{}_4$	20[c]	23
4	**18**	$[H(OEt_2)_2]BAr^F{}_4$	420[d]	>99[e]
5	**19•Cl**	-	40[c]	9[e]
6	**19•PF_6**	-	20[c]	9[e]
7	**24**[f]	-	120	>99
8	**25**[f,g]	-	1440	19

[a] Reaction conditions, unless otherwise noted: CH_2Cl_2 or CD_2Cl_2 solvent, [norbornene] : [Ru] = 100, initial [Ru] = 10 mM, RT; % conversion determined by ^1H NMR analysis. [b]Additive: 10 mM $[H(OEt_2)_2]BAr^F{}_4$. [c] Extreme viscosity prevents effective stirring after this time. [d] Solution was periodically diluted with CH_2Cl_2 (1 mL/h) during the reaction. [e] % yield (isolated); intractable polymer precipitated by addition of MeOH and dried under vacuum. [f] Ref. 8d. [g] 40 °C.

Polymerizations were carried out in dichloromethane solvent; use of chloroform was precluded for reactions involving **18** owing to spontaneous chlorination to generate **19**, which could be observed by ^{31}P NMR analysis (30% after 18 h at RT). Quantitative polymerization of norbornene via **18** is successful at high initial monomer concentration (1.0 M), though periodic dilution is required to enable stirring. Under dilute conditions ([NBE] = 0.078 M), conversions consistently plateaued at ~20%, suggesting catalyst

decomposition. An inverse correlation between catalytic performance and concentration was likewise noted for the Grubbs' catalyst $RuCl_2(CH\text{-}CH{=}CPh_2)(PCy_3)_2$.[32]

Once isolated, the polymeric products were insoluble, precluding GPC analyses and suggesting the predominance of high molecular weight chains. The latter are a manifestation of slow rates of initiation vs. propagation, which is typical for Ru-vinylidene catalysts.[1,8c-f] Slow initiation is particularly acute for catalysts **19•Cl** and **19•PF$_6$** which yield highly intractable poly(norbornene): at conversions above 8% the extremely viscous solutions *resisted even dilution.* These qualitative observations support the suggestion that the presence of a trichloride bridging unit may retard ROMP catalysis at the initiation step, widening the discrepancy between the relative rates of initiation and propagation, and undermining control over polymer properties.[1] Attempts to enhance initiation rates by addition of the chloride-abstracting agent $NaBAr^F_4$ to **19•PF$_6$** were ineffective, owing to the kinetic inertness of the $Ru_2(\mu\text{-}Cl)_3$ group on the timescale of ROMP reactions (Section 4.5.2).

Complex **18** is more active than its triphenylphosphine analogue $RuCl_2(C{=}CHBu^t)(PPh_3)_2$ (**25**, entry 8),[8d] attesting to the activating effect of the more basic alkylphosphine ligands.[31,33] However, tricyclohexylphosphine analogue $RuCl_2(C{=}CHBu^t)(PCy_3)_2$[8d] (**24**, entry 7) is significantly more active than **18**. The different activities may reflect, in part, a difference in initiation mechanisms: while the monophosphine catalysts proceed via phosphine dissociation,[33] initiation by the

diphosphine systems are thought to involve an associative mechanism.[31] The sterically demanding ligand sphere of **18** would almost certainly inhibit an initial associative step.

As an alternative initiation strategy, abstraction of an anionic ligand may enhance metathesis activity.[1,23] Indeed, addition of the non-coordinating acid $[H(OEt_2)_2]BAr^F_4$ (Ar^F = 3,5-bis(trifluoromethyl)phenyl)[34] dramatically enhances the ROMP activity of **18** (entries 3 and 4), presumably via protonolysis of a perfluorophenoxide ligand.* While the nature of the catalytic precursor is still under investigation, preliminary experiments indicate that a single Ru-vinylidene product is formed (IR: ν(C=C) 1611 cm^{-1}; ^{31}P NMR δ_P 72.6, s).

4.10. Conclusions

The forgoing describes the synthesis and ROMP activity of a novel ruthenium vinylidene complex bearing pentafluorophenoxide ligands (**18**), and its dichloro derivative (**19•Cl**). In contrast with **18**, the dichloro species exists as a dinuclear structure. The stability of the $Ru_2(\mu\text{-}Cl)_3$ unit, as evidenced by the chemical inertness of **19**, emerges as a central issue in the design, synthesis, and catalytic applications of chlororuthenium complexes. The trichloride bridge represents a potential obstacle in

* While in principle protonolysis of a phosphine donor is also plausible, this seems unlikely in view of *in situ* ^{31}P NMR experiments which show a single new P-containing species (δ_P 72.6, s), and no evidence of the protonated dcypb.

catalysis, hindering initiation in ROMP. The stability of the $Ru_2(\mu\text{-}Cl)_3$ entity can, however, facilitate *ligand*-based reactions with nucleophiles, as illustrated by the facile deprotonation of vinylidene ligands of **19** by perfluorophenoxide to yield σ-acetylide complex **20**.

4.11. References and Notes

(1) Amoroso, D.; Yap, G. P. A.; Fogg, D. E. *Organometallics* **2002**, *21*, 3335.

(2) (a) Coalter, J. N.; Bollinger, J. C.; Eisenstein, O.; Caulton, K. G. *New J. Chem.* **2000**, *24*, 925. (b) Sanford, M. S.; Henling, L. M.; Day, M. W.; Grubbs, R. H. *Angew. Chem. Int. Ed.* **2000**, *39*, 3451. (c) Coalter, J. N.; Huffman, J. C.; Caulton, K. G. *J. Chem. Soc. Chem. Commun.* **2001**, 1158.

(3) Snelgrove, J. L.; Conrad, J. C.; Yap, G. P. A.; Fogg, D. E. *Inorg. Chim. Acta* **2003**, *345*, 268.

(4) Conrad, J. C.; Amoroso, D.; Yap, G. P. A.; Fogg, D. E. *J. Am. Chem. Soc.*, in press, 2003.

(5) Tena, M. A.; Nürnberg, O.; Werner, H. *Chem. Ber.* **1993**, *126*, 1597.

(6) Very recent work by the Fogg group indicates that this deprotonation behaviour is almost certainly driven by steric constraints within the coordination sphere, which promote interaction between the alkylidene proton and the phenoxide oxygen. Strategies for the selective synthesis of alkylidene complexes bearing phenoxide ligands may require careful matching of steric parameters between neutral L-donor ligand(s) and incoming pseudohalide: Conrad, J. C.; Amoroso, D.; Czechura, P.; Yap, G. P. A.; Fogg, D. E. *J. Am. Chem. Soc.* **2003**, submitted.

(7) (a) Bruneau, C.; Dixneuf, P. H. *Acc. Chem. Res.* **1999**, *32*, 311. (b) Bruce, M. I. *Chem. Rev.* **1991**, *91*, 197.

(8) (a) Louie, J.; Grubbs, R. H. *Angew. Chem. Int. Ed.* **2001**, *40*, 247. (b) Saoud, M.; Romerosa, A.; Peruzzini, M. *Organometallics* **2000**, *19*, 4005. (c) Schwab, P.; Grubbs, R. H.; Ziller, J. W. *J. Am. Chem. Soc.* **1996**, *118*, 100. (d) Katayama, H.; Ozawa, F. *Chem. Lett.* **1998**, 67. (e) del Rio, I.; van Koten, G. *Tet. Lett.* **1999**, *40*, 1401. (f) Katayama, H.; Yoshida, T.; Ozawa, F. *J. Organomet. Chem.* **1998**, *562*, 203.

(9) (a) Bielawski, C. W.; Morita, T.; Grubbs, R. H. *Macromolecules*, **2000**, *33*, 678. (b) Katayama, H.; Yonezawa, F.; Nagao, M.; Ozawa, F. *Macromolecules*, **2002**, *35*, 1133.

(10) Scheirs, J.; Böhm, L. L.; Boot, J. C.; Leevers, P. S. *Trends Polym. Sci.* **1996**, *4*, 408.

(11) Wakatsuki, Y.; Koga, N.; Yamakazi, H.; Morokuma, K. *J. Am. Chem. Soc.* **1994**, *116*, 8105.

(12) Amoroso, D.; Yap, G. P. A.; Fogg, D. E. *Can. J. Chem.* **2001**, *79*, 958.

(13) (a) Amoroso, D.; Haaf, M.; Yap, G. P. A.; R.West; Fogg, D. E. *Organometallics* **2002**, *21*, 534. (b) Drouin, S. D.; Amoroso, D.; Yap, G. P. A.; Fogg, D. E. *Organometallics* **2002**, *21*, 1042.

(14) Cotton, F. A.; Wilkinson, G. *Advanced Inorganic Chemistry*; Third ed.; John Wiley & Sons: Toronto, 1988.

(15) Martin, M.; Gevert, O.; Werner, H. *J. Chem. Soc., Dalton Trans.* **1996**, 2275.

(16) (a) Hartwig, J. F.; Andersen, R. A.; Bergman, R. G. *Organometallics* **1991**, *10*, 1875. (b) Osakada, K.; Ohshiro, K.; Yamamoto, A. *Organometallics* **1991**, *10*, 404.

(17) (a) Gonzalez-Herrero, P.; Weberndörfer, B.; Ilg, K.; Wolf, J. *Organometallics* **2001**, *20*, 3672. (b) Stüer, W.; Wolf, J.; Werner, H.; Schwab, P.; Schultz, M. *Angew. Chem. Int. Ed.* **1998**, *37*, 3421. (c) Wolf, J.; Stüer, W.; Grunwald, C.; Werner, H.; Schwab, P.; Schultz, M. *Angew. Chem. Int. Ed.* **1998**, *37*, 1124.

(18) (a) Koelle, U.; Hörnig, A.; Englert, U. *Organometallics* **1994**, *13*, 4064. (b) Curnow, O. J.; Hughes, R. P. *J. Am. Chem. Soc.* **1992**, *114*, 5895.

(19) (a) Bugno, C. D.; Pasquali, M.; Leoni, P.; Sabatino, P.; Braga, D. *Inorg. Chem.* **1989**, *28*, 1390. (b) Gramstad, T.; Husebye, S.; Maartmann-Moe, K. *Acta. Chem. Scand. Ser. B.* **1987**, *41*, 555. (c) Gramstad, T.; Husebye, S.; Maartmann-Moe, K. *Acta. Chem. Scand. Ser. B.* **1986**, *40*, 26. (d) Gramstad, T.; Husebye, S.; Maartmann-Moe, K. *Acta. Chem. Scand. Ser. B.* **1985**, *39*, 767.

(20) Slugovc, C.; Mereiter, K.; Zobetz, E.; Schmid, R.; Kirchner, K. *Organometallics* **1996**, *15*, 5275.

(21) Seddon, E. A.; Seddon, K. R. *The Chemistry of Ruthenium*; Elsevier: Amsterdam, 1984.

(22) (a) Albinati, A.; Jiang, Q.; Rüegger, H.; Venanzi, L. M. *Inorg. Chem.* **1993**, *32*, 4940. (b) Cotton, F. A.; Torralba, R. C. *Inorg. Chem.* **1991**, *30*, 2196. (c) Rhodes, L. F.; Sorato, C.; Venanzi, L. M.; Bachechi, F. *Inorg. Chem.* **1988**, *27*, 604. (d) see also Chapter 5 of this thesis.

(23) Hansen, S. M.; Volland, M. A. O.; Rominger, F.; Eisenträger, F.; Hofmann, P. *Angew. Chem. Int. Ed.* **1999**, *38*, 1273.

(24) (a) Bianchini, C.; Innocenti, P.; Peruzzini, M.; Romerosa, A.; Zanobini, F. *Organometallics* **1996**, *15*, 272. (b) M. A. J. Tenorio, M. A. J.; Puerta, M. C.; Valerga, P. *Organometallics* **2000**, *19*, 1333.

(25) Bianchini, C.; Casares, J. A.; Peruzzini, M.; Romerosa, A.; Zanobini, F. *J. Am. Chem. Soc.* **1996**, *118*, 4585.

(26) Castro, E. A.; Angel, M.; Arellano, D.; Santos, J. *J. Org. Chem.* **2001**, *66*, 6571.

(27) (a) Katawa, Y.; Sato, M. *Organometallics*, **1997**, *16*, 1093. (b) Sun, Y.; Taylor, N. J.; Carty, A. *Organometallics*, **1992**, *11*, 4293.

(28) Alcock, N. W.; Raspin, K. A. *J. Chem. Soc., A* **1969**, 2108.

(29) (a) Crozat, M. M.; Watkins, S. F. *J. Chem. Soc. Dalton Trans.* **1972**, 2513. (b) Cotton, F. A.; Ucko, D. A. *Inorg. Chim. Acta* **1971**, *6*, 161. (c) Summerville, R. H.; Hoffmann, R. *J. Am. Chem. Soc.* **1979**, *101*, 3821.

(30) Kawata, Y.; Sato, M. *Organometallics* **1997**, *16*, 1093.

(31) Amoroso, D.; Fogg, D. E. *Macromolecules* **2000**, *33*, 2815.

(32) Hillmyer, M. A.; Laredo, W. R.; Grubbs, R. H. *Macromolecules* **1995**, *28*, 6311.

(33) Dias, E. L.; Nguyen, S. T.; Grubbs, R. H. *J. Am. Chem. Soc.* **1997**, *119*, 3887.

(34) Brookhart, M.; Grant, B.; Volpe, A. F. J. *Organometallics* **1992**, *11*, 3920.

CHAPTER 5

Synthesis and Catalytic Activity of Electron-Rich Hydridocarbonyl Complexes of Ruthenium

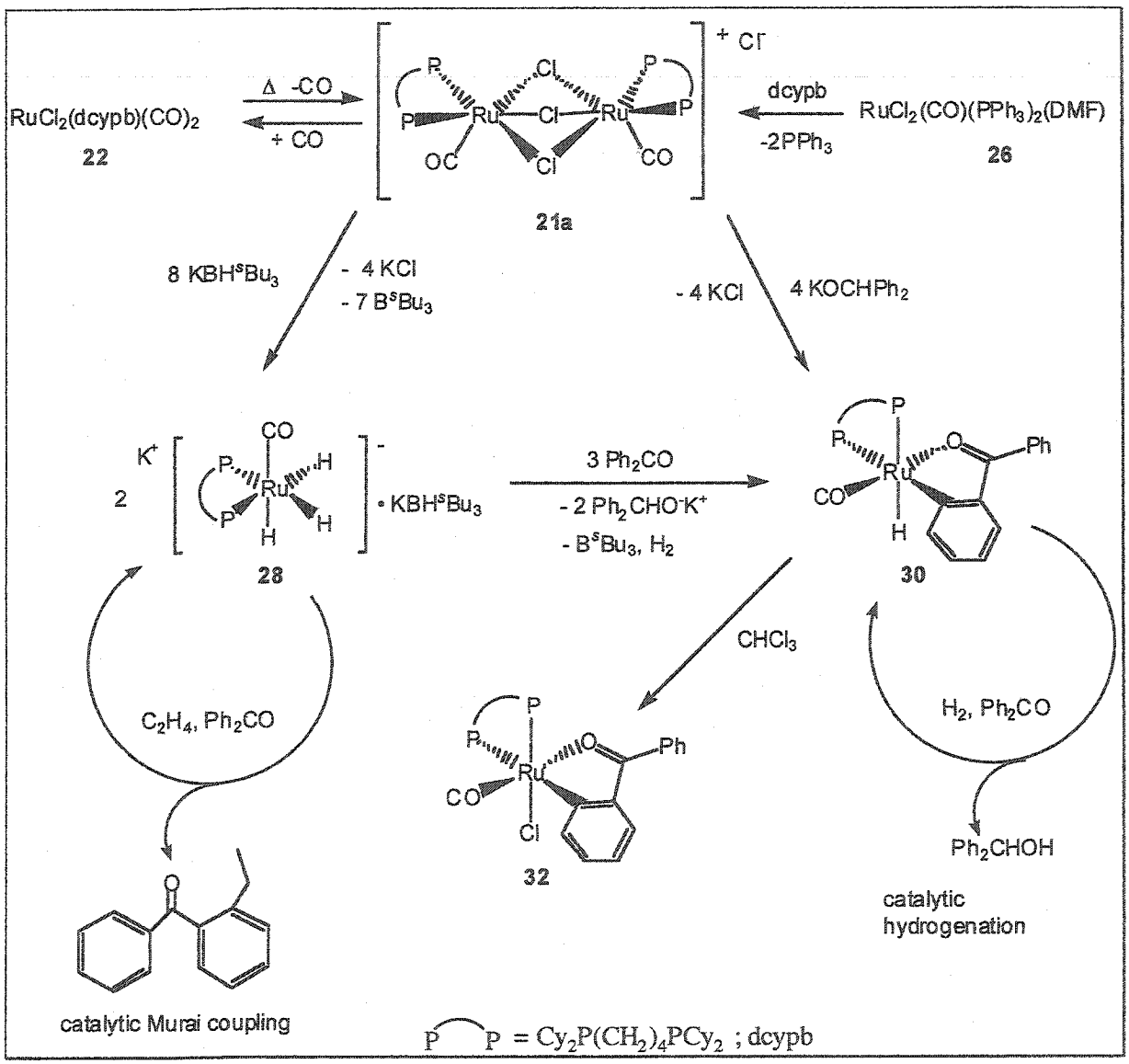

Figure 5.1 Pictorial summary of Chapter 5.

* Parts of this chapter have been published:
Drouin, S. D.; Amoroso, D.; Yap, G. P. A.; Fogg, D. E. *Organometallics*, **2002**, *201* 1042.

5.1. Introduction

Mono- and dicarbonyl complexes of ruthenium catalyze a wide range of organic transformations.[1-6] Recent reports suggest involvement of ruthenium carbonyl complexes in the oxidative arylation of acrylates,[2] silane alcoholysis,[3] dehydrosilylation of alkenes,[4] and alkene-alkyne cross-coupling reactions.[5]

While use of bulky, electron-rich alkylphosphine ligands can enhance some types of Ru(II) activity,[7] including metathesis catalysis,[8,9] there have been relatively few investigations into the catalytic potential of ruthenium *carbonyl* complexes bearing such ligands. Examples include a report by Yi detailing the activity of $RuHCl(CO)(PCy_3)_2$ (**13**) for the hydrovinylation[6] and dehydrosilylation[4] of alkenes. Collaborative work by Oro and Werner describes high activity of $RuHCl(CO)(P^iPr_3)_2$ in the transfer- and H_2-hydrogenation of a range of unsaturated substrates,[10a] and in the stereoselective hydrosilylation of terminal alkynes.[10b-h] Our own work (Chapter 3) illustrated the increased hydrogenation activity associated with the presence of a CO ligand in **13**, vs. $RuHCl(H_2)(PCy_3)_2$ (**4**).

Few examples have been described of Ru(II)-CO complexes bearing *chelating* electron-rich diphosphines, ligands which offer the combined effects of electronic activation and enhanced robustness.[11] To the best of our knowledge, the present work represents the first published report[12] of *catalytic* data for such species.

Chapter 5 References: p 175

This chapter describes the synthesis and characterization of a robust catalytic precursor, $Ru_2Cl_4(dcypb)_2(CO)_2$ (**21**), which, in solution, is observed in three different isomeric forms. Stoichiometric transformations of **21** are described, including formation of a novel ionic trihydride complex, K[*fac*-RuH_3(dcypb)(CO)] (**28**). Complex **28** is active for Murai coupling, and exceptionally active for hydrogenation catalysis.

5.2. Dichlorocarbonyl Complexes

5.2.1. Preparation of [{Ru(dcypb)(CO)}$_2$(μ-Cl)$_3$]Cl (21a)

Reaction of $RuCl_2(CO)(PPh_3)_2(DMF)$ (**26**)[13] with 1 equiv dcypb effects clean transformation into dinuclear species [{Ru(dcypb)(CO)}$_2$(μ-Cl)$_3$]Cl (**21a**). The complex is assigned the geometry shown in Figure 5.2 on the basis of $^{31}P\{^1H\}$ and $^{13}C\{^1H\}$ NMR data, and X-ray crystallography.

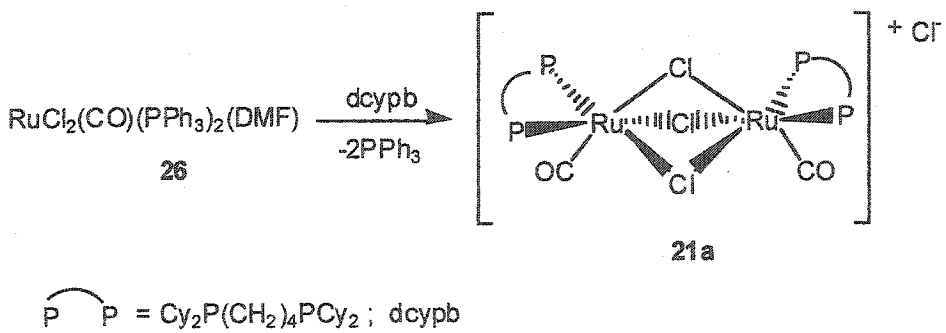

Figure 5.2 Preparation of ionic dinuclear complex **21a**.

The dinuclear formulation is also supported by microanalysis and electrospray mass spectrometry data; the latter reveal the molecular ion for the cation. Observation of a pair of ^{31}P NMR doublets for **21a** ($CDCl_3$: δ_P 50.8, 42.5; $^2J_{PP}$ = 23 Hz) attests to the chemical inequivalence of the two phosphorus nuclei within a given dcypb ligand, and the equivalence of the two halves of the dimer. A similar pattern is observed for dppb analogs $[Ru(L)(dppb)]_2(\mu\text{-}Cl)_3]PF_6$ (L = PhCN, MeCN).[14] Observation of a $^{13}C\{^1H\}$ NMR triplet for the carbonyl ligand confirms that this ligand is cis to two ^{31}P nuclei (δ 200; $^2J_{PC}$ = 15 Hz). A single infrared ν(CO) band is present. The ionic formulation of **21a** is supported by reactivity data: the ^{31}P NMR pattern is unchanged following abstraction of the Cl^- counterion by $TlPF_6$. The latter reaction afforded $[\{Ru(dcypb)(CO)\}_2(\mu\text{-}Cl)_3]PF_6$ (**21a•PF$_6$**) in 81% yield. Its identity is supported by microanalysis.

5.2.2 Molecular Structure of $[\{Ru(dcypb)(CO)\}_2(\mu\text{-}Cl)_3]Cl$ (21a)

X-ray quality crystals of **21a** formed at RT on dissolving the crude product in benzene. An ORTEP diagram is shown in Figure 5.3, bond lengths and angles in Table 5.1. Crystallographic characterization confirms the face-sharing bioctahedral structure with bridging chloride ligands, a common structural motif in Ru(II) species.[14-20,21-23] A C_2 axis of symmetry through the centre (Cl1) of the bridging unit relates the two halves of the polyhedron. The

structure manifests the compression of cofacial Cl-Ru-Cl angles (76.93(11) – 80.62(11)°) usual for $Ru_2(\mu\text{-}Cl)_3$ face-sharing bioctahedra.[18-20] The Ru-Ru separation (3.384(4) Å) indicates the absence of a metal-metal bond.[21-23] Ru-Cl (2.463(3) – 2.495(3) Å) and Ru-P (and 2.327(3) – 2.352(4) Å) bond lengths fall within the usual ranges, as do Ru-Cl-Ru angles (85.57(10) – 85.83(10)°).[18-20] P-Ru-P angles (average 92.7°) compare well with those in $Ru_2Cl_5(dcypb)_2$ (average 94.4°).[24] C-O bond lengths, averaging 1.144 Å, are comparable to those in *mer*, cis-$RuCl_2(CO)(PPh_2Me)_3$[25] (1.167 Å) and in *cct*-$[RuCl_2(CO)_2(PhCH_2PPh_2)_2]$[26] (1.13 Å) The Ru-C distances in **21a**, averaging 1.834 Å, are notably shorter than the value of 1.948 Å for *cct*-$[RuCl_2(CO)_2(PhCH_2PPh_2)_2]$,[26] likely reflecting a slightly greater extent of π-backbonding within the electron-rich dcypb complex.

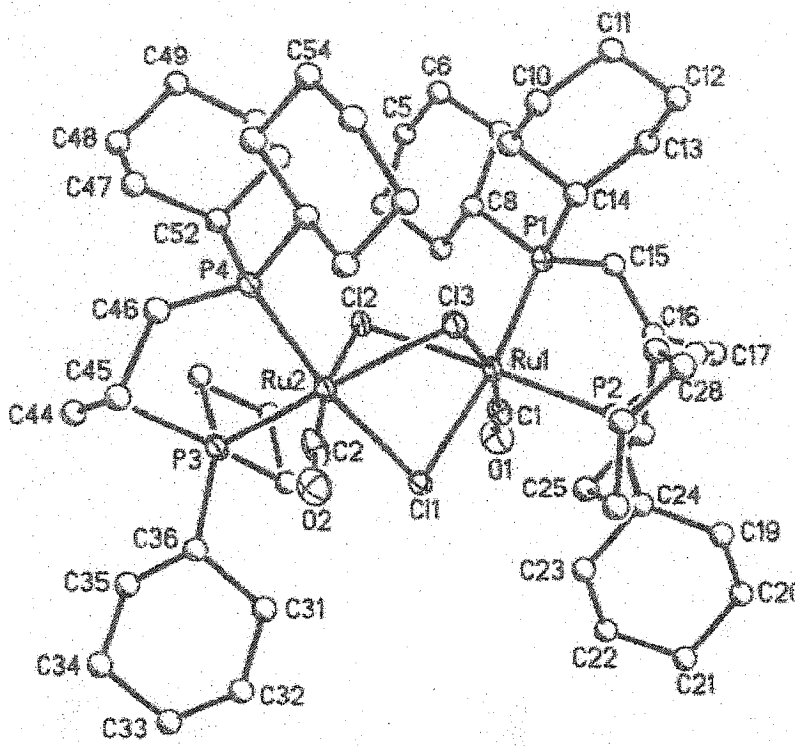

Figure 5.3 ORTEP diagram for $[\{Ru(CO)(dcypb)\}_2(\mu\text{-}Cl)_3]Cl$ (**21a**). Thermal ellipsoids shown at 30% probability level; hydrogen atoms, chloride counter ion, and co-crystallized solvent molecules omitted for clarity.

Table 5.1 Selected bond lengths (Å) and angles (deg) for $[\{Ru(CO)(dcypb)\}_2(\mu\text{-}Cl)_3]Cl$ (**21a**)

Bond Distances (Å)		Bond Angles (deg)	
Ru(1)-P(1)	2.335(4)	C(1)-Ru(1)-P(1)	91.2(4)
Ru(1)-P(2)	2.352(4)	C(1)-Ru(1)-P(2)	91.9(4)
Ru(2)-P(3)	2.346(4)	C(2)-Ru(2)-P(4)	90.4(4)
Ru(2)-P(4)	2.327(3)	P(1)-Ru(1)-Cl(1)	171.52(12)
Ru(1)-C(1)	1.856(15)	P(2)-Ru(1)-Cl(2)	172.02(13)
Ru(2)-C(2)	1.812(14)	P(4)-Ru(2)-Cl(1)	171.32(12)
C(1)-O(1)	1.124(14)	P(3)-Ru(2)-Cl(3)	170.25(12)
C(2)-O(2)	1.163(14)	P(2)-Ru(1)Cl(1)	96.09(12)
Ru(1)-Cl(1)	2.478(3)	P(1)-Ru(1)-Cl(3)	98.45(12)
Ru(1)-Cl(2)	2.501(3)	P(2)-Ru(1)-Cl(3)	95.53(12)
Ru(1)-Cl(3)	2.481(3)	P(1)-Ru(1)-P(2)	92.21(12)
Ru(2)-Cl(1)	2.485(3)	C(2)-Ru(2)-P(3)	92.1(4)
Ru(2)-Cl(2)	2.463(3)	O(1)-C(1)-Ru(1)	173.2(13(1)
Ru(2)-Cl(3)	2.495(3)	O(2)-C(2)-Ru(2)	175.4(12)

5.2.3. Isomeric Forms of $Ru_2Cl_4(CO)_2(dcypb)_2$ (21)

On the basis of the ^{31}P and ^{13}C NMR data, the structure of **21a** was originally formulated as an edge-bridged dimer (Figure 5.4);[12] the face-bridged structure was revealed subsequently upon crystallographic analysis. Clearly, NMR data do not distinguish between the neutral centrosymmetric structure and its ionic face-bridged isomer. A similar ambiguity was found for the dppb analogue $Ru_2Cl_4(PhCN)_2(dppb)_2$.[14,27,28]

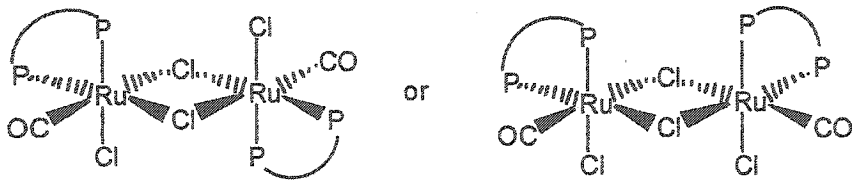

Figure 5.4 Edge-bridged dinuclear structures.

While the face-sharing structure (**21a**) is the only species observed in $CHCl_3$ or CH_2Cl_2, two other isomers are also evident by *in situ* ^{31}P NMR analysis in benzene, chlorobenzene, or THF (C_6D_6: two singlets at δ 40.6, 34.4 alongside the doublets of **21a** at δ 55.3, 42.3) The singlets are tentatively assigned to the neutral, symmetrical transoid- and cisoid-CO dimers **21b** and **21c** (Figure 5.5). In related work by Dino Amoroso of this group, the transoid isomer (**21b**) was characterized by X-ray analysis following its serendipitous crystallization from solutions containing the dicarbonyl species $RuCl_2(CO)_2$(dcypb) (**22**);[24] thermal decarbonylation of **22** is discussed in the next section. Closely related $[RuCl_2(CO)(PP)]_2(\mu\text{-}Cl)_2$ complexes (PP = 2 P^iPr_2Me, $^tBu_2PCH_2CH_2PBu^t_2$ (d'bpe)) have been proposed to exist as mixtures of cisoid and transoid isomers (NMR evidence).[11,29] In the case of the P^iPr_2Me complex, the ionic form corresponding to **21a** was also observed (^{31}P NMR data).[29]

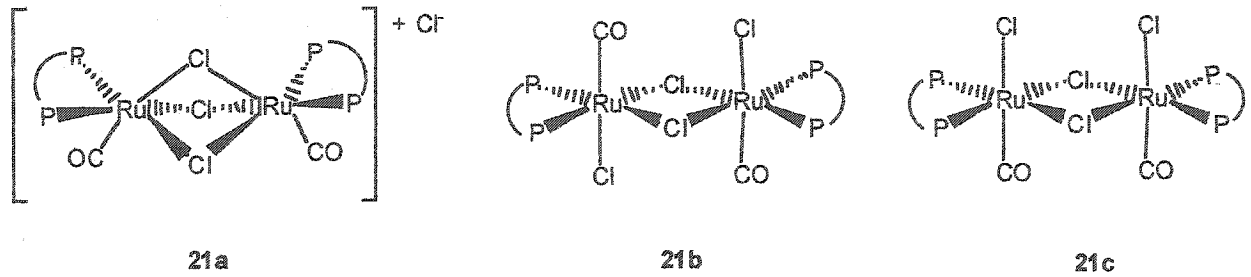

Figure 5.5 Isomeric forms of $[RuCl_2(dcypb)(CO)_2]_2$ (**21**).

^{31}P EXSY NMR experiments on mixtures of all three isomers of **21** (Figure 5.6) reveal site-exchange between the inequivalent phosphines of **21a**. Similar dynamic behaviour has been reported for ^{31}P NMR spectra of dppb analogs $[\{Ru(L)(dppb)\}_2(\mu\text{-}Cl)_3]PF_6$ (L = PhCN, MeCN)[14] and $[L(dppb)Ru(\mu\text{-}Cl)_3RuCl(dppb)]$ (L = Me_2S, C_4H_8S).[30] No loss of PP coupling is evident, however, and it is thus likely that the exchange mechanism for **21a** involves motion of the flexible dcypb backbone rather than dechelation.

The ^{31}P EXSY experiments also correlate the signals for **21b** and **21c**, indicating that these species are related by a chemical equilibrium. Although the timescale of exchange of **21b/21c** with **21a** is outside the ^{31}P T_1 window,* chemical evidence indicates that all three species **21a-c** may exist in equilibrium. This evidence includes (a) quantitative crystallization of **21a** (characterized by X-ray diffraction) from a benzene solution containing all three species,

* T_1 relaxation time for ^{31}P nuclei of **2c** is 650 ms at RT, 121 MHz.

(b) observation of all three species by ^{31}P NMR analysis on redissolving **21a** in THF or chlorobenzene, (c) complete transformation of **21b/c** into **21a** on stripping off the solvent and redissolving in $CDCl_3$, affording a homogeneous solution in which only signals for **21a** are observed by ^{31}P NMR analysis, and (d) quantitative transformation of **21a-c** into **21a**•PF_6 by reaction with $TlPF_6$. Neither the ^{1}H NMR nor the IR spectra differ appreciably between isomers **21a-c**. ^{13}C NMR data for **21b** and **21c** in C_6D_6, chlorobenzene, or THF could not be obtained owing to crystallization of **21a** over several hours in solution, which rapidly depletes the concentration of **21**.

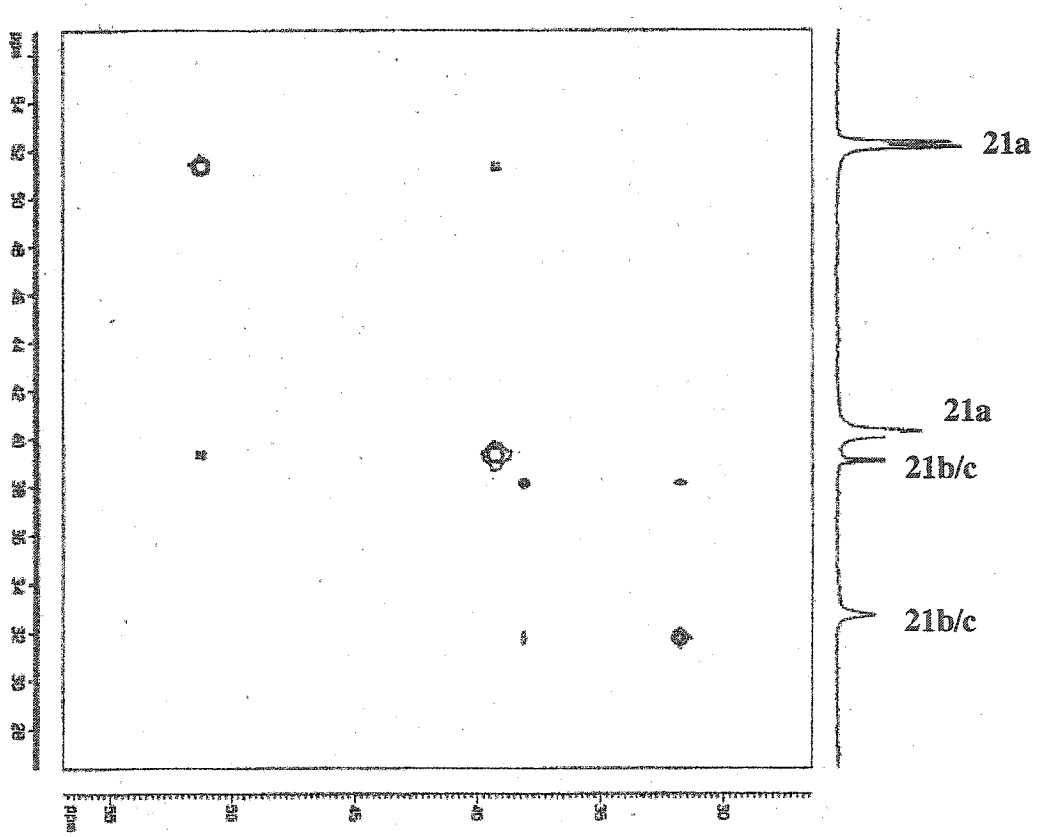

Figure 5.6 ^{31}P NMR EXSY spectrum of $[RuCl_2(CO)(dcypb)]_2$ (**21**) in chlorobenzene.

The energetic relationship between the edge- and face-sharing forms of **21** is of interest given the ubiquitousness of the trichloride-bridged structures in Ru(II) chemistry. The solvent-dependent relationship between the isomers **21a-c** may correlate with solvent effects in catalysis. Related work has shown that activation of the hydrogenation precursor [(DMSO)(PP)Ru(μ-Cl)$_3$Ru(PP)Cl] requires MeOH or EtOH solvents; ROH coordinates to one metal centre, cleaving a chloride bridge to give the active catalyst precursor [(DMSO)(PP)ClRu(μ-Cl)$_2$RuCl(ROH)(PP)] (PP = (R)-(R)-3-benzyl-2,4-bis(diphenylphosphino)pentane) (Figure 5.7).[31] The role of alcohol in cleaving such chloride-bridged dimers may have general implications for catalysis. Thus, coordinatively saturated hydrogenation catalysts of type Ru$_2$(μ-Cl)$_3$ have shown significantly enhanced activities in alcohol vs. hydrocarbon solvents.[32]

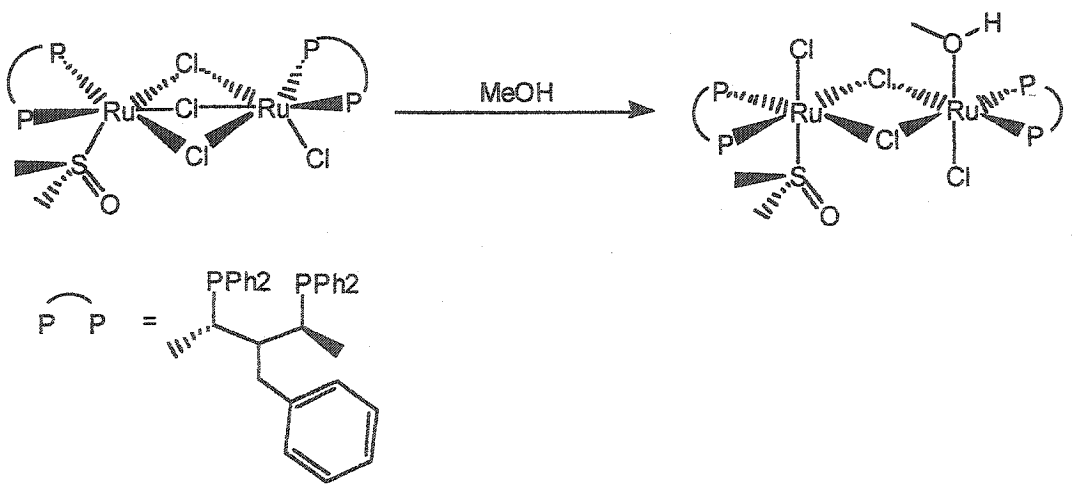

Figure 5.7. Transformation of inactive face-bridged dimer into a catalytically active species.[31]

Future work in our laboratory will apply theoretical methods to evaluate the relative barriers to interconversion between the different isomers of **21**. An experimental approach to this problem, via the use of temperature-dependent ^{31}P NMR spectroscopy and lineshape analysis, is prohibited by the low solubility of **21a**. In this regard, it is worth noting that the complexity of this system, where there is dynamic exchange between four sites with mutual coupling between two (P_A and P_B of **21a**), exceeds the capabilities of current modeling programs for lineshape analysis.[33,34]

5.2.4. Stability of [{Ru(CO)(dcypb)}$_2$(μ-Cl)$_3$]Cl (21a)

Complex **21a** is air-stable in the solid state and in solution. The chemical inertness of this complex is also manifested by slow rates of carbonylation. At room temperature, reaction of **21a** under 1 atm CO in $CHCl_3$ requires several days for complete transformation to bis-CO complex[24] $RuCl_2(CO)_2$(dcypb), observed by ^{31}P NMR analysis as a mixture of *ccc* (**22a**, 95%) and *tcc* (**22b**, 5%) isomers (Figure 5.8). Carbonylation is faster in EtOH, and **22b** precipitates as the major product within 18 h. Observation of faster rates in EtOH supports the inference, noted above, that alcohol helps to break the $Ru_2(\mu\text{-}Cl)_3$ bridging unit, and thus facilitates chemical transformations.

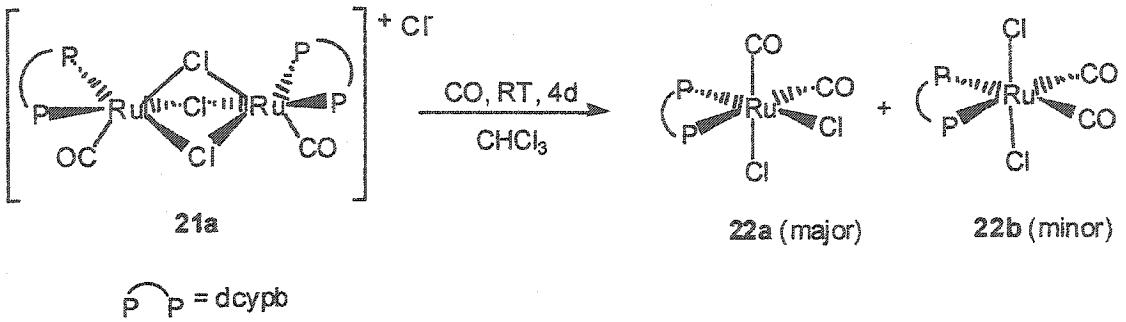

Figure 5.8 Carbonylation of $[\{Ru(CO)(dcypb)\}_2(\mu\text{-}Cl)_3]Cl$ (**21a**).

The relative inertness of **21a** to carbonylation is likewise found in the reaction of vinylidene complex $[\{Ru(dcypb)(C{=}CHBu^t)\}_2(\mu\text{-}Cl)_3]Cl$ (Chapter 4, Section 4.5.1) with CO. Even under 1 atm CO at prolonged reflux in chlorobenzene, **21a** is formed as the major product, rather than **22**. Similar robustness is implied in other work, where the face-bridged structure [(PP)(DMSO)Ru(μ-Cl)$_3$Ru(PP)Cl] (PP = (R)–(R) 3-benzyl-2,4-bis(diphenylphosphino)pentane) is the only species observed by NMR analysis in DMSO at RT. Only at high temperatures (90 °C) in DMSO is the edge-bridged symmetrical dimer [(PP)(DMSO)Ru(μ-Cl)$_2$RuCl(DMSO)(PP)] observed (Figure 5.9).[31]

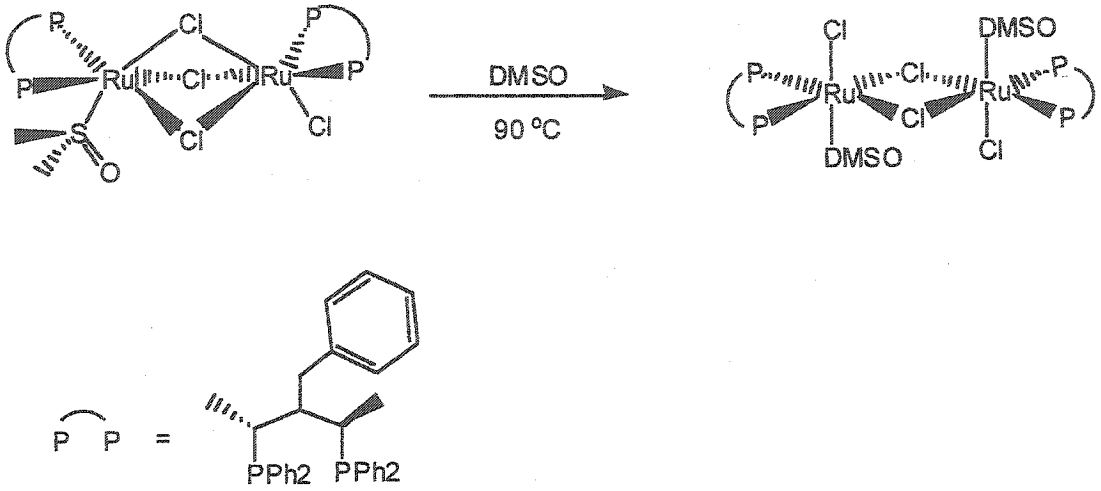

Figure 5.9. Thermal cleavage of a chloride bride to form edge-sharing dinuclear species.[31]

5.2.5. Formation of 21a via Thermal Decarbonylation of $RuCl_2(CO)_2$(dcypb) (22).

Carbonylation of **21a** is reversible; under nitrogen, **21a** is reformed quantitatively from a solution of **22a/22b** in refluxing MeOH (Figure 5.10). Similar decarbonylation behaviour has been noted for analogues $RuCl_2(L_2)(CO)_2$ (L_2 = d'bpe[11] or dppe[35]) which form edge-bridged dimeric structures on prolonged heating in alcohol solvents. Similar transformations have also been induced photochemically ($L_2 = (PMe_2Ph)_2$[36] or bpy[37]).

It may be noted that use of methanol as a decarbonylating solvent is highly unusual, this substrate more usually acting as a source of the carbonyl ligand.[17,38] In other solvents (EtOH, THF, benzene, or toluene), formation of **21a** is accompanied by appearance of new product(s) **27**, observed as overlapping peaks centered at δ_P 20 in the ^{31}P NMR spectrum. Bubbling nitrogen

through an ethanol solution of **22b** (3.5 h, 60 °C) yields a mixture of **21a** (50% of total integration) and **27**. Formation of **27** in non-alcohol solvents rules out the possibility that it may be a solvated intermediate $RuCl_2L_2(CO)(ROH)$, earlier proposed on the basis of IR evidence.[35] Its identity is further discussed below.

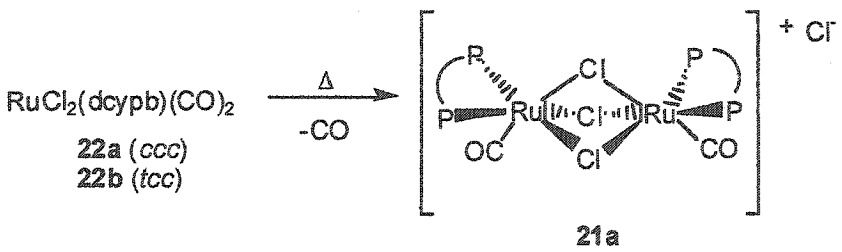

Figure 5.10 Preparation of ionic complex **21a** via thermal decarbonylation of **22**.

5.2.6. Isomerization Behaviour and Stability of Solvated $RuCl_2(dcypb)(CO)_2$ (22a/b)

Though stable in $CHCl_3$, **22b** slowly isomerizes to **22a** in benzene or THF, manifesting in these solvents a thermodynamic preference for the *ccc* form, in which only one CO is trans to a labilizing P donor. Similar behaviour has been noted for related monodentate phosphine complexes $RuCl_2(CO)_2L_2$ (L = PPh_3, PMe_3, PMe_2Ph, PPh_2Me,[25] $(PhCH_2)_nPPh_{3-n}$[26]). Facile dissociation of a CO ligand trans to another, labilizing CO has likewise been invoked to rationalize the superior catalytic activity of *ttt*-$RuCl_2(CO)_2L_2$ complexes relative to their *ctc* isomers.[39]

Isomerization via dissociation and subsequent recapture of a CO ligand is well established for $RuCl_2L_2(CO)_2$ complexes.[25,36] Dimerization of the coordinatively unsaturated intermediate $RuCl_2L_2(CO)$ can lead to dinuclear byproducts, $[RuCl_2(CO)L_2]_2$,[36] consistent with the facile dimerization of **22a/b** discussed in Section 5.2.5.

The enhanced rate of isomerization of **22b** in THF vs. benzene (90% after 28 h for THF, vs. 10% after 18 h for C_6D_6), is surprising in view of the observed inhibition of isomerization by neutral donors (H_2, olefin) for the related $RuCl_2L_2(CO)_2$ systems.[39] Stabilization of the coordinatively unsaturated intermediate $RuCl_2(CO)$(dcypb) by THF is suggested by the minimal production of byproduct(s) **27** (δ_P 20, *vide supra*) in this solvent; only 10% **27** is observed after 28 h. When **22b** is dissolved in *benzene*, ^{31}P NMR signals for **27** are prominent after 48 h (40% **27**, 13% **22a**, 47% **22b**). In marked contrast with **22b**, isomer **22a** is stable in both C_6H_6 and THF: neither isomerization nor formation of **27** occurs over 24 h at RT.

While the identity of **27** is unknown, it may possibly form by dechelation of one end of the dcypb ligand. Side products arising from dissociation of one phosphine ligand have been observed on photochemical isomerization of *cct*-$RuCl_2(CO)_2LL'$ (L = PMe_2Ph, L' = $P(OMe)_3$ or $P(OMe)_2Ph$).[36] This behaviour would be facilitated by the labilizing trans-effect of the CO ligand in the case of **22b**.

5.3. Hydridocarbonyl Complexes

5.3.1. Formation of K[*fac*-RuH_3(CO)(dcypb)] (28)

Given the central role of Ru-hydride complexes in catalysis (Chapter 1), we were interested in exploring the utility of **21** as a precursor for related hydride derivatives. Transition metal hydrides are commonly prepared by reaction of halide (or hydridohalide) precursors with alkali metal hydrides in tetrahydrofuran. Use of potassium tri-*sec*-butyl borohydride as a soluble hydride reagent offers a stoichiometrically precise alternative. Reaction of **21** with two, four, or six equivalents of KBH^sBu_3 affords a single phosphorus-containing product (**22**; δ_P 59.3 (s), THF), accompanied by unreacted **21**. Complete transformation is achieved only on use of eight equivalents of hydride (Figure 5.11). The structure of **28** is assigned based on NMR and IR spectroscopy, and X-ray diffraction. Several unidentified minor products are observed in the ^{31}P NMR spectrum on use of <8 equiv of KHB^sBu_3 in benzene. That these are due to irreversible decomposition in the absence of excess borohydride in this solvent is indicated by clean transformation of **21** to **28** on use of 8 equiv KBH^sBu_3, but not on *sequential* addition of borohydride (2 × 4 equiv) to the benzene solution.

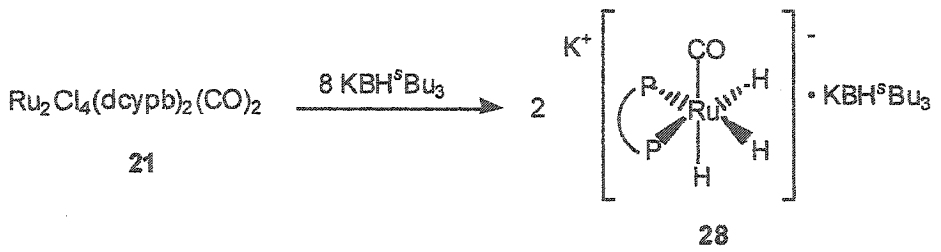

Figure 5.11 Preparation of ionic trihydride complex K[*fac*-$RuH_3(CO)$(dcypb)] (**28**)

The requirement for "excess" hydride is due in part* to formation of an anionic trihydride species, examples of which have been reported in Ru and Os systems containing trans-disposed P^iPr_3 or cis-PMe_2Ph ligands.[40,41] Consistent with formation of [*fac*-$RuH_3(CO)$(dcypb)]$^-$ is the appearance of two hydride signals, in 2:1 ratio, by ^1H NMR analysis; the cis geometry of the chelating diphosphine in **28**, coupled with the destabilizing influence of a trans-dihydride geometry,[42] precludes formation of a *mer*[40] isomer. The hydride signals comprise the AA'B component of a AA'BXX' spin system. The upfield portion (H_A, $H_{A'}$) is a second order multiplet, with a pattern identical to that previously shown for the magnetically inequivalent hydride ligands in [K(1-aza-18-crown-6)][*fac*-$OsH_3(CO)(P^iPr_3)_2$][40] and K[*fac*-$RuH_3(PPh_3)_2$].[43] The downfield hydride signal H_B appears as a broadened, distorted triplet, from which the P-H coupling constant can be extracted (δ_H -9.29, $^2J_{HPcis}$ = 22 Hz). In the previously reported systems, H_B appears as a triplet of triplets.[40,43] The H-H couplings are not resolved in **28**, but decoupling of

* Observation of apparently unreacted KHB^sBu_3 (spectroscopically detected in the product oil; δ_H -1.0; ν(B-H) 1901 (m) cm^{-1}) was initially puzzling, as was the required stoichiometry. Both are accounted for by the presence of a stabilizing interaction between a Ru-H bond and the potassium ion of an intact KHB^sBu_3 molecule (*vide infra*).

the phosphorus signal permits measurement of a $^2J_{HH}$ value of 4.8 Hz for this signal. A single hydride stretching band (1834 cm^{-1}) is present in the infrared spectrum.

Efforts to confirm the presence of the presumed potassium counter-ion by microanalysis were frustrated by the high solubility of **28** and its tendency to form oils, which hampered separation from boron and potassium byproducts. Small amounts of **28** were isolated as a fine powder from cold pentane, but underwent decomposition on drying under high vacuum. Exhaustive dehydrogenation of the dcypb ligand on exposure of $Ru_2(Cl)(N_2)(dcypb)_2(\mu\text{-}Cl)_3$ (**16**) to vacuum has been described in a related report.[24] Such behaviour appears to be general for labile or coordinatively unsaturated dcypb[24,44] or PCy_3[45] complexes of ruthenium, and may also be a feature of the P^iPr_3 systems.[40]

5.3.2. Molecular Structure of K[RuH_3(CO)(dcypb)] (28)

Storage of **28** as an oil at RT resulted in serendipitous formation of crystals suitable for X-ray analysis. Selected bond distances and angles are listed in Table 5.2. The crystal structure (Figure 5.12) shows a $[RuH_3(PP)(CO)]^-\ldots K^+\ldots KBH^sBu_3$ entity, in which the Ru center possesses the *fac* geometry deduced spectroscopically, and the potassium counter-ion interacts with all three hydride ligands (located and refined with a riding model), as well as a solvating toluene molecule. The Ru-based anion in **28** is a distorted octahedron, in which the P-Ru-P angle of

100.51(7) indicates compression of the hydride face. This angle, and the average Ru-H distance of 1.63(3) Å, are comparable to features present in [K(18-crown-6)][*fac*-$H_3Ru(PPh_3)_3$].[46]

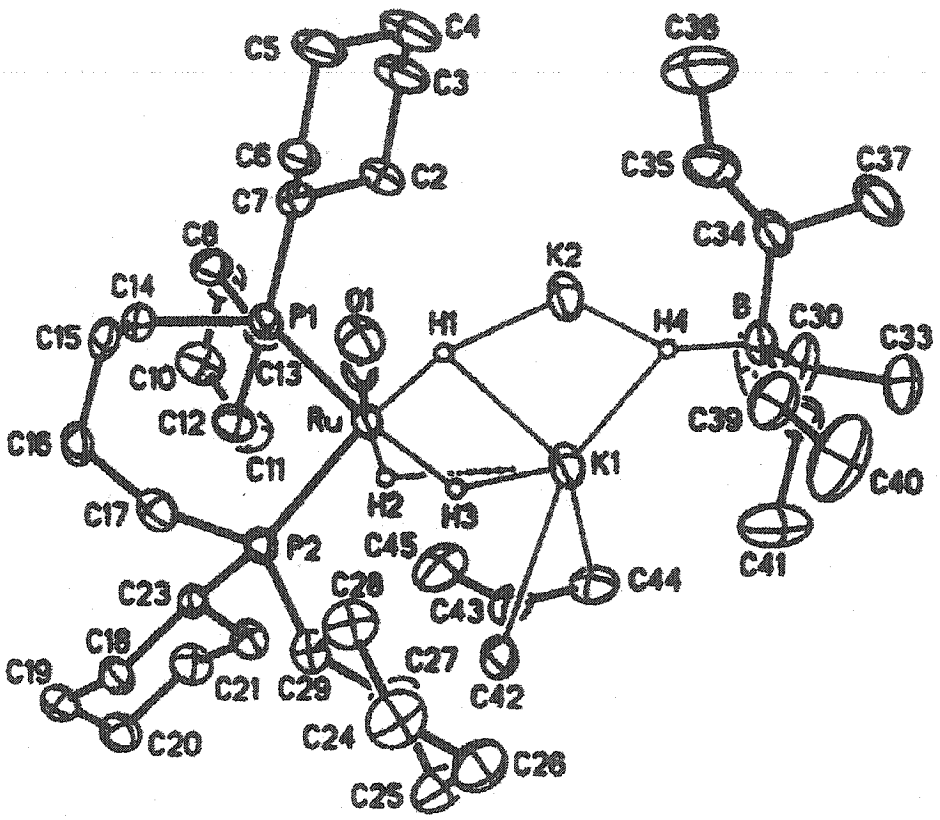

Figure 5.12 Molecular structure and atomic numbering of K[*fac*-$RuH_3(CO)(dcypb)$]KBH^sBu_3•0.5 toluene (**28**). Thermal ellipsoids are depicted at 30% probability level; non-metal hydrogens are omitted for clarity.

Chapter 5 References: p 175

Table 5.2 Selected bond lengths (Å) and angles (deg) for complex **28**.

Bond distances (Å)		Bond angles (deg)	
Ru-P(1)	2.335(2)	P(1)-Ru-P(2)	100.51(7)
Ru-P(2)	2.3375(19)	C(1)-Ru-P(1)	98.8(2)
Ru-C(1)	1.807(7)	C(1)-Ru-P(2)	90.9(2)
Ru-H(1)	1.63(3)	O(1)-C(1)-Ru	175.0(6)
Ru-H(2)	1.64(3)	C(1)-Ru-K(1)	123.4(2)
Ru-H(3)	1.63(3)	C(1)-Ru-K(2)	56.8(2)
O(1)-C(1)	1.201(7)	P(1)-Ru-K(1)	117.01(6)
K(1)-H(1)	2.63(5)	P(2)-Ru-K(1)	120.76(5)
K(1)-H(3)	2.64(5)	P(1)-Ru-K(2)	112.29(6)
K(2)-H(1)	2.82(5)	P(2)-Ru-K(2)	136.03(6)
K(1)-H(2)	2.67(5)	K(1)-Ru-K(2)	69.17(4)
K(2)-H(4)	2.44(6)	Ru-K(1)-B	108.58(14)
K(1)-H(4)	2.57(6)	B-K(2)-Ru	112.35(15)
B-H(4)	1.32(6)	Ru-K(2)-K(1)	53.81(3)
K(1)-C(42)	3.251(8)	Ru-K(1)-K(2)	57.02(3)
K(1)-C(43)	3.197(7)	Ru-C(1)-K(2)	92.5(3)
K(1)-C(44)	3.260(7)	C(34)-B-K(1)	131.2(5)
K(2)-O(1)#2	2.650(5)	C(34)-B-K(2)	74.6(4)
K(2)-O(1)#1	3.103(5)	C(14)-P(1)-Ru	118.8(2)
Ru-K(1)	3.3998(17)	C(17)-P(2)-Ru	113.3(2)
Ru-K(2)	3.5337(16)	C(7)-P(1)-Ru	114.6(2)
B-K(1)	3.577(8)	C(13)-P(1)-Ru	117.5(2)
B-K(2)	3.284(8)	C(23)-P(2)-Ru	120.8(2)
B-C(30)	1.656(11)	C(29)-P(2)-Ru	116.7(2)
B-C(34)	1.645(11)	C(30)-B-K(1)	82.1(4)
K(1)-K(2)	3.937(2)	C(30)-B-K(2)	146.9(5)

More unexpected is the presence in **28** of a "solvating", intact KBH^tBu_3 molecule, the K^+ ion of which is associated with a ruthenium-based hydride, the boron hydride, and the carbonyl oxygen of a neighbouring Ru molecule (for CO...K^+ interaction, see Figure 5.11). While

examples of transition metal-borohydride interactions are well established, and in some cases afford isolable species,[47] this is, to our knowledge, the first crystallographically characterized example of a metal hydride stabilized by an intact borohydride molecule within the third coordination sphere. Tight hydride-K^+ ion pairing (*vide infra*), in conjunction with shielding of the potassium ions by *sec*-butyl, cyclohexyl, and (for K(1)), toluene groups, renders the entire complex highly lipophilic, resulting in extreme solubility in hydrocarbon solvents, including pentane. This effect is reminiscent of Caulton's observation of high hydrocarbon solubility in $K_2Os_2H_6(PMe_2Ph)_6$, in which the potassium counter-ions are enfolded by two phosphine phenyl rings in a centrosymmetric dimer.[41] The stoichiometric requirements noted earlier imply that interactions with *both* K^+ and KBH^sBu_3 are necessary to stabilize the anionic trihydride complex (the former alone is insufficient, as indicated by decomposition of **28** on use of 6 equiv borohydride in benzene; see Section 5.3.1).

A portion of the ion-pair structure for **28** is shown in Figure 5.13. Bridging interactions between K(2) and the carbonyl oxygens are present in one dimension, with sandwiching of a toluene molecule between adjacent K(1) cations in a second. Interaction of metal cations with a carbonyl oxygen is common in hydridocarbonylmetalates;[48] occupation of this site by K(2) in **28** leaves K(1) free to bind the hydride face. Potassium-carbon distances (3.20 - 3.26 Å) are comparable with other arene-K^+ interactions.[41,49] Two distinct crystallographic inversion centers are present. The K(2) ion and its symmetry-generated pair are bridged by a carbonyl oxygen,

with an interatomic separation of 4.679(2) Å, while a second inversion center is located at the center of the toluene molecule coordinated to K(1), with a K...(centroid) distance of 3.015(2) Å, or an effective K...K distance of 6.030(2) Å. The closest K...K interatomic separation, 3.937(2) Å, occurs between the symmetry-unique K(1) and K(2) ions bridged by the borohydride anion. Potassium ion K(1) is approximately equidistant between Ru-H and B-H entities, with K...H distances ranging from 2.57(6)-2.67(5) Å, while K(2) is more closely associated with the borohydride B-H (K(2)...H(4), 2.44(6) Å; K(2)...H(1), 2.82(5) Å). Intimate potassium-hydride ion-pairing in both second and third coordination spheres is indicated by these values; cf. distances of 2.52-3.02 Å for the tight ion pair in $[KH_3Os(PMe_2Ph)_3]_2$.[41]

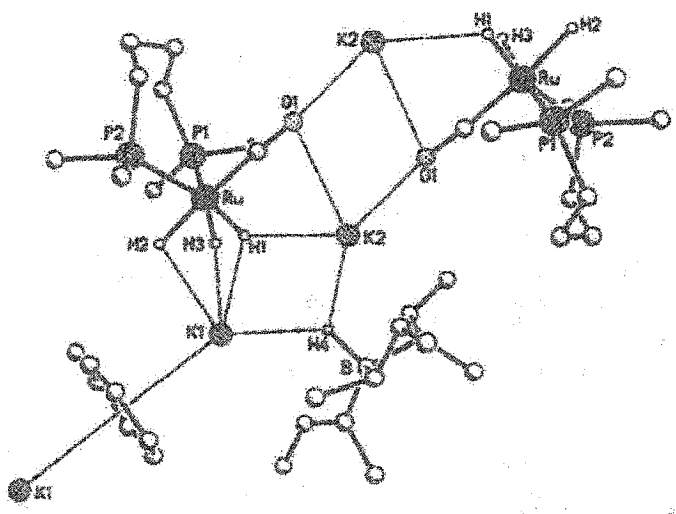

Figure 5.13 Schematic diagram illustrating the position of K^+ ions within the packing of K[*fac*-$RuH_3(CO)(dcypb)$]KBH^sBu_3•toluene (**28**) units. For clarity, cyclohexyl groups are abbreviated to a single carbon.

5.3.3. Catalysis

The hydrogenation activity of **28** (Table 5.3) compares favourably with that of the important Noyori systems containing chelating diphosphine and 1,2-diamine ligands.[50,51] Thus, **28** effects reduction of benzophenone at *one atmosphere* of H_2 and 60 °C in isopropanol, in comparison to the requirement for H_2 pressures of 8 atm using $RuCl_2[P(C_6H_4\text{-}4\text{-}CH_3)_3]_2(NH_2CH_2CH_2NH_2)$ (**29**) (entries 1, 4).[51] The exceptionally high hydrogenation activity of **28**, mediated by intermediate **30** (*vide infra*), is retained on large scale (entry 7): reduction of 100 g of benzophenone (2.7 M ketone, [S]:[C] = 20 000:1) reached 48% conversion within 1 h (TOF = 9600 h^{-1}). On distilling off the acetone byproduct,[52] 90% conversion is attained within a further 2 h. Characterization of orthometallated complex **30**, (an intermediate in the hydrogenation reaction) is detailed in the next section.

Table 5.3 Reduction of benzophenone to benzhydrol[a]

Entry	Catalyst	pH_2 (atm)	Solvent	Conversion (%)
1	**29**	8	^{i}PrOH	99[b, c]
2	**28**	8	C_6H_6	100[b]
3	**28**	2	C_6H_6	67
4	**28**	1	^{i}PrOH	96
5	**28**	0	^{i}PrOH	55
6	**30**	1	^{i}PrOH	95
7	**30**	1	^{i}PrOH	90[d]

[a] Reactions carried out at 60 °C for 24 h, using 0.34 mM [Ru]; $[Ph_2CO]$:[Ru] = 3000:1, unless otherwise stated. [b] Reaction at 35 °C for 18 h. [c] Ref. 51. [d] Reaction using 100 g (0.55 mol, 2.75 M) of benzophenone ([Ru] = 0.138 mM; $[Ph_2CO]$:[Ru] = 20 000:1) at reflux for 3 h, acetone removed by distillation after 1 h.

Hydrogenation via **28** proceeds in both aromatic and isopropanol solvent, the latter being associated with higher activity, possibly owing to protonation of the trihydride to generate catalytically-active $[RuH_2(H_2)(dcypb)(CO)]$.[53] Both H_2-hydrogenation and transfer hydrogenation pathways are accessible for **28**, as indicated by partial retention of activity in isopropanol under N_2 (entry 5). In this regard it is worth noting the possibility, which cannot be ruled out at this stage, of inhibition by N_2, an effective ligand in other Ru-dcypb chemistry.[24] Efficient transfer hydrogenation of benzophenone under Ar or N_2 was previously reported, albeit at much higher catalyst loadings (0.1-0.5 mol% Ru, vs. 0.005 mol% for **28**).[54,55] The very high activity of **28** is particularly notable given the emerging view that an NH group in the ligand set is required for efficient ketone hydrogenation.[50,52] Very recently, Gimeno and coworkers reported that phosphine-imine ligands devoid of an NH functionality performed better than phosphine-secondary amine ligands in transfer hydrogenation of ketones.[56]

The hydrogenation activity of **28** prompted a preliminary evaluation of its activity for *ortho*-functionalization of aromatic ketones (Figure 5.14), for which an orthometallated intermediate[1d,57,58] is proposed similar to that described[53] for benzophenone hydrogenation. First described by Murai less than ten years ago, such C=C/C-H coupling reactions are much less developed than hydrogenation catalysis.[1d,57] Relatively few variants on the original $Ru(H)_2(CO)(PPh_3)_3$ catalyst systems have been explored, though a recent breakthrough described RT coupling using $Ru(H)_2(H_2)_2(PCy_3)_2$ as precursor.[59] The potential Murai activity of systems

containing the "$RuH_2(PP)$" (PP = chelating dialkylphosphine) structural motif is of particular interest, as loss of monodentate phosphine has emerged as a potentially important contributor to deactivation pathways.[60] Complex **28** shows modest activity, but improved stability over the PCy_3 systems, which were unstable at elevated temperatures. Thus, 58% conversion of benzophenone to 2-ethylbenzophenone is found after 22 h at 60°C under 260 psi ethylene (1.5 mM **28**; 23.7 mM Ph_2CO).

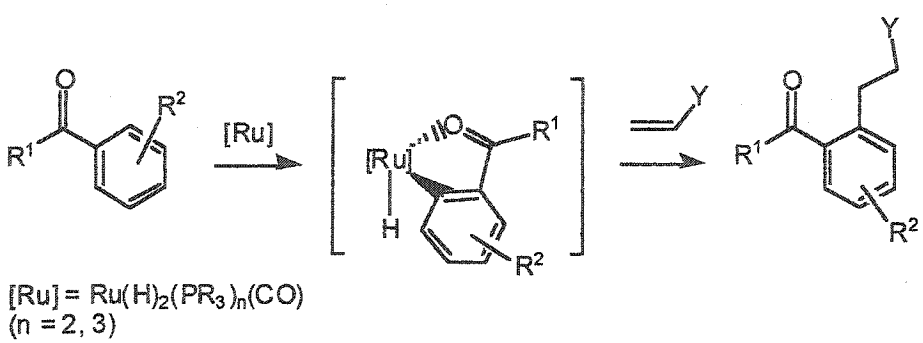

Figure 5.14 Murai coupling catalyzed by ruthenium dihydride complexes.

5.3.4. Identification of a catalytic intermediate

^{31}P NMR analysis of catalyst solutions following hydrogenation revealed a single species, identified as RuH[*o*-C(O)(Ph)C_6H_4](CO)(dcypb) (**30**) on the basis of NMR, XRD, and elemental analysis. In stoichiometric experiments, **28** was completely converted to **30** in the presence of a threefold excess of benzophenone (Figure 5.15, Route A), two equivalents of the ketone being converted to $KOCHPh_2$ (δ_H 5.67, C_6D_6). No benzhydrol (Ph_2CHOH; δ_H 5.49 (d, $^3J_{HH}$ = 3.6 Hz),

C_6D_6) was observed by ^{1}H NMR or IR spectroscopy, but a peak for dissolved H_2 was present for reactions carried out in a sealed system, implying the reaction sequence depicted. There was no evidence of the presumed $RuH_2(CO)$(dcypb) intermediate, in contrast to the corresponding reaction of K[*fac*-$RuH_3(PPh_3)_3$], in which the greater steric protection afforded by the trans-PPh_3 ligands permitted observation of $RuH_2(PPh_3)_3$ en route to RuH[*o*-$C(O)(Ph)C_6H_4$]$(PPh_3)_3$.[53b] The *ortho* proton of benzophenone is identified as the source of the hydride ligand in **30**, rather than the hydride originally present in **28**, on the basis of a labelling experiment in which benzophenone was reacted with trideuteride **28-d$_3$** (itself prepared by treating **21a** with 8 equiv $LiDBEt_3$). A hydride signal corresponding to that originally observed for **30** (δ_H -6.32) was observed, which integrated 1:1 against an isolated aromatic proton of the benzophenone ligand.

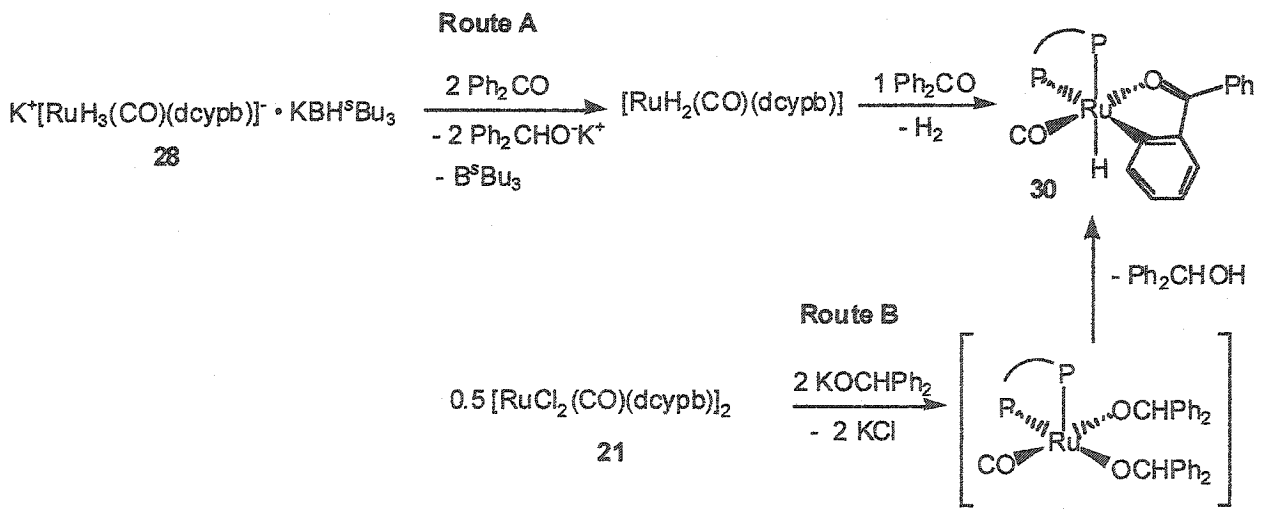

Figure 5.15 Synthetic routes to RuH[*o*-$C(O)(Ph)C_6H_4$](CO)(dcypb) (**30**). One of two enantiomeric forms of **30** is shown.

Structure **30** represents a resting state in catalytic hydrogenation of benzophenone via **28**, as indicated by the observation of essentially identical activity for catalysis via isolated **30** (Table 5.3, entry 6). Its PPh_3 analogue has been proposed as a key intermediate in *ortho*-functionalization of benzophenone.[57,58] However, the markedly lower Murai activity of **30** vs. **28** (26% vs. 58% under the conditions above) suggest that the orthometallated species is not on the reaction coordinate for Murai coupling, but is in fact a catalytic *sink* in this chemistry. Indeed, substrate chelation may represent a general deactivation pathway for such catalysts. A recent report on the performance of the original Murai catalyst $RuH_2(CO)(PPh_3)_3$ shows complete inhibition of activity resulting from orthometallation of the acetophenone substrate to give $RuH(o\text{-}C_6H_4C(O)CH_3)(CO)(PPh_3)_2$.[61] The observation of some activity for **30** may arise from the reversibility of Ru insertion into the *ortho* C-H bond.[57b] While it has been suggested that catalysis by complexes containing a carbonyl ligand proceeds via initial loss of CO, the experimental evidence is limited.[59,62] Firstly, the inactivity of $Ru(H)_2(CO)(PPh_3)_3$ under CO pressure[62] is likely due to formation of $Ru(H)_2(CO)_2(PPh_3)_2$, rather than simply suppression of CO loss.[63] Secondly, comparative catalytic studies indicate that the presence of a CO ligand inhibits the activity of *orthometallated* complexes:[59,61] it is clearly not detrimental to the behaviour of the parent systems, including $Ru(H)_2(CO)(PPh_3)_2$ itself.[1d,57,61] The latter distinction was masked in earlier work by the common assumption that the orthometallated species lay on the reaction path for catalysis.

Direct reaction of **21** with $KOCHPh_2$ (Figure 5.15, Route B) provides a cleaner and more efficient route to **30**. Formation of **30** by either method is signalled by a colour change from yellow to red. Although the transformation is quantitative, as judged by ^{31}P NMR spectroscopy, high solubility limits isolated yields of **30** to 51%. Observation of a doublet of doublets in the hydride region of the ^{1}H NMR spectrum (-6.3; $^{2}J_{PPtrans}$ = 90 Hz; $^{2}J_{PPcis}$ = 24 Hz), signifies the presence of a hydride ligand trans to one phosphorus nucleus, and cis to the other. Consistent with this is the ^{31}P NMR spectrum, which shows a pair of doublets (25.7, 30.5; $^{2}J_{PP}$ = 20 Hz). ^{31}P-^{1}H HMQC experiments correlate the upfield phosphorus resonance with an aromatic proton that appears as a doublet of doublets (9.00 ppm). In the $^{1}H\{^{31}P\}$ NMR spectrum, the latter collapses to a doublet, and the hydride signal collapses to a singlet. In conjunction with the $^{13}C\{^{1}H\}$ NMR data, which shows a new quaternary carbon signal far downfield (δ_C 215), as a doublet of doublets split by cis and trans phosphines, this provides unambiguous evidence for orthometallation of the benzophenone ligand. An infrared band of medium intensity appears for Ru-H (1859 cm^{-1}), accompanied by a weak band for the carbonyl functionality within the η^2-O=C(Ph)(C_6H_4) ligand (1580 cm^{-1}). The low energy of the latter band is consistent with chelation of the ketone.[64] Related complexes containing monodentate phosphines have been described in other work.[53,59,61,65]

One equivalent of Ph_2CHOH is evolved in formation of **30** via **21**, suggesting that reaction proceeds via reductive elimination of alcohol from a bis(alkoxide) intermediate (Figure

5.15, Route B). In contrast, reactions of monophosphine analogs $RuCl_2(CO)(PPh_3)_2(DMF)$ (**26**) or $RuCl_2(CO)(PCy_3)_2$ (**14**) with $KOCHPh_2$ involved β-elimination of benzophenone (and disproportionation in the case of **26**), terminating in Ru hydride complexes (Figures 5.16 and 5.17). The principal products were $RuH_2(CO)(PPh_3)_3$ and $RuHCl(CO)(PCy_3)_2$ (**13**) (for the PPh_3 and PCy_3 reactions, respectively); in both cases unidentified side-products were also observed. Both hydride species were identified by their characteristic NMR spectra. [5,66]

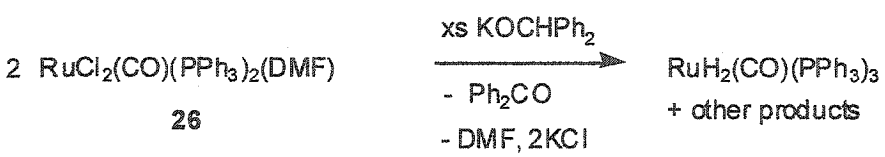

Figure 5.16 Disproportionation by reaction of $RuCl_2(CO)(PPh_3)_2(DMF)$ (**26**) with $KOCHPh_2$.

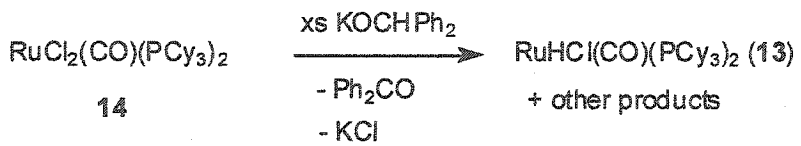

Figure 5.17 Reaction of $RuCl_2(CO)(PCy_3)_2$ (**14**) with $KOCHPh_2$.

5.3.5. Molecular Structure of RuH[*o*-C(O)(Ph)(C_6H_4)](CO)(dcypb) (30)

Crystals of **30** suitable for X-ray analysis were obtained by slow concentration from toluene solution (Figure 5.18). Selected bond distances and angles are listed in Table 5.4. This structure is the first crystallographically characterized example of a Ru-hydride complex containing orthometallated benzophenone; related, chloride-containing species, including acetophenone derivatives, have been reported in other chemistry.[53,59,61,65] The five-membered metallacycle in **30** constrains significant deviations from regular octahedral geometry; the O(1)-Ru-C(29) angle of 77.24(10)°, in particular, is highly compressed relative to the ideal value of 90°, as also found in RuCl[*o*-C_6H_3MeC(O)C_6H_4Me](CO)(PMe_2Ph)$_2$ (**31**).[65] The fused five- and six-membered rings in **30** are coplanar, while the non-metallated ring is tilted ca. 45° out of this plane, relieving the interaction between the hydrogen atoms on C(33) and C(35). The P-Ru-P bite angle (99.44(3)°) is close to that observed for **28**, a consequence of the steric demand of the dcypb ligand.[24] The Ru-C(29) bond length for the orthometallated carbon trans to phosphine is marginally longer than that observed for **31**, in which the trans position is occupied by a chloride ligand (2.056(3) Å) for **30**, vs. 1.987(19) and 2.044(17) Å for the two independent molecules in the asymmetric unit for **31**).

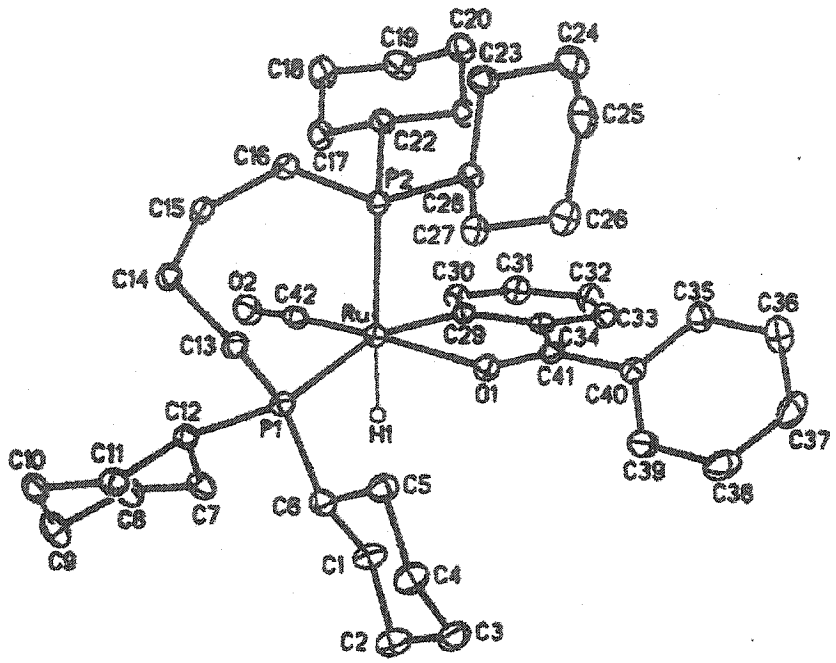

Figure 5.18 Molecular structure and atomic numbering of RuH[*o*-C(O)(Ph)(C_6H_4)](CO)(dcypb) (**30**). Thermal ellipsoids depicted at 30% probability level; non-metal hydrogens are omitted for clarity.

Table 5.4 Selected bond lengths (Å) and angles (deg) for Complex **30**

Bond distances (Å)		Bond angles (deg)	
Ru-P(1)	2.3753(9)	P(1)-Ru-P(2)	99.44(3)
Ru-P(2)	2.4237(8)	C(42)-Ru-P(1)	91.09(10)
Ru-C(42)	1.814(3)	C(42)-Ru-P(2)	96.11(9)
Ru-C(29)	2.056(3)	O(1)-Ru-P(2)	90.27(5)
Ru-O(1)	2.144(2)	O(1)-Ru-P(1)	94.13(6)
Ru-H(1)	1.48(2)	C(16)-P(2)-Ru	117.99(9)
O(1)-C(41)	1.259(3)	C(13)-P(1)-Ru	119.42(10)
O(2)-C(42)	1.166(3)	C(28)-P(2)-Ru	115.43(10)
P(1)-C(13)	1.846(3)	C(12)-P(1)-Ru	113.17(10)
P(1)-C(12)	1.859(3)	C(6)-P(1)-Ru	116.44(10)
P(2)-C(16)	1.858(3)	C(28)-P(2)-Ru	115.43(10)
P(2)-C(28)	1.861(3)	C(22)-P(2)-Ru	116.46(10)
		O(2)-C(42)-Ru	176.8(3)

5.3.6. Reaction of RuH[*o*-C(O)(Ph)C_6H_4](CO)(dcypb) (30) with Chlorinated Solvents

The tendency of metal hydride species to undergo chlorination often precludes the use of chlorinated solvents for catalytic hydrogenation reactions.[67] Indeed, hydride complex **30** reacts immediately and quantitatively with chloroform or dichloromethane to form the chloro derivative **32** (Figure 5.19).

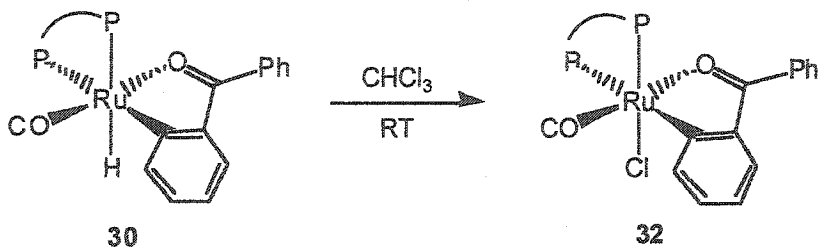

30 **32**

Figure 5.19 Chlorination of RuH[*o*-C(O)(Ph)C_6H_4](CO)(dcypb) (**30**).

The identity of **32** is confirmed by microanalysis, and its structural similarity to **30** is evident from spectroscopic analysis. The ^{1}H NMR spectrum of **32** is virtually identical to that of **30**, lacking only the characteristic high-field hydride multiplet. The two inequivalent phosphorus centres are represented by a pair of doublets (δ_P 46.0 and 6.2, J_{PP} = 17 Hz) in the ^{31}P NMR spectrum. Three sets of peaks for the quaternary carbons appear in the ^{13}C NMR spectrum. Furthest downfield is a doublet of doublets at 210.6 ppm, assigned to the carbonyl carbon given the absence of any correlations in the ^{1}H - ^{13}C HMQC NMR spectrum. A doublet of doublets at 204 ppm can be assigned to the metallated carbon based on its correlation with the *ortho*-proton

(δ_H = 8.62 ppm (dd)) by HMQC analysis. An apparent doublet at 210 ppm (rather than the expected triplet) is assigned to the acyl-carbon. A strong infrared band at 1926 cm^{-1} confirms the presence of the carbonyl ligand, while the acyl C=O stretch is represented by a weak band at 1579 cm^{-1}.

5.4. Conclusions

The foregoing describes a general route into the chemistry of monocarbonyl ruthenium complexes containing the basic, bulky diphosphine dcypb. While, in solution, dimeric complex $[RuCl_2(dcypb)(CO)]_2$ (**21**) can be observed in three different isomeric forms, it precipitates preferentially as the face-sharing ionic complex $[\{Ru(dcypb)(CO)\}_2(\mu\text{-}Cl)_3]Cl$ (**21a**). The chemical inertness of complex **21a**, evidenced by its stability toward air and by slow rates of carbonylation, is attributed in part to the thermodynamic stability of the trichoride bridging unit. Facile formation of such $Ru_2(\mu\text{-}Cl)_3$ structures is a common occurrence in ruthenium chemistry and may represent a general obstacle in catalysis via Ru(II) dichloro complexes, unless bridge-cleaving reactions (by, for example, alcohol solvents) are accessible.

Complex **21a** provides a stable and synthetically valuable precursor to key catalytic species, including novel, anionic trihydride $K[RuH_3(CO)(dcypb)]\bullet KBH^sBu_3$ (**28**). Complex **28** is susceptible to decomposition in the absence of the stabilizing interactions provided by $H\ldots K^+$ and $CO\ldots K^+$ involving the potassium counter-ion and an intact borohydride molecule in the third

Chapter 5 References: p 175

coordination sphere. Restraint of decomposition permits us to redirect the heightened reactivity of **28** toward the challenging problems of catalytic hydrogenation and *ortho*-functionalization of benzophenone. Exceptionally high activity is found in hydrogenation, permitting reduction at 1 atm H_2. An orthometallated intermediate implicated in catalytic hydrogenation was identified and crystallographically characterized; this species may represent a catalytic sink in the Murai chemistry. Current efforts utilizing **28** and related species are aimed at developing a protocol for *tandem* Murai-hydrogenation, a potentially valuable route to pharmaceutically-relevant benzhydrol derivatives.

Chapter 5 References: p 175

5.5. References

(1) Recent reviews: (a) General Ru-catalysis: Naota, T.; Takaya, H.; Murahashi, S.-I. *Chem. Rev.* **1998**, *98*, 2599. (b) Lewis Acid and Base Catalysis: Murahashi, S.-I.; Takaya, H. *Acc. Chem. Res.* **2000**, *33*, 225. (c) Epoxidation and aziridination of alkenes: Che, C.-M.; Yu, W.-Y. *Pure Appl. Chem.* **1999**, *71*, 281. (d) Murai catalysis: Murai, S.; Kakiuchi, F.; Sekine, S.; Tanaka, Y.; Kamatani, A.; Sonoda, M.; Chatani, N. *Nature* **1993**, *366*, 529. (e) C-C bond formation: Trost, B. M.; Toste, D.; Pinkerton, A. B. *Chem. Rev.* **2001**, *101*, 2067.

(2) Weissman, H.; Song, X.; Milstein, D. *J. Am. Chem. Soc.* **2001**, *123*, 337.

(3) Chung, M.-K.; Ferguson, G.; Robertson, V.; Schlaf, M. *Can. J. Chem.* **2001**, *79*, 949.

(4) Yi, C. S.; He, Z.; Lee, D. W. *Organometallics* **2000**, *19*, 2036.

(5) Yi, C. S.; Lee, D. W.; Chen, Y. *Organometallics* **1999**, *18*, 2043.

(6) Yi, C. S.; He, Z.; Lee, D. W. *Organometallics* **2001**, *20*, 802.

(7) Chapter 3 of this thesis.

(8) Trnka, T. M.; Grubbs, R. H. *Acc. Chem. Res.* **2001**, *34*, 18.

(9) Amoroso, D.; Fogg, D. E. *Macromolecules* **2000**, *33*, 2815.

(10) (a) Esteruelas, M. A.; Herrero J.; Oro L. A. *Organometallics*, **1993**, *12*, 2377. (b) Esteruelas, M. A.; Sola, E.; Oro, L. A.; Werner, H.; Meyer, U. *J. Mol. Catal.*, **1988**, *45*, 1. (c) Esteruelas, M. A.; Valero, C.; Oro, L. A.; Meyer, U.; Werner, H. *Inorg. Chem.*, **1991**, *30*, 1159. (d) Esteruelas, M. A.; Sola, E.; Oro, L. A.; Werner, H.; Meyer, U. *J. Mol. Catal.*, **1989**, *53*, 43. (e) Werner, H.; Meyer, U.; Esteruelas, M. A.; Sola, E.; Oro, L. A.; Valero, C. *Organometallics*, **1993**, *12*, 663. (f) Andriollo, A.; Esteruelas, M. A.; Meyer, U.; Oro, L. A.; Sanchez-Delago, R. A.; Sola, E.; Valero, C.; Werner, H. *J. Am. Chem. Soc.*, **1989**, *111*, 7431. (g) Esteruelas, M. A.; Sola, E.; Oro, L. A.; Meyer, U.; Werner, H. *Angew. Chem. Int Ed. Engl.*,**1988**,*27*, 1563. (h) Esteruelas, M. A.; Oro, L. A.; Valero, C. *Organometallics*, **1992**, *11*, 3362.

(11) Gottschalk-Gaudig, T.; Folting, K.; Caulton, K. G. *Inorg. Chem.* **1999**, *38*, 5241.

(12) Drouin, S. D.; Amoroso, D.; Yap, G. P. A.; Fogg, D. E. *Organometallics* **2002**, *21*, 1042.

(13) James, B. R.; Markham, L. D.; Hui, B. C.; Rempel, G. L. *J. Chem. Soc., Dalton Trans.* **1973**, 2247.

(14) Fogg, D. E.; James, B. R. *Inorg. Chem.* **1997**, *36*, 1961.

(15) Huang, D.; Folting, K.; Caulton, K. G. *Inorg. Chem.* **1996**, *35*, 7035.

(16) Ohta, T.; Tonomura, Y.; Nozaki, K.; Takaya, H.; Mashima, K. *Organometallics* **1996**, *15*, 1521.

(17) Seddon, E. A.; Seddon, K. R. *The Chemistry of Ruthenium*; Elsevier: Amsterdam, 1984.

(18) Albinati, A.; Jiang, Q.; Rüegger, H.; Venanzi, L. M. *Inorg. Chem.* **1993**, *32*, 4940.

(19) Cotton, F. A.; Torralba, R. C. *Inorg. Chem.* **1991**, *30*, 2196.

(20) Rhodes, L. F.; Sorato, C.; Venanzi, L. M.; Bachechi, F. *Inorg. Chem.* **1988**, *27*, 604.

(21) Crozat, M. M.; Watkins, S. F. *J. Chem. Soc. Dalton Trans.* **1972**, 2513.

(22) Cotton, F. A.; Ucko, D. A. *Inorg. Chim. Acta* **1971**, *6*, 161.

(23) Summerville, R. H.; Hoffmann, R. *J. Am. Chem. Soc.* **1979**, *101*, 3821.

(24) Amoroso, D.; Yap, G. P. A.; Fogg, D. E. *Can. J. Chem.* **2001**, *79*, 958.

(25) Krassowski, D. W.; Nelson, J. H.; Brower, K. R.; Hauenstein, D.; Jacobson, R. A. *Inorg. Chem.* **1988**, *27*, 4294.

(26) Wilkes, L. M.; Nelson, J. H.; Mitchener, J. P.; Babich, M. W.; Riley, W. C.; Helland, B. J.; Jacobson, R. A.; Cheng, M. Y.; Seff, K.; McCusker, L. B. *Inorg. Chem.* **1982**, *21*, 1376.

(27) Joshi, A. M.; Thorburn, I. S.; Rettig, S. J.; James, B. R. *Inorg. Chim. Acta* **1992**, *198-200*, 283.

(28) Fogg, D. E.; James, B. R. *Inorg. Chem.* **1995**, *34*, 2557.

(29) Marchenko, A. V.; Huffman, J. C.; Valerga, P.; Tenorio, M. J.; Puerta, M. C.; Caulton, K. G. *Inorg. Chem.* **2001**, *40*, 6444.

(30) MacFarlane, K. S.; Joshi, A. M.; Rettig, S. J.; James, B. R. *Inorg. Chem.* **1996**, *35*, 7304.

(31) Bianchini, C.; Barbaro, P.; Scapacci, G.; Zanobini, F. *Organometallics* **2000**, *19*, 2450.

(32) Fogg, D. E.; James, B. R.; Kilner, M. *Inorg. Chim. Acta* **1994**, *222*, 85.

(33) Personal communication with Dr. Glenn Facey, NMR Facilities Manager, University of Ottawa, 2001.

(34) Bain, A. D., 2000, MEXICO, The McMaster Program for Lineshape Analysis, http://www.chemistry.mcmaster.ca/faculty/bain/mexiter.tar.

(35) Grocott, S. C.; Wild, S. B. *Inorg. Chem.* **1982**, *21*, 3535.

(36) Barnard, C. F. J.; Daniels, J. A.; Jeffery, J.; Mawby, R. J. *J. Chem. Soc. Dalton Trans.* **1976**, 953.

(37) Deacon, G. B.; Kepert, C. M.; Sahely, N.; Skelton, B. W.; Spiccia, L.; Thomas, N. C.; White, A. H. *J. Chem. Soc., Dalton Trans.* **1999**, 275.

(38) *Inorganic Reactions and Methods*; Zuckerman, J. J., Ed.; VCH, 1987; Vol. 2.

(39) Krassowski, D. W.; Nelson, J. H. *J. Organomet. Chem.* **1988**, *356*, 93.

(40) Gusev, D. G.; Lough, A. J.; Morris, R. H. *J. Am. Chem. Soc.* **1998**, *120*, 13138.

(41) Huffman, J. C.; Green, M. A.; Kaiser, S. L.; Caulton, K. G. *J. Am. Chem. Soc.* **1985**, *107*, 5111.

(42) Yandulov, D. V.; Huang, D.; Huffman, J. C.; Caulton, K. G. *Inorg. Chem.* **2000**, *39*, 1919, and references therein.

(43) Fordyce, W. A.; Wilczynski, R.; Halpern, J. *J. Organomet. Chem.* **1985**, *296*, 115.

(44) (a) Leitner, W.; Six, C. *Chem. Ber.* **1997**, *130*, 555. (b) Six, C.; Gabor, B.; Görls, H.; Mynott, R.; Philipps, P.; Leitner, W. *Organometallics*, **1999**, *18*, 3316.

(45) (a) Christ, M. L.; Sabo-Etienne, S.; Chaudret, B. *Organometallics* **1995**, *14*, 1082. (b) Borowski, A. F.; Sabo-Etienne, S.; Christ, M. L.; Donnadieu, B.; Chaudret, B. *Organometallics* **1996**, *15*, 1427. (c) Mauthner, K.; Soldouzi, K. M.; Mereitner, K.; Schmid, R.; Kirchner, K. *Organometallics* **1999**, *18*, 4681.

(46) Chan, A. S. C.; Shieh, H. S. *J. Chem. Soc., Chem. Commun.* **1985**, 1379.

(47) Marks, T. J.; Kolb, J. R. *Chem. Rev.* **1977**, *77*, 263.

(48) Darensbourg, M. Y.; Ash, C. E. *Adv. Organomet. Chem.* **1987**, *27*, 1.

(49) Pez, G. P.; Grey, R. A.; Corsi, J. *J. Am. Chem. Soc.* **1981**, *103*, 7528.

(50) Noyori, R.; Ohkuma, T. *Angew. Chem. Int. Ed. Engl.* **2001**, *40*, 40.

(51) Ohkuma, T.; Koizumi, M.; Ikehira, H.; Yokozawa, T.; Noyori, R. *Organic Letters* **2000**, *2*, 659.

(52) Noyori, R.; Hashiguchi, S. *Acc. Chem. Res.* **1997**, *30*, 97, and references therein.

(53) (a) Halpern, J. *Pure Appl. Chem.*, **1987**, *59*, 173. (b) Linn, D. E.; Halpern, J. *J. Organomet. Chem.* **1987**, *330*, 155.

(54) Kelson, E. P.; Phengsy, P. P. *J. Chem. Soc., Dalton Trans.* **2000**, 4023.

(55) Dani, P.; Karlen, T.; Gossage, R. A.; Gladiali, S.; van Koten, G. *Angew. Chem. Int. Ed.* **2000**, *39*, 743.

(56) Crochet, P.; Gimeno, J.; Garcia-Granda, S.; Borge, J. *Organometallics* **2001**, *20*, 4369.

(57) (a) Murai, S.; Chatani, N.; Kakiuchi, F. *Pure Appl. Chem.*, **1997**, *69*, 589. (b) Kakiuchi, F.; Sekine, S.; Tanaka, Y.; Kamatani, A.; Sonoda, M.; Chatani, N.; Murai, S. *Bull. Chem. Soc. Jpn.* **1995**, *68*, 62.

(58) (a) Matsubara, T.; Koga, N.; Musaev, D. G.; Morokuma, K. *Organometallics*, **2000**, *19*, 2318. (b) Matsubara, T.; Koga, N.; Musaev, D. G.; Morokuma, K. *J. Am. Chem. Soc.* **1998**, *120*, 12692.

(59) Guari, Y.; Sabo-Etienne, S.; Chaudret, B. *J. Am. Chem. Soc.* **1998**, *120*, 4228.

(60) Busch, S.; Leitner, W. *Adv. Synth. Catal.* **2001**, *343*, 192.

(61) Jazzar, R. F. R.; Mahon, M. F.; Whittlesey, M. K. *Organometallics* **2001**, *20*, 3745.

(62) Trost, B. M.; Imi, K.; Davies, I. W. *J. Am. Chem. Soc.* **1995**, *117*, 5371.

(63) Cotton, F. A.; Bruce, M. I.; Stone, F. G. A. *J. Chem. Soc. A* **1968**, 2162.

(64) Cole-Hamilton, D. J.; Wilkinson, G. *New J. Chem.* **1977**, *1*, 141.

(65) Dauter, Z.; Mawby, R. J.; Reynolds, C. D.; Saunders, D. R. *J. Chem. Soc. Dalton Trans.* **1985**, 1235.

(66) Ahmad, N.; Levison, J. J.; Robinson, S. D.; Uttley, M. F. In *Inorg. Synth.*; Parshall, G. W., Ed.; McGraw-Hill: New York, 1974; Vol. 15; pp 45.

(67) James, B. R. In *Comprehensive Organometallic Chemistry*; Wilkinson, G., Ed.; Pergamon Press: New York, 1982; Vol. 8, Chapter 51, and references therein.

CHAPTER 6

A Robust Ruthenium Metathesis Precursor Bearing a Chelating Iminopyrrolato Ligand

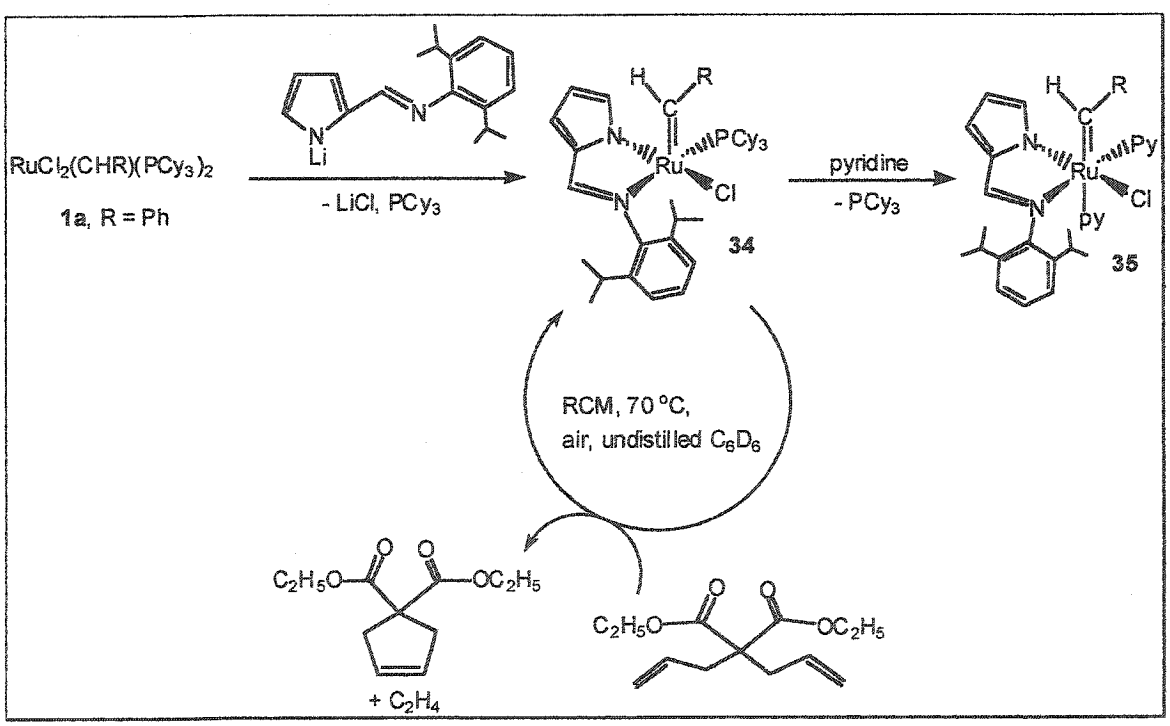

Figure 6.1 Pictorial summary of Chapter 6.

6.1. Introduction

Chelating iminopyrrolato ligands have recently emerged as effective scaffolds in the design of ethylene polymerization catalysts.[1-3] Iminopyrrolato ligands differ from the ubiquitous salicylaldimine-Schiff base ligands (Figure 6.2) by forming five-membered, rather than six-membered chelate rings.[4] They are easily prepared from commercially available precursors such as aniline and pyrrole-2-carbaldehyde, and their electronic and steric properties can be tuned via selective functionalization of the imino moiety.[5]

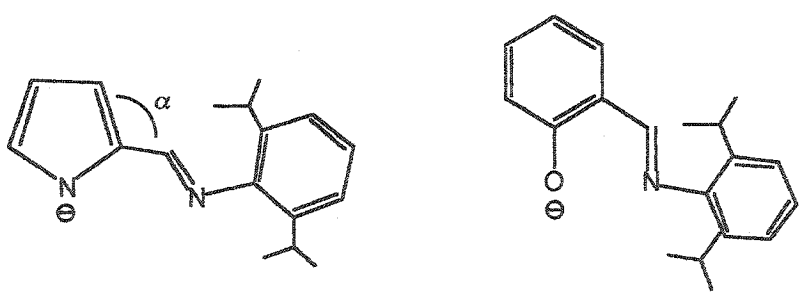

iminopyrrolato ligand (NN′) salicylaldiminato ligand

Figure 6.2 Monoiminopyrrolato (NN′) and Schiff base (exemplified by a salicylaldiminato structure) ligands, each bearing the 2,6-diisopropylphenyl substituent; exocyclic angle, α shown for NN′.

On coordination (Figure 6.3), iminopyrrolato ligands typically exhibit narrow bite angles (70 – 85°),[2,3,5] enforced by the rigid, wide exocyclic angle of the pyrrolyl unit (α, Figure 6.2).[3] This rigidity plays a role in determining the denticity of ligand coordination. For example, bis(iminopyrrolato) complexes of iron, cobalt, and zirconium generally

chelate as bidentate ligands, with one dangling imino group, as shown in Figure 6.3 B. In mono(imino)pyrrolato complexes, ligand rigidity may induce preferential bidentate, rather than monodentate, coordination. Certainly, the available spectroscopic data[3,5] indicate that the NN′ ligand remains fixedly chelated on coordination. This behaviour is attractive for the design of sterically well-defined catalysts, and inspires the work described herein.

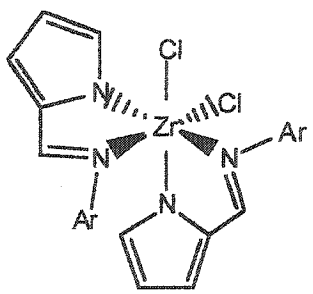

mono(imino)pyrrolato complex (**A**)

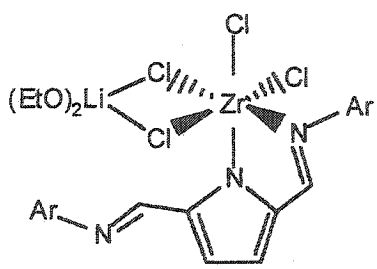

bis(imino)pyrrolato complex (**B**)

Ar = 2,6-diisopropylphenyl

Figure 6.3. Examples of known iminopyrrolato complexes.[3]

To date, there have been no reports of olefin metathesis catalysts bearing iminopyrrolato ligands, though a range of Schiff base Ru-alkylidene complexes were recently reported (Figure 6.4).[6-8] In addition to olefin metathesis catalysis, Ru-Schiff base

complexes catalyze a variety of transformations, including Kharasch addition,[9,10] atom transfer radical polymerization,[8,11] and enol ester synthesis.[9]

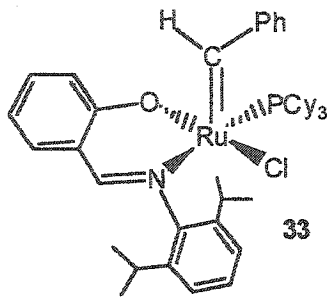

33

Figure 6.4 Metathesis catalyst **33**, representative of a series of related ruthenium alkylidene complexes bearing Schiff base ligands.[6,7]

In general, Schiff base complexes such as **33** are more robust, though less active for olefin metathesis, than the parent catalyst, $RuCl_2(PCy_3)_2(CHPh)$ (**1a**).[6,7] Metathesis catalysis via **33** is thought to occur via initial dissociation of the N(imine) "arm";[7] this lability affords entry into the catalytic cycle, but also reduces the spatial definition at the active site. In targeting an iminopyrrolato analogue of **33**, it is of interest to know whether metathesis activity can be achieved despite the anticipated "strong bite" of the NN′ ligand. This chapter describes the synthesis of two novel ruthenium iminopyrrolato complexes, one of which is a structural analogue of the Schiff base complex **33**. Reported also are the catalytic activities of these novel complexes for the ring closing metathesis (RCM) of diethyl diallylmalonate. The present work represents a preliminary step toward

the development of a novel class of asymmetric metathesis catalysts. Chiral variants on the NN′ structure, including (oxazolinyl)[12] and (oxazinyl)pyrroyl[13] ligands, are accessible, and their potential for the design of novel Ru-based metathesis catalysts will be explored in future work.

6.2. Preparation of RuCl(NN′)(PCy_3)(CHPh) (34)

The ligand precursor, mono(arylimino)pyrrole 2-C_4H_3NH[CH=N(2,6-$^iPr_2$-C_6H_3)] (HNN′), was prepared by condensation of pyrrole-2-carbaldehyde with 2,6-diisopropylaniline.[14] Lithiation of HNN′ with *n*-BuLi was accomplished in high yield by a literature route[3] and the isolated product was stored at –35 °C for several months without apparent degradation (^{1}H NMR). Reaction of LiNN′ with the benzylidene precursor $RuCl_2(PCy_3)_2$(CHPh) (**1a**) yields mononuclear iminopyrrolide complex **34** (Figure 6.5). The proposed structure is based on spectroscopic data, microanalysis, and crystallographic characterization.

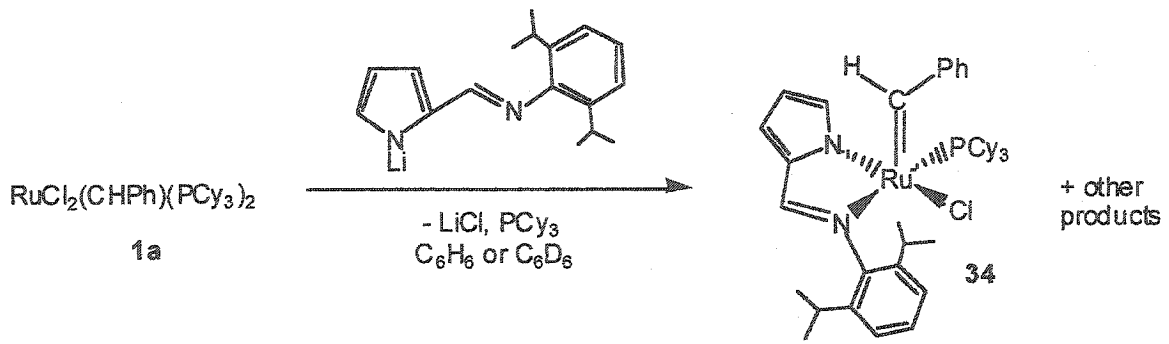

Figure 6.5 Preparation of iminopyrrolato-benzylidene complex **34**.

Despite the implicit 1:1 stoichiometry for the above reaction, an excess of LiNN′ (1.6 equiv) is required for complete reaction of **1a**, suggesting that side reaction(s) compete effectively with formation of **34**. Indeed, the *in situ* yield of **34** is approximately 78% (^{1}H NMR), and unidentified byproducts are observed by ^{31}P NMR analysis (δ_P 55, 26, 25, total integration ca. 22%). *In situ* ^{1}H NMR experiments indicate that the excess LiNN′ reagent is reduced to the pyrrole, HNN′. While the nature of the reducing agent(s) remains elusive, control experiments have demonstrated the inertness of LiNN′ toward the known products (PCy_3 and **34**) in C_6D_6, suggesting that **1a** itself is involved in the side reaction. Once isolated, product **34** is stable in both hydrocarbon and chlorinated solvents, and, thus dissolved, shows no decomposition on exposure to air for 72 h, as determined by ^{1}H NMR integration relative to an internal standard (triphenylmethane). Isolated yields of **34** are low (35-40%), owing to its extreme solubility in all solvents, including hexanes.

The ^{1}H NMR spectrum of **34** reveals the alkylidene proton as a doublet at 20.0 ppm ($^3J_{HP}$ = 11.6 Hz), split by the ^{31}P nucleus of the PCy_3 ligand. The magnitude of this HP coupling (> 10 Hz) suggests that the carbene plane is oriented parallel to the Ru-P bond axis.[15] The imino proton at δ_H 7.7 (d, $^4J_{HP}$ = 3.9 Hz) is also coupled to ^{31}P; both of these resonances collapse to singlets in the phosphorus-decoupled spectrum. Restricted rotation about the N-C (imino-aryl) bond is implied by the chemically inequivalence of the isopropyl groups, which are observed as two separate methine septets and four methyl

doublets in the ^{1}H NMR spectrum (C_6D_6). This inequivalence indicates that rotation about each aryl-methine C-C bond is inhibited; it is, surprisingly, maintained even at 70 °C. Likewise, the ^{13}C NMR spectrum shows a distinct peak for each ^{i}Pr-substituted aromatic position (142.8 and 142.0 ppm); these assignments are supported by correlation experiments (HMBC) which show long-range coupling to the ^{i}Pr protons. In the ^{1}H NMR spectrum, broad peaks in the characteristic locations of 7.1, 6.8 and 6.5 ppm are assigned to the C3-, C5- and C4-positions of the pyrrolyl ring, respectively, on the basis of correlation experiments (COSY, HMQC, HMBC) and related literature reports.[3,5,16] In the ^{13}C NMR spectrum, a doublet at 303.5 ppm ($^{2}J_{CP}$ = 14.1 Hz) confirms the presence of the alkylidene ligand. The C5-, and C4-pyrrolyl signals, located at 142.2 and 114.7 ppm, respectively, are consistent with other complexes of NN', showing little sensitivity to the nature of the metal centre.[3,14,16]

6.3. Molecular Structure of RuCl(NN')(PCy_3)(CHPh) (34)

Crystals of 34 suitable for X-ray analysis were grown from a concentrated toluene solution. An ORTEP diagram is shown in Figure 6.6, selected bond lengths and angles in Table 6.1. The geometry at ruthenium is a distorted square pyramid in which the benzylidene ligand occupies the apical site and the PCy_3 group is trans to $N_{(imine)}$ in the equatorial plane. The four "equatorial" bonds are, in fact, angled toward the vacant site,

as manifested by the angles for P-Ru-N(2) (159.56(8)°) and N(1)-Ru-Cl (164.39(8)°). The torsion angle about ∠P-Ru-C18-C24 is 129.6(3)°, implying a dihedral angle (∠P-Ru-C(18)-H_α) that is close to zero and thus consistent with the large J_{HP} coupling constant (11.6 Hz) for this complex (*vide supra*). The bite angle of the iminopyrrolato ligand (79.04(10)°), while slightly wider than in related Ti and Zr complexes $Zr(NN')_2(NMe_3)_2$ (average 70.1°)[3] and $Ti(N_AN_B)_2Cl_2$ (average 75.9°, N_AN_B = 2-(PhNCH)C_4H_3N),[2] is considerably more acute than the O-Ru-N angle in salicylaldiminato analogue **33** (88.9(2)°).[6] The sum of the bond angles around N(1) is 360°, attesting to the planarity of the pyrrolyl unit. The exocyclic angle of 132.6(3)° for C(3)-C(4)-C(5) is consistent with values found in previous work; this value is maintained in both free and coordinated iminopyrrolato ligands.[3] The aromatic plane of the diisopropylphenyl unit is orthogonal to the fused ring system, an orientation which accommodates the steric demand of the isopropyl substituents and which is maintained on dissolution, as judged from the complexity of the ^{1}H NMR spectrum (noted above). The Ru-C(18) (carbene carbon) bond distance (1.828(4) Å) is similar to that in **33** (1.850(6) Å),[6] and in $RuCl_2$(=CH-*p*-$C_6H_4Cl)(PCy_3)_2$ (1.838(3) Å).[17] The Ru-N(2) (imine nitrogen) bond length (2.149(2) Å) is marginally longer than the Ru-N(1) (pyrrolyl nitrogen) distance (2.065(3) Å), consistent with the trend in M-N bond distances for other iminopyrrolato complexes.[3,5] Ru-Cl and Ru-P bond distances of 2.3869(8) and 2.3474(8) Å, respectively, are typical and similar

to those in **33** (2.382(2) and 2.345(2) Å)[6] and in $RuCl_2(CO)(PCy_3)_2$ (2.400(2) Å and 2.3811(5) Å, respectively).[18]

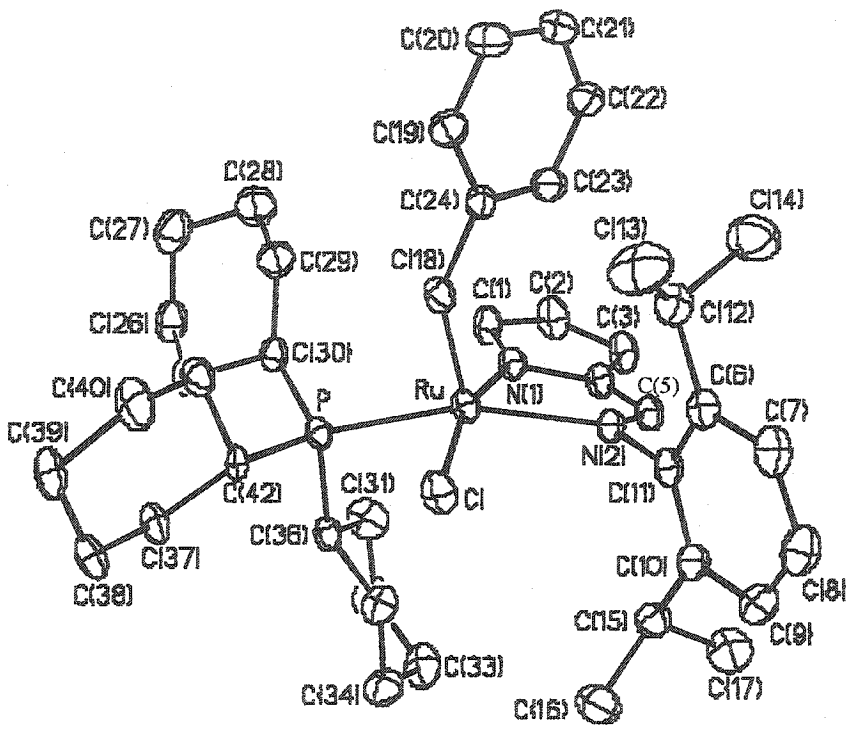

Figure 6.6 ORTEP diagram for $RuCl(NN')(PCy_3)(CHPh)$ (**34**). Thermal ellipsoids shown at 30% probability level; hydrogen atoms are omitted for clarity.

Table 6.1 Selected bond lengths (Å) and angles (deg) for RuCl(NN′)(PCy_3)(CHPh) (**34**)

Bond Distances (Å)		Bond Angles (deg)	
Ru-C(18)	1.828(4)	C(18)-Ru-N(1)	98.49(13)
Ru-P	2.3474(8)	C(18)-Ru-N(2)	105.72(12)
Ru-N(1)	2.065(3)	N(1)-Ru-N(2)	79.04(10)
Ru-N(2)	2.149(2)	N(1)-Ru-Cl	164.39(8)
Ru-Cl	2.3869(8)	N(2)-Ru-P	159.56(8)
C(18)-C(24)	1.479(5)	C(18)-Ru-Cl	93.74(11)
N(2)-C(5)	1.307(4)	C(18)-Ru-P	94.69(10)
		C(24)-C(18)-Ru	134.2(2)

6.4. Preparation of RuCl(NN′)($py)_2$(CHPh) (35)

The tricyclohexylphosphine ligand of **34** undergoes facile displacement by pyridine to yield the bis(pyridine) complex RuCl(NN′)($py)_2$(CHPh) (**35**, Figure 6.7), which was isolated as a yellow-green microcrystalline solid. Characterization is based on spectroscopic evidence and microanalysis. The ^{13}C NMR spectrum of **35** shows the alkylidene ligand as a singlet at 316.6 ppm. In the ^{1}H NMR spectrum, the alkylidene proton is observed as a characteristically low-field peak at 20.51 ppm, and the presence of two pyridine ligands is supported by the relative integration of the aromatic signals. In related work, preferential binding of two, rather than a single pyridine ligand has been noted for complexes **36**-**38** (Figure 6.8).[19,20]

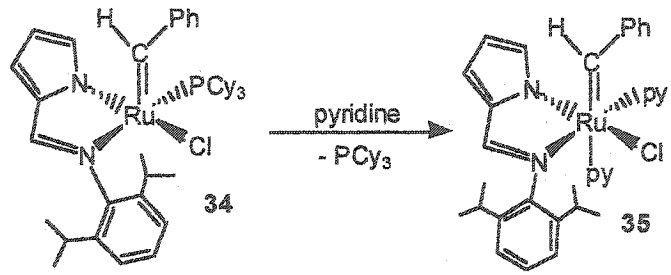

Figure 6.7. Preparation of bis(pyridine) complex $RuCl(NN')(py)_2(CHPh)$ (**35**).

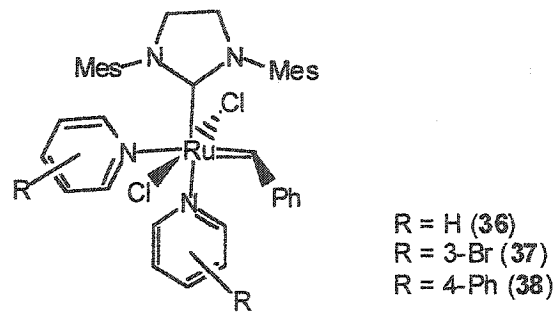

Figure 6.8. Ru-alkylidene complexes reported by Grubbs et al.: complexes preferentially bind two, rather than one, pyridine ligand.[19,20]

Small amounts of a new product (~10%) are formed on drying solid **35** under high vacuum (500 mTorr, 18 h). The product is tentatively identified as the mono(pyridine) derivative on the basis of ^{1}H NMR analysis, which shows a corresponding decrease in the relative area of the aromatic signals, and a new alkylidene peak, located at 19.70 ppm; the latter peak disappears immediately on addition of pyridine to the sample. Loss of one pyridine ligand has also been noted on exposure of Grubbs catalyst **36** to high vacuum.[19]

6.5. Catalytic RCM via Iminopyrrolato Complexes

Preliminary investigations were undertaken into the activities of complexes **34** and **35** for ring-closing metathesis (RCM) of diethyl diallylmalonate (Figure 6.9). Although inactive at room temperature, **34** is a robust catalyst at 70 °C, performing RCM in presence of air, in non-distilled, non-degassed solvent (Table 6.2, entry 1).

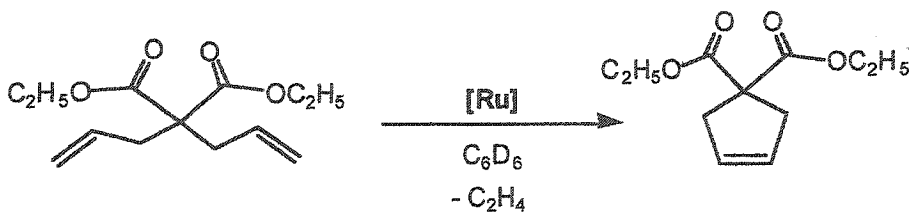

Figure 6.9 RCM of diethyl diallylmalonate by ruthenium complexes.

Table 6.2 RCM of Diethyl diallylmalonate Catalyzed by $RuCl(NN^{i})(PCy_3)(CHPh)$ (**34**) and $RuCl(NN^{i})(py)_2(CHPh)$ (**35**).[a]

entry	catalyst	temp (°C)	solvent	Additive	Time (min)	conv (%)[b]
1	**34**	70	C_6D_6	-	480	100
2	**34**	70	[c]	-	1440	50
3[d]	**34**	70	C_6D_6	-	1440	45
4[d]	**34**	70	C_6D_6	PCy_3[e]	1440	4
5[d]	**34**	70	C_6D_6	CuCl[f]	1440	100
6	**34**	23	C_6D_6	$TlPF_6$[g]	1440	0
7	**34**	70	C_6D_6	$TlPF_6$[h]	20	33
8	**34**	70	C_6D_6	$TlPF_6$[g]	10	100
9[d]	**35**	70	C_6D_6	-	1440	10
10	**35**	70	C_6D_6	-	1440	0

[a] Conditions, unless otherwise noted: performed in air, using non-degassed solvent, [Ru] = 7.7 mM; 5 mol % Ru. [b] Determined by ^1H NMR analysis. [c] In neat substrate: 13 μmol Ru in 500 μL (2.1 mmol) diethyl diallylmalonate. [d] Performed under nitrogen in degassed C_6D_6. [e] 5.8 μmol (1 equiv per Ru). [f] 58 μmol (10 equiv per Ru). [g] 29 μmol (5 equiv per Ru). [h] 5.8 μmol (1 equiv per Ru).

Exclusive selectivity for RCM over intermolecular (ADMET) processes is noted; even in the absence of solvent (70 °C), ^1H NMR analysis showed no evidence of competitive oligomerization by **34**, though catalyst degradation limited conversions to ≤ 60% under these conditions (entry 2). Inactivity at ambient temperature is attributed to the low lability of both P and N_{imino} donors, a feature also exhibited by the Schiff base analogues, including **33**.[6,7] Further evidence for this stability comes from the absence of any correlation between coordinated and free PCy_3 in ^{31}P NMR EXSY experiments at 70

°C, which shows that there is no phosphine exchange on the NMR timescale. Observation of four separate methyl doublets in the ^{1}H NMR spectrum at 70 °C likewise suggests that the iminopyrrolato chelate is non-fluxional. Stoichiometric NMR experiments show no evidence of a propagating species. Failure to observe a propagating species, or free PCy_3, by NMR analysis suggests that the catalysis is carried via trace amounts (< 5%) of an active species. Similar observations have been noted for other Ru metathesis catalysts, including Schiff base analogues of **34**[7] and tris(pyrazolyl)borate derivative $Ru(Tp)(PCy_3)(CHPh)$.[21] The catalytic activity of **34** indicates that there is dissociation of one of the two neutral ligands in the basal plane of the square pyramid. The following catalytic data suggest that initiation occurs via phosphine, rather than imine, dissociation: (1) inhibition of activity on addition of free PCy_3 (entries 4 vs. 3), and (2) enhanced RCM activity on addition of the known phosphine scavenger,[22] CuCl (entries 5 vs. 3). These results contrast with the behaviour of the related Schiff base precursors, which are thought to operate via initial imine dissociation.[7]

The activity of **34** is lower on exclusion of air (entry 3 vs. 1), perhaps because oxidation of PCy_3 is suppressed. A similar effect is found in catalytic hydrogenation via $RhCl(PPh_3)_3$[23] and trans-$IrCl(CO)(PPh_3)_2$,[24] and in hydrosilylation by $RuCl_2(PPh_3)_3$,[25] all of which are accelerated in the presence of small amounts of oxygen.

As an alternative to loss of a neutral donor ligand, loss of chloride can be induced to create a vacant site cis to the alkylidene ligand.[22,26-28] Addition of $TlPF_6$, despite its

poor solubility in benzene, dramatically increases the rate of metathesis by **34**: vigorous bubbling of ethylene occurs at the surface of the $TlPF_6$ granules, and RCM of diethyl diallylmalonate is complete within 10 min at 70 °C (entry 8). Poor solubility of $TlPF_6$ in C_6D_6 may account for the necessity of heating, and for the non-stoichiometric rate enhancement (entries 7, 8). Current work is aimed at isolating and characterizing the catalytic precursor derived by reaction of **34** with $TlPF_6$ and, ultimately, at optimizing its catalytic activity.

The low activity of pyridine complex **35** (entry 9) is surprising in view of the emerging view that substitution of phosphine by pyridine enhances metathesis activity in ruthenium precursors.[19,20,29] Although the precise origins of the low activity of **35** have not yet been identified, it is possible that the required dissociation of *two* pyridine ligands (vs. a single phosphine in **34**), represents a kinetic disadvantage in this context. The relative instability of complex **35** vs. **34** may also account for its poor activity, if the rate of decomposition competes effectively with catalysis. The instability of complex **35** on exposure to air is indicated by the loss of characteristic alkylidene peak in the ^1H NMR spectrum, and by its inactivity for RCM in air (Table 6.2, entry 10).

6.6. Conclusions

The foregoing describes the preparation and metathesis activity of the novel iminopyrrolato complex RuCl(NN′)(PCy_3)(CHPh) (**34**). The robustness of catalyst **34** reflects significant steric protection at the metal centre. The spectroscopic and catalytic data suggest that activation of **34** occurs via initial phosphine, rather than imine, dissociation. Strong chelation of the iminopyrrolato (NN′) ligand is an attractive feature for the design of sterically well-defined catalysts; incorporation of chirality in NN′ is a promising strategy for the preparation of stereoselective analogues of **34**. Replacement of the PCy_3 ligand in **34** by two pyridine ligands resulted in a dramatic decrease in both catalytic activity and robustness, perhaps implying a stronger binding of pyridine to these electron-rich late metal systems than has been generally recognized.

6.7. References

(1) Yoshida, Y.; Saito, J.; Mitani, M.; Takagi, Y.; Matsui, S.; Ishii, S.; Nakano, T.; Kashiwa, N.; Fujita, T. *Chem. Commun.* **2002**, *1298*.

(2) Yoshida, Y.; Matsui, S.; Takagi, Y.; Mitani, M.; Nakano, T.; Tanaka, H.; Kashiwa, N.; Fujita, T. *Organometallics* **2001**, *20*, 4793.

(3) Dawson, D. M.; Walker, D. A.; Thornton-Pett, M.; Bochmann, M. *J. Chem. Soc., Dalton Trans.* **2000**, 459.

(4) Blaser, H.-U. *Chem. Rev.* **1992**, *92*, 935.

(5) Hao, H.; Bhandari, S.; Ding, Y.; Roesky, H. W.; Magull, J.; Schmidt, H.-G.; Noltemeyer, M.; Cui, C. *Eur. J. Inorg. Chem.* **2002**, 1060.

(6) Chang, S.; Jones, L.; Wang, C.; Henling, L. M.; Grubbs, R. H. *Organometallics* **1998**, *17*, 3460.

(7) DeClercq, B.; Verpoort, F. *Adv. Synth. Catal.* **2002**, *344*, 639.

(8) DeClercq, B.; Verpoort, F. *Macromolecules* **2002**, *35*, 8943.

(9) DeClercq, B.; Verpoort, F. *Tet. Lett.* **2001**, *42*, 8959.

(10) DeClercq, B.; Verpoort, F. *Catal. Lett.* **2002**, *83*, 9.

(11) DeClercq, B.; Verpoort, F. *J. Organomet. Chem.* **2003**, *672*, 11.

(12) Mazet, C.; Gade, L. H. *Chem. Eur. J.* **2002**, *8*, 4308.

(13) Mazet, C.; Gade, L. H. *Inorg. Chem.* **2003**, *42*, 210.

(14) Matsuo, Y.; Mashima, K.; Tani, K. *Chem. Lett.* **2000**, 1114.

(15) Schwab, P.; Grubbs, R. H.; Ziller, J. W. *J. Am. Chem. Soc.* **1996**, *118*, 100.

(16) Matsuo, Y.; Mashima, K.; Tani, K. *Organometallics* **2001**, *20*, 3510.

(17) Schwab, P.; France, M. B.; Ziller, J. W.; Grubbs, R. H. *Angew. Chem. Int. Ed. Engl.* **1995**, *34*, 2039.

(18) Chapter 3 of this thesis.

(19) Sanford, M. S.; Love, J. A.; Grubbs, R. H. *Organometallics* **2001**, *20*, 5314.

(20) Love, J. A.; Morgan, J. P.; Trnka, T. M.; Grubbs, R. H. *Angew. Chem. Int. Ed.* **2002**, *41*, 4035.

(21) Sanford, M. S.; Henling, L. M.; Grubbs, R. H. *Organometallics* **1998**, *17*, 5384.

(22) Dias, E. L.; Nguyen, S. T.; Grubbs, R. H. *J. Am. Chem. Soc.* **1997**, *119*, 3887.

(23) van Bekkum, H.; van Rantwijk, F.; van de Putte, T. *Tet. Lett.* **1969**, 1.

(24) James, B. R.; Memon, N. A. *Can. J. Chem.* **1968**, *46*, 217.

(25) Gulinski, J.; James, B. R.; Marciniec, B. *J. Organomet. Chem.* **1995**, *499*, 173.

(26) Hansen, S. M.; Volland, M. A. O.; Rominger, F.; Eisenträger, F.; Hofmann, P. *Angew. Chem. Int. Ed.* **1999**, *38*, 1273.

(27) Amoroso, D.; Yap, G. P. A.; Fogg, D. E. *Organometallics* **2002**, *21*, 3335.

(28) Chapter 4 of this thesis.

(29) Dias, E. L. Ph. D. Thesis, California Institute of Technology, 1998.

CHAPTER 7

Conclusions and Recommendations for Future Work

The work summarized in this thesis illustrates the versatile catalytic chemistry of ruthenium alkylphosphine complexes. Successful tandem ROMP-hydrogenation methodology is described in Chapter 3; this chemistry rests on the ease of transforming Ru(II) alkylidene complexes into hydride derivatives. Depending on the reaction conditions, several different hydride products can form on hydrogenolysis of $RuCl_2(PCy_3)_2(CHPh)$ (**1a**). Strategic transformations at the active site were targeted and, ultimately, reversible cycling between ROMP and hydrogenation chemistry was achieved. Use of methanol and base in the reduction step allowed complete hydrogenation of polymeric olefins at the surprisingly low hydrogenation pressure of 1 atm. This exceptional hydrogenation activity was attributed, in part, to formation of the active hydrogenation catalyst $RuHCl(CO)(PCy_3)_2$ (**13**). Future work in this laboratory will further probe the contributions of MeOH solvent in the hydrogenation chemistry. The tandem metathesis-hydrogenation methodology is currently being applied to other catalytic initiators and substrates, including RCM and CM substrates. Development of *asymmetric* tandem metathesis-hydrogenation processes is an ultimate goal of this work.

In order to more fully realize the potential of Ru(II) complexes in homogeneous catalysis, it is desirable to minimize formation of trichloride-bridged dinuclear structures.

Such species can function as a catalytic sink in chemistry mediated by mononuclear, dichlororuthenium catalysts. Use of alternative anionic ligands in place of the ubiquitous chlorides can, advantageously, inhibit such bimolecular deactivation. The mononuclear structural motif is stabilized by incorporating perfluorophenoxide "pseudohalide" ligands. Thus, vinylidene complex $Ru(OC_6F_5)_2$(dcypb)(=C=CHBu^t) (**18**) exists as a stable mononuclear structure, whereas its dichloro analogue, **19•Cl**, is a face-bridged dimer. Comparative studies of ROMP via **18** and **19•Cl** indicate that **18** initiates more efficiently than the dinuclear complex. Future work in this area will probe the potential of fluorinated aryloxides as *modular* pseudohalides in the design of new catalysts. Very exciting recent work by Jay Conrad of this group suggests that chiral, chelating perfluorophenoxides are effective scaffolds for preparation of robust, *stereoselective* metathesis catalysts.

The tendency of dichloro complexes to form $Ru_2(\mu\text{-}Cl)_3$ structures was also recognized in the chemistry of carbonyl complex $Ru_2Cl_4(CO)_2(dcypb)_2$ (**21**), which in solution can exist in three different isomeric forms. Of these, the trichloride-bridged isomer **21a** always predominates. The stability of **21a** is reflected by its inertness toward oxygen and its startlingly low reactivity toward CO. This stability is advantageous for the high-yield preparation and storage of **21**. On reaction with a standard hydride reagent, **21** is easily transformed into the highly active hydrogenation catalyst K[*fac*-$RuH_3(CO)$(dcypb)] (**28**). Activity of the latter complex for Murai coupling opens the

possibility of effecting tandem Murai-hydrogenation chemistry on diaryl ketones, a subject of current investigation in this laboratory.

Our interest in alternative anionic ligands led us to novel pyrrolato derivatives. Thus, replacement of a chloride ligand in **1a** by a chelating iminopyrrolato ligand, yields the robust, mononuclear $RuCl(NN')(PCy_3)(CHPh)$ (**34**). Complex **34** was found to be an active metathesis catalyst, effecting RCM in the presence of oxygen and moisture. Activation of **34** probably occurs via initial phosphine, rather than imine, dissociation. Strong chelation of the iminopyrrolato (NN′) ligand is an attractive feature for the design of sterically well-defined catalysts; future work in this area will investigate the possibility of incorporating chirality in the NN′ scaffold.

APPENDICES

Appendix A

Polymer Characterization

The isolated polymers were characterized by IR (as thin films on a NaCl plate), and ^{1}H and $^{13}C\{^{1}H\}$ NMR spectroscopy. Full characterization data for the related unsaturated polymers is included for comparison. Molecular weights (M_n) and PDI values were determined by GPC in CH_2Cl_2 using polystyrene standards (instrumental and procedural details on page 16).

Poly(octene). IR (neat; cm^{-1}): 3004 (m; =CH), 2922 (s; CH_3, CH_2), 2852 (s; CH_3, CH_2), 1464 (m; CH_2), 967 (m; CH=CH *trans*), 721 (w; CH=CH *cis*). ^{1}H NMR ($CDCl_3$, δ): 5.38 (br m, 2 H, olefinic), 2.01 (br m, 4 H, 2 × C*H*$_2$), 1.32 (br m, 8 H, 4 × C*H*$_2$). $^{13}C\{^{1}H\}$ NMR ($CDCl_3$): δ 130.3, 129.9, 32.6, 29.7, 29.2, 29.1, 29.0, 27.2. GPC (CH_2Cl_2): PDI = 1.42 ± 0.24; 10^{-4} M_n = 5.3 ± 1.4, average of three trials.

Hydrogenated Poly(octene) (Polyethylene). IR (neat; cm^{-1}) 2915 (m; CH_3, CH_2), 2850 (m; CH_3, CH_2), 1470 (m; CH_2). ^{1}H NMR ($CDCl_3$): δ 1.27 (br s) ppm. $^{13}C\{^{1}H\}$ NMR ($CDCl_3$): δ 29.4, 29.4, 29.2, 28.3 ppm. GPC data could not be obtained due to insolubility in CH_2Cl_2 at RT.

Poly(5-bromo-1-octene) (poly-9). IR (neat; cm^{-1}) 3005 (m; =C-H), 2934 (m; CH_3, CH_2), 2857 (m; CH_3, CH_2), 1660 (m, C=C), 1444 (m; CH_2), 1364 (w; CH), 969 (m; CH=CH, *trans*), 727 (w; C-Br). ^{1}H NMR ($CDCl_3$, δ): 5.40 (m, 2 H, olefinic), 4.02 (m, 1 H, C*H*Br), 2.35-1.20 (m, 10 H, 5 × C*H*$_2$).^{13}C NMR ($CDCl_3$, δ): 130.94, 130.58, 129.81, 129.34, 129.05, 128.50, 57.81(*C*-Br),

38.92, 38.64, 31.88, 30.54, 27.56, 27.35, 26.54, 25.39. GPC (CH_2Cl_2): 10^{-4} M_n = 6.0 ± 1.5, PDI = 1.41 ± 0.22, average of two trials.

Hydrogenated Poly-9: IR (neat; cm^{-1}): 2928 (m; CH_3, CH_2), 2855 (m; CH_3, CH_2), 1460 (m; CH_2), 1370 (w; CH), 723 (w; C-Br). ^1H NMR ($CDCl_3$, δ): 4.03 (m, 1 H, C*H*Br), 1.98-1.10 (m, 14 H, 7 × CH_2). ^{13}C NMR ($CDCl_3$, δ): 59.53 (*C*-Br), 39.73, 29.93, 29.55, 28.11. GPC (CH_2Cl_2): 10^{-4} M_n = 4.5 ± 1.6, PDI = 1.38 ± 0.24, average of two trials.

Poly(5-methoxy-1-octene)(poly-10): IR (neat, cm^{-1}): 2937 (m; CH_3, CH_2), 2856 (m; CH_3, CH_2), 2820 (m; CH_3, CH_2), 1457 (m; CH_2), 1368 (w; CH), 1099 (m; C-O-C), 968 (m; CH=CH, *trans*), 725 (m; CH=CH, *cis*). ^1H NMR ($CDCl_3$, δ): 5.39 (m, 2 H, olefinic), 3.30 (s, 3 H, OCH_3), 3.13 (m, 1 H, C*H*O), 2.01 (m, 4 H, 2 × CH_2CHOMe), 1.42 (m, 6 H, 3 × CH_2). ^{13}C NMR ($CDCl_3$, δ): 130.91, 130.80, 130.46, 130.33, 80.82, 57.02, 34.02, 33.58, 33.46, 33.34, 28.97, 27.94, 25.90, 25.77, 23.64. GPC (CH_2Cl_2): 10^{-4} M_n = 6.3 ± 1.6, PDI = 1.40 ± 0.22, average of two trials.

Hydrogenated Poly-10: IR (neat, cm^{-1}): 2931 (m; CH_3, CH_2), 2855 (m; CH_3, CH_2), 2819 (m; CH_3, CH_2), 1461 (m; CH_2), 1370 (w; CH), 1098 (m; C-O-C). ^1H NMR ($CDCl_3$, δ): 3.33 (s, 3 H, OCH_3), 3.13 (m, 1 H, C*H*O), 1.05-1.65 (m, 14 H, 7 × CH_2). ^{13}C NMR ($CDCl_3$, δ): 81.58, 57.00, 34.02, 34.06, 30.50, 25.87. GPC (CH_2Cl_2): 10^{-4} M_n = 6.3 ± 1.4, PDI = 1.40 ± 0.25, average of two trials.

Poly(5-acetoxy-1-octene) (poly-11): IR(neat, cm^{-1}): 2938 (m; CH_3, CH_2), 2861 (m; CH_3, CH_2), 1730 (s; C=O), 1635 (m; C=C), 1455 (m; CH_2), 1374 (w; CH), 1250 (m; C-C(=O)-O), 1024 (m;

C-O), 970 (m; CH=CH, *trans*), 732 (w; CH=CH, *cis*). ^{1}H NMR ($CDCl_3$, δ): 5.40 (m, 2 H, olefin), 4.83 (m, 1 H, C*H*OAc), 2.12-1.87 (br, 7 H, CO_2CH_3, 2 × CH_2CHOAc), 1.67-1.39 (br, 2 H, CH_2), 1.39-1.13 (br, 4 H, 2 × CH_2). ^{13}C NMR ($CDCl_3$, δ): 170.84 (CO_2Me), 130.35, 130.19, 129.88, 129.77, 129.68, 129.61, 129.31, 129.10, 73.67 (HCOAc), 73.23 (CO_2CH_3), 33.92, 32.38, 28.41, 27.00, 26.96, 25.32, 25.34, 25.17, 24.85, 23.20, 23.16, 21.26. GPC (CH_2Cl_2): 10^{-4} M_n = 3.6 ± 2.1, PDI = 1.17 ± 0.25, average of two trials.

Hydrogenated Poly-11: IR (neat, cm^{-1}): 2932 (m; CH_3, CH_2), 2857 (m; CH_3, CH_2), 1735 (s; C=O), 1440 (m; CH_2), 1373 (w; CH), 1244 (m; C(O)-O), 1021 (m; C-O). ^{1}H NMR ($CDCl_3$, δ): 4.82 (m, 1 H, C*H*OAc), 1.98 (s, 3 H, CO_2CH_3), 1.46 (m, 4 H, 2 × CH_2CHOAc), 1.23 (br, 10 H, 5 × CH_2). ^{13}C NMR ($CDCl_3$, δ): 170.91 (*C*=O), 74.32 (HCOAc), 34.22, 32.20, 29.50, 29.41, 27.25, 25.33, 23.01, 21.32. GPC (CH_2Cl_2): 10^{-4} M_n = 6.1 ± 1.8, PDI = 1.23 ± 0.22, average of two trials.

Poly(12). IR (neat, cm^{-1}) 2975 (m; =C-H), 2928 (s; CH_3, CH_2), 2864 (s; CH_2, CH_3), 1656 (m; C=C), 1453 (m; CH_2), 1387 (m; CH), 1113 (m; C-O-C), 967 (m; ring), 915 (w; CH=CH *trans*), 734 (m, CH=CH *cis*). ^{1}H NMR ($CDCl_3$, δ): 5.25, 5.17 (br m, 2 H, olefinic), 3.37-3.05 (br s, 6 H; includes singlet for OCH_3 at δ 3.35), 2.89-1.01 (br m, 6 H). ^{13}C{^{1}H} NMR ($CDCl_3$, δ): 134.1, 136.9, 132.1, 131.0, 129.7, 74.9 (*C*HO) , 58.8 (OCH_3), 46.3, 44.7, 44.2, 42.2, 42.5, 41.4, 39.2, 39.7, 37.0, 36.2. GPC (CH_2Cl_2): 10^{-4} M_n = 3.00 ± 0.14, PDI = 1.04 ± 0.01, average of two trials.

Hydrogenated Poly(12): IR (neat; cm^{-1}): 2919 (m; CH_3, CH_2), 2737 (s; CH_3, CH_2), 1437 (s; CH_2), 1386 (m; CH), 1114 (m; C-O-C), 959 (m; ring). ^1H NMR ($CDCl_3$, δ): 3.52-3.25 (br s, 6 H; includes singlet for OCH_3 at δ 3.35), 2.31-0.55 (br m, 10 H). $^{13}C\{^1H\}$ NMR ($CDCl_3$, δ): 74.7 (*C*HO), 58.8 (OCH_3), 46.3, 44.5, 44.2, 43.0, 41, 39.2, 38.7, 36.1, 35.0. GPC (CH_2Cl_2): 10^{-4} M_n = 2.97 ± 0.17, PDI = 1.03 ± 0.01, average of two trials.

Appendix B

Crystallographic Information for $RuCl_2(PCy_3)_2(DMA)$ (6)

Structural determination of $RuCl_2(PCy_3)_2(DMA)$. A suitable crystal was selected, mounted on a thin, glass fiber using paraffin oil and cooled to the data collection temperature. Data were collected on a Bruker AXS SMART 1k CCD diffractometer using 0.3° ω-scans at 0, 90, and 180° in ϕ. Initial unit-cell parameters were determined from 60 data frames collected at different sections of the Ewald sphere. Semi-empirical absorption corrections based on equivalent reflections were applied.[1]

Systematic absences in the diffraction data and unit-cell parameters were uniquely consistent with the reported space group. The structure was solved by direct methods, completed with difference Fourier syntheses and refined with full-matrix least-squares procedures based on F^2. All hydrogen atoms were treated as idealized contributions. All scattering factors are contained in the SHELXTL 6.12 program library.[2]

---

(1) SADABS, Bruker AXS, Madison, WI, 2000.

(2) Sheldrick, G. M., SHELXTL V5.10, Siemens Analytical X-ray Instruments Inc., Madison WI 1997.

Table B.1. Crystal Data and Structure Refinement Details for $RuCl_2(H_2)(PCy_3)_2(DMA)$ (**6**).

Empirical formula	$C_{40}\,H_{75}\,Cl_2\,N\,O\,P_2\,Ru$
Formula weight	819.92
Temperature	203(2) K
Wavelength	0.71073 Å
Crystal system, space group	Orthorhombic, Pnma
Unit cell dimensions	a = 17.831(2) A alpha = 90 deg.
	b = 23.980(3) A beta = 90 deg.
	c = 9.6048(9) A gamma = 90 deg.
Volume	4106.9(9) $Å^3$
Z, Calculated density	4, 1.326 Mg/m^3
Absorption coefficient	0.621 mm^{-1}
F(000)	1752
Crystal size	0.1 x 0.1 x 0.1 mm
Theta range for data collection	1.70 to 24.71 deg.
Limiting indices	0<=h<=20, 0<=k<=28, 0<=l<=11
Reflections collected / unique	32693 / 3589 [R(int) = 0.2310]
Completeness to theta =	24.71 99.9 %
Absorption correction	Semi-empirical from equivalents
Max. and min. transmission	0.862144 and 0.494348
Refinement method	Full-matrix least-squares on F^2
Data / restraints / parameters	3589 / 0 / 227
Goodness-of-fit on F^2	1.056
Final R indices [I>2sigma(I)]	R1 = 0.0670, wR2 = 0.1568
R indices (all data)	R1 = 0.1179, wR2 = 0.1799
Extinction coefficient	0.0074(8)
Largest diff. peak and hole	0.905 and -0.954 $e.Å^{-3}$

Definition of R indices: $R_1 = \Sigma(F_o - F_c)/\Sigma(F_o)$; $wR_2 = [\Sigma[w(F_o^2 - F_c^2)^2]/\Sigma[w(F_o^2)^2]]^{1/2}$

Table B.2. Bond lengths [Å] and angles [deg] for $RuCl_2(H_2)(PCy_3)_2(DMA)$ (**6**).

Ru-O(1)	2.323(7)
Ru-P(1)	2.3707(16)
Ru-P(1)#1	2.3707(16)
Ru-Cl(1)	2.423(4)
Ru-Cl(2)	2.428(6)
P(1)-C(6)	1.845(6)
P(1)-C(18)	1.848(7)
P(1)-C(12)	1.856(6)
O(1)-C(19)	1.212(13)
N(1)-C(19)	1.292(14)
N(1)-C(22)	1.466(16)
N(1)-C(21)	1.475(15)
C(1)-C(2)	1.524(10)
C(1)-C(6)	1.538(8)
C(2)-C(3)	1.502(11)
C(3)-C(4)	1.506(10)
C(4)-C(5)	1.529(9)
C(5)-C(6)	1.525(9)
C(7)-C(12)	1.519(8)
C(7)-C(8)	1.550(9)
C(8)-C(9)	1.511(10)
C(9)-C(10)	1.513(10)
C(10)-C(11)	1.528(9)
C(11)-C(12)	1.532(9)
C(13)-C(14)	1.512(9)
C(13)-C(18)	1.514(9)
C(14)-C(15)	1.495(10)
C(15)-C(16)	1.525(10)
C(16)-C(17)	1.527(9)
C(17)-C(18)	1.532(9)
C(19)-C(20)	1.548(16)
O(1)-Ru-P(1)	97.78(4)
O(1)-Ru-P(1)#1	97.78(4)
P(1)-Ru-P(1)#1	164.29(8)
O(1)-Ru-Cl(1)	90.21(19)
P(1)-Ru-Cl(1)	91.07(4)

P(1)#1-Ru-Cl(1)	91.07(4)
O(1)-Ru-Cl(2)	83.35(19)
P(1)-Ru-Cl(2)	89.81(5)
P(1)#1-Ru-Cl(2)	89.81(5)
Cl(1)-Ru-Cl(2)	173.55(13)
C(6)-P(1)-C(18)	101.6(3)
C(6)-P(1)-C(12)	110.1(3)
C(18)-P(1)-C(12)	101.8(3)
C(6)-P(1)-Ru	111.0(2)
C(18)-P(1)-Ru	118.4(2)
C(12)-P(1)-Ru	113.0(2)
C(19)-O(1)-Ru	159.1(8)
C(19)-N(1)-C(22)	125.7(12)
C(19)-N(1)-C(21)	116.4(11)
C(22)-N(1)-C(21)	117.9(11)
C(2)-C(1)-C(6)	111.2(6)
C(3)-C(2)-C(1)	110.9(6)
C(2)-C(3)-C(4)	111.8(6)
C(3)-C(4)-C(5)	111.2(6)
C(6)-C(5)-C(4)	110.6(6)
C(5)-C(6)-C(1)	108.1(5)
C(5)-C(6)-P(1)	119.0(5)
C(1)-C(6)-P(1)	114.8(4)
C(12)-C(7)-C(8)	110.9(6)
C(9)-C(8)-C(7)	110.6(6)
C(8)-C(9)-C(10)	110.7(6)
C(9)-C(10)-C(11)	111.6(6)
C(10)-C(11)-C(12)	110.4(5)
C(7)-C(12)-C(11)	110.3(5)
C(7)-C(12)-P(1)	114.1(4)
C(11)-C(12)-P(1)	117.3(4)
C(14)-C(13)-C(18)	111.7(6)
C(15)-C(14)-C(13)	112.3(6)
C(14)-C(15)-C(16)	110.1(6)
C(15)-C(16)-C(17)	111.0(6)
C(16)-C(17)-C(18)	111.2(6)
C(13)-C(18)-C(17)	109.8(6)
C(13)-C(18)-P(1)	112.5(4)
C(17)-C(18)-P(1)	110.2(4)

O(1)-C(19)-N(1)	125.5(13)
O(1)-C(19)-C(20)	119.8(11)
N(1)-C(19)-C(20)	114.7(12)

Appendix C

Crystallographic Information for $Ru(OC_6F_5)_2(dcypb)[C{=}CH(Bu^t)]$ (18)

Structural determination of $Ru(OC_6F_5)_2(dcypb)[C{=}CH(Bu^t)]$. A suitable crystal was selected, mounted on a thin, glass fiber using paraffin oil and cooled to the data collection temperature. Data were collected on a Bruker AXS SMART 1k CCD diffractometer using 0.3° ω-scans at 0, 90, and 180° in ϕ. Initial unit-cell parameters were determined from 60 data frames collected at different sections of the Ewald sphere. Semi-empirical absorption corrections based on equivalent reflections were applied.[1]

Systematic absences in the diffraction data and unit-cell parameters were uniquely consistent with the reported space group. The structure was solved by direct methods, completed with difference Fourier syntheses and refined with full-matrix least-squares procedures based on F^2. All hydrogen atoms were treated as idealized contributions. All scattering factors are contained in the SHELXTL 6.12 program library.[2]

---

(1) SADABS, Bruker AXS, Madison, WI, 2000.

(2) Sheldrick, G. M., SHELXTL V5.10, Siemens Analytical X-ray Instruments Inc., Madison WI 1997.

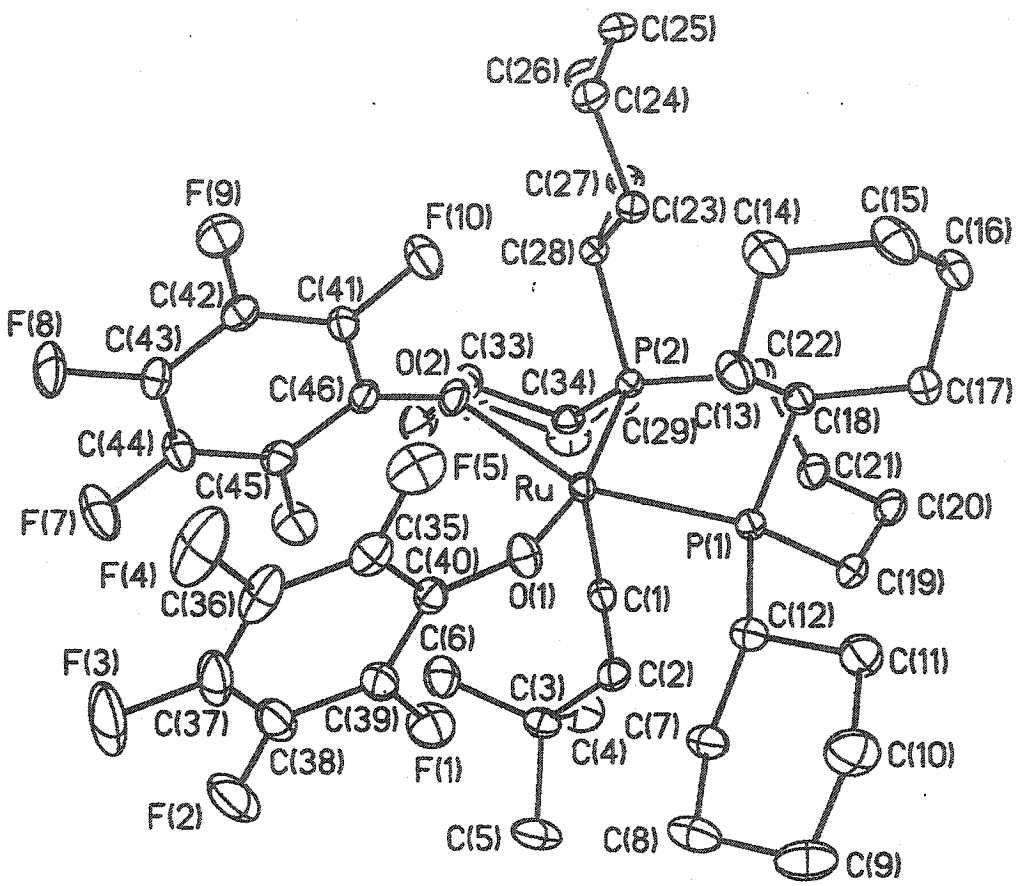

Figure C.1. ORTEP diagram of $Ru(OC_6F_5)_2(dcypb)[C{=}CH(Bu^t)]$ (**18**) showing all cyclohexyl groups. Thermal ellipsoids shown at 30% probability level. For clarity, hydrogen atoms are omitted.

Table C.1. Crystal Data and Structure Refinement Details for $Ru(OC_6F_5)_2(dcypb)[C{=}CH(Bu^t)]$ (**18**)

Empirical formula	$C_{46}H_{62}F_{10}O_2P_2Ru$
Formula weight	999.97
Temperature	203(2) K
Wavelength	0.71073 Å
Crystal system, space group	Monoclinic, P2(1)/n
Unit cell dimensions	a = 13.9203(15) Å α = 90°
	b = 17.5657(19) Å β = 91.803(2)°
	c = 18.877(2) Å γ = 90°
Volume	4613.5(9) $Å^3$
Z, Calculated density	4, 1.440 Mg/m^3
Absorption coefficient	0.486 mm^{-1}
F(000)	2072
Crystal size	0.20 x 0.20 x 0.10 mm
θ range for data collection	1.58 to 28.91 deg.
Limiting indices	-18<=h<=18, -23<=k<=22, -18<=l<=25
Reflections collected / unique	31550 / 10720 [R(int) = 0.0287]
Completeness to θ =	8.91, 88.2 %
Max. and min. transmission	1.000000 and 0.860258
Refinement method	Full-matrix least-squares on F^2
Data / restraints / parameters	10720 / 0 / 550
Goodness-of-fit on F^2	1.009
Final R indices [I >2sigma(I)]	R1 = 0.0353, wR2 = 0.0782
R indices (all data)	R1 = 0.0529, wR2 = 0.0871
Largest diff. peak and hole	0.929 and -0.565 $e.Å^{-3}$

Definition of R indices: $R_1 = \Sigma(F_o - F_c)/\Sigma(F_o)$; $wR_2 = [\Sigma[w(F_o^2 - F_c^2)^2]/\Sigma[w(F_o^2)^2]]^{1/2}$

Table C.2. Bond lengths [Å] and angles [deg] for $Ru(OC_6F_5)_2$(dcypb)[C=CH(Bu^t)] (**18**).

Ru-C(1)	1.793(2)
Ru-O(2)	2.0342(16)
Ru-O(1)	2.1260(18)
Ru-P(2)	2.3143(6)
Ru-P(1)	2.3309(7)
P(1)-C(19)	1.844(2)
P(1)-C(18)	1.852(2)
P(1)-C(12)	1.858(2)
P(2)-C(22)	1.829(2)
P(2)-C(28)	1.861(2)
P(2)-C(34)	1.864(3)
F(1)-C(39)	1.349(3)
F(2)-C(38)	1.351(4)
F(3)-C(37)	1.356(3)
F(4)-C(36)	1.338(4)
F(5)-C(35)	1.339(3)
F(6)-C(45)	1.341(3)
F(7)-C(44)	1.343(3)
F(8)-C(43)	1.345(3)
F(9)-C(42)	1.345(3)
F(10)-C(41)	1.349(3)
O(1)-C(40)	1.305(3)
O(2)-C(46)	1.326(3)
C(1)-C(2)	1.316(3)
C(2)-C(3)	1.523(4)
C(3)-C(6)	1.524(4)
C(3)-C(4)	1.530(4)
C(3)-C(5)	1.541(4)
C(7)-C(12)	1.538(3)
C(7)-C(8)	1.536(4)
C(8)-C(9)	1.509(5)
C(9)-C(10)	1.518(5)
C(10)-C(11)	1.535(4)
C(11)-C(12)	1.543(4)
C(13)-C(14)	1.523(4)
C(13)-C(18)	1.538(3)

C(14)-C(15)	1.527(4)
C(15)-C(16)	1.514(4)
C(16)-C(17)	1.527(3)
C(17)-C(18)	1.540(3)
C(19)-C(20)	1.530(3)
C(20)-C(21)	1.527(4)
C(21)-C(22)	1.541(3)
C(23)-C(24)	1.530(3)
C(23)-C(28)	1.532(4)
C(24)-C(25)	1.522(4)
C(25)-C(26)	1.513(5)
C(26)-C(27)	1.540(4)
C(27)-C(28)	1.542(3)
C(29)-C(30)	1.531(4)
C(29)-C(34)	1.540(4)
C(30)-C(31)	1.519(5)
C(31)-C(32)	1.522(5)
C(32)-C(33)	1.527(4)
C(33)-C(34)	1.535(3)
C(35)-C(36)	1.399(4)
C(35)-C(40)	1.403(4)
C(36)-C(37)	1.373(5)
C(37)-C(38)	1.352(5)
C(38)-C(39)	1.380(4)
C(39)-C(40)	1.399(4)
C(41)-C(42)	1.383(3)
C(41)-C(46)	1.391(4)
C(42)-C(43)	1.378(4)
C(43)-C(44)	1.376(4)
C(44)-C(45)	1.376(3)
C(45)-C(46)	1.400(3)
C(1)-Ru-O(2)	103.50(9)
O(2)-Ru-O(1)	88.21(7)
C(1)-Ru-P(2)	90.19(8)
O(2)-Ru-P(2)	82.31(5)
O(1)-Ru-P(2)	166.16(6)
C(1)-Ru-P(1)	85.49(7)
O(2)-Ru-P(1)	150.38(6)
O(1)-Ru-P(1)	84.85(5)

P(2)-Ru-P(1)	98.45(2)
C(19)-P(1)-C(18)	108.45(11)
C(19)-P(1)-C(12)	102.05(11)
C(18)-P(1)-C(12)	107.19(11)
C(19)-P(1)-Ru	121.71(9)
C(18)-P(1)-Ru	105.60(8)
C(12)-P(1)-Ru	111.14(8)
C(22)-P(2)-C(28)	102.76(10)
C(22)-P(2)-C(34)	105.53(11)
C(28)-P(2)-C(34)	106.46(11)
C(22)-P(2)-Ru	118.38(8)
C(28)-P(2)-Ru	110.77(8)
C(34)-P(2)-Ru	111.94(8)
C(40)-O(1)-Ru	134.59(17)
C(46)-O(2)-Ru	132.81(15)
C(2)-C(1)-Ru	177.6(2)
C(1)-C(2)-C(3)	130.2(2)
C(6)-C(3)-C(2)	111.6(2)
C(6)-C(3)-C(4)	110.3(3)
C(2)-C(3)-C(4)	109.0(2)
C(6)-C(3)-C(5)	109.6(2)
C(2)-C(3)-C(5)	107.8(2)
C(4)-C(3)-C(5)	108.5(2)
C(12)-C(7)-C(8)	109.9(2)
C(9)-C(8)-C(7)	111.8(2)
C(10)-C(9)-C(8)	110.3(3)
C(9)-C(10)-C(11)	111.1(3)
C(10)-C(11)-C(12)	111.5(2)
C(7)-C(12)-C(11)	110.2(2)
C(7)-C(12)-P(1)	111.74(18)
C(11)-C(12)-P(1)	115.94(17)
C(14)-C(13)-C(18)	111.2(2)
C(13)-C(14)-C(15)	111.1(3)
C(16)-C(15)-C(14)	110.8(2)
C(15)-C(16)-C(17)	111.5(2)
C(16)-C(17)-C(18)	110.4(2)
C(17)-C(18)-C(13)	110.9(2)
C(17)-C(18)-P(1)	117.64(16)
C(13)-C(18)-P(1)	110.71(16)

C(20)-C(19)-P(1)	123.53(17)
C(21)-C(20)-C(19)	117.7(2)
C(20)-C(21)-C(22)	113.9(2)
C(21)-C(22)-P(2)	116.41(16)
C(24)-C(23)-C(28)	111.1(2)
C(23)-C(24)-C(25)	111.9(2)
C(26)-C(25)-C(24)	111.5(2)
C(25)-C(26)-C(27)	111.6(2)
C(26)-C(27)-C(28)	110.7(2)
C(23)-C(28)-C(27)	109.5(2)
C(23)-C(28)-P(2)	112.01(16)
C(27)-C(28)-P(2)	115.36(18)
C(30)-C(29)-C(34)	110.7(2)
C(31)-C(30)-C(29)	111.3(3)
C(30)-C(31)-C(32)	111.3(3)
C(31)-C(32)-C(33)	111.9(3)
C(32)-C(33)-C(34)	111.6(2)
C(33)-C(34)-C(29)	111.1(2)
C(33)-C(34)-P(2)	111.58(18)
C(29)-C(34)-P(2)	117.18(18)
F(5)-C(35)-C(36)	118.6(3)
F(5)-C(35)-C(40)	119.1(2)
C(36)-C(35)-C(40)	122.2(3)
F(4)-C(36)-C(37)	120.5(3)
F(4)-C(36)-C(35)	119.5(4)
C(37)-C(36)-C(35)	119.9(3)
F(3)-C(37)-C(38)	120.7(4)
F(3)-C(37)-C(36)	119.7(4)
C(38)-C(37)-C(36)	119.5(3)
F(2)-C(38)-C(37)	120.0(3)
F(2)-C(38)-C(39)	119.5(3)
C(37)-C(38)-C(39)	120.6(3)
F(1)-C(39)-C(38)	118.0(3)
F(1)-C(39)-C(40)	118.8(2)
C(38)-C(39)-C(40)	123.1(3)
O(1)-C(40)-C(39)	124.5(2)
O(1)-C(40)-C(35)	121.1(2)
C(39)-C(40)-C(35)	114.4(2)
F(10)-C(41)-C(42)	118.2(2)

F(10)-C(41)-C(46)	119.3(2)
C(42)-C(41)-C(46)	122.5(2)
F(9)-C(42)-C(43)	119.7(2)
F(9)-C(42)-C(41)	120.3(2)
C(43)-C(42)-C(41)	120.0(2)
F(8)-C(43)-C(44)	120.8(2)
F(8)-C(43)-C(42)	120.2(2)
C(44)-C(43)-C(42)	119.1(2)
F(7)-C(44)-C(43)	119.1(2)
F(7)-C(44)-C(45)	120.3(2)
C(43)-C(44)-C(45)	120.6(2)
F(6)-C(45)-C(44)	119.0(2)
F(6)-C(45)-C(46)	118.9(2)
C(44)-C(45)-C(46)	122.1(2)
O(2)-C(46)-C(41)	121.2(2)
O(2)-C(46)-C(45)	122.7(2)
C(41)-C(46)-C(45)	115.8(2)

Appendix D

Crystallographic Information for $Tl\{[Ru(C{\equiv}CBu^t)(dcypb)]_2(\mu\text{-}Cl)_3\}$ (20)

A suitable crystal was selected, mounted on a thin, glass fiber using paraffin oil and cooled to the data collection temperature. Data were collected on a Bruker AXS SMART 1k CCD diffractometer using 0.3° ω-scans at 0, 90, and 180° in ϕ. Initial unit-cell parameters were determined from 60 data frames collected at different sections of the Ewald sphere. Semi-empirical absorption corrections based on equivalent reflections were applied.[1]

Systematic absences in the diffraction data and unit-cell parameters were consistent with *C*2/*c* (No. 15) and *Cc* (No. 9). Solution in the centrosymmetric space group option yielded chemically reasonable and computationally stable results of refinement. The structure was solved by direct methods, completed with difference Fourier syntheses and refined with full-matrix least-squares procedures based on F^2. The compound molecule is located at a two-fold axis. All hydrogen atoms were treated as idealized contributions. All scattering factors are contained in the SHELXTL 6.12 program library.[2]

---

(1) Brucker AXS, SADABS, Madison, WI, 2000.

(2) Sheldrick, G. M., SHELXTL V5.10, Siemens Analytical X-ray Instruments Inc., Madison WI 1997.

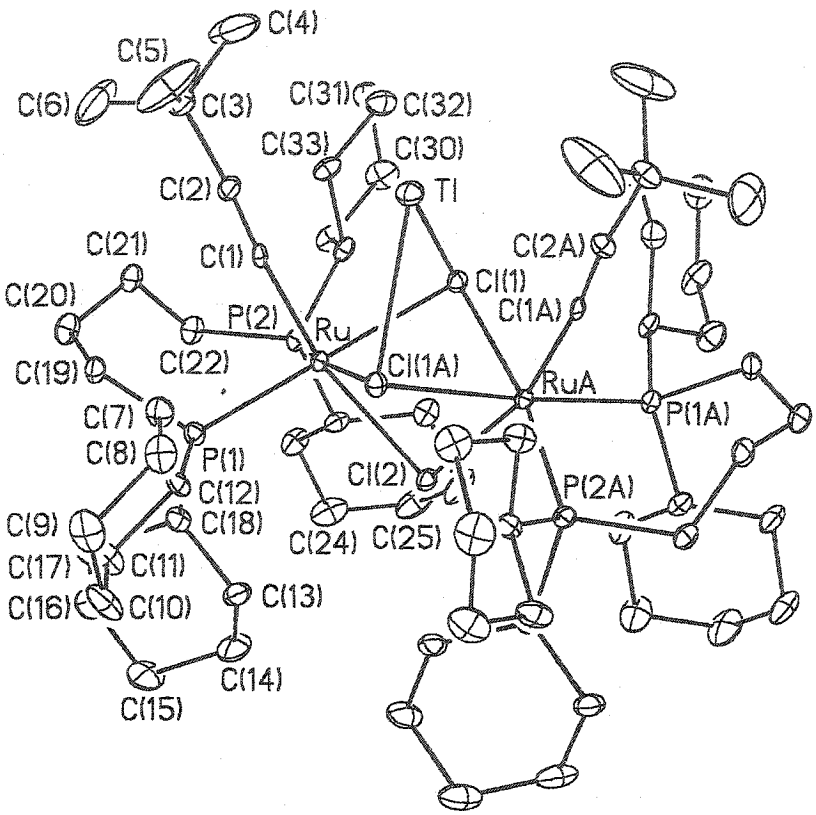

Figure D.1. ORTEP of Tl{[Ru(C≡CBu^t)(dcypb)]$_2$(μ-Cl)$_3$} (**20**), including cyclohexyl groups. Thermal ellipsoids are shown at 30% probability level. Hydrogen atoms are omitted for clarity.

Table D.1. Crystal data and structure refinement for Tl{[Ru(C≡CBu^t)(dcypb)]$_2$(μ-Cl)$_3$} (**20**)

Empirical formula	$C_{68}H_{122}Cl_3P_4Ru_2Tl$
Formula weight	1576.40
Temperature	203(2) K
Wavelength	0.71073 Å
Crystal system, space group	Monoclinic, C2/c
Unit cell dimensions	a = 14.8162(14) Å α = 90°
	b = 20.2544(19) Å β = 97.025(2)°
	c = 24.548(2) Å γ = 90°
Volume	7311.4(12) Å^3
Z, Calculated density	4, 1.432 Mg/m^3
Absorption coefficient	2.840 mm^{-1}
F(000)	3240
Crystal size	0.05 x 0.05 x 0.03 mm
Theta range for data collection	1.67 to 28.99 deg.
Limiting indices	-19<=h<=19, -27<=k<=26, -30<=l<=31
Reflections collected / unique	25223 / 8711 [R(int) = 0.0908]
Completeness to theta	28.99 89.6 %
Absorption correction	Semi-empirical from equivalents
Max. and min. transmission	0.9196 and 0.8710
Refinement method	Full-matrix least-squares on F^2
Data / restraints / parameters	8711 / 0 / 353
Goodness-of-fit on F^2	1.000
Final R indices [I>2sigma(I)]	R1 = 0.0572, wR2 = 0.0704
R indices (all data)	R1 = 0.1193, wR2 = 0.0831
Largest diff. peak and hole	1.210 and -1.160 e.Å^{-3}

Definition of R indices: $R_1 = \Sigma(F_o - F_c)/\Sigma(F_o)$; $wR_2 = [\Sigma[w(F_o^2 - F_c^2)^2]/\Sigma[w(F_o^2)^2]]^{1/2}$

Table D.2. Bond lengths [Å] and angles [deg] for $Tl\{[Ru(C{\equiv}CBu^t)(dcypb)]_2(\mu\text{-}Cl)_3\}$ (**20**)

Tl-Cl(1)#1	2.9157(13)
Tl-Cl(1)	2.9157(13)
Ru-C(1)	1.989(5)
Ru-P(2)	2.2699(15)
Ru-P(1)	2.2865(14)
Ru-Cl(1)	2.5211(13)
Ru-Cl(1)#1	2.5459(13)
Ru-Cl(2)	2.5506(14)
Cl(1)-Ru#1	2.5459(13)
Cl(2)-Ru#1	2.5506(14)
P(1)-C(19)	1.847(5)
P(1)-C(18)	1.873(5)
P(1)-C(12)	1.874(5)
P(2)-C(22)	1.845(5)
P(2)-C(34)	1.866(5)
P(2)-C(28)	1.880(5)
C(1)-C(2)	1.211(7)
C(2)-C(3)	1.509(7)
C(3)-C(6)	1.488(9)
C(3)-C(5)	1.503(9)
C(3)-C(4)	1.498(9)
C(7)-C(12)	1.543(7)
C(7)-C(8)	1.549(7)
C(8)-C(9)	1.510(8)
C(9)-C(10)	1.517(8)
C(10)-C(11)	1.530(8)
C(11)-C(12)	1.544(7)
C(13)-C(14)	1.520(8)
C(13)-C(18)	1.541(7)
C(14)-C(15)	1.540(8)
C(15)-C(16)	1.507(8)
C(16)-C(17)	1.525(8)
C(17)-C(18)	1.541(7)
C(19)-C(20)	1.540(7)
C(20)-C(21)	1.540(7)

C(21)-C(22)	1.545(7)
C(23)-C(24)	1.533(7)
C(23)-C(28)	1.540(7)
C(24)-C(25)	1.521(9)
C(25)-C(26)	1.527(8)
C(26)-C(27)	1.537(7)
C(27)-C(28)	1.545(7)
C(29)-C(30)	1.528(8)
C(29)-C(34)	1.540(7)
C(30)-C(31)	1.527(8)
C(31)-C(32)	1.511(8)
C(32)-C(33)	1.534(7)
C(33)-C(34)	1.534(7)
Cl(1)#1-Tl-Cl(1)	67.60(5)
C(1)-Ru-P(2)	94.20(14)
C(1)-Ru-P(1)	88.31(14)
P(2)-Ru-P(1)	92.62(5)
C(1)-Ru-Cl(1)	90.11(14)
P(2)-Ru-Cl(1)	91.66(5)
P(1)-Ru-Cl(1)	175.53(5)
C(1)-Ru-Cl(1)#1	89.63(14)
P(2)-Ru-Cl(1)#1	170.48(5)
P(1)-Ru-Cl(1)#1	96.20(5)
Cl(1)-Ru-Cl(1)#1	79.61(5)
C(1)-Ru-Cl(2)	164.05(14)
P(2)-Ru-Cl(2)	96.90(4)
P(1)-Ru-Cl(2)	102.56(4)
Cl(1)-Ru-Cl(2)	78.18(4)
Cl(1)#1-Ru-Cl(2)	77.73(4)
Ru-Cl(1)-Ru#1	86.35(4)
Ru-Cl(1)-Tl	86.45(4)
Ru#1-Cl(1)-Tl	86.00(4)
Ru-Cl(2)-Ru#1	85.63(6)
C(19)-P(1)-C(18)	104.2(2)
C(19)-P(1)-C(12)	99.9(2)
C(18)-P(1)-C(12)	106.1(2)
C(19)-P(1)-Ru	116.49(18)
C(18)-P(1)-Ru	116.27(18)
C(12)-P(1)-Ru	112.14(17)

C(22)-P(2)-C(34)	102.3(2)
C(22)-P(2)-C(28)	102.9(2)
C(34)-P(2)-C(28)	103.3(2)
C(22)-P(2)-Ru	119.46(18)
C(34)-P(2)-Ru	115.48(17)
C(28)-P(2)-Ru	111.45(18)
C(2)-C(1)-Ru	172.9(5)
C(1)-C(2)-C(3)	170.9(6)
C(6)-C(3)-C(5)	109.6(7)
C(6)-C(3)-C(4)	108.4(7)
C(5)-C(3)-C(4)	107.2(7)
C(6)-C(3)-C(2)	110.7(5)
C(5)-C(3)-C(2)	110.4(5)
C(4)-C(3)-C(2)	110.3(5)
C(12)-C(7)-C(8)	110.7(5)
C(9)-C(8)-C(7)	110.7(5)
C(8)-C(9)-C(10)	110.7(5)
C(9)-C(10)-C(11)	111.4(5)
C(10)-C(11)-C(12)	111.9(5)
C(7)-C(12)-C(11)	108.3(5)
C(7)-C(12)-P(1)	111.1(4)
C(11)-C(12)-P(1)	118.6(4)
C(14)-C(13)-C(18)	110.8(5)
C(13)-C(14)-C(15)	111.1(6)
C(16)-C(15)-C(14)	110.6(5)
C(15)-C(16)-C(17)	111.3(5)
C(16)-C(17)-C(18)	110.8(5)
C(13)-C(18)-C(17)	110.0(5)
C(13)-C(18)-P(1)	113.1(4)
C(17)-C(18)-P(1)	119.2(4)
C(20)-C(19)-P(1)	124.0(4)
C(19)-C(20)-C(21)	117.8(4)
C(20)-C(21)-C(22)	113.4(5)
C(21)-C(22)-P(2)	116.2(4)
C(24)-C(23)-C(28)	111.5(5)
C(25)-C(24)-C(23)	111.9(5)
C(24)-C(25)-C(26)	111.6(5)
C(25)-C(26)-C(27)	109.9(5)
C(26)-C(27)-C(28)	110.6(5)

C(23)-C(28)-C(27)	110.1(4)
C(23)-C(28)-P(2)	119.0(4)
C(27)-C(28)-P(2)	112.0(4)
C(30)-C(29)-C(34)	111.3(5)
C(32)-C(31)-C(30)	110.6(5)
C(31)-C(32)-C(33)	111.6(5)
C(32)-C(33)-C(34)	110.9(5)
C(33)-C(34)-C(29)	108.4(4)
C(33)-C(34)-P(2)	115.0(4)
C(29)-C(34)-P(2)	116.7(4)

Symmetry transformations used to generate equivalent atoms:

#1 -x+2,y,-z+1/2

Appendix E

Crystallographic Information for $\{[Ru(C{=}CH^tBu)(dcypb)]_2(\mu\text{-}Cl)_2\}\cdot 2BAr^F{}_4$ (23)

A suitable crystal was selected, mounted on thin, glass fiber using paraffin oil and cooled to the data collection temperature. Data were collected on a Bruker AXS SMART 1k CCD diffractometer using 0.3° ω-scans at 0, 90, and 180° in ϕ. Initial unit-cell parameters were determined from 60 data frames collected at different sections of the Ewald sphere. Semi-empirical absorption corrections based on equivalent reflections were applied.[1]

No symmetry higher than triclinic was observed in the diffraction data and solution in the centrosymmetric space group option yielded chemically reasonable and computationally stable results of refinement. The structure was solved by direct methods, completed with difference Fourier syntheses and refined with full-matrix least-squares procedures based on F^2. The dimeric dication was located at the inversion centre. All nonhydrogen atoms were refined with anisotropic displacement parameters. All hydrogen atoms were treated as idealized contributions. All scattering factors are contained in the SHELXTL 6.12 program library.[2]

---

(1) SADABS, Bruker AXS, Madison, WI, 2000.

(2) Sheldrick, G. M., SHELXTL V5.10, Siemens Analytical X-ray Instruments Inc., Madison WI 1997.

Table E.1. Crystal data and structure refinement for $\{[Ru(C{=}CH^tBu)(dcypb)]_2(\mu\text{-}Cl)_2\}\bullet 2BAr^F{}_4$ (23)

Empirical formula	$C_{132}H_{148}B_2Cl_2F_{48}P_4Ru_2$
Formula weight	3065.04
Temperature	203(2) K
Wavelength, Å	0.71073 Å
Crystal system, space group	Triclinic, P-1
Unit cell dimensions	a = 14.563(2) A α = 68.003(2) deg.
	b = 15.219(3) A β = 76.178(2) deg.
	c = 17.602(3) A γ = 86.912(2) deg.
Volume	3509.7(10) $Å^3$
Z, Calculated density	1, 1.450 Mg/m^3
Absorption coefficient	409 mm^{-1}
F(000)	F(000) 1564
Crystal size	0.30 x 0.20 x 0.20 mm
θ range for data collection	1.44 to 28.71 deg.
Limiting indices	-18<=h<=18, -20<=k<=16, -22<=l<=17
Reflections collected / unique	19818 / 14279 [R(int) = 0.0283]
Completeness to θ =	28.71 78.6 %
Absorption correction	Semi-empirical from equivalents
Max. and min. transmission	0.9226 and 0.8870
Refinement method	Full-matrix least-squares on F^2
Data / restraints / parameters	14279 / 0 / 856
Goodness-of-fit on F^2	1.017
Final R indices [I >2sigma(I)]	R1 = 0.0642, wR2 = 0.1356
R indices (all data)	R1 = 0.0982, wR2 = 0.1549
Largest diff. peak and hole	1.255 and -1.019 $e.A^{-3}$

Definition of R indices: $R_1 = \Sigma(F_o - F_c)/\Sigma(F_o)$; $wR_2 = [\Sigma[w(F_o^2 - F_c^2)^2]/\Sigma[w(F_o^2)^2]]^{1/2}$

Table E.2. Bond lengths (Å) and angles (deg) for {[Ru(C=CH^{t}Bu)(dcypb)]$_2$(μ-Cl)$_2$}•2BAr$^F{}_4$ (**23**)

Ru-C(1)	1.798(4)
Ru-P(2)	2.3210(12)
Ru-P(1)	2.3594(12)
Ru-Cl	2.4500(12)
Ru-Cl#1	2.5159(11)
P(1)-C(19)	1.840(4)
P(1)-C(18)	1.860(4)
P(1)-C(12)	1.861(4)
P(2)-C(22)	1.831(5)
P(2)-C(28)	1.843(5)
P(2)-C(34)	1.870(4)
Cl-Ru#1	2.5159(11)
B-C(56)	1.647(6)
B-C(48)	1.647(6)
B-C(40)	1.652(7)
B-C(64)	1.655(7)
C(1)-C(2)	1.308(6)
C(2)-C(3)	1.528(6)
C(3)-C(4)	1.530(7)
C(3)-C(5)	1.527(6)
C(3)-C(6)	1.542(6)
C(7)-C(8)	1.527(7)
C(7)-C(12)	1.543(6)
C(8)-C(9)	1.528(7)
C(9)-C(10)	1.532(8)
C(10)-C(11)	1.530(7)
C(11)-C(12)	1.547(6)
C(13)-C(14)	1.530(6)
C(13)-C(18)	1.533(6)
C(14)-C(15)	1.532(7)
C(15)-C(16)	1.531(6)
C(16)-C(17)	1.549(7)
C(17)-C(18)	1.545(6)
C(19)-C(20)	1.538(7)
C(20)-C(21)	1.536(7)

C(21)-C(22)	1.550(7)
C(23)-C(24)	1.525(7)
C(23)-C(28)	1.547(6)
C(24)-C(25)	1.523(8)
C(25)-C(26)	1.529(9)
C(26)-C(27)	1.548(8)
C(27)-C(28)	1.539(7)
C(29)-C(34)	1.535(8)
C(29)-C(30)	1.549(7)
C(30)-C(31)	1.532(9)
C(31)-C(32)	1.507(9)
C(32)-C(33)	1.537(7)
C(33)-C(34)	1.540(7)
C(35)-C(36)	1.397(7)
C(35)-C(40)	1.402(6)
C(36)-C(37)	1.387(6)
C(36)-C(41)	1.500(7)
C(37)-C(38)	1.394(7)
C(38)-C(39)	1.389(6)
C(38)-C(42)	1.497(6)
C(39)-C(40)	1.409(6)
C(41)-F(2)	1.284(7)
C(41)-F(3)	1.288(7)
C(41)-F(1)	1.301(7)
C(42)-F(6)	1.342(6)
C(42)-F(5)	1.334(6)
C(42)-F(4)	1.337(6)
C(43)-C(44)	1.391(7)
C(43)-C(48)	1.404(7)
C(44)-C(45)	1.398(8)
C(44)-C(49)	1.499(9)
C(45)-C(46)	1.391(8)
C(46)-C(47)	1.397(6)
C(46)-C(50)	1.498(7)
C(47)-C(48)	1.403(6)
C(49)-F(8)	1.276(9)
C(49)-F(9)	1.296(8)
C(49)-F(7)	1.324(10)
C(50)-F(11)	1.324(7)

C(50)-F(10)	1.325(7)
C(50)-F(12)	1.335(7)
C(51)-C(52)	1.392(7)
C(51)-C(56)	1.402(7)
C(52)-C(53)	1.392(7)
C(52)-C(57)	1.512(9)
C(53)-C(54)	1.376(7)
C(54)-C(55)	1.394(6)
C(54)-C(58)	1.491(7)
C(55)-C(56)	1.401(6)
C(57)-F(14)	1.285(8)
C(57)-F(15)	1.325(10)
C(57)-F(13)	1.349(10)
C(58)-F(18)	1.259(6)
C(58)-F(16)	1.282(6)
C(58)-F(17)	1.301(6)
C(59)-C(60)	1.394(7)
C(59)-C(64)	1.406(6)
C(60)-C(61)	1.396(7)
C(60)-C(65)	1.503(7)
C(61)-C(62)	1.399(6)
C(62)-C(63)	1.393(7)
C(62)-C(66)	1.495(7)
C(63)-C(64)	1.403(6)
C(65)-F(19)	1.319(7)
C(65)-F(20)	1.333(6)
C(65)-F(21)	1.345(6)
C(66)-F(24)	1.335(6)
C(66)-F(22)	1.335(6)
C(66)-F(23)	1.350(6)
C(1)-Ru-P(2)	89.06(13)
C(1)-Ru-P(1)	86.98(13)
P(2)-Ru-P(1)	98.76(4)
C(1)-Ru-Cl	108.66(13)
P(2)-Ru-Cl	90.70(4)
P(1)-Ru-Cl	161.94(4)
C(1)-Ru-Cl#1	104.01(14)
P(2)-Ru-Cl#1	163.85(4)
P(1)-Ru-Cl#1	91.46(4)

Cl-Ru-Cl#1	76.28(4)
C(19)-P(1)-C(18)	107.8(2)
C(19)-P(1)-C(12)	102.9(2)
C(18)-P(1)-C(12)	107.31(19)
C(19)-P(1)-Ru	119.67(15)
C(18)-P(1)-Ru	109.08(14)
C(12)-P(1)-Ru	109.42(15)
C(22)-P(2)-C(28)	106.1(2)
C(22)-P(2)-C(34)	104.4(2)
C(28)-P(2)-C(34)	108.5(2)
C(22)-P(2)-Ru	116.96(16)
C(28)-P(2)-Ru	104.68(14)
C(34)-P(2)-Ru	115.66(16)
Ru-Cl-Ru#1	103.72(4)
C(56)-B-C(48)	109.2(4)
C(56)-B-C(40)	112.9(4)
C(48)-B-C(40)	108.0(3)
C(56)-B-C(64)	107.1(3)
C(48)-B-C(64)	110.1(4)
C(40)-B-C(64)	109.6(4)
C(2)-C(1)-Ru	178.4(4)
C(1)-C(2)-C(3)	125.7(4)
C(4)-C(3)-C(5)	111.4(4)
C(4)-C(3)-C(2)	108.9(4)
C(5)-C(3)-C(2)	109.7(4)
C(4)-C(3)-C(6)	109.1(4)
C(5)-C(3)-C(6)	109.0(4)
C(2)-C(3)-C(6)	108.7(4)
C(8)-C(7)-C(12)	110.4(4)
C(7)-C(8)-C(9)	111.9(5)
C(10)-C(9)-C(8)	110.7(4)
C(11)-C(10)-C(9)	112.1(4)
C(10)-C(11)-C(12)	109.5(4)
C(7)-C(12)-C(11)	109.2(4)
C(7)-C(12)-P(1)	112.5(3)
C(11)-C(12)-P(1)	116.4(3)
C(14)-C(13)-C(18)	110.7(4)
C(13)-C(14)-C(15)	111.5(4)
C(16)-C(15)-C(14)	111.4(4)

C(15)-C(16)-C(17)	110.5(4)
C(18)-C(17)-C(16)	108.8(4)
C(13)-C(18)-C(17)	109.5(3)
C(13)-C(18)-P(1)	112.0(3)
C(17)-C(18)-P(1)	118.4(3)
C(20)-C(19)-P(1)	121.9(3)
C(21)-C(20)-C(19)	117.5(4)
C(20)-C(21)-C(22)	114.6(4)
C(21)-C(22)-P(2)	113.5(3)
C(24)-C(23)-C(28)	110.5(4)
C(23)-C(24)-C(25)	110.9(5)
C(24)-C(25)-C(26)	110.8(5)
C(25)-C(26)-C(27)	112.0(5)
C(28)-C(27)-C(26)	108.8(4)
C(27)-C(28)-C(23)	109.2(4)
C(27)-C(28)-P(2)	117.7(3)
C(23)-C(28)-P(2)	110.3(3)
C(34)-C(29)-C(30)	111.2(5)
C(31)-C(30)-C(29)	110.7(5)
C(32)-C(31)-C(30)	111.0(5)
C(31)-C(32)-C(33)	111.7(5)
C(34)-C(33)-C(32)	110.3(5)
C(29)-C(34)-C(33)	110.3(4)
C(29)-C(34)-P(2)	112.3(3)
C(33)-C(34)-P(2)	115.4(3)
C(36)-C(35)-C(40)	122.8(4)
C(37)-C(36)-C(35)	120.8(4)
C(37)-C(36)-C(41)	119.2(4)
C(35)-C(36)-C(41)	120.0(4)
C(36)-C(37)-C(38)	117.9(4)
C(37)-C(38)-C(39)	120.7(4)
C(37)-C(38)-C(42)	119.8(4)
C(39)-C(38)-C(42)	119.5(4)
C(38)-C(39)-C(40)	123.0(4)
C(35)-C(40)-C(39)	114.8(4)
C(35)-C(40)-B	126.0(4)
C(39)-C(40)-B	119.2(4)
F(2)-C(41)-F(3)	105.1(6)
F(2)-C(41)-F(1)	104.8(6)

F(3)-C(41)-F(1)	104.2(6)
F(2)-C(41)-C(36)	114.4(5)
F(3)-C(41)-C(36)	113.9(5)
F(1)-C(41)-C(36)	113.4(5)
F(6)-C(42)-F(5)	105.4(5)
F(6)-C(42)-F(4)	104.9(4)
F(5)-C(42)-F(4)	107.2(5)
F(6)-C(42)-C(38)	113.3(4)
F(5)-C(42)-C(38)	113.7(4)
F(4)-C(42)-C(38)	111.8(4)
C(44)-C(43)-C(48)	122.4(5)
C(43)-C(44)-C(45)	120.7(5)
C(43)-C(44)-C(49)	120.6(5)
C(45)-C(44)-C(49)	118.7(5)
C(46)-C(45)-C(44)	118.0(5)
C(45)-C(46)-C(47)	120.9(5)
C(45)-C(46)-C(50)	120.3(5)
C(47)-C(46)-C(50)	118.8(5)
C(46)-C(47)-C(48)	121.9(5)
C(43)-C(48)-C(47)	116.1(4)
C(43)-C(48)-B	119.5(4)
C(47)-C(48)-B	124.2(4)
F(8)-C(49)-F(9)	107.2(7)
F(8)-C(49)-F(7)	104.3(8)
F(9)-C(49)-F(7)	103.1(8)
F(8)-C(49)-C(44)	113.7(7)
F(9)-C(49)-C(44)	114.9(6)
F(7)-C(49)-C(44)	112.6(6)
F(11)-C(50)-F(10)	105.1(5)
F(11)-C(50)-F(12)	103.8(6)
F(10)-C(50)-F(12)	106.7(5)
F(11)-C(50)-C(46)	113.1(5)
F(10)-C(50)-C(46)	113.9(5)
F(12)-C(50)-C(46)	113.3(5)
C(52)-C(51)-C(56)	122.6(5)
C(51)-C(52)-C(53)	120.5(5)
C(51)-C(52)-C(57)	120.2(5)
C(53)-C(52)-C(57)	119.2(5)
C(54)-C(53)-C(52)	118.4(4)

C(53)-C(54)-C(55)	120.5(4)
C(53)-C(54)-C(58)	119.9(4)
C(55)-C(54)-C(58)	119.5(4)
C(54)-C(55)-C(56)	122.9(4)
C(55)-C(56)-C(51)	114.9(4)
C(55)-C(56)-B	121.8(4)
C(51)-C(56)-B	123.2(4)
F(14)-C(57)-F(15)	107.7(8)
F(14)-C(57)-F(13)	109.0(9)
F(15)-C(57)-F(13)	102.1(6)
F(14)-C(57)-C(52)	113.9(5)
F(15)-C(57)-C(52)	112.3(7)
F(13)-C(57)-C(52)	111.1(7)
F(18)-C(58)-F(16)	108.5(6)
F(18)-C(58)-F(17)	104.3(6)
F(16)-C(58)-F(17)	102.3(5)
F(18)-C(58)-C(54)	113.9(4)
F(16)-C(58)-C(54)	114.6(5)
F(17)-C(58)-C(54)	112.2(5)
C(60)-C(59)-C(64)	123.0(4)
C(59)-C(60)-C(61)	121.0(4)
C(59)-C(60)-C(65)	120.8(5)
C(61)-C(60)-C(65)	118.1(5)
C(62)-C(61)-C(60)	117.5(4)
C(63)-C(62)-C(61)	120.5(4)
C(63)-C(62)-C(66)	119.0(4)
C(61)-C(62)-C(66)	120.5(4)
C(62)-C(63)-C(64)	123.6(4)
C(63)-C(64)-C(59)	114.6(4)
C(63)-C(64)-B	124.2(4)
C(59)-C(64)-B	121.3(4)
F(19)-C(65)-F(20)	106.6(5)
F(19)-C(65)-F(21)	106.0(5)
F(20)-C(65)-F(21)	105.3(5)
F(19)-C(65)-C(60)	113.4(5)
F(20)-C(65)-C(60)	113.2(4)
F(21)-C(65)-C(60)	111.7(4)
F(24)-C(66)-F(22)	106.9(5)

F(24)-C(66)-F(23)	105.3(4)
F(22)-C(66)-F(23)	105.8(5)
F(24)-C(66)-C(62)	112.5(4)
F(22)-C(66)-C(62)	114.1(4)
F(23)-C(66)-C(62)	111.6(4)

Symmetry transformations used to generate equivalent atoms:
#1 -x+1,-y+1,-z+1

Appendix F

Crystallographic Information for $[\{Ru(CO)(dcypb)\}_2(\mu\text{-}Cl)_3]^+Cl^-$ (21a)

This complex crystallized rapidly from a saturated benzene solution. Despite several attempts, this compound consistently yielded very small, multiple crystals. The data reported herein represents the best effort. A crystal was selected, mounted on a thin, glass fiber using paraffin oil and cooled to the data collection temperature. Data were collected on a Bruker AXS SMART 1k CCD diffractometer using 0.3° ω-scans at 0, 90, and 180° in ϕ. Initial unit-cell parameters were determined from 60 data frames collected at different sections of the Ewald sphere. Semi-empirical absorption corrections based on equivalent reflections were applied.[1] No data were observed beyond 42° (2θ) and the data set was truncated accordingly.

Systematic absences in the diffraction data, and unit-cell parameter were consistent with the reported space group $P2_1/n$ (No. 14). The structure was solved by direct methods, completed with difference Fourier syntheses and refined with full-matrix least-squares procedures based on F^2. A chloride counterion and four cocrystallized benzene solvent molecules were located in the asymmetric unit. In order to conserve a favourable data/parameter ratio, all the non-carbonyl carbon atoms were refined isotropically and all phenyl groups were refined as idealized, rigid, flat hexagons. All non-hydrogen, non-carbon atoms and the carbonyl carbon atoms were refined with

anisotropic displacement coefficients. All hydrogen atoms were treated as idealized contributions. All scattering factors are contained in the SHELXTL 6.12 program library.[2]

---

(1) SADABS, Bruker AXS, Madison, WI, 2000.

(2) Sheldrick, G. M., SHELXTL V5.10, Siemens Analytical X-ray Instruments Inc., Madison WI 1997.

Table F.1. Crystal data and structure refinement for $\{[Ru(CO)(dcypb)]_2(\mu\text{-}Cl)_3\}^+Cl^-$ (**21a**).

Empirical formula	$C_{82}H_{128}Cl_4O_2P_4Ru_2$
Formula weight	1613.66
Temperature	203(2) K
Wavelength, Å	0.71073
Crystal system, space group	Monoclinic, P2(1)/n
Unit cell dimensions	a = 15.3703(19) Å α = 90 deg.
	b = 18.721(2) Å β = 99.027(3) deg.
	c = 28.156(4) Å γ = 90 deg.
Volume	8001.7(17) Å^3
Z, Calculated density	4, 1.339 Mg/m^3
Absorption coefficient	0.636 mm^{-1}
F(000)	3408
Crystal size	0.05 x 0.05 x 0.05 mm
θ range for data collection	1.31 to 20.81 deg.
Limiting indices	-15<=h<=15, 0<=k<=18, 0 <= l <= 28
Reflections collected / unique	63347 / 8378 [R(int) = 0.4158]
Completeness to θ =	20.81, 100.0 %
Absorption correction	Semi-empirical from equivalents
Max. and min. transmission	0.928076 and 0.779953
Refinement method	Full-matrix least-squares on F^2
Data / restraints / parameters	8378 / 0 / 399
Goodness-of-fit on F^2	1.002
Final R indices [I >2sigma(I)]	R1 = 0.0704, wR2 = 0.1533
R indices (all data)	R1 = 0.1639, wR2 = 0.1935
Largest diff. peak and hole	0.865 and -0.773 e.A^{-3}

Definition of R indices: $R_1 = \Sigma(F_o - F_c)/\Sigma(F_o)$; $wR_2 = [\Sigma[w(F_o^2 - F_c^2)^2]/\Sigma[w(F_o^2)^2]]^{1/2}$

Table F.2. Bond lengths (Å) and angles (deg) for $\{[Ru(CO)(dcypb)]_2(\mu\text{-}Cl)_3\}^+Cl^-$ (**21a**)

Ru(1)-C(1)	1.856(15)
Ru(1)-P(1)	2.335(4)
Ru(1)-P(2)	2.352(4)
Ru(1)-Cl(1)	2.478(3)
Ru(1)-Cl(3)	2.481(3)
Ru(1)-Cl(2)	2.501(3)
Ru(2)-C(2)	1.812(14)
Ru(2)-P(4)	2.327(3)
Ru(2)-P(3)	2.346(4)
Ru(2)-Cl(2)	2.463(3)
Ru(2)-Cl(1)	2.485(3)
Ru(2)-Cl(3)	2.495(3)
O(1)-C(1)	1.124(14)
O(2)-C(2)	1.163(14)
P(1)-C(8)	1.852(12)
P(1)-C(15)	1.863(12)
P(1)-C(14)	1.864(12)
P(2)-C(18)	1.833(12)
P(2)-C(30)	1.859(13)
P(2)-C(24)	1.867(12)
P(3)-C(36)	1.852(12)
P(3)-C(42)	1.851(12)
P(3)-C(43)	1.860(12)
P(4)-C(58)	1.849(12)
P(4)-C(46)	1.850(13)
P(4)-C(52)	1.874(12)
C(3)-C(8)	1.526(16)
C(3)-C(4)	1.544(16)
C(4)-C(5)	1.491(17)
C(5)-C(6)	1.533(16)
C(6)-C(7)	1.490(16)
C(7)-C(8)	1.564(16)
C(9)-C(10)	1.512(16)
C(9)-C(14)	1.538(15)
C(10)-C(11)	1.520(17)
C(11)-C(12)	1.504(17)
C(12)-C(13)	1.509(17)

C(13)-C(14)	1.529(16)
C(15)-C(16)	1.529(16)
C(16)-C(17)	1.536(16)
C(17)-C(18)	1.523(16)
C(19)-C(24)	1.539(16)
C(19)-C(20)	1.558(16)
C(20)-C(21)	1.529(17)
C(21)-C(22)	1.488(18)
C(22)-C(23)	1.510(17)
C(23)-C(24)	1.541(16)
C(25)-C(30)	1.492(16)
C(25)-C(26)	1.578(19)
C(26)-C(27)	1.52(2)
C(27)-C(28)	1.468(19)
C(28)-C(29)	1.526(17)
C(29)-C(30)	1.580(16)
C(31)-C(32)	1.503(16)
C(31)-C(36)	1.552(16)
C(32)-C(33)	1.534(18)
C(33)-C(34)	1.524(18)
C(34)-C(35)	1.516(17)
C(35)-C(36)	1.532(16)
C(37)-C(42)	1.512(15)
C(37)-C(38)	1.523(17)
C(38)-C(39)	1.471(17)
C(39)-C(40)	1.537(17)
C(40)-C(41)	1.511(17)
C(41)-C(42)	1.538(16)
C(43)-C(44)	1.523(16)
C(44)-C(45)	1.512(16)
C(45)-C(46)	1.519(16)
C(47)-C(48)	1.540(16)
C(47)-C(52)	1.549(15)
C(48)-C(49)	1.509(16)
C(49)-C(50)	1.521(16)
C(50)-C(51)	1.535(16)
C(51)-C(52)	1.555(16)
C(53)-C(58)	1.535(16)
C(53)-C(54)	1.565(17)

C(54)-C(55)	1.471(18)
C(55)-C(56)	1.536(17)
C(56)-C(57)	1.541(17)
C(57)-C(58)	1.542(17)
C(59)-C(60)	1.3900
C(59)-C(64)	1.3900
C(60)-C(61)	1.3900
C(61)-C(62)	1.3900
C(62)-C(63)	1.3900
C(63)-C(64)	1.3900
C(65)-C(66)	1.3900
C(65)-C(70)	1.3900
C(66)-C(67)	1.3900
C(67)-C(68)	1.3900
C(68)-C(69)	1.3900
C(69)-C(70)	1.3900
C(71)-C(72)	1.3900
C(71)-C(76)	1.3900
C(72)-C(73)	1.3900
C(73)-C(74)	1.3900
C(74)-C(75)	1.3900
C(75)-C(76)	1.3900
C(77)-C(78)	1.3900
C(77)-C(82)	1.3900
C(78)-C(79)	1.3900
C(79)-C(80)	1.3900
C(80)-C(81)	1.3900
C(81)-C(82)	1.3900
C(1)-Ru(1)-P(1)	91.2(4)
C(1)-Ru(1)-P(2)	91.9(4)
P(1)-Ru(1)-P(2)	92.21(12)
C(1)-Ru(1)-Cl(1)	90.2(4)
P(1)-Ru(1)-Cl(1)	171.52(12)
P(2)-Ru(1)-Cl(1)	96.09(12)
C(1)-Ru(1)-Cl(3)	167.5(4)
P(1)-Ru(1)-Cl(3)	98.45(12)
P(2)-Ru(1)-Cl(3)	95.53(12)
Cl(1)-Ru(1)-Cl(3)	79.06(10)
C(1)-Ru(1)-Cl(2)	95.0(4)

P(1)-Ru(1)-Cl(2)	91.53(12)
P(2)-Ru(1)-Cl(2)	172.02(13)
Cl(1)-Ru(1)-Cl(2)	80.03(10)
Cl(3)-Ru(1)-Cl(2)	76.93(11)
C(2)-Ru(2)-P(4)	90.4(4)
C(2)-Ru(2)-P(3)	92.1(4)
P(4)-Ru(2)-P(3)	93.28(12)
C(2)-Ru(2)-Cl(2)	169.8(4)
P(4)-Ru(2)-Cl(2)	97.29(12)
P(3)-Ru(2)-Cl(2)	94.23(12)
C(2)-Ru(2)-Cl(1)	90.8(4)
P(4)-Ru(2)-Cl(1)	171.32(12)
P(3)-Ru(2)-Cl(1)	95.28(11)
Cl(2)-Ru(2)-Cl(1)	80.62(11)
C(2)-Ru(2)-Cl(3)	95.6(4)
P(4)-Ru(2)-Cl(3)	92.69(11)
P(3)-Ru(2)-Cl(3)	170.25(12)
Cl(2)-Ru(2)-Cl(3)	77.36(11)
Cl(1)-Ru(2)-Cl(3)	78.64(10)
Ru(1)-Cl(1)-Ru(2)	85.83(10)
Ru(2)-Cl(2)-Ru(1)	85.82(11)
Ru(1)-Cl(3)-Ru(2)	85.57(10)
C(8)-P(1)-C(15)	99.6(6)
C(8)-P(1)-C(14)	106.2(5)
C(15)-P(1)-C(14)	108.3(6)
C(8)-P(1)-Ru(1)	112.6(4)
C(15)-P(1)-Ru(1)	119.0(4)
C(14)-P(1)-Ru(1)	110.1(4)
C(18)-P(2)-C(30)	99.1(6)
C(18)-P(2)-C(24)	100.8(5)
C(30)-P(2)-C(24)	104.6(6)
C(18)-P(2)-Ru(1)	116.9(4)
C(30)-P(2)-Ru(1)	118.1(4)
C(24)-P(2)-Ru(1)	114.7(4)
C(36)-P(3)-C(42)	106.1(6)
C(36)-P(3)-C(43)	101.0(6)
C(42)-P(3)-C(43)	98.7(5)
C(36)-P(3)-Ru(2)	115.4(4)
C(42)-P(3)-Ru(2)	116.2(4)

C(43)-P(3)-Ru(2)	117.1(4)
C(58)-P(4)-C(46)	100.3(6)
C(58)-P(4)-C(52)	106.0(6)
C(46)-P(4)-C(52)	108.5(6)
C(58)-P(4)-Ru(2)	113.8(4)
C(46)-P(4)-Ru(2)	117.5(4)
C(52)-P(4)-Ru(2)	109.8(4)
O(1)-C(1)-Ru(1)	173.2(13)
O(2)-C(2)-Ru(2)	175.4(12)
C(8)-C(3)-C(4)	109.6(10)
C(5)-C(4)-C(3)	113.5(12)
C(4)-C(5)-C(6)	110.3(12)
C(7)-C(6)-C(5)	113.0(11)
C(6)-C(7)-C(8)	109.6(10)
C(3)-C(8)-C(7)	109.3(10)
C(3)-C(8)-P(1)	114.1(8)
C(7)-C(8)-P(1)	114.3(8)
C(10)-C(9)-C(14)	109.3(10)
C(9)-C(10)-C(11)	111.0(11)
C(12)-C(11)-C(10)	112.5(12)
C(11)-C(12)-C(13)	111.5(12)
C(12)-C(13)-C(14)	111.6(11)
C(9)-C(14)-C(13)	110.7(10)
C(9)-C(14)-P(1)	112.1(8)
C(13)-C(14)-P(1)	119.1(9)
C(16)-C(15)-P(1)	120.1(9)
C(15)-C(16)-C(17)	114.1(11)
C(18)-C(17)-C(16)	118.1(11)
C(17)-C(18)-P(2)	117.6(9)
C(24)-C(19)-C(20)	109.2(10)
C(21)-C(20)-C(19)	110.1(11)
C(22)-C(21)-C(20)	112.5(12)
C(23)-C(22)-C(21)	114.1(12)
C(22)-C(23)-C(24)	110.4(11)
C(19)-C(24)-C(23)	109.3(10)
C(19)-C(24)-P(2)	113.6(8)
C(23)-C(24)-P(2)	116.5(8)
C(30)-C(25)-C(26)	111.0(12)
C(27)-C(26)-C(25)	107.9(13)

C(28)-C(27)-C(26)	110.9(14)
C(27)-C(28)-C(29)	112.3(14)
C(28)-C(29)-C(30)	109.4(11)
C(25)-C(30)-C(29)	111.7(11)
C(25)-C(30)-P(2)	114.9(9)
C(29)-C(30)-P(2)	110.9(9)
C(32)-C(31)-C(36)	112.1(10)
C(31)-C(32)-C(33)	111.4(12)
C(34)-C(33)-C(32)	110.8(12)
C(35)-C(34)-C(33)	110.2(12)
C(34)-C(35)-C(36)	112.4(11)
C(35)-C(36)-C(31)	107.6(10)
C(35)-C(36)-P(3)	114.0(9)
C(31)-C(36)-P(3)	117.5(9)
C(42)-C(37)-C(38)	113.5(11)
C(39)-C(38)-C(37)	112.8(12)
C(38)-C(39)-C(40)	109.2(12)
C(41)-C(40)-C(39)	111.8(12)
C(40)-C(41)-C(42)	112.2(11)
C(37)-C(42)-C(41)	111.4(10)
C(37)-C(42)-P(3)	115.5(9)
C(41)-C(42)-P(3)	114.7(8)
C(44)-C(43)-P(3)	116.8(9)
C(45)-C(44)-C(43)	119.8(11)
C(44)-C(45)-C(46)	114.0(11)
C(45)-C(46)-P(4)	123.0(9)
C(48)-C(47)-C(52)	109.1(10)
C(49)-C(48)-C(47)	113.0(11)
C(48)-C(49)-C(50)	110.5(11)
C(49)-C(50)-C(51)	111.6(11)
C(50)-C(51)-C(52)	109.4(10)
C(51)-C(52)-C(47)	110.7(10)
C(51)-C(52)-P(4)	111.8(8)
C(47)-C(52)-P(4)	115.9(8)
C(58)-C(53)-C(54)	110.6(11)
C(55)-C(54)-C(53)	112.4(12)
C(54)-C(55)-C(56)	112.8(13)
C(55)-C(56)-C(57)	110.9(12)
C(58)-C(57)-C(56)	109.5(11)

C(53)-C(58)-C(57)	110.0(10)
C(53)-C(58)-P(4)	113.1(9)
C(57)-C(58)-P(4)	112.5(9)
C(60)-C(59)-C(64)	120.0
C(61)-C(60)-C(59)	120.0
C(60)-C(61)-C(62)	120.0
C(61)-C(62)-C(63)	120.0
C(64)-C(63)-C(62)	120.0
C(63)-C(64)-C(59)	120.0
C(66)-C(65)-C(70)	120.0
C(67)-C(66)-C(65)	120.0
C(66)-C(67)-C(68)	120.0
C(69)-C(68)-C(67)	120.0
C(68)-C(69)-C(70)	120.0
C(69)-C(70)-C(65)	120.0
C(72)-C(71)-C(76)	120.0
C(73)-C(72)-C(71)	120.0
C(74)-C(73)-C(72)	120.0
C(73)-C(74)-C(75)	120.0
C(76)-C(75)-C(74)	120.0
C(75)-C(76)-C(71)	120.0
C(78)-C(77)-C(82)	120.0
C(79)-C(78)-C(77)	120.0
C(80)-C(79)-C(78)	120.0
C(79)-C(80)-C(81)	120.0
C(82)-C(81)-C(80)	120.0
C(81)-C(82)-C(77)	120.0

Symmetry transformations used to generate equivalent atoms:

#1 –x+1, -y+1, -z+1

Appendix G

Crystallographic Information for K[*fac*-$RuH_3(CO)$(dcypb)]KBH^nBu_3 (28)

X-ray quality crystals of this complex (as a toluene solvate) formed over a period of 3 d at RT from an oil of the crude material. Suitable crystals were selected, mounted on thin, glass fibers using paraffin oil and cooled to the data collection temperature. Data were collected on a Bruker AX SMART 1k CCD diffractometer using 0.3° ω-scans at 0, 90, and 180° in ϕ. Unit-cell parameters were determined from 60 data frames collected at different sections of the Ewald sphere. Semi-empirical absorption corrections based on equivalent reflections were applied.[1] No symmetry higher than triclinic was observed. Refinement in the centrosymmetric space group options yielded computationally stable and chemically reasonable results of refinement. The structures were solved by direct methods, completed with difference Fourier syntheses and refined with full-matrix least-squares procedures based on F^2. The hydride ligands were located from the Fourier electron density difference maps and were refined with a riding model. A half-occupied toluene molecule was located cocrystallized at an inversion center in the asymmetric unit. Phenyl rings were refined as flat hexagonal rigid bodies. All other non-hydrogen atoms were refined with anisotropic displacement parameters. Hydrogen atoms not directly

coordinated as hydride ligands were treated as idealized contributions. All scattering factors are contained in the SHEXTL 5.10 program library.[2]

---

(1) Blessing, R. *Acta Cryst.* **1995**, *A51*, 33.

(2) Sheldrick, G. M., SHELXTL V5.10, Siemens Analytical X-ray Instruments Inc., Madison WI 1997.

Table G.1. Crystal data and structure refinement for K[*fac*-$RuH_3(CO)$(dcypb)]KBH^sBu_3•0.5 toluene (**28**)

empirical formula	$C_{44.50}\,H_{87}\,B\,K_2\,O\,P_2\,Ru$
Formula weight	890.16
crystal size, mm	0.10 x 0.08 x 0.05
temperature, K	203(2)
wavelength, Å	0.71073
crystal system, space group	Triclinic, P–1
a, Å	12.7045(19)
b, Å	14.274(2)
c, Å	16.288(2)
α, deg	70.154(3)
β, deg	71.340(3)
γ, deg	64.262(2)
Volume, $Å^3$	2450.2(6)
Z	2
D_{calcd}, g/cm^3	1.207
μ(Mo Kα), cm^{-1}	5.85
F(000)	958
Range θ collected, deg	1.36-20.81
no. of rflns	21969
no. of indep rflns	5141
no. of rflns obsd (>2σ(I))	5141
R(int)	0.1034
max. and min. transmission	0.928076 and 0.760371
data/restraints/parameters	5141/477/481
goodness-of-fit on F^2	1.030
final R_1, wR_2 indices (I>2σ(I))[a]	0.0505, 0.1055
final R_1, wR_2 indices (all data)	0.0923, 0.1184
largest diff peak and hole, $eÅ^{-3}$	0.510 and -0.415

[a] Definition of R indices: $R_1 = \Sigma(F_o - F_c)/\Sigma(F_o)$; $wR_2 = [\Sigma[w(F_o^2 - F_c^2)^2]/\Sigma[w(F_o^2)^2]]^{1/2}$

Table G.2. Bond lengths [Å] and angles [deg] for K[*fac*-$RuH_3(CO)$(dcypb)]KBH^sBu_3• 0.5 toluene (**28**).

Ru-C(1)	1.807(7)
Ru-P(1)	2.335(2)
Ru-P(2)	2.3375(19)
Ru-K(1)	3.3998(17)
Ru-K(2)	3.5337(16)
Ru-H(1)	1.63(3)
Ru-H(2)	1.64(3)
Ru-H(3)	1.63(3)
B-C(38)	1.620(11)
B-C(34)	1.645(11)
B-C(30)	1.656(11)
B-H(4)	1.32(6)
B-K(2)	3.284(8)
B-K(1)	3.577(8)
K(1)-C(43)	3.197(7)
K(1)-C(42)	3.251(8)
K(1)-C(44)	3.260(7)
K(1)-C(31)	3.343(8)
K(1)-C(42)#1	3.353(8)
K(1)-C(44)#1	3.360(8)
K(1)-C(43)#1	3.424(8)
K(1)-K(2)	3.937(2)
K(1)-H(1)	2.63(5)
K(1)-H(2)	2.67(5)
K(1)-H(3)	2.64(5)
K(1)-H(4)	2.57(6)
K(2)-O(1)#2	2.650(5)
K(2)-C(1)	2.958(6)
K(2)-O(1)	3.103(5)
K(2)-C(39)	3.241(8)
K(2)-C(34)	3.260(8)
K(2)-C(35)	3.448(9)
K(2)-K(2)#2	4.679(3)
K(2)-H(1)	2.82(5)
K(2)-H(4)	2.44(6)
O(1)-C(1)	1.201(7)

O(1)-K(2)#2	2.650(5)
P(1)-C(14)	1.850(7)
P(1)-C(13)	1.860(7)
P(1)-C(7)	1.869(7)
P(2)-C(17)	1.859(6)
P(2)-C(29)	1.862(7)
P(2)-C(23)	1.864(6)
C(2)-C(7)	1.520(9)
C(2)-C(3)	1.524(9)
C(3)-C(4)	1.521(10)
C(4)-C(5)	1.521(10)
C(5)-C(6)	1.533(9)
C(6)-C(7)	1.520(9)
C(8)-C(9)	1.534(9)
C(8)-C(13)	1.538(9)
C(9)-C(10)	1.499(9)
C(10)-C(11)	1.525(10)
C(11)-C(12)	1.549(9)
C(12)-C(13)	1.530(9)
C(14)-C(15)	1.550(9)
C(15)-C(16)	1.525(9)
C(16)-C(17)	1.529(9)
C(18)-C(23)	1.529(8)
C(18)-C(19)	1.540(8)
C(19)-C(20)	1.506(9)
C(20)-C(21)	1.498(9)
C(21)-C(22)	1.527(8)
C(22)-C(23)	1.522(8)
C(24)-C(25)	1.517(9)
C(24)-C(29)	1.527(9)
C(25)-C(26)	1.505(9)
C(26)-C(27)	1.503(10)
C(27)-C(28)	1.519(10)
C(28)-C(29)	1.530(9)
C(30)-C(31)	1.315(10)
C(30)-C(33)	1.524(9)
C(31)-C(32)	1.472(10)
C(34)-C(35)	1.516(10)
C(34)-C(37)	1.525(9)

C(35)-C(36)	1.429(11)
C(38)-C(39)	1.525(9)
C(38)-C(41)	1.571(10)
C(39)-C(40)	1.494(10)
C(42)-C(44)#1	1.357(11)
C(42)-C(43)	1.368(11)
C(42)-K(1)#1	3.353(8)
C(43)-C(44)	1.392(11)
C(43)-C(45)	1.459(17)
C(43)-K(1)#1	3.424(8)
C(44)-C(42)#1	1.357(11)
C(44)-K(1)#1	3.360(8)
C(1)-Ru-P(1)	98.8(2)
C(1)-Ru-P(2)	90.9(2)
P(1)-Ru-P(2)	100.51(7)
C(1)-Ru-K(1)	123.4(2)
P(1)-Ru-K(1)	117.01(6)
P(2)-Ru-K(1)	120.76(5)
C(1)-Ru-K(2)	56.8(2)
P(1)-Ru-K(2)	112.29(6)
P(2)-Ru-K(2)	136.03(6)
K(1)-Ru-K(2)	69.17(4)
C(38)-B-C(34)	113.4(6)
C(38)-B-C(30)	110.5(6)
C(34)-B-C(30)	114.7(7)
C(38)-B-K(2)	92.1(4)
C(34)-B-K(2)	74.6(4)
C(30)-B-K(2)	146.9(5)
C(38)-B-K(1)	100.5(4)
C(34)-B-K(1)	131.2(5)
C(30)-B-K(1)	82.1(4)
K(2)-B-K(1)	69.89(16)
C(43)-K(1)-C(42)	24.5(2)
C(43)-K(1)-C(44)	24.9(2)
C(42)-K(1)-C(44)	42.8(2)
C(43)-K(1)-C(31)	106.6(2)
C(42)-K(1)-C(31)	122.4(2)
C(44)-K(1)-C(31)	82.3(2)
C(43)-K(1)-C(42)#1	42.42(19)

C(42)-K(1)-C(42)#1	48.5(3)
C(44)-K(1)-C(42)#1	23.63(18)
C(31)-K(1)-C(42)#1	74.4(2)
C(43)-K(1)-C(44)#1	42.5(2)
C(42)-K(1)-C(44)#1	23.62(18)
C(44)-K(1)-C(44)#1	49.1(3)
C(31)-K(1)-C(44)#1	112.3(3)
C(42)#1-K(1)-C(44)#1	41.43(19)
C(43)-K(1)-Ru	105.50(17)
C(42)-K(1)-Ru	94.63(15)
C(44)-K(1)-Ru	130.11(18)
C(31)-K(1)-Ru	142.33(19)
C(42)#1-K(1)-Ru	143.12(15)
C(44)#1-K(1)-Ru	104.56(16)
C(43)-K(1)-C(43)#1	49.2(3)
C(42)-K(1)-C(43)#1	41.57(19)
C(44)-K(1)-C(43)#1	41.7(2)
C(31)-K(1)-C(43)#1	88.7(3)
C(42)#1-K(1)-C(43)#1	23.26(19)
C(44)#1-K(1)-C(43)#1	23.66(19)
Ru-K(1)-C(43)#1	127.62(18)
C(43)-K(1)-B	145.4(2)
C(42)-K(1)-B	143.9(2)
C(44)-K(1)-B	121.3(2)
C(31)-K(1)-B	44.89(19)
C(42)#1-K(1)-B	103.5(2)
C(44)#1-K(1)-B	120.8(2)
Ru-K(1)-B	108.58(14)
C(43)#1-K(1)-B	103.1(2)
C(43)-K(1)-K(2)	161.81(18)
C(42)-K(1)-K(2)	141.52(17)
C(44)-K(1)-K(2)	172.79(19)
C(31)-K(1)-K(2)	91.50(16)
C(42)#1-K(1)-K(2)	150.36(17)
C(44)#1-K(1)-K(2)	131.48(16)
Ru-K(1)-K(2)	57.02(3)
C(43)#1-K(1)-K(2)	135.02(16)
B-K(1)-K(2)	51.56(14)
O(1)#2-K(2)-C(1)	90.98(18)

O(1)#2-K(2)-O(1)	71.43(16)
C(1)-K(2)-O(1)	22.68(14)
O(1)#2-K(2)-C(39)	106.01(18)
C(1)-K(2)-C(39)	127.7(2)
O(1)-K(2)-C(39)	121.23(18)
O(1)#2-K(2)-C(34)	100.46(18)
C(1)-K(2)-C(34)	165.3(2)
O(1)-K(2)-C(34)	171.55(17)
C(39)-K(2)-C(34)	57.8(2)
O(1)#2-K(2)-B	128.04(19)
C(1)-K(2)-B	141.0(2)
O(1)-K(2)-B	157.54(19)
C(39)-K(2)-B	48.2(2)
C(34)-K(2)-B	29.1(2)
O(1)#2-K(2)-C(35)	94.26(19)
C(1)-K(2)-C(35)	145.0(2)
O(1)-K(2)-C(35)	153.41(19)
C(39)-K(2)-C(35)	83.8(2)
C(34)-K(2)-C(35)	25.93(18)
B-K(2)-C(35)	46.9(2)
O(1)#2-K(2)-Ru	118.45(11)
C(1)-K(2)-Ru	30.73(14)
O(1)-K(2)-Ru	53.37(9)
C(39)-K(2)-Ru	123.72(16)
C(34)-K(2)-Ru	134.87(14)
B-K(2)-Ru	112.35(15)
C(35)-K(2)-Ru	122.62(17)
O(1)#2-K(2)-K(1)	167.59(13)
C(1)-K(2)-K(1)	83.42(14)
O(1)-K(2)-K(1)	104.89(10)
C(39)-K(2)-K(1)	86.11(14)
C(34)-K(2)-K(1)	83.54(14)
B-K(2)-K(1)	58.54(15)
C(35)-K(2)-K(1)	84.21(16)
Ru-K(2)-K(1)	53.81(3)
O(1)#2-K(2)-K(2)#2	38.96(10)
C(1)-K(2)-K(2)#2	52.97(14)
O(1)-K(2)-K(2)#2	32.48(9)
C(39)-K(2)-K(2)#2	120.00(15)

C(34)-K(2)-K(2)#2	139.37(15)
B-K(2)-K(2)#2	164.16(16)
C(35)-K(2)-K(2)#2	129.44(16)
Ru-K(2)-K(2)#2	82.77(4)
K(1)-K(2)-K(2)#2	136.35(6)
C(1)-O(1)-K(2)#2	149.9(5)
C(1)-O(1)-K(2)	71.8(4)
K(2)#2-O(1)-K(2)	108.57(16)
C(14)-P(1)-C(13)	101.6(3)
C(14)-P(1)-C(7)	101.8(3)
C(13)-P(1)-C(7)	99.6(3)
C(14)-P(1)-Ru	118.8(2)
C(13)-P(1)-Ru	117.5(2)
C(7)-P(1)-Ru	114.6(2)
C(17)-P(2)-C(29)	99.3(3)
C(17)-P(2)-C(23)	100.2(3)
C(29)-P(2)-C(23)	103.3(3)
C(17)-P(2)-Ru	113.3(2)
C(29)-P(2)-Ru	116.7(2)
C(23)-P(2)-Ru	120.8(2)
O(1)-C(1)-Ru	175.0(6)
O(1)-C(1)-K(2)	85.5(4)
Ru-C(1)-K(2)	92.5(3)
C(7)-C(2)-C(3)	111.9(6)
C(4)-C(3)-C(2)	111.3(7)
C(5)-C(4)-C(3)	110.2(7)
C(4)-C(5)-C(6)	110.4(6)
C(7)-C(6)-C(5)	112.3(6)
C(2)-C(7)-C(6)	110.3(6)
C(2)-C(7)-P(1)	113.2(5)
C(6)-C(7)-P(1)	113.7(5)
C(9)-C(8)-C(13)	111.5(6)
C(10)-C(9)-C(8)	111.7(7)
C(9)-C(10)-C(11)	111.3(6)
C(10)-C(11)-C(12)	110.8(6)
C(13)-C(12)-C(11)	111.3(6)
C(12)-C(13)-C(8)	108.6(5)
C(12)-C(13)-P(1)	112.7(5)
C(8)-C(13)-P(1)	117.4(5)

C(15)-C(14)-P(1)	117.8(5)
C(16)-C(15)-C(14)	115.7(6)
C(15)-C(16)-C(17)	118.1(6)
C(16)-C(17)-P(2)	118.7(5)
C(23)-C(18)-C(19)	111.3(6)
C(20)-C(19)-C(18)	112.0(6)
C(21)-C(20)-C(19)	111.7(6)
C(20)-C(21)-C(22)	111.0(6)
C(23)-C(22)-C(21)	111.9(6)
C(22)-C(23)-C(18)	108.8(5)
C(22)-C(23)-P(2)	116.4(4)
C(18)-C(23)-P(2)	115.6(4)
C(25)-C(24)-C(29)	113.8(6)
C(26)-C(25)-C(24)	111.1(6)
C(27)-C(26)-C(25)	110.7(7)
C(26)-C(27)-C(28)	112.0(7)
C(27)-C(28)-C(29)	112.0(6)
C(24)-C(29)-C(28)	108.1(6)
C(24)-C(29)-P(2)	112.8(5)
C(28)-C(29)-P(2)	112.5(5)
C(31)-C(30)-C(33)	118.2(7)
C(31)-C(30)-B	126.0(7)
C(33)-C(30)-B	115.8(6)
C(30)-C(31)-C(32)	133.0(8)
C(30)-C(31)-K(1)	96.6(6)
C(32)-C(31)-K(1)	121.4(6)
C(35)-C(34)-C(37)	114.0(7)
C(35)-C(34)-B	116.2(6)
C(37)-C(34)-B	114.0(7)
C(35)-C(34)-K(2)	84.0(5)
C(37)-C(34)-K(2)	148.5(6)
B-C(34)-K(2)	76.3(4)
C(36)-C(35)-C(34)	120.5(9)
C(36)-C(35)-K(2)	103.4(6)
C(34)-C(35)-K(2)	70.1(4)
C(39)-C(38)-C(41)	106.3(7)
C(39)-C(38)-B	115.7(6)
C(41)-C(38)-B	114.4(6)
C(40)-C(39)-C(38)	114.6(7)

C(40)-C(39)-K(2)	147.5(6)
C(38)-C(39)-K(2)	95.6(4)
C(44)#1-C(42)-C(43)	121.9(9)
C(44)#1-C(42)-K(1)	82.7(5)
C(43)-C(42)-K(1)	75.5(5)
C(44)#1-C(42)-K(1)#1	74.3(5)
C(43)-C(42)-K(1)#1	81.3(5)
K(1)-C(42)-K(1)#1	131.5(3)
C(42)-C(43)-C(44)	118.7(8)
C(42)-C(43)-C(45)	122.8(12)
C(44)-C(43)-C(45)	118.5(12)
C(42)-C(43)-K(1)	80.0(5)
C(44)-C(43)-K(1)	80.1(4)
C(45)-C(43)-K(1)	107.0(7)
C(42)-C(43)-K(1)#1	75.4(5)
C(44)-C(43)-K(1)#1	75.6(4)
C(45)-C(43)-K(1)#1	122.2(7)
K(1)-C(43)-K(1)#1	130.8(3)
C(42)#1-C(44)-C(43)	119.5(8)
C(42)#1-C(44)-K(1)	82.0(5)
C(43)-C(44)-K(1)	75.0(4)
C(42)#1-C(44)-K(1)#1	73.7(5)
C(43)-C(44)-K(1)#1	80.8(5)
K(1)-C(44)-K(1)#1	130.9(3)

Symmetry transformations used to generate equivalent atoms:

#1 -x+1,-y+1,-z

#2 -x,-y+1,-z+1

Appendix H

Crystallographic Information for RuH[*o*-C(O)(Ph)(C_6H_4)](CO)(dcypb) (30)

X-ray quality crystals were obtained by slow evaporation of a toluene solution. Suitable crystals were selected, mounted on thin, glass fibers using paraffin oil and cooled to the data collection temperature. Data were collected on a Bruker AX SMART 1k CCD diffractometer using 0.3° ω-scans at 0, 90, and 180° in ϕ. Unit-cell parameters were determined from 60 data frames collected at different sections of the Ewald sphere. Semi-empirical absorption corrections based on equivalent reflections were applied.[1] No symmetry higher than triclinic was observed. Refinement in the centrosymmetric space group options yielded computationally stable and chemically reasonable results of refinement. The structures were solved by direct methods, completed with difference Fourier syntheses and refined with full-matrix least-squares procedures based on F^2. The hydride ligand was located from the Fourier electron density difference maps and was refined with a riding model. Phenyl rings were refined as flat hexagonal rigid bodies. All other non-hydrogen atoms were refined with anisotropic displacement parameters. Hydrogen atoms not directly coordinated as hydride ligands were treated as idealized contributions. All scattering factors are contained in the SHEXTL 5.10 program library.[2]

---

(1) SADABS, Bruker AXS, Madison, WI, 2000.

(2) Sheldrick, G. M., SHELXTL V5.10, Siemens Analytical X-ray Instruments Inc., Madison WI 1997.

Table H.1. Crystal data and refinement parameters for RuH[*o*-C(O)(Ph)(C_6H_4)](CO)(dcypb) (**30**)

empirical formula	$C_{42}H_{62}O_2P_2Ru$
Formula weight	761.93
crystal size, mm	0.10 x 0.10 x 0.03
temperature, K	203(2)
wavelength, Å	0.71073
crystal system, space group	Triclinic, P–1
a, Å	11.4140(11)
b, Å	12.4646(12)
c, Å	14.7309(14)
α, deg	105.770(2)
β, deg	95.353(2)
γ, deg	105.010(2)
Volume, Å^3	1917.6(3)
Z	2
D_{calcd}, g/cm^3	1.320
μ(Mo Kα), cm^{-1}	5.26
F(000)	808
Range θ collected, deg	1.46-28.67
no. of rflns	14922
no. of indep rflns	8631
no. of rflns obsd (>2σ(I))	8631
R(int)	0.0426
max. and min. transmission	0.928074 and 0.814151
data/restraints/parameters	8631/0/428
goodness-of-fit on F^2	1.015
final R_1, wR_2 indices (I>2σ(I))[a]	0.0439, 0.0714
final R_1, wR_2 indices (all data)	0.0815, 0.0774
largest diff peak and hole, eÅ^{-3}	0.495 and -0.588

[a] Definition of R indices: $R_1 = \Sigma(F_o - F_c)/\Sigma(F_o)$; $wR_2 = [\Sigma[w(F_o^2 - F_c^2)^2]/\Sigma[w(F_o^2)^2]]^{1/2}$

Table H.2. Bond lengths [Å] and angles [deg] for RuH[*o*-C(O)(Ph)(C_6H_4)](CO)(dcypb) (**30**)

Ru-C(42)	1.814(3)
Ru-C(29)	2.056(3)
Ru-O(1)	2.144(2)
Ru-P(1)	2.3753(9)
Ru-P(2)	2.4237(8)
P(1)-C(13)	1.846(3)
P(1)-C(12)	1.859(3)
P(1)-C(6)	1.860(3)
P(2)-C(16)	1.858(3)
P(2)-C(28)	1.861(3)
P(2)-C(22)	1.866(3)
O(1)-C(41)	1.259(3)
O(2)-C(42)	1.166(3)
C(1)-C(2)	1.522(4)
C(1)-C(6)	1.539(4)
C(2)-C(3)	1.522(4)
C(3)-C(4)	1.519(4)
C(4)-C(5)	1.531(4)
C(5)-C(6)	1.534(4)
C(7)-C(8)	1.520(4)
C(7)-C(12)	1.539(4)
C(8)-C(9)	1.520(4)
C(9)-C(10)	1.513(4)
C(10)-C(11)	1.525(4)
C(11)-C(12)	1.536(4)
C(13)-C(14)	1.531(4)
C(14)-C(15)	1.523(4)
C(15)-C(16)	1.537(4)
C(17)-C(22)	1.530(4)
C(17)-C(18)	1.524(4)
C(18)-C(19)	1.498(4)
C(19)-C(20)	1.518(4)
C(20)-C(21)	1.531(4)
C(21)-C(22)	1.529(4)
C(23)-C(24)	1.524(4)
C(23)-C(28)	1.541(4)

C(24)-C(25)	1.525(4)
C(25)-C(26)	1.524(4)
C(26)-C(27)	1.527(4)
C(27)-C(28)	1.524(4)
C(29)-C(30)	1.414(4)
C(29)-C(34)	1.421(4)
C(30)-C(31)	1.368(4)
C(31)-C(32)	1.397(4)
C(32)-C(33)	1.381(4)
C(33)-C(34)	1.401(4)
C(34)-C(41)	1.448(4)
C(35)-C(40)	1.379(4)
C(35)-C(36)	1.387(4)
C(36)-C(37)	1.372(5)
C(37)-C(38)	1.371(5)
C(38)-C(39)	1.378(4)
C(39)-C(40)	1.393(4)
C(40)-C(41)	1.487(4)
C(42)-Ru-C(29)	95.87(12)
C(42)-Ru-O(1)	170.99(11)
C(29)-Ru-O(1)	77.24(10)
C(42)-Ru-P(1)	91.09(10)
C(29)-Ru-P(1)	163.62(8)
O(1)-Ru-P(1)	94.13(6)
C(42)-Ru-P(2)	96.11(9)
C(29)-Ru-P(2)	94.55(8)
O(1)-Ru-P(2)	90.27(5)
P(1)-Ru-P(2)	99.44(3)
C(13)-P(1)-C(12)	100.50(14)
C(13)-P(1)-C(6)	100.18(13)
C(12)-P(1)-C(6)	104.82(14)
C(13)-P(1)-Ru	119.42(10)
C(12)-P(1)-Ru	113.17(10)
C(6)-P(1)-Ru	116.44(10)
C(16)-P(2)-C(28)	101.51(13)
C(16)-P(2)-C(22)	100.42(14)
C(28)-P(2)-C(22)	102.46(13)
C(16)-P(2)-Ru	117.99(9)
C(28)-P(2)-Ru	115.43(10)

C(22)-P(2)-Ru	116.46(10)
C(41)-O(1)-Ru	115.90(18)
C(2)-C(1)-C(6)	110.6(2)
C(1)-C(2)-C(3)	111.6(3)
C(4)-C(3)-C(2)	111.0(3)
C(3)-C(4)-C(5)	112.2(3)
C(6)-C(5)-C(4)	110.6(2)
C(5)-C(6)-C(1)	108.8(3)
C(5)-C(6)-P(1)	114.3(2)
C(1)-C(6)-P(1)	112.5(2)
C(8)-C(7)-C(12)	111.0(3)
C(7)-C(8)-C(9)	110.8(3)
C(10)-C(9)-C(8)	111.5(3)
C(9)-C(10)-C(11)	111.9(3)
C(12)-C(11)-C(10)	110.2(2)
C(11)-C(12)-C(7)	108.0(2)
C(11)-C(12)-P(1)	116.8(2)
C(7)-C(12)-P(1)	115.8(2)
C(14)-C(13)-P(1)	117.3(2)
C(15)-C(14)-C(13)	116.4(3)
C(14)-C(15)-C(16)	114.6(2)
C(15)-C(16)-P(2)	115.4(2)
C(22)-C(17)-C(18)	112.6(3)
C(19)-C(18)-C(17)	111.4(3)
C(18)-C(19)-C(20)	111.0(3)
C(19)-C(20)-C(21)	111.3(3)
C(22)-C(21)-C(20)	110.5(3)
C(21)-C(22)-C(17)	109.6(2)
C(21)-C(22)-P(2)	114.0(2)
C(17)-C(22)-P(2)	111.4(2)
C(24)-C(23)-C(28)	110.4(3)
C(25)-C(24)-C(23)	111.2(3)
C(26)-C(25)-C(24)	111.0(2)
C(27)-C(26)-C(25)	111.3(3)
C(28)-C(27)-C(26)	111.4(3)
C(27)-C(28)-C(23)	108.7(2)
C(27)-C(28)-P(2)	112.1(2)
C(23)-C(28)-P(2)	116.5(2)
C(30)-C(29)-C(34)	115.1(3)

C(30)-C(29)-Ru	130.0(2)
C(34)-C(29)-Ru	114.7(2)
C(31)-C(30)-C(29)	122.0(3)
C(30)-C(31)-C(32)	122.1(3)
C(33)-C(32)-C(31)	118.1(3)
C(32)-C(33)-C(34)	120.2(3)
C(33)-C(34)-C(29)	122.5(3)
C(33)-C(34)-C(41)	123.1(3)
C(29)-C(34)-C(41)	114.1(3)
C(40)-C(35)-C(36)	120.5(3)
C(37)-C(36)-C(35)	119.9(3)
C(38)-C(37)-C(36)	120.1(3)
C(37)-C(38)-C(39)	120.4(3)
C(38)-C(39)-C(40)	120.2(3)
C(35)-C(40)-C(39)	118.8(3)
C(35)-C(40)-C(41)	122.4(3)
C(39)-C(40)-C(41)	118.7(3)
O(1)-C(41)-C(34)	117.8(3)
O(1)-C(41)-C(40)	117.3(3)
C(34)-C(41)-C(40)	124.9(3)
O(2)-C(42)-Ru	176.8(3)

Appendix I

Crystallographic Information for RuCl(NN′)(PCy_3)(CHPh) (34)

X-ray quality crystals were obtained by slow evaporation of a saturated toluene solution. A suitable crystal was selected, mounted on a thin, glass fiber using paraffin oil and cooled to the data collection temperature. Data were collected on a Bruker AXS SMART 1k CCD diffractometer using 0.3° ω-scans at 0, 90, and 180° in ϕ. Initial unit-cell parameters were determined from 60 data frames collected at different sections of the Ewald sphere. Semi-empirical absorption corrections based on equivalent reflections were applied.[1]

Systematic absences in the diffraction data are consistent with *C*2/*c* (No. 15) and *Cc* (No. 9). Solution in the centrosymmetric space group option yielded chemically reasonable and computationally stable results of refinement. The structure was solved by direct methods, completed with difference Fourier syntheses and refined with full-matrix least-squares procedures based on F^2. One of the cyclohexyl rings in the phosphine ligand was found disordered in two conformations with a roughly 50/50 refined site occupancy distribution and was each restrained to an ideal chair conformation with chemically identical atoms refined with common atomic displacement parameters. All hydrogen

atoms were treated as idealized contributions. All scattering factors are contained in the SHELXTL 6.12 program library.[2]

---

(1) Brucker AXS, SADABS, Madison, WI, 2000.
(2) Sheldrick, G. M., SHELXTL V5.10, Siemens Analytical X-ray Instruments Inc., Madison WI 1997.

Table I.1. Crystal data and structure refinement for $RuCl(NN')(PCy_3)(CHPh)$ (**34**).

Empirical formula	$C_{42}\ H_{60}\ Cl\ N_2\ P\ Ru$
Formula weight	760.41
Temperature	203(2) K
Wavelength	0.71073 Å
Crystal system, space group	Monoclinic, C2/c
Unit cell dimensions	a = 40.258(4) Å α = 90°
	b = 12.4998(12) Å β = 115.323(2)°
	c = 17.7071(16) Å γ = 90°
Volume	8054.3(13) $Å^3$
Z, Calculated density	8, 1.254 Mg/m^3
Absorption coefficient	0.525 mm^{-1}
F(000)	3216
Crystal size	0.20 x 0.20 x 0.10 mm
Theta range for data collection	1.72 to 29.08°
Limiting indices	-53<=h<=52, -9<=k<=14, -23<=l<=15
Reflections collected / unique	11429 / 8338 [R(int) = 0.0203]
Completeness to theta = 29.08	77.3 %
Absorption correction	Semi-empirical from equivalents
Max. and min. transmission	0.9494 and 0.9022
Refinement method	Full-matrix least-squares on F^2
Data / restraints / parameters	8338 / 36 / 443
Goodness-of-fit on F^2	1.064
Final R indices [I>2sigma(I)]	R_1 = 0.0442, wR_2 = 0.0915
R indices (all data)	R_1 = 0.0731, wR_2 = 0.1038
Largest diff. peak and hole	0.562 and -1.298 $e.Å^{-3}$

Definition of R indices: $R_1 = \Sigma(F_o - F_c)/\Sigma(F_o)$; $wR_2 = [\Sigma[w(F_o^2 - F_c^2)^2]/\Sigma[w(F_o^2)^2]]^{1/2}$

Table I.2. Bond lengths [Å] and angles [deg] for $RuCl(NN')(PCy_3)(CHPh)$ (**34**)

Ru-C(18)	1.828(4)
Ru-N(1)	2.065(3)
Ru-N(2)	2.149(2)
Ru-P	2.3474(8)
Ru-Cl	2.3869(8)
N(1)-C(1)	1.342(4)
N(1)-C(4)	1.390(4)
N(2)-C(5)	1.307(4)
N(2)-C(11)	1.439(4)
P-C(42)	1.864(9)
P-C(36)	1.864(3)
P-C(30)	1.862(4)
P-C(42')	1.904(11)
C(1)-C(2)	1.401(4)
C(2)-C(3)	1.378(5)
C(3)-C(4)	1.405(4)
C(4)-C(5)	1.398(5)
C(6)-C(7)	1.394(5)
C(6)-C(11)	1.408(5)
C(6)-C(12)	1.505(5)
C(7)-C(8)	1.378(6)
C(8)-C(9)	1.375(6)
C(9)-C(10)	1.398(5)
C(10)-C(11)	1.396(5)
C(10)-C(15)	1.523(5)
C(12)-C(13)	1.510(5)
C(12)-C(14)	1.529(6)
C(15)-C(17)	1.539(5)
C(15)-C(16)	1.541(5)
C(18)-C(24)	1.479(5)
C(19)-C(20)	1.385(6)
C(19)-C(24)	1.388(5)
C(20)-C(21)	1.375(6)
C(21)-C(22)	1.367(6)
C(22)-C(23)	1.380(5)
C(23)-C(24)	1.399(5)
C(25)-C(26)	1.528(5)

C(25)-C(30)	1.543(4)
C(26)-C(27)	1.504(6)
C(27)-C(28)	1.533(6)
C(28)-C(29)	1.517(6)
C(29)-C(30)	1.524(5)
C(31)-C(32)	1.526(5)
C(31)-C(36)	1.529(4)
C(32)-C(33)	1.508(6)
C(33)-C(34)	1.512(5)
C(34)-C(35)	1.522(5)
C(35)-C(36)	1.535(5)
C(37)-C(38)	1.530(12)
C(37)-C(42)	1.543(8)
C(38)-C(39)	1.511(11)
C(39)-C(40)	1.533(9)
C(40)-C(41)	1.530(12)
C(41)-C(42)	1.524(11)
C(37')-C(38')	1.528(14)
C(37')-C(42')	1.542(11)
C(38')-C(39')	1.507(13)
C(39')-C(40')	1.510(13)
C(40')-C(41')	1.535(14)
C(41')-C(42')	1.521(13)
C(18)-Ru-N(1)	98.49(13)
C(18)-Ru-N(2)	105.72(12)
N(1)-Ru-N(2)	79.04(10)
C(18)-Ru-P	94.69(10)
N(1)-Ru-P	97.29(7)
N(2)-Ru-P	159.56(8)
C(18)-Ru-Cl	93.74(11)
N(1)-Ru-Cl	164.39(8)
N(2)-Ru-Cl	88.36(7)
P-Ru-Cl	91.31(3)
C(1)-N(1)-C(4)	106.1(3)
C(1)-N(1)-Ru	142.0(2)
C(4)-N(1)-Ru	111.9(2)
C(5)-N(2)-C(11)	116.7(3)
C(5)-N(2)-Ru	111.1(2)
C(11)-N(2)-Ru	131.19(19)

C(42)-P-C(36)	104.5(3)
C(42)-P-C(30)	113.0(3)
C(36)-P-C(30)	103.74(16)
C(42)-P-C(42')	15.4(3)
C(36)-P-C(42')	103.9(4)
C(30)-P-C(42')	98.7(3)
C(42)-P-Ru	111.30(19)
C(36)-P-Ru	104.97(10)
C(30)-P-Ru	117.74(10)
C(42')-P-Ru	125.3(3)
N(1)-C(1)-C(2)	111.0(3)
C(3)-C(2)-C(1)	106.9(3)
C(2)-C(3)-C(4)	106.5(3)
N(1)-C(4)-C(5)	117.3(3)
N(1)-C(4)-C(3)	109.5(3)
C(5)-C(4)-C(3)	132.6(3)
N(2)-C(5)-C(4)	119.6(3)
C(7)-C(6)-C(11)	117.9(4)
C(7)-C(6)-C(12)	121.0(3)
C(11)-C(6)-C(12)	121.2(3)
C(8)-C(7)-C(6)	121.0(4)
C(7)-C(8)-C(9)	120.2(4)
C(8)-C(9)-C(10)	121.4(4)
C(11)-C(10)-C(9)	117.7(3)
C(11)-C(10)-C(15)	122.4(3)
C(9)-C(10)-C(15)	119.9(4)
C(10)-C(11)-C(6)	121.7(3)
C(10)-C(11)-N(2)	119.2(3)
C(6)-C(11)-N(2)	119.0(3)
C(6)-C(12)-C(13)	113.2(4)
C(6)-C(12)-C(14)	111.8(3)
C(13)-C(12)-C(14)	110.4(4)
C(10)-C(15)-C(17)	111.2(3)
C(10)-C(15)-C(16)	110.8(3)
C(17)-C(15)-C(16)	110.8(4)
C(24)-C(18)-Ru	134.2(2)
C(20)-C(19)-C(24)	120.9(4)
C(21)-C(20)-C(19)	119.7(4)
C(22)-C(21)-C(20)	120.2(4)

C(21)-C(22)-C(23)	120.8(4)
C(22)-C(23)-C(24)	119.9(4)
C(19)-C(24)-C(23)	118.4(3)
C(19)-C(24)-C(18)	117.4(3)
C(23)-C(24)-C(18)	124.1(3)
C(26)-C(25)-C(30)	110.4(3)
C(27)-C(26)-C(25)	111.7(4)
C(26)-C(27)-C(28)	111.0(4)
C(29)-C(28)-C(27)	112.3(4)
C(28)-C(29)-C(30)	110.9(3)
C(29)-C(30)-C(25)	110.2(3)
C(29)-C(30)-P	115.8(2)
C(25)-C(30)-P	116.2(2)
C(32)-C(31)-C(36)	111.3(3)
C(33)-C(32)-C(31)	112.4(4)
C(32)-C(33)-C(34)	110.1(3)
C(33)-C(34)-C(35)	110.6(4)
C(34)-C(35)-C(36)	111.9(3)
C(31)-C(36)-C(35)	109.1(3)
C(31)-C(36)-P	115.0(3)
C(35)-C(36)-P	109.8(2)
C(38)-C(37)-C(42)	110.0(9)
C(39)-C(38)-C(37)	112.0(11)
C(38)-C(39)-C(40)	111.7(9)
C(41)-C(40)-C(39)	111.5(10)
C(40)-C(41)-C(42)	110.1(11)
C(41)-C(42)-C(37)	109.1(9)
C(41)-C(42)-P	112.0(7)
C(37)-C(42)-P	115.2(5)
C(38')-C(37')-C(42')	109.7(12)
C(39')-C(38')-C(37')	111.8(13)
C(40')-C(39')-C(38')	112.4(13)
C(39')-C(40')-C(41')	110.1(12)
C(42')-C(41')-C(40')	111.3(13)
C(41')-C(42')-C(37')	109.8(12)
C(41')-C(42')-P	112.0(8)
C(37')-C(42')-P	114.4(7)